

**DEMON2K: Density-Functional Theory (DFT)
for Chemical Physicists/Physical Chemists**
Workbook Number 1 (Abraham's Workbook)



DEMON stands for *densité de Montréal*. For obvious reasons, the unofficial DEMON logo is a demon or devil, mostly just for fun. This is a picture of Jun Maekawa's devil which is one of the most famous origami devils.

Mark Earl CASIDA

Laboratoire de Spectrométrie, Interactions et Chimie théorique (SITH), Département de Chimie Moléculaire (DCM, UMR CNRS/UGA 5250), Institut de Chimie Moléculaire de Grenoble (ICMG, FR2607), Université Grenoble Alpes (UGA) 301 rue de la Chimie, BP 53, F-38041 Grenoble Cedex 9, FRANCE

e-mail: mark.casida@univ-grenoble-alpes.fr

Date of Publication: January 19, 2022 (MS 0.23)

Contents

1 Preliminaries	5
1.1 Preface	5
1.2 Installation	6
1.3 Lesson 0: Running the Program	8
2 Hydrogen Atom Calculations: Basis Sets and Functionals	11
2.1 Lesson 1: The Orbital Basis Set	11
2.1.1 LCAO approximation	11
2.1.2 Dirac-Roothaan Representation	13
2.1.3 GTOs	15
2.1.4 BASIS file	17
2.1.5 Exercise	19
2.2 Lesson 2: Density Functionals	20
2.2.1 Brief Review of Kohn-Sham Theory	21
2.2.2 Some Exact Conditions	23
2.2.3 Brief Review of Functionals	26
2.2.4 Exercise	31
3 H₂⁺ and H₂: Functionals, Potential Energy Curves, and Geometry Optimizations	33
3.1 Lesson 3: The Radical Dissociation Problem	33
3.1.1 LiH: Fractional Charge Problem (FCP)	33
3.1.2 Back to H ₂ ⁺ : What Should We Expect?	37
3.1.3 Exercise	42
3.2 Lesson 4: Treating Multideterminantal Problems by Symmetry-Breaking	43
3.2.1 Preliminaries	43
3.2.2 Excited States	46
3.2.3 Spin-Coupling Theory	48
3.2.4 Dissociation Limits	53
3.2.5 Symmetry Breaking and Spin Contamination	56
3.2.6 Exercise	58
3.3 Lesson 5: Analytic Gradients and Geometry Optimization	61
3.3.1 Variational Calculus	63
3.3.2 Mathematical Formalism and the Hellmann-Feynman Theorem	66
3.3.3 Numerical Method and Pulay Forces	68
3.3.4 Walking on the Potential Energy Surface	72
3.3.5 Exercises	75

4 Lesson 6: Singlet Oxygen, ${}^1\Delta$ O₂	79
4.0.1 Different Types of Oxygen	79
4.0.2 Oxygen Electronic States from DFT	89
4.0.3 Exercises	96
5 Answers	103
5.1 Lesson 1 Answers	103
5.1.1 Raw Results	103
5.1.2 Analysis	110
5.2 Lesson 2 Answers	120
5.2.1 Hartree-Fock	120
5.2.2 Hartree	121
5.2.3 X α	122
5.2.4 LDA	124
5.2.5 GGAs	125
5.2.6 mGGAs	128
5.2.7 Hybrids	131
5.2.8 Trends	132
5.3 Lesson 3 Answers	134
5.3.1 Raw Data	134
5.3.2 Concluding Discussion	140
5.3.3 M062X	144
5.4 Lesson 4 Answers	144
5.4.1 Raw Data	144
5.4.2 Concluding Discussion	148
5.5 Lesson 5 Answers	152
5.5.1 Functional Derivatives	152
5.5.2 SCF Convergence and Forces	156
5.5.3 How Good a Guess Do We Need?	159
5.6 Lesson 6 Answers	160
5.6.1 No Symmetry Breaking	160
5.6.2 With Symmetry Breaking	162
5.6.3 Conclusion	165
A Installing LINUX on a Mac Notebook	167
A.1 Step 1: VIRTUALBOX Installation	167
A.2 Step 2: LINUX Installation	168
A.3 Step 3: Creation of a Virtual Machine	168

Chapter 1

Preliminaries

“All models are approximations. Essentially, all models are wrong, but some are useful. However, the approximate nature of the model must always be born in mind.” — George BOX (famous statistician)

1.1 Preface

“A chemist who is not a physicist is nothing at all.” — Robert Bunsen who, besides being famous for his Bunsen burner, helped to pioneer the use of physical methods, notably spectroscopy, as tools for chemistry

This is a workbook for learning density-functional theory (DFT). It is aimed at chemical physicists/physical chemists. Once upon a time there was a difference between being a chemical physicist and being a physical chemist. At that time, physical chemistry consisted of thermodynamics, kinetics, and various aspects of electrochemistry. While mathematical, the mathematics needed was not as sophisticated as that needed to do quantum mechanics. So the development of quantum mechanics as a tool for investigating chemistry was done in physics departments by chemical physicists. Those days are now in the distant past as quantum mechanics has been taught in chemistry departments since at least the 1970s. The blurring of the border between physics and chemistry continues now at the nano-interface between theoretical solid-state physics and quantum chemistry as physicists look at smaller and smaller structures and chemists look at larger and larger structures. Truly the two terms chemical physicist and physical chemist have become synonymous in recent years!

DFT is a quantum chemical theory which tries to do as much possible with the charge density, rather than with wave functions. This means that much hard work has been and is being done in the building of density-functionals (DFAs for “density-functional approximations”) so that the actual calculations can be kept as simple as possible. Nevertheless it is a mistake to use DFT to study molecular systems without first becoming at least a little familiar with its formalism and the differences between how DFT should work *in principle* and how DFAs work *in practice*. This workbook has as its primary objective to help you fill in this gap between principle and practice. While this workbook does contain a fair amount of theory, the reader will want to supplement this workbook with a basic courses on quantum chemistry and DFT. Indeed, this workbook is really aimed at understanding via practical calculations using the DEMON2K program. The choice of this program comes from the author’s own experience with the code and from its ready availability. Most of what is learned with DEMON2K is just as relevant to using other quantum chemistry programs that do DFT.



Cameroon flag



Dr. Anne ETINDELE



Abraham PONRA

Figure 1.1: Our collaborators from Cameroon.

DEMON2K [1] is an efficient quantum chemistry program which (I feel) should be better known, perhaps especially in the Developing Countries. The only real obstacle to the wider dissemination of DEMON2K is primarily one of information. My hope is that workbooks such as this one may help to fill the information void. Ultimately I would like this to be a small workbook that could be given to a new student for learning how to do basic electronic structure programs through the use of the DEMON2K program. The main advantage of the DEMON2K program for the student is that it is free. The main advantage for the deMon developers is that we can expand our user base and develop the program to better meet the needs of that user base.

In the short term, this workbook is intended to help Abraham PONRA who is a student of Anne ETINDELE in Cameroon to get started on his PhD project with DEMON2K (Fig. 1.1). My plan is that each chapter should be an exercise aimed at learning some particular point and that these points should lead to calculations directly related to Abraham's project. Somewhat unexpectedly Lesson 6 developed into publishable work comparing density functionals [2]. This is a nice example of how teaching and research can go hand-in-hand and of how good ideas do not always require huge amounts of computing power.

At a more personal level, this is also an excuse for me to take some time to get to know some of the more recent innovations in DEMON2K. There is no better way to learn something than by teaching it! Not only have I been enjoying writing the lessons but I have also been enjoying *doing* them. I suggest that the student may have as much to learn from studying my answers as they had from trying the exercises in the first place.

1.2 Installation

DEMON2K should run under most UNIX operating systems. If you do not have a computer running UNIX, it is possible to run UNIX on top of WINDOWS on a PC or on top of the APPLE operating system. Appendix A explains how Nabila Oozeer installed UNIX on her Mac notebook without removing the APPLE operating system.

Let us assume that you have succeeded in finding or creating a UNIX environment. Let us see how you can install DEMON2K on your machine by looking at how I installed it on my machine. Specifically I installed a binary version on my portable computer which runs CENTOS LINUX. Installation involved several steps:

1. Going to http://www.demon-software.com/public_html/download/binary/download.html?

2. Filling in the form:

First name: Mark

Family name: Casida

Institution: Université Grenoble Alpes

email: mark.casida@univ-grenoble-alpes.fr

Platform: deMon2k 5.0: x86 Linux

Submit **Clear**

3. Creating a suitable directory for unpacking:

```
/home/mcasida/ENGINEERING/workbook/deMon->ls
deMon2k.5.0.x86_linux.tgz
```

4. Changing to that directory and unpacking it:

```
> cd /home/mcasida/ENGINEERING/workbook/deMon
> gunzip deMon2k.5.0.x86_linux.tgz
> ls
deMon2k.5.0.x86_linux.tar
>tar xvf deMon2k.5.0.x86_linux.tar
AUXIS
BASIS
binary
ECPS
FFDS
MCPS
> ls
AUXIS BASIS binary deMon2k.5.0.x86_linux.tar ECPS FFDS MCPS
```

The executable is the file called **binary**. There are also several other files: **BASIS** contains a library of orbital basis sets, **AUXIS** contains a library of auxiliary basis sets for fitting the charge density and exchange correlation (xc) terms, **ECPS** and **MCPS** contain effective core potentials and model core potentials (two very similar concepts) respectively, and **FFDS** contains force field parameters for molecular modeling.

5. Creating a simple input file `deMon.inp` containing:

```

TITLE 02 (Basis: GEN-A3*/6-311++G**)
MULTI 3
#
VXCTYPE VWN
#
PRINT MOS
VISUALIZATION MOLDEN FULL
#
# --- GEOMETRY ---
#
GEOMETRY CARTESIAN ANGSTROM
0      0.000000    0.000000    0.603500
0      0.000000    0.000000   -0.603500

```

This is a single point calculation for the O₂ molecule in its triplet ground state using the LDA.

6. Run the program directly in the directory with the binary:

```

> ./binary < deMon.inp >& deMon.out
> ls
AUXIS binary                  deMon.inp  deMon.mol  deMon.out  ECPS  MCPS
BASIS deMon2k.5.0.x86_linux.tar deMon.mem  deMon.new  deMon.rst  FFDS
> vi deMon.out

```

The program ran correctly, creating several additional files, including the main output in `deMon.out`, a restart file `deMon.rst`, one used for molecular visualization `deMon.mol`, and the files `deMon.mem` and `deMon.new`. The program seems to be working just fine.

1.3 Lesson 0: Running the Program

Right now you have a directory (which I will call the `deMon_root` directory) which contains your executable, BASIS directory, AUXIS directory, etc. For various reasons, you do not want to run in the `deMon_root` directory. Instead, it is convenient to create a SHELL program (which I call `run.csh`) to run DEMON2K for you and do any clean up you might want to do afterwards. This section provides a simple example of how this is done.

Note that the ending `run.csh` indicates that this program is written in C SHELL (`csh`). Other options are possible, but I like C SHELL. My program is intended to be small and easily modifiable so that, once you understand it, you can adjust it to your own purposes and start to build your own SHELL programs.

My program may be run in any directory of your account. It will look for a DEMON2K input file named `xxx.inp` in the same directory where “`xxx`” can be pretty much anything. Since DEMON2K always reads input from a file called `deMon.inp`, the file `xxx.inp` will have to be copied to `deMon.inp`. Also `run.csh` will have to copy the DEMON2K executable and any essential directories to the present directory. The job is then run. Once the job has finished, the output file `deMon.out` is renamed

`xxx.out` (same “`xxx`” as for `xxx.inp`) and all the unimportant files are removed. In order to keep things simple, `run.csh` runs `DEMON2K` in foreground.

Here is the contents of `run.csh` which I have placed in the directory
`/home/mcasida/ENGINEERING/workbook/examples`.

```
#!/bin/csh
# The previous line indicates that this is a C-shell file
# -----
# Program to run deMon in the present working directory.
# To use: Create an input file with the name xxx.inp where
# xxx can be anything. Execute with
# /home/mcasida/ENGINEERING/workbook/examples/run.csh xxx
# The job runs interactively in foreground.
# -----
set xxx = $1
echo "Input file \"$xxx.inp"
set PWD = `pwd'
echo "The present working directory is \"$PWD"
set deMon_root = /home/mcasida/ENGINEERING/workbook/deMon # location of deMon files
echo "Using directories and executables from \"$deMon_root"
#
# copy essential files to the present working directory
#
cp $deMon_root/BASIS $PWD # copy the BASIS file to the run directory
cp $deMon_root/AUXIS $PWD # copy the AUXIS file to the run directory
cp $deMon_root/binary $PWD/deMon.x # copy the executable to the run directory
cp $xxx.inp deMon.inp
#
# run deMon
#
./deMon.x
#
# clean up
\rm BASIS
\rm AUXIS
mv deMon.out $xxx.out
\rm deMon.*
# -----
# End of file
# -----
```

Note that comments begin with the “number sign” (#) except for the first line in `run.csh` which tells my computer that this is a `csh` program. The program needs to be made executable:

```
> chmod ugo+x run.csh
```

Let us see how the program works. I have copied the input file from Sec. 1.2 to the directory
`/HOME/MCASIDA/ENGINEERING/WORKBOOK/EXAMPLES/LESSON0` as the file `02.inp`. Here is a transcript of my session:

```
> ls
02.inp
> cat 02.inp
TITLE 02 (Basis: GEN-A3*/6-311++G**)
MULTI 3
#
VXCTYPE VWN
#
PRINT MOS
VISUALIZATION MOLDEN FULL
#
# --- GEOMETRY ---
#
#
GEOMETRY CARTESIAN ANGSTROM
0      0.000000    0.000000    0.603500
0      0.000000    0.000000   -0.603500
> /home/mcasida/ENGINEERING/workbook/examples/run.csh 02
Input file 02.inp
The present working directory is /home/mcasida/ENGINEERING/workbook/examples/Lesson0
Using directories and executables from /home/mcasida/ENGINEERING/workbook/deMon
> ls
02.inp  02.out
```

In addition to the input file 02.inp, I now have my output file 02.out but nothing else. This is enough to get us started.

Chapter 2

Hydrogen Atom Calculations: Basis Sets and Functionals

Lessons are arranged, at least for now in this initial version, by order of complexity of the molecules treated. It makes sense to begin with the hydrogen atom whose analytic solution is both well known and usually taught in both chemistry and physics curricula.

2.1 Lesson 1: The Orbital Basis Set

The objective here is to gain some understanding of the orbital basis sets used in DEMON2K via a little theory followed by an exercise consisting of calculations on the hydrogen atom.

2.1.1 LCAO approximation

It is well-known that the many-body problem cannot be solved exactly and so approximations are needed. However physicists (by which I generally mean solid-state physicists who are used to doing periodic calculations on metals and semiconductors) and chemists (by which I generally mean physical chemists/chemical physicists who are used to doing calculations on molecules) typically build their approximations based upon different physical pictures. For a physicist, the first approximation is that of an idealized metal where the wave functions of the conduction electrons are plane waves. These plane waves are delocalized over physical (x, y, z) space but localized in momentum space and lend themselves to Fourier transform methods. For a chemist, on the other hand, molecules are thought of as made up of atoms which interact to make bonding molecular orbitals (MOs), nonbonding MOs, and antibonding MOs. The simplest approximation is that each MO is a Linear Combination of Atomic Orbitals (AOs.) Although this LCAO approximation is only a first approximation to more accurate descriptions of the electronic structure of molecules, it is still at the heart of much of chemical thinking. Each MO ψ_i is expanded in terms of AOs χ_μ as,

$$\begin{aligned} \psi_i(\vec{r}) &= \sum_{\mu} \chi_{\mu}(\vec{r}) C_{\mu,i} \\ (\psi_1(\vec{r}) &\quad \psi_2(\vec{r}) \quad \cdots \psi_n(\vec{r})) = (\chi_1(\vec{r}) \quad \chi_2(\vec{r}) \quad \cdots \chi_m(\vec{r})) \begin{bmatrix} C_{1,1} & C_{1,2} & \cdots & C_{1,n} \\ C_{2,1} & C_{2,2} & \cdots & C_{2,n} \\ \vdots & \vdots & \ddots & \vdots \\ C_{m,1} & C_{m,2} & \cdots & C_{m,n} \end{bmatrix}, \quad (2.1) \end{aligned}$$

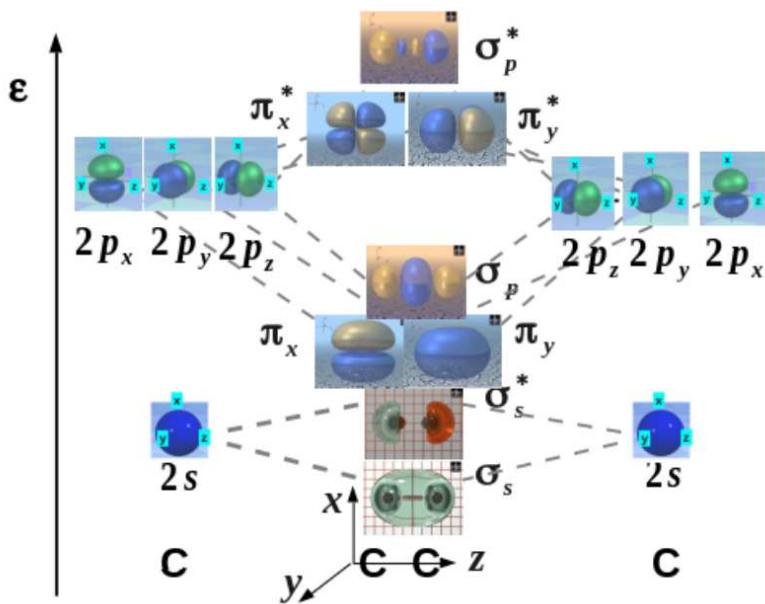


Figure 2.1: Part of the solution to last year’s final exam in the first-year course (CHI 131) that I teach. Notice how AOs with $S > 0$ come together to create MOs with lower energy than the corresponding AOs (i.e., are bonding) while AOs with $S < 0$ come together to create MOs with higher energy than the corresponding AOs (i.e., are antibonding).

where the $C_{\mu,i}$ are referred to as MO coefficients. Notice how Latin indices are used for MOs and Greek indices are used for AOs. This is a very consistent practice throughout the Quantum Chemistry literature. Also capital Latin and Greek letters (such as Ψ) are reserved for many-electron quantities while small Latin and Greek letters (such as ψ) are reserved for 1-electron (e.g., MO) quantities, but there are some exceptions as capital letters are frequently used for matrices for historical reasons.

Each AO is naturally enough centered on an atom (often referred to as a “center”). True AOs on any given center are orthonormal (or, more exactly, may be chosen to be orthonormal),

$$S_{\mu,\nu} = \langle \chi_\mu | \chi_\nu \rangle = \int \chi_\mu^*(\vec{r}) \chi_\nu(\vec{r}) d\vec{r} = \delta_{\mu,\nu} = \begin{cases} 1 & \text{if } \mu = \nu \\ 0 & \text{if } \mu \neq \nu \end{cases}. \quad (2.2)$$

However AOs from different atoms are *not* orthonormal and chemists are used to visualizing how the AOs interact:

$$S_{\mu,\nu} \begin{cases} > 0 & \Rightarrow \text{ bonding} \\ = 0 & \Rightarrow \text{ nonbonding} \\ < 0 & \Rightarrow \text{ antibonding} \end{cases} \quad (2.3)$$

This is adequate to describe the simple AO/MO correlation diagrams found in first-year University chemistry courses (e.g., Fig. 2.1.)

2.1.2 Dirac-Roothaan Representation

Sometimes it is useful to use a more compact representation. This is made possible using Dirac's bras and kets. The bras and kets are related to the wavefunctions by,

$$\begin{aligned}\psi(\vec{r}) &= \langle \vec{r} | \psi \rangle \\ \phi^*(\vec{r}) &= \langle \phi | \vec{r} \rangle.\end{aligned}\quad (2.4)$$

Then,

$$\begin{aligned}\langle \phi | \psi \rangle &= \int \phi^*(\vec{r}) \psi(\vec{r}) d\vec{r} \\ &= \int \langle \phi | \vec{r} \rangle \langle \vec{r} | \psi \rangle d\vec{r} \\ &= \langle \phi | \left(\int | \vec{r} \rangle \langle \vec{r} | d\vec{r} \right) | \psi \rangle.\end{aligned}\quad (2.5)$$

Note how this implies the completeness relation,

$$\hat{1} = \int | \vec{r} \rangle \langle \vec{r} | d\vec{r}. \quad (2.6)$$

In bra-ket notation, Eq. (2.1) is written as,

$$|\psi_i\rangle = \sum_{\mu} |\chi_{\mu}\rangle C_{\mu,i}, \quad (2.7)$$

or,

$$\vec{\psi}^\dagger = \vec{\chi}^\dagger \mathbf{C}, \quad (2.8)$$

where,

$$\begin{aligned}\vec{\psi}^\dagger &= (| \psi_1 \rangle \quad | \psi_2 \rangle \quad \cdots | \psi_n \rangle) \\ \vec{\chi}^\dagger &= (| \chi_1 \rangle \quad | \chi_2 \rangle \quad \cdots | \chi_m \rangle) \\ \mathbf{C} &= \begin{bmatrix} C_{1,1} & C_{1,2} & \cdots & C_{1,n} \\ C_{2,1} & C_{2,2} & \cdots & C_{2,n} \\ \vdots & \vdots & \ddots & \vdots \\ C_{m,1} & C_{m,2} & \cdots & C_{m,n} \end{bmatrix}.\end{aligned}\quad (2.9)$$

Similarly,

$$\begin{aligned}\vec{\phi} &= \begin{pmatrix} \langle \psi_1 | \\ \langle \psi_2 | \\ \ddots \\ \langle \psi_n | \end{pmatrix} \\ \vec{\chi} &= \begin{pmatrix} \langle \chi_1 | \\ \langle \chi_2 | \\ \ddots \\ \langle \chi_m | \end{pmatrix}.\end{aligned}\quad (2.10)$$

I call this combination of Dirac notation and matrix notation “Dirac-Roothaan notation” because the first time I saw it was in an article by Roothaan. This allows us to write some things very compactly:

$$\begin{aligned}\mathbf{S} &= \vec{\chi}\vec{\chi}^\dagger \Rightarrow \text{Overlap matrix} \\ \mathbf{H} &= \vec{\chi}\hat{h}\vec{\chi}^\dagger \Rightarrow \text{Orbital Hamiltonian matrix} \\ \hat{P} &= \vec{\chi}^\dagger\mathbf{S}^{-1}\vec{\chi} \Rightarrow \text{Resolution-of-the-identity.}\end{aligned}\quad (2.11)$$

Note that the resolution-of-the-indentity (RI) only gives the identity operator, $\hat{1}$, in the limit of a complete basis set. Nevertheless, *assuming* that the RI projector is the identity operator provides a quick way to find the matrix form of the orbital equation that can be found more rigorously from the variational principle. This equation is solved in DEMON2K and other quantum chemistry programs:

$$\begin{aligned}\hat{h}|\psi_i\rangle &= \epsilon_i|\psi_i\rangle \\ \vec{\chi}\hat{h}\hat{P}|\psi_i\rangle &= \epsilon_i\vec{\chi}|\psi_i\rangle \\ \vec{\chi}\hat{h}\vec{\chi}^\dagger\mathbf{S}^{-1}\vec{\chi}|\psi_i\rangle &= \epsilon_i\vec{\chi}|\psi_i\rangle \\ \mathbf{H}\vec{C}_i &= \epsilon_i\mathbf{S}\vec{C}_i,\end{aligned}\quad (2.12)$$

where,

$$\vec{C}_i = \mathbf{S}^{-1}\vec{\chi}|\psi_i\rangle, \quad (2.13)$$

is the i th column of the matrix \mathbf{C} of MO coefficients because,

$$\begin{aligned}|\psi_i\rangle &= \vec{\chi}^\dagger\vec{C}_i \\ \vec{\chi}|\psi_i\rangle &= \vec{\chi}\vec{\chi}^\dagger\vec{C}_i \\ \vec{\chi}|\psi_i\rangle &= \mathbf{S}\vec{C}_i \\ \vec{C}_i &= \mathbf{S}^{-1}\vec{\chi}|\psi_i\rangle.\end{aligned}\quad (2.14)$$

One nice thing about the Dirac-Roothaan representation is that it provides useful tools for dealing with basis sets which are *not* orthonormal, which is almost always the case in quantum chemistry.

It is worth repeating that the matrix form of the orbital equation solved in most quantum chemistry program is,

$$\mathbf{H}\vec{C}_i = \epsilon_i\mathbf{S}\vec{C}_i, \quad (2.15)$$

which is a sort of generalized eigenvalue problem. It is often solved using Lödwin’s method which involves taking the square root of the overlap matrix:

$$\begin{aligned}\mathbf{H}\mathbf{S}^{-1/2}\mathbf{S}^{+1/2}\vec{C}_i &= \epsilon_i\mathbf{S}^{+1/2}\mathbf{S}^{+1/2}\vec{C}_i \\ (\mathbf{S}^{-1/2}\mathbf{H}\mathbf{S}^{-1/2})\left(\mathbf{S}^{+1/2}\vec{C}_i\right) &= \epsilon_i\left(\mathbf{S}^{+1/2}\vec{C}_i\right) \\ \tilde{\mathbf{H}}\tilde{\vec{C}}_i &= \epsilon_i\tilde{\vec{C}}_i,\end{aligned}\quad (2.16)$$

where objects indicated with a tilde are sometimes called the symmetrized quantities,

$$\begin{aligned}\tilde{\mathbf{H}} &= \mathbf{S}^{-1/2}\mathbf{H}\mathbf{S}^{-1/2} \\ \tilde{\vec{C}}_i &= \mathbf{S}^{+1/2}\vec{C}_i.\end{aligned}\quad (2.17)$$

A final calculation is then needed to retrieve the true MO coefficients,

$$\vec{C}_i = \mathbf{S}^{-1/2}\tilde{\vec{C}}_i. \quad (2.18)$$

2.1.3 GTOs

The LCAO approximation is only a starting point for accurate approximations which use more elaborate basis sets. There are many excellent reviews of the basis sets used in quantum chemistry (e.g., Ref. [3, 4]). These should be studied. My goal here is only to give a minimal overview.

Although some programs (e.g., DMOL [5]) actually start with real atomic orbitals obtained from atomic calculations on many-electron atoms, most programs take a different approach.

True AOs look roughly like hydrogen atom orbitals which take the familiar form,

$$\chi_{n,l,m}(\vec{r}) = Y_{l,m}(\theta, \phi) R_{n,l}(r), \quad (2.19)$$

where the radial function is a polynomial times an exponential. For example,

$$\begin{aligned} R_{1s}(r) &= 2 \left(\frac{Z}{a_0} \right)^{3/2} e^{-Zr/a_0} \\ R_{2s}(r) &= \frac{1}{\sqrt{2}} \left(\frac{Z}{a_0} \right)^{3/2} \left(1 - \frac{Zr}{2a_0} \right) e^{-Zr/a_0} \\ R_{2p}(r) &= \frac{1}{2\sqrt{6}} \left(\frac{Z}{a_0} \right)^{5/2} r e^{-Zr/a_0}, \end{aligned} \quad (2.20)$$

where a_0 is the Bohr radius and Z is the atomic number of the 1-electron atom. As the nodes in the radial wave function are due to the requirement that the higher energy orbitals be orthogonal to the lower energy orbitals and as this orthogonalization emerges naturally in variational calculations, it is enough to use Slater-type orbitals (STOs) of the form,

$$\chi_{n,l,m}(\vec{r}) \propto Y_{l,m}(\theta, \phi) r^{n-1} e^{-\zeta r/a_0}. \quad (2.21)$$

In many-electron atoms, the real atomic number Z is replaced by an effective atomic number ζ (Greek letter *zeta*) which may, for example, be determined by Slater's rules [6]. The problem with spherical-harmonic STOs in the form of Eq. (2.21) is that these STOs are complex valued which is a problem both for visualization and because it increases computation times. However spherical-harmonic orbitals may be made the real and imaginary parts if necessary,

$$\begin{aligned} Y_{0,0} &= \frac{1}{2\sqrt{\pi}} \\ Y_{1,0} &= \frac{1}{2} \sqrt{\frac{3}{\pi}} \frac{z}{r} \\ \Re e Y_{1,1} &= \frac{1}{2} \sqrt{\frac{3}{2\pi}} \frac{x}{r} \\ \Im m Y_{1,1} &= \frac{1}{2} \sqrt{\frac{3}{2\pi}} \frac{y}{r}. \end{aligned} \quad (2.22)$$

This allows the spherical STOs to be replaced by cartesian STOs of the form,

$$\chi_{l_x, l_y, l_z}(\vec{r}) \propto x^{l_x} y^{l_y} z^{l_z} e^{-\zeta r/a_0}. \quad (2.23)$$

Here $l = l_x + l_y + l_z$ is more or less the azimuthal quantum number except that certain combinations actually lead to functions of lower azimuthal quantum number. For example, there is no $d_{x^2+y^2+z^2}$

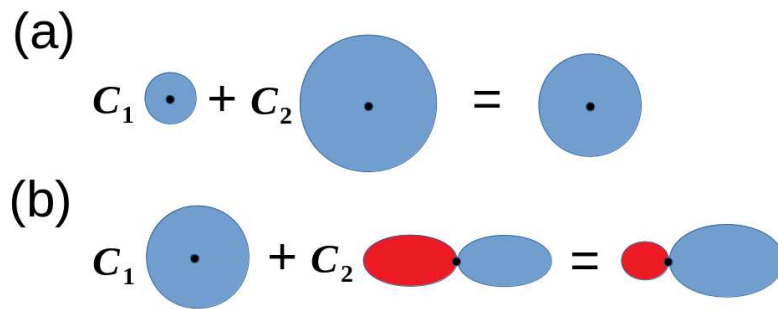


Figure 2.2: Illustration of the effects of using (a) a double ζ basis set and (b) a polarization function.

function because $x^2 + y^2 + z^2 = r^2$ is spherically symmetric, hence an s function. STOs are used in some programs, such as ADF [7], electron repulsion integrals involving more than two centers are difficult to evaluate using STOs.

Instead it is better to use Gaussian-type orbitals (GTOs) of either the spherical-harmonic or cartesian type. These differ from STOs by the replacement $\exp(-\zeta r/a_0)$ by $\exp(-\alpha r^2/a_0^2)$ to make primitive GTOs,

$$\chi_{l_x, l_y, l_z}(\vec{r}; \alpha) \propto x^{l_x} y^{l_y} z^{l_z} e^{-\alpha r^2/a_0^2}. \quad (2.24)$$

Fixed linear combinations of primitive GTOs make contracted GTOs of the form,

$$\chi_\mu(\vec{r}) \propto x^{l_x} y^{l_y} z^{l_z} \sum_i e^{-\alpha_i r^2/a_0^2} d_i. \quad (2.25)$$

Here the d_i are the contraction coefficients and the α_i are the exponentials. DEMON2K uses a GTO basis set.

Contracted GTOs may resemble STOs as in the case of the STO-3G basis minimal basis set where each STO is approximated by a linear combination of three primitive GTOs. Note that a *minimal basis set* corresponds to the case where there is one orbital for each core and for each valence orbital (whether the latter are occupied or not). This partly justifies the common practice of referring to GTOs as AOs.

One criticism which is sometimes made of GTOs by physicists who are used to planewave codes is that there is no single parameter (like the wave number cut-off) that can be used to control the convergence of the basis set. It is possible to control the convergence of a GTO basis set in a systematic way by using, for example, even-tempered Gaussians which are known to provide a uniform coverage of the function space and by systematically enlarging the angular degree of freedom by increasing the largest azimuthal quantum number l in the basis set. However this is rarely done because chemists usually want the *smallest* basis set which is adequate for studying the molecular system (or systems) of interest to them. So the usual strategy is to expand the minimal basis set in two ways.

The first way is to double or triple (double ζ or triple ζ) the number of AOs (i.e., really GTOs) so as to allow expansion or contraction of the AO by variational optimization of, for example, a linear combination of a smaller and a larger GTO of the same type (Fig. 2.2a.) The second way is to include polarization functions of higher angular momentum than in the minimal basis which may be used to describe an angular deformation of an atom or polarization of a bond (Fig. 2.2b.) Clearly these tight or diffuse or polarization functions are no longer atomic orbitals, but it is still common practice to call them AOs.

A convenient place to find GTO basis sets is at the **Basis Set Exchange**:
<https://www.basissetexchange.org/>. You can even download GTO basis sets specifically in DEMON2K format!

2.1.4 BASIS file

The DEMON2K BASIS file is a library of orbital basis sets. For example, for the hydrogen atoms, the file includes the following orbital basis sets:

1. O-HYDROGEN HYDROGEN H (41) (DZV) (DZV-LDA)
2. O-HYDROGEN HYDROGEN H (41/1) (DZVP) (DZVP-LDA) [8]
3. O-HYDROGEN HYDROGEN H (DZV-GGA)
4. O-HYDROGEN HYDROGEN H (DZVP-GGA) [9]
5. O-HYDROGEN HYDROGEN H (41/11*) (TZVP)
6. O-HYDROGEN HYDROGEN H (3) (STO-3G) [10]
7. O-HYDROGEN HYDROGEN H (6-31G**) [11, 12]
8. O-HYDROGEN HYDROGEN H (6-311G**) [13]
9. O-HYDROGEN HYDROGEN H (DEF2-TZVPP) [14]
10. O-HYDROGEN HYDROGEN H (3111/11) (EPR) (EPR-III) [15]
11. O-HYDROGEN HYDROGEN H (311/1) (IGLO-II) [16]
12. O-HYDROGEN HYDROGEN H (3111/11) (IGLO-III) [16]
13. O-HYDROGEN HYDROGEN H (LIC) [17]
14. O-HYDROGEN HYDROGEN H (SAD) [18]
15. O-HYDROGEN HYDROGEN H (41/1*) (TZVP-FIP1) [19]
16. O-HYDROGEN HYDROGEN H (41/1*/1+) (TZVP-FIP2) [19]
17. O-HYDROGEN HYDROGEN H (DZ-ANO) [20]
18. O-HYDROGEN HYDROGEN H (cc-pVTZ) [21]
19. O-HYDROGEN HYDROGEN H (AUG-CC-PVDZ) [22]
20. O-HYDROGEN HYDROGEN H (AUG-CC-PVTZ) [22]
21. O-HYDROGEN HYDROGEN H (AUG-CC-PVQZ) [22]
22. O-HYDROGEN HYDROGEN H (AUG-CC-PV5Z) [22]
23. O-HYDROGEN HYDROGEN H (AUG-PCJ-0) [23]

24. O-HYDROGEN H (AUG-PCJ-1) [23]
25. O-HYDROGEN H (AUG-PCJ-2) [23]
26. O-HYDROGEN H (AUG-PCJ-3) [23]
27. O-HYDROGEN H (AUG-PCJ-4) [23]
28. O-HYDROGEN HYDROGEN H (LANL2DZ) [24]

It is also possible to input your own basis set (possibly one downloaded from the **Basis Set Exchange**) via the standard DEMON2K input file.

Let us take a look at the format of one of these basis sets to get an idea of what the numbers mean:

O-HYDROGEN HYDROGEN H (SAD)

```

5
1 0 4
 33.8650140000      0.0060680000
   5.0947880000      0.0453160000
   1.1587860000      0.2028460000
   0.3258400000      0.5037090000
2 0 1
  0.1027410000      1.0000000000
3 0 1
  0.0324000000      1.0000000000
2 1 2
  1.1588000000      0.1884400000
  0.3258000000      0.8824200000
3 1 2
  0.1027000000      0.1178000000
  0.0324000000      0.0042000000

```

This is an example of a Sadlej field-induced polarisation basis which is specifically designed for efficient calculation of molecular polarizabilities. The number “5” after the title tells us that this basis set consists of 5 contracted GTOs. The next line “1 0 4” tells us the following lines describe the first (“1”) s-type ($l = 0$) function which is a contraction of 4 primitive GTOs. The exponents and contraction coefficients are:

$1s$

1. $\alpha_1 = 33.8650140000, d_1 = 0.0060680000$
2. $\alpha_2 = 5.0947880000, d_2 = 0.0453160000$
3. $\alpha_3 = 1.1587860000, d_3 = 0.2028460000$
4. $\alpha_4 = 0.3258400000, d_4 = 0.5037090000$

The line “2 0 1” announces the next basis function which is the second s-type function consisting of a single primitive GTO:

$1s'$

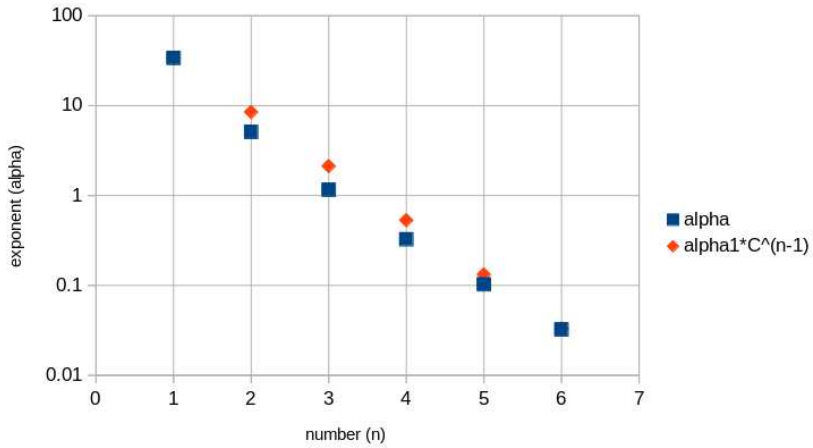


Figure 2.3: The exponents in the Sadlej basis set showing that they form a rough geometric series of the form $\alpha_n = \alpha_1 * (C^{n-1})$ where $C = 0.25$.

1. $\alpha_1 = 0.1027410000, d_1 = 1.0000000000$

The line “3 0 1” announces the third basis function which is the third *s*-type function consisting of a single primitive GTO:

$1s''$

1. $\alpha_1 = 0.0324000000, d_1 = 1.0000000000$

Figure 2.3 shows how the exponents form a rough geometric series. This is not an accident but instead a property that has to be satisfied when GTOs provide a uniform coverage of function space [25]. Continuing on to the next lines: The line “2 1 2” announces the first set of *p*-type functions consisting of the contraction of two primitive GTOs:

$2p_x, 2p_y, 2p_z$

1. $\alpha_1 = 1.1588000000, d_1 = 0.1884400000$

2. $\alpha_2 = 0.3258000000, d_2 = 0.8824200000$

This is followed by the line “3 1 2” which announces the second set of *p*-type functions which also consists of the contraction of two primitive GTOs:

$2p'_x, 2p'_y, 2p'_z$

1. $\alpha_1 = 0.1027000000, d_1 = 0.1178000000$

2. $\alpha_2 = 0.0324000000, d_2 = 0.0042000000$

The total size of the basis set is $m = 3$ *s*-type functions + 2 sets of 3 *p*-type functions = 9 AOs.

2.1.5 Exercise

Copy the following input file and run DEMON2K:

```

TITLE H (Basis: GEN-A3*/STO-3G)
MULTI 2
#
VXCTYPE VWN
#
PRINT MOS
#
# --- GEOMETRY ---
#
#
GEOMETRY CARTESIAN ANGSTROM
H    0.000000    0.000000    0.000000
#
AUXIS (GEN-A3*)
BASIS (STO-3G)

```

For each basis set note down:

1. The size of the basis set (number of AOs)
2. The total energy in Ha (hartrees)
3. The spin α and spin β orbital energies

Discuss your results.

2.2 Lesson 2: Density Functionals

Lesson 1 showed that (at least within the limitations of the given grid and auxiliary basis set), a (spin-unrestricted) calculation on the hydrogen atom leads to a total energy of -0.47972 Ha when the LDA is used, rather than to the exact answer of -0.5 Ha that most of us have seen multiple times in our courses. This happens because, although density-functional *theory* (DFT) is an exact formal theory, practical calculations require the use of density-functional *approximations* (DFAs) which are not exact.

I think it is very important to understand the difference between DFT and DFAs and why both are necessary. Let us begin with the well-known joke about the spherical cow. From the Wikipedia entry entitled “Spherical cow”:

“Milk production at a dairy farm was low, so the farmer wrote to the local university, asking for help from academia. A multidisciplinary team of professors was assembled, headed by a theoretical physicist, and two weeks of intensive on-site investigation took place. The scholars then returned to the university, notebooks crammed with data, where the task of writing the report was left to the team leader. Shortly thereafter the physicist returned to the farm, saying to the farmer, ‘I have the solution, but it works only in the case of spherical cows in a vacuum’.”

This joke illustrates the tendency of physicists to seek exact solutions to idealized problems. For us, DFT is a sort of spherical cow where we can work out all sorts of exact results while DFAs represent a herd of real cows.

However we are also masters of genetic manipulation in the sense that we need not be content with only those real cows in our herd but we, as a community, may also invent new DFA cows. Which brings us to another important point: What makes one DFA better than another DFA? In principle it is how closely it fulfills the exact conditions laid down by DFT. DFT is the target that we may never be able to hit but which gives direction and purpose to our design of DFAs:

Le but n'est pas toujours placé pour être atteint, mais pour servir de mire ou de direction

“The target is not always meant to be hit, but rather to show where we should aim.” —

Joseph Joubert (p. 221 of *Receuil des pensées de M. Joubert* by F.-R. De Chateaubriand, 1838)

In this lesson, we will take first look at one of the exact conditions that should be satisfied by a density functional. This condition goes by a number of names, including that the exact density functional should be free of any self-interaction error (SIE) [26], should show a particle-number derivative discontinuity (PNDD) [27, 28], and should not have any delocalization error (DE) or static correlation error (SCE) [29]. We then make a very brief survey of different types of functionals. Finally the lesson focuses on finding the degree to which the DFAs available in DEMON2K suffer from or are free from SIE.

One final thing should really be said before we go any further. This is that

DFAs typically do worst for small symmetric systems but often do very well for larger systems.

Thus the hydrogen atom is a worst case scenario. This is encouraging for those of us who see DFT as a way to extend *ab initio* accuracy to larger systems. However, in recent years, difficulties have also emerged for DFAs and larger systems, typically having to do with charge distributions in semiconducting polymers and van der Waals interactions. Nevertheless DFT still proves amazing useful for large systems, *provided the DFAs used are first validated against experiment or reliable ab initio calculations for similar properties of similar molecules*. For now let us concentrate on smaller systems where calculations are rapid and failures can be dramatic!

2.2.1 Brief Review of Kohn-Sham Theory

Let us first review the Kohn-Sham formulation of DFT [30]. The total energy expression is,

$$E = \sum_i n_i \langle \psi_i | \hat{t} + v | \psi_i \rangle + E_H[\rho] + E_{xc}[\rho], \quad (2.26)$$

where $\hat{t} = -(1/2)\nabla^2$ is the kinetic energy operator, v is the external potential representing attraction to the nuclei, and the ψ_i are the Kohn-Sham orbitals whose occupation numbers are the n_i . The ψ_i are assumed to be orthonormal in Kohn-Sham theory,

$$\langle \psi_i | \psi_j \rangle = \delta_{i,j}. \quad (2.27)$$

There are also two functionals in the energy expression (2.26). The first is what physicists often call the Hartree energy but which chemists usually call the Coulomb term (and designate by J). I will write it as,

$$E_H[\rho] = \frac{1}{2} \int \int \frac{\rho(1)\rho(2)}{r_{1,2}} d1d2, \quad (2.28)$$

where the numbers “1” and “2” stand for the coordinates of electrons 1 and 2 respectively including spin. It is a functional (i.e., a function of a function) of the charge density,

$$\rho(1) = \sum_i n_i |\psi_i(1)|^2. \quad (2.29)$$

(Note that physicists often write this same quantity as $n(1)$.) The exchange-correlation (xc) energy functional $E_{xc}[\rho]$ is known exactly and can be expressed using the Levy-Lieb constrained variational formalism [31, 32], but this is not practical for calculations. Hence $E_{xc}[\rho]$ is approximated in practice.

Minimizing the energy expression (2.26) subject to the orthonormality condition (2.27) may be done using the Lagrange multiplier formalism:

$$0 = \frac{\delta}{\delta \psi_i^*(1)} \left[E[\psi_i, \psi_i^*] - \sum_i n_i \epsilon_i (\langle \psi_i | \psi_i \rangle - 1) \right]. \quad (2.30)$$

The functional derivative $\delta F[f]$ of a functional $F[f]$ of a function $f(1)$, if it exists, is defined by,

$$\delta F[f] = F[f + \delta f] - F[f] = \int \frac{\delta F[f]}{\delta f(1)} \delta f(1) d1, \quad (2.31)$$

for an arbitrary infinitesimally small variation δf . (See Ref. [33] for a detailed presentation of the theory of functionals and functional derivatives.) Equation (2.30) becomes,

$$0 = n_i (\hat{t} + v(1) + v_H(1) + v_{xc}(1)) \psi_i(1) - n_i \epsilon_i \psi_i(1), \quad (2.32)$$

where the Hartree potential,

$$v_H(1) = v_H[\rho](1) = \int \frac{\rho(2)}{r_{1,2}} d2, \quad (2.33)$$

and the xc potential,

$$v_{xc}(1) = v_{xc}[\rho](1) = \frac{\delta E_{xc}[\rho]}{\delta \rho(1)}. \quad (2.34)$$

Equation (2.32) may be rewritten as,

$$\hat{h} \psi_i(1) = \epsilon_i \psi_i(1), \quad (2.35)$$

where,

$$\hat{h} = \hat{t} + v(1) + v_H(1) + v_{xc}(1), \quad (2.36)$$

is the Kohn-Sham (orbital) hamiltonian.

Note that,

$$\frac{\delta E[\psi_i, \psi_i^*]}{\delta (n_i \psi_i^*(1))} = \hat{h} \psi_i(1). \quad (2.37)$$

This allows a rapid proof of Janak's theorem [34]:

$$\begin{aligned} \frac{\partial E}{\partial n_i} &= \int \frac{\delta E[\psi_i, \psi_i^*]}{\delta (n_i \psi_i^*(1))} \frac{\partial (n_i \psi_i^*(1))}{\partial n_i} d1 \\ &= \int (\hat{h} \psi_i(1)) \psi_i^*(1) d1 \\ &= \int \psi_i^*(1) \hat{h} \psi_i(1) d1 \\ &= \langle \psi_i | \hat{h} | \psi_i \rangle \\ &= \epsilon_i. \end{aligned} \quad (2.38)$$

This provides a way of calculating the ionization potential IP_i of a molecule M associated with removal of an electron from orbital ψ_i , namely,

$$\begin{aligned}\text{IP}_i &= E(\text{M}^+) - E(\text{M}) \\ &= - \int_0^1 \frac{\partial E}{\partial n_i} d1 \\ &= - \int_0^1 \epsilon_i(n_i) d1 \\ &\approx -\epsilon_i(n_i = 1/2).\end{aligned}\tag{2.39}$$

The last approximation (known as Slater's transition orbital method) becomes exact when the $\epsilon_i(n_i)$ is a linear function of n_i . In practice with most functionals it is roughly linear. This will be addressed in more detail below.

2.2.2 Some Exact Conditions

DFT is sometimes criticized as lacking the property of systematic improvability that we have come to expect from wave function methods. However this is not entirely correct as one may hope to improve DFAs by systematically improving as many of the known conditions on the exact xc functional as possible. We discuss only a few related exact conditions here. These are so intimately interrelated that I tend to view these as one exact condition viewed from different points of view.

Highest Occupied Molecular Orbital (HOMO) Energy The asymptotic behavior of the charge density at large distances ("large r ") from a molecule has been extensively studied (Refs. [35, 36] contain reviews) and is known to go as

$$\rho(\vec{r}) \underset{r \rightarrow \infty}{\longrightarrow} \text{const} \times e^{-2\sqrt{2\text{IP}}r},\tag{2.40}$$

where IP is the ionization potential. As the the large r behavior of the density is dominated by the HOMO, we conclude that the HOMO energy in exact Kohn-Sham theory must be equal to exactly minus the IP. This is the

Kohn-Sham Koopmans' theorem: $\epsilon_H = -\text{IP}$, where H stands for the HOMO.

In practice, $-\epsilon_i + \text{const} \approx \text{IP}_i$ where the constant depends upon the functional (see, e.g., Ref. [37]). In particular, electrons are typically *underbound* with the usual DFAs.

Self-Interaction Error We have seen that the Kohn-Sham Koopmans' theorem does not hold for LDA calculations on the hydrogen atom. In particular,

Self-interaction error (SIE): The xc potential fails to cancel the spurious Hartree repulsion of an electron with itself in one-electron systems.

The SIE must also be present in many-electron systems but is difficult to define exactly. The most famous attempt to correct the SIE is the Perdew-Zunger self-interaction correction (SIC) [26],

$$E_{xc}[\rho] \rightarrow E_{xc}[\rho] - \sum_i^{occ} (E_H[\rho_i] + E_{xc}[\rho_i]),\tag{2.41}$$

where $\rho_i(1) = |\psi_i(1)|^2$ and the sum is over occupied (spin) orbitals. The corresponding xc potential has the SIC,

$$v_{xc}[\rho](1) \rightarrow v_{xc}[\rho](1) - \sum_i^{occ} (v_H[\rho_i](1) + v_{xc}[\rho_i](1)) . \quad (2.42)$$

The main difficulty with this SIC is that it is not invariant under a unitary transformation of the occupied orbitals so that a proper implementation involves finding the unitary transformation which minimizes the total energy. Unfortunately most implementations of the Perdew-Zunger SIC are incorrect (including Perdew and Zunger's) in the sense that this unitary transformation is not done.

Particle Number Derivative Discontinuity (PNDD) Janak's theorem uses the concept of fractional occupation number, but what does it mean to have a system with a fractional number of electrons? An answer was proposed by Perdew, Parr, Levy, and Balduz [38] in terms of a weighted ensemble consisting of a fraction $f_N = n_H$ of molecules in their ground state with N electrons and a fraction $f_{N-1} = 1 - n_H$ of molecules in their ground state with $N - 1$ electrons,

$$E(n_H) = n_H E_N(M) + (1 - n_H) E_{N-1}(M^+) . \quad (2.43)$$

Here n_H is the occupation number of the highest-occupied molecular (spin) orbital (HOMO). Then

$$\frac{\partial E(n_H)}{\partial n_H} = E_N(M) - E_{N-1}(M^+) = -\text{IP}_H \quad (2.44)$$

rigorously. Similarly we may consider adding electrons to the lowest unoccupied molecular (spin) orbital to obtain

$$E(n_L) = n_L E_{N+1}(M^-) + (1 - n_L) E_N(M) . \quad (2.45)$$

Then

$$\frac{\partial E(n_L)}{\partial n_L} = E_{N+1}(M^-) - E_N(M) = -\text{EA}_L , \quad (2.46)$$

where EA stands for the electron affinity of the molecule. Equations (2.43) and (2.45) are exact in this theory. They also tell us that the energy is piecewise linear in the number of electrons and therefore that the orbital energy derivative in Janak's theorem does not exist for an integer number of electrons.

Particle Number Derivative Discontinuity:

$$\frac{\partial E}{\partial n} = \begin{cases} -\text{IP} & ; N - \delta \\ \not\exists & ; N \\ -\text{EA} & ; N + \delta \end{cases} . \quad (2.47)$$

This is the famous PNDD (see also the articles by Perdew and Levy [27] and by Sham and Schlüter [28]). As almost all practical DFAs are continuously differentiable, the best we can expect is

$$\epsilon_H = \frac{\partial E}{\partial n_H} \approx -\frac{\text{IP} + \text{EA}}{2} . \quad (2.48)$$

For the hydrogen atom, IP = 0.5 Ha and EA = 0.0277161 Ha [39], so we expect that $\epsilon_{1s} \approx -0.2639$ Ha. This compares well with the LDA value of -0.269 Ha found in Lesson 1.

Cohen, Mori-Sánchez, and Yang published a very nice paper *Science* in 2008 [29] proposing that the failure of the total energy to be piece-wise linear when a fraction of an electron (DE) or a fraction

of spin (SCE) is transferred from one atom to another could be used to measure the error in density functionals and illustrated it with the examples of the dissociation of H_2^+ , H_2 , and aqueous solvation of Cl^- . These examples bring home the importance of what has already been explained above and are proposed as a guide for designing better functionals.

The only way to explain the nondifferentiability of the energy with respect to particle number is to assume a sudden jump in the xc potential when a new orbital begins to be populated. This jump must be nearly constant over all space as an infinitesimal population of a new orbital can only result in an infinitesimal change in the charge density and hence of the orbitals. The exception is asymptotically at large r when the density is going to zero. This asymptotic behavior depends only on the HOMO and so it changes in a discontinuous manner whenever a new orbital is populated even infinitesimally, providing a physical explanation of why the xc potential must have a PNDD.

Krieger-Li-Iafrate (KLI) Model The Perdew-Zunger SIC is not the right way to correct the SIE because it does not treat the PNDD correctly. Instead insight may be obtained from the KLI approximation to the optimized effective potential (OEP). The OEP is the answer to the question,

“What is the local potential v_x whose orbitals minimize the Hartree-Fock energy expression?”

Alternatively the OEP is the answer to the question,

“What is the local potential v_x for a system whose linear response to the perturbation $\hat{\Sigma}_x - v_x$ is zero?”

Here $\hat{\Sigma}_x$ is the Hartree-Fock exchange potential (often denoted by $-\hat{K}$ by chemists). An equation for finding the OEP was first proposed in 1953 a half-page article by Sharp and Horton [40] and then solved by Talman and Shadwick [41]. (See Refs. [42, 36] for an extension that includes electron correlation.)

Instead of looking at that solution we will look at an approximate solution which was suggested in a footnote in the Sharp-Horton paper [40] and later found to be an excellent approximation to the OEP by Krieger, Li, and Iafrate [43, 44]. The “derivation” given here is only heuristic but produces the KLI approximation in a way that it meant to provide more of a feeling for how it works than might a more rigorous approach. We assume that the exchange-only Kohn-Sham orbitals satisfying,

$$\left(\hat{h}_H[\rho] + v_x \right) \psi_i = \epsilon_i^{KS} \psi_i, \quad (2.49)$$

are *on average* the same as the Hartree-Fock orbitals satisfying,

$$\left(\hat{h}_H[\rho] + \hat{\Sigma}_x \right) \psi_i = \epsilon_i^{HF} \psi_i. \quad (2.50)$$

Among other things, “on average” means that we may treat the density ρ and hence the Hartree orbital Hamiltonian $\hat{h}[\rho]$ as the same. Taking the difference of Eqs. (2.49) and (2.50) gives,

$$\left(v_x(1) - \hat{\Sigma}_x \right) \psi_i(1) = (\epsilon_i^{KS} - \epsilon_i^{HF}) \psi_i(1). \quad (2.51)$$

As Eq. (2.51) is only supposed to be correct “on average,” left multiply by $n_i \psi_i^*(1)$ and sum to get,

$$v_x(1)\rho(1) - \sum_i n_i \psi_i^*(1) \hat{\Sigma}_x \psi_i(1) = \sum_i n_i (\epsilon_i^{KS} - \epsilon_i^{HF}) |\psi_i(1)|^2, \quad (2.52)$$

or

$$v_x(1) = v_x^S(1) + \text{DDC}(1), \quad (2.53)$$

where

$$v_x^S(1) = \frac{\sum_i n_i \psi_i^*(1) \hat{\Sigma}_x \psi_i(1)}{\rho(1)} \quad (2.54)$$

is Slater's potential [45] and

$$\text{DDC}(1) = \frac{\sum_i n_i (\epsilon_i^{KS} - \epsilon_i^{HF}) |\psi_i(1)|^2}{\rho(1)} \quad (2.55)$$

is the derivative discontinuity correction (DDC). The LDA is a first approximation to Slater's potential. The DDC is in principle a nonconstant function but it is roughly constant because, to a first approximation, ϵ_i^{KS} and ϵ_i^{HF} differ mainly by an additive constant [37]. Setting $\epsilon_H^{KS} = \epsilon_H^{HF}$ makes this additive constant very nearly zero and assures the correct $v_x \rightarrow 0$ behavior as $r \rightarrow \infty$ [46, 47]. Here "H" stands for the HOMO. Unexpectedly OEP orbital energies seem to provide a better approximation than HF orbital energies to experimental IPs [47]. Equation (2.53) emphasizes that most DFAs behave like the Slater potential while the exact xc potential has a DDC which causes a sudden jump everytime a new orbital is even partly filled.

It should be mentioned that the KLI approximation (2.53) is not invariant to a unitary transformation of the occupied orbitals. However this may be fixed by a slight variation in the derivation of equation to give,

$$v_x(1) = v_x^S(1) + \frac{\sum_{i,j} n_i \psi_i(1) \langle \psi_i | v_x - \hat{\Sigma}_x | \psi_j \rangle \psi_j^*(1)}{\rho(1)}. \quad (2.56)$$

This goes by several names including localized Hartree-Fock [48], the common energy denominator approximation (CEDA) [49], and the effective local potential (ELP) [50]. It has the added advantage of having better numerical stability than does a direct solution of the OEP equation.

2.2.3 Brief Review of Functionals

DFAs sometimes seem like an incomprehensible zoo of miscellaneous acronyms. However John Perdew took a lead from the Bible story of Jacob who fell asleep in the desert and dreamed of a ladder between heaven and earth with angles ascending and descending. In particular, Perdew imagined a ladder of DFAs (Fig. 2.4) where each rung of the ladder represents the inclusion of a new variable that may be used to build DFAs [51, 52]. This might make it seem to provide a systematic way to improve DFAs, but all that is really guaranteed is that DFAs on higher rungs of the ladder will require greater computational resources. Nevertheless there is a tendency for functionals from higher rungs of the ladder to be more accurate than those from lower rungs of the ladder (see, e.g., Ref. [53]). Let us examine the rungs one by one with comments on what is currently available in DEMON2K.

Hartree

We have not even reached the first rung of the ladder! Hartree calculations may be carried out with DEMON2K using the keyword,

NONE No exchange-correlation functional is used.

This is primarily of theoretical interest.

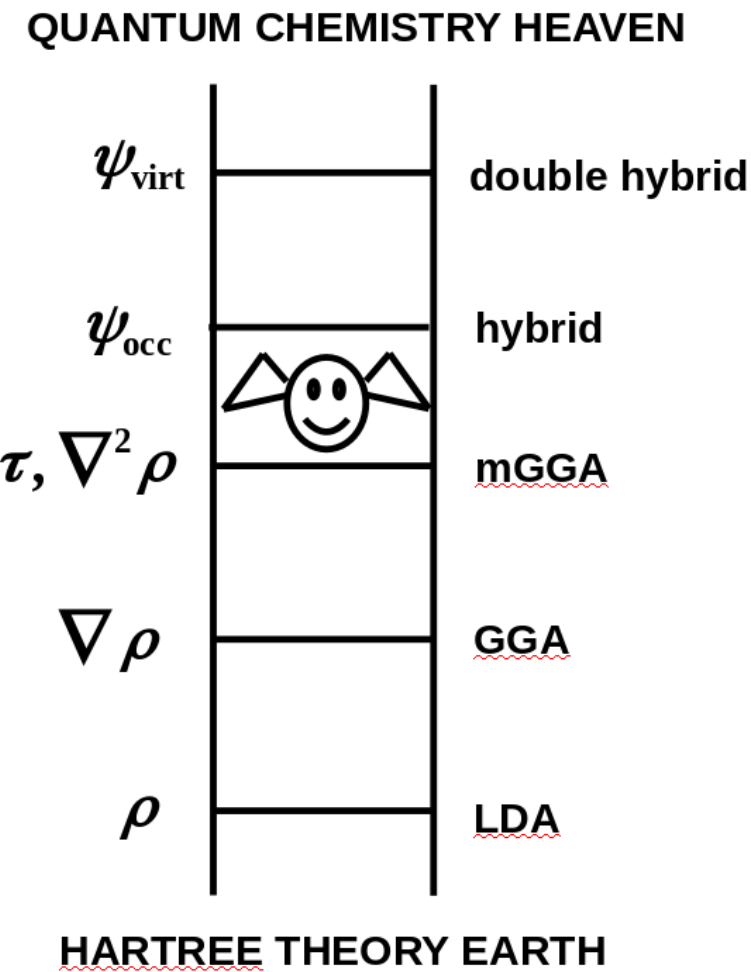


Figure 2.4: John Perdew's vision of a Jacob's ladder for DFAs. On the left of the ladder are the new variables which may be used to make functionals once that rung is reached. On the right is the name usually given to that level of approximation. In the middle is a user drawn as an angel in the spherical approximation. It is important that the user be able to climb the ladder towards more accurate calculations but also to be able to descend the ladder when less resource intensive calculations are adequate and needed for particular problems.

Local (Spin) Density Approximation (LDA)

“We do not expect an accurate description of chemical bonding.” — Kohn and Sham on the LDA [30]

As the quote indicates, when Kohn and Sham first proposed the LDA in their seminal paper, they did not expect it to work very well for molecules. In fact, molecular geometries are remarkably good at the LDA level in many cases but bond energies are typically overestimated.

The LDA assumes that the xc density $e_{xc}(\rho(\vec{r}))$ locally at each point \vec{r} is the same as the xc density in a homogeneous electron gas (HEG) of the same density $\rho(\vec{r})$. Neglecting spin we may write this as,

$$E_{xc}^{LDA}[\rho] = \int e_{xc}^{\text{HEG}}(\rho(\vec{r}))\rho(\vec{r}) d\vec{r}. \quad (2.57)$$

Implementing the LDA requires a calculation of the xc-energy density for the HEG. Only the exchange-part is known analytically. The correlation part and its spin-dependence need to be fit. Here is a list of LDA fittings implemented in DEMON2K:

VWN Dirac exchange with local VWN correlation [54, 55]

PZ81 Dirac exchange with local PZ81 correlation [54, 26]

PW92 Dirac exchange with local PW92 correlation [54, 56]

These should give very similar answers as they are all fits to accurate calculations of the properties of the HEG. *Warning:* GAUSSIAN’s VWN5 keyword is everyone else’s VWN.

An additional keyword

XALPHA X α calculation. The default α value is 0.75. A user defined α value can be selected with the X = <Real> option [45].

has been included. The X α method is a very old exchange-only method due to Slater which involves an empirical parameter chosen to fit Hartree-Fock energies. It is primarily only of historical interest.

Generalized Gradient Approximations (GGAs)

GGAs help to correct the overbinding problem of the LDA. Neglecting spin and focusing only on exchange, a typical GGA has the form,

$$E_{xc}^{GGA}[\rho] = \int \rho^{4/3}(\vec{r})F(x(\vec{r})) d\vec{r}, \quad (2.58)$$

where the enhancement factor $F(x)$ depends upon the reduced gradient,

$$x(\vec{r}) = \frac{|\nabla\rho(\vec{r})|}{\rho^{2/3}(\vec{r})}. \quad (2.59)$$

Many people think that GGAs are most sensitive to the electron density near the nucleus where the density varies the most quickly. However GGAs really depend upon the reduced gradient which only becomes large in the outer regions of the electron density where bonding is important. One consequence is that GGAs correct binding energies primarily by correcting atomic energies rather than by correcting molecular energies. Here is a list of GGAs implemented in DEMON2K:

PW86 GGA exchange [57, 58] with P86 GGA correlation [59, 60].

BLYP GGA [61] exchange with LYP GGA correlation [62, 63, 64]

OLYP HC01 GGA exchange [65] with LYP GGA correlation [63, 61, 64]

PW91 GGA exchange and correlation [66]

PW91SSF PW91 with full spin scaling function [66]

PBE GGA exchange and correlation [67, 68].

PBESSF PBE with full spin scaling function [67, 68].

PBESOL PBE GGA exchange and correlation for solids [69, 70].

KT1/2/3 KT1-3 GGA exchange and correlation for NMR shieldings [71, 72].

S011 GGA exchange and correlation [73].

N12 GGA exchange and correlation [74].

GAM GGA exchange and correlation [75].

CAP GGA exchange and correlation [76].

Meta GGAs (mGGAs)

The new functional dependence allowed with mGGAs is on the local kinetic energy density,

$$\tau(\vec{r}) = \sum_p n_p \psi_p(\vec{r}) \nabla^2 \psi_p(\vec{r}). \quad (2.60)$$

Note that there is some indication that this local kinetic energy density contains comparable information to the Laplacian of the charge density $\nabla^2 \rho(\vec{r})$ [77].

VS98 meta-GGA exchange and correlation [78, 79].

PKZB meta-GGA exchange and correlation [80, 81].

TPSS meta-GGA exchange and correlation [82, 83].

M06L meta-GGA exchange and correlation [84].

M11L meta-GGA exchange and correlation [85].

MN12 meta-GGA exchange and correlation [86].

Hybrid Functionals

“Obituary: Density-Functional Theory (1927-1993)”

— Peter Gill announcing the murder of pure DFT by hybrid functionals [87]

Hybrid functionals contain a portion of “Hartree-Fock” or “exact” exchange, where quotes have been used because the Hartree-Fock exchange integral is calculated using the DFT orbitals. These functionals were first proposed by Axel Becke [88] on the basis of adiabatic connection theory [89] in order to get closer to the thermodynamic limit of “chemical accuracy” — namely 1 kcal/mol (4.184 kJ/mol). Becke’s original idea was to retain the local xc potential using an OEP-like procedure. However, as this was never done, the orbital energies no longer have the same meaning as in the exact Kohn-Sham DFT and must be reclassified as *generalized* Kohn-Sham DFT [90].

FOCK Variational fitted Fock exchange (i.e., Hartree-Fock) [91].

B3LYP GGA hybrid exchange and correlation [92, 93].

BH&H Becke half-and-half GGA hybrid exchange and correlation [88].

PBE0 GGA hybrid exchange and correlation [94, 95].

M062X meta-GGA hybrid exchange and correlation [96].

M06HF meta-GGA hybrid exchange and correlation [96].

M06 meta-GGA hybrid exchange and correlation [96].

Fifth Rung DFAs

These are functionals which also depend upon the virtual (i.e., unoccupied) orbitals. They typically emerge in the form of DFT-based many-body perturbation theory (MBPT) and seem to depart from the basic hope of DFT that the hard work is done in designing the DFA but the computations are relatively simple. These belong to the most computationally-intensive rung of Jacob’s ladder. Time-dependent DFT (TD-DFT) is often formulated in a way that it uses virtual orbitals and so it could be considered to belong to the fifth rung of Jacob’s ladder. If we accept this, then it is the only member of the fifth rung that you will find in the version of DEMON2K that you are using here. Nevertheless there are private versions of DEMON2K that seem to building fifth rung approaches, so let us review a little about them here.

One of the earliest approaches is based upon the fluctuation-dissipation theorem which makes use of the generalized susceptibility,

$$\chi(\mathbf{1}, \mathbf{2}) = \frac{\delta\rho(\mathbf{1})}{\delta v_{\text{app}}(\mathbf{2})}, \quad (2.61)$$

where $\mathbf{i} = (i, t_i)$. This is available from TD-DFT. It may be used to calculate the correlation energy via the fluctuation-dissipation theorem,

$$E_{\text{corr}} = \frac{1}{2} \int_0^1 d\lambda \int \frac{i\chi_\lambda(\mathbf{1}, \mathbf{2}) - \chi_0(\mathbf{1}, \mathbf{2})}{r_{1,2}} d\mathbf{1}d\mathbf{2}. \quad (2.62)$$

This is actually a very old result (see. e.g., Ref. [97] p. 152). The parameter λ is a prefactor which “turns on” the electron repulsion in a sort of adiabatic connection between the noninteracting

system with generalized susceptibility χ_0 and the interacting system with generalized susceptibility χ_1 . Reference [98] provides one example of a fifth-rung functional derived from this approach.

Another approach, still maintaining the MBPT flavor of the fifth rung, is based upon mixing MP2 and DFT correlation to improve the correlation energy. These are the so-called double hybrids of which one example may be found in Ref. [99].

Is There a Best DFA?

So what functionals are best? Many functionals have been developed over the years, not infrequently with particular properties in mind. The result is such a zoo of functionals that it can be difficult for even the expert to know which functional to choose. In practice, some seem to work better for some molecules and some properties than do others. *What is a user to do?*

One approach is to go to a colleague and ask them. Or you can go to the literature and see what other people are using. Note that going to the literature or asking a colleague often both amount to asking which is the most *popular* functional, not necessarily which is the *best* functional. Marcel Swart runs a DFT Poll whose results you may find at

<https://www.marcelswart.eu/dft-poll/index.html>

This does not really tell you which is the best but it does tell you which functionals are the most popular among those who responded to the poll. I do not know to what extent we may call this science but it is amusing and it is useful to know what functionals are trending!

In the past decades, data bases have emerged containing reliable experimental or sometimes reliable *ab initio* properties for increasingly large sets of molecules. (See, e.g., Ref. [53].) These have been tremendously valuable for people who develop new functionals and it is tempting to judge the quality of a functional by how well it fares with these data sets. Certainly this has a more solid scientific basis than any popularity poll. However, you should be aware, that even the most extensive of these data bases still represents a limited class of molecules and properties. If your problem is outside of this well-studied zone, then you are on your own. This is why validating your functional is still necessary.

Here is some old fashioned, but I think still important advice:

Always validate your choice of functional for the problem you want to study!

That is, research problems usually involve specific properties of specific molecules which have (hopefully) not yet been studied (so that there is something new to learn!) Make sure that you have the best functional for your problem by choosing several functionals and applying them to a well-studied molecule with similar properties to the ones that interest you. In the best scenario, all the functionals will give similar results and so you can be reasonably confident that the choice of functional is not a critical issue for your problem. But it often happens that there are striking differences and that some functionals are better for making predictions for the class of molecules and properties which interest you.

2.2.4 Exercise

Copy the following input file and run DEMON2K for VSCTYPE VWN and for the other functionals mentioned above:

```
TITLE H functionals
MULTI 2
#
VXCTYPE VWN
#
PRINT MOS
#
# --- GEOMETRY ---
#
#
GEOMETRY CARTESIAN ANGSTROM
H      0.000000    0.000000    0.000000
#
AUXIS (GEN-A3*)
BASIS (LIC)
```

Note that calculations with mGGAs require the extra keyword BASIS. For example:

```
VXCTYPE VS98
```

to

```
VXCTYPE BASIS VS98
```

For each functional set note down:

1. The total energy in Ha (hartrees)
2. The spin α and spin β orbital energies

Discuss your results.

Chapter 3

H_2^+ and H_2 : Functionals, Potential Energy Curves, and Geometry Optimizations

3.1 Lesson 3: The Radical Dissociation Problem

*DFA*s typically do worst for small symmetric systems but often do very well for larger systems.

This is our first lesson dealing with a molecule—namely H_2^+ . It qualifies as one of the small symmetric systems that create problems for DFAs. In this case the problem is getting the correct dissociation behavior,



All of the fundamental (and deeply interrelated) reasons mentioned in Lesson 2 have been used to explain why DFAs struggle to describe Eq. (3.1) correctly: self-interaction error (SIE), delocalization error (DE), and the particle number derivative discontinuity (PNDD). Clearly these problems might also be expected to arise when a radical R^\bullet reacts with a neutral molecule M,



which is not that uncommon a process in chemistry.

3.1.1 LiH: Fractional Charge Problem (FCP)

Before proceeding further we should add one more problem which is closely related to the SIE, DE, and PNDD. I will call this the fractional charge problem (FCP). There is no particular relation with H_2^+ except that the FCP gives us an excuse to go more deeply into the PNDD which we will then use to help us understand the famous problem of incorrect long-distance behavior of the H_2^+ potential energy curve. Of course, users of DFT also need to be aware of the FCP for its own sake.

A particular case of the FCP, discussed in Ref. [38] is the charge transfer reaction between at “infinite” (i.e., very large but finite) separation,



Most chemists will recognize this as a spontaneous reaction. Here is some data to help us think:

$$\begin{aligned} \text{EA(Li)} &= \text{EA}(\text{Li}^-) = 0.0227 \text{ Ha} [100] \\ \text{EA(H)} &= \text{EA}(\text{H}^-) = 0.0277 \text{ Ha} [39] \\ \text{IP(H)} &= 0.5000 \text{ Ha} [\text{textbook result}] \\ \text{IP(Li)} &= 0.1981 \text{ Ha} [101] \\ \text{IP}(\text{Li}^+) &= 2.780 \text{ Ha} [102]. \end{aligned} \quad (3.4)$$

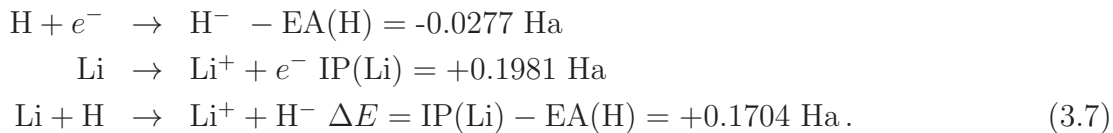
The Mulliken electronegativity of an atom A is,

$$\chi(A) = \frac{\text{IP}(A) + \text{EA}(A)}{2}, \quad (3.5)$$

so

$$\begin{aligned} \chi(\text{Li}) &= 0.1104 \text{ Ha} \\ \chi(\text{H}) &= 0.2638 \text{ Ha}, \end{aligned} \quad (3.6)$$

and H is more electronegative than Li. Hence we expect to see the transfer of an electron from Li to H. Nevertheless the reaction is endothermic at infinite separation



It only becomes energetically favorable (i.e., exothermic) at sufficiently small finite separation R because

$$\Delta E = \text{IP}(\text{Li}) - \text{EA}(\text{H}) - \frac{1}{R}. \quad (3.8)$$

In fact, $\Delta E < 0$ for $R < 5.869$ bohr = 3.106 Å. So this is actually the case where the two atoms should remain neutral when “well separated.” In the LDA, the electrons neither remain neutral nor transfer an electron. Instead, a fraction of an electron is transferred:

“For separated LiH the local density approximation’ displays no derivative discontinuity, and so it minimizes the energy incorrectly at the configuration $\text{Li}^{+0.25}\text{H}^{-0.25}$. The spin-restricted Hartree-Fock approximation leads to an even worse dissociation limit, $\text{Li}^{+0.45}\text{H}^{-0.45}$.¹

— Ref. [38]

How can this be and what (if anything) does it have to do with the properties of the exact functional? Remember that the exact functional (DFT) is the target at which we should aim when constructing density functional approximations (DFAs)!

Let us consider the system when charge is transferred: $\text{Li}^+ + \text{H}^-$. In Lesson 2, we learned that minus the HOMO energy in exact DFT is the IP of the system. But what is the IP for $\text{Li}^+ + \text{H}^-$? Well, the $\text{IP}(\text{Li}^+) = 2.780$ Ha [102] and $\text{IP}(\text{H}^-) = 0.0277$ Ha, so neither can be $\text{IP}(\text{Li}^+ + \text{H}^-)$. The only way out of this dilemma is to shift one of the atomic potential energy curves relative to the other as shown schematically in Fig. 3.1. But wait! There is a discontinuity in the figure at $x = 50$ bohr. How can this be? If this is a region with no charge density, then Kohn-Sham theory can actually tell us nothing about this region. However what if the charge density is small but not zero? There

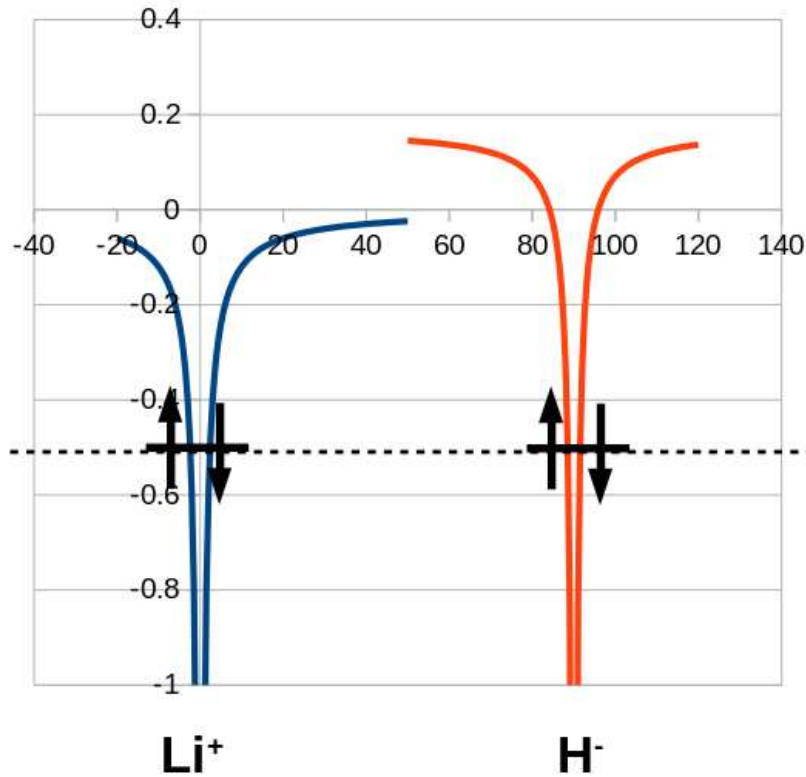


Figure 3.1: Guesstimated cartoon of the exact DFT potentials for well-separated Li^+ and H^- . (Energy units are Ha and distance units are bohr, but this picture needs to be taken with a large grain of salt!)

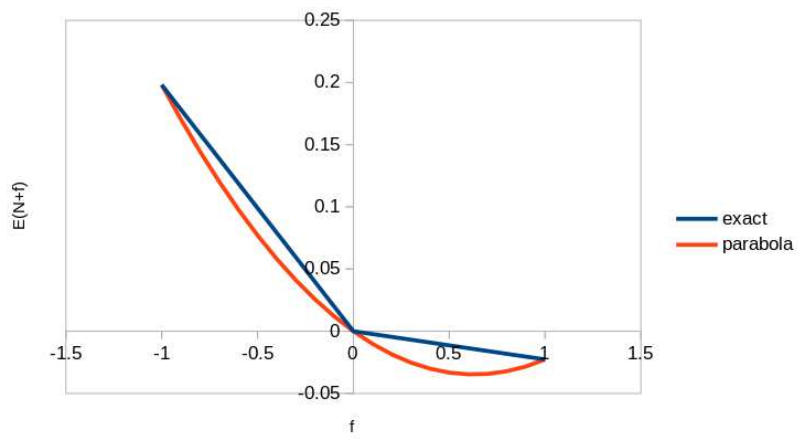


Figure 3.2: Exact and parabolic estimate (DFA) energy curves for the lithium atom (where the energy zero has been chosen as the total energy of the neutral atom.)

is active research in this area (e.g., Ref. [103]) and the answer seems to be that the potential forms a sort of δ -function-like barrier separating the two atoms.

Of course, DFAs do not have any such strange discontinuities. Figure 3.2 shows the exact

$$E(N + f) = [fE(N + 1) + (1 - f)E(N)] \theta(f) + ((1 + f)E(N) - fE(N - 1)) \theta(-f), \quad (3.9)$$

where

$$\theta(x) = \begin{cases} 1 & ; \quad x > 0 \\ 0 & ; \quad x < 0 \end{cases} \quad (3.10)$$

is the usual Heaviside function. In contrast DFAs will be smoother and may be approximated by a parabola to a first approximation,

$$\begin{aligned} E(N + f) &= af^2 + bf + c \\ a &= \frac{\text{IP} - \text{EA}}{2} \\ b &= -\frac{\text{IP} + \text{EA}}{2} \\ c &= E(N) \\ \text{IP} &= E(N - 1) - E(N) \\ \text{EA} &= E(N) - E(N + 1). \end{aligned} \quad (3.11)$$

Interestingly, Slater's transition orbital approximation is exact in this approximation,

$$\begin{aligned} \epsilon_H(N - \frac{1}{2}) &= -\text{IP} \\ \epsilon_H(N + \frac{1}{2}) &= -\text{EA}. \end{aligned} \quad (3.12)$$

More generally, by Janak's theorem,

$$\epsilon_H(N + f) = 2af + b = (\text{IP} - \text{EA})f - \frac{\text{IP} + \text{EA}}{2}. \quad (3.13)$$

We may now estimate the amount of charge transferred from Li to H when a DFA is used because a fraction f of an electron should be transferred until the HOMO energy is the same for Li^{+f} and for H^{-f} . From Eq. (3.13),

$$\begin{aligned} \epsilon_H(\text{Li}^{+f}) &= \epsilon_H(\text{H}^{-f}) \\ (\text{IP(Li)} - \text{EA(Li)}) (-f) - \frac{\text{IP(Li)} + \text{EA(Li)}}{2} &= (\text{IP(H)} - \text{EA(H)}) f - \frac{\text{IP(H)} + \text{EA(H)}}{2}. \end{aligned} \quad (3.14)$$

Solving gives,

$$\begin{aligned} f &= \frac{1}{2} \frac{(\text{IP(H)} - \text{IP(Li)}) + (\text{EA(H)} - \text{EA(Li)})}{(\text{IP(H)} - \text{IP(Li)}) - (\text{EA(H)} - \text{EA(Li)})} \\ &= \frac{1}{2} \frac{(0.5 \text{ Ha} - 0.1981 \text{ Ha}) + (0.0277 \text{ Ha} - 0.0227 \text{ Ha})}{(0.5 \text{ Ha} - 0.1981 \text{ Ha}) - (0.0277 \text{ Ha} - 0.0227 \text{ Ha})} \\ &= 0.5168. \end{aligned} \quad (3.15)$$

So the prediction is for $\text{Li}^{+0.5}\text{H}^{-0.5}$. Although this is not in quantitative agreement with the result reported in Ref. [38], it does indeed show why we expect only a fraction of the charge of an electron to be transferred.

3.1.2 Back to H_2^+ : What Should We Expect?

The hydrogen molecule cation, H_2^+ , has been called the “simplest molecule” because it has only two atoms (for which $Z = 1$) and only one electron. This is also our first chance to focus on “chemistry” in the sense of reactivity as H_2^+ dissociates into H^+ and a neutral radical H^\bullet ,



With the usual energy zero (corresponding to infinitely separated electrons and nuclei), the energy of completely dissociated H_2^+ is just the energy of the neutral radical, which is exactly -0.5 Ha. As we are also interested in the reaction path we can calculate the potential energy curve (PEC) as a function of the internuclear distance R . Let us ask first about the applicability of exact DFT to this system and then about the consequences of using a DFA without a PNDD. We will see that the lack of a proper treatment of the PNDD leads to an incorrect dissociation behavior.

Let us first consider the applicability of exact DFT. This is a question of non-interacting v -representability. Can we find a system of non-interacting electrons whose ground state gives the same charge density as the ground state of H_2^+ ? If so, can we calculate it? As H_2^+ is a very simple system, there is a trivial answer. The Kohn-Sham wave function ψ that solves

$$(\hat{t} + v) \psi(\vec{r}) = \epsilon \psi(\vec{r}) \quad (3.17)$$

is the given by the square root of the density,

$$\psi(\vec{r}) = \sqrt{\rho(\vec{r})} . \quad (3.18)$$

Note that this wave function has no nodes so we do not have to worry about the possibility of phase changes. The Kohn-Sham potential is then

$$v(\vec{r}) = \epsilon - \frac{\hat{t}\psi(\vec{r})}{\psi(\vec{r})} , \quad (3.19)$$

where \hat{t} is the kinetic energy operator. If all is done correctly, then, according to what we know about the HOMO energy in exact DFT, the eigenvalue $\epsilon = -0.5$ Ha will lead to $v(\vec{r})$ in the limit of large distances from the molecule. So this system is indeed noninteracting v -representable and this is true for all internuclear distances R . (Caveat: When R is very large, the density between the two nuclei is effectively zero. This creates a computational difficulty but not a conceptual one as the density is formally always nonzero at this point.)

In order to actually do this calculation, we would need an accurate solution of the Schrödinger equation for H_2^+ . We will not need this for this lesson, but we will need a PEC. If we are not very demanding, then calculating an approximate PEC only requires writing about a program about a dozen lines long [107]. However the H_2^+ Born-Oppenheimer problem is separable in elliptical coordinates and the remaining one-dimensional problem may be solved exactly using numerical integration. So an accurate PEC has long been known for H_2^+ . We will also need accurate PECs for H_2^{2+} and for H_2 . Sharp’s review in *Atomic Data* [108] provides an excellent overview of the various ground and excited-state potential energy surfaces of these molecules. Figures 2 and 3 of that paper show very nice plots of potential energy curves. Accurate results are tabulated in Table 3.1. The numbers in this table are *not* taken from the plots in Sharp’s review. Instead, the values for the H_2 potential energy curve in this table were taken from the very accurate Born-Oppenheimer calculations of Kolos and Roothaan using the Hylleraas method (Table IV of Ref. [106].) Also given are spin-restricted

Table 3.1: Collected ground state potential energy curves for H_2^{2+} , H_2^+ , and H_2 . See text. All values are in atomic units (distances are bohr and energies are Ha.)

R (bohr)	Energy (Ha)			
	H_2^{2+}	H_2^+ [104, 105]	H_2 [106]	RHF H_2
0.8	+1.2500000	-0.1090030	-1.020175	-0.9807128
0.9	+1.1111111	-0.2805032	-1.083651	-1.0443116
1.0	+1.0000000	-0.4034420	-1.124517	-1.0851144
1.1	+0.9090909	-0.4926148	-1.150043	-1.1104338
1.2	+0.8333333	-0.5576986	-1.164930	-1.1250078
1.3	+0.7692308	-0.6052379	-1.172323	-1.1723230
1.35	+0.7407407	-0.6239064	-1.173934	-1.1333790
1.39	+0.7194245	-0.6368097	-1.174420	-1.1336510
1.40	+0.7242857	-0.6397790	-1.174442	-1.1336167
1.41	+0.7092199	-0.6426514	-1.174428	-1.1335442
1.45	+0.6896552	-0.6532229	-1.174022	-1.1328956
1.5	+0.6666667	-0.6645509	-1.172828	-1.1313624
1.6	+0.6250000	-0.6818903	-1.168538	-1.1263398
1.8	+0.5555556	-0.7007217	-1.154985	-1.1109541
2.0	+0.5000000	-0.7055500	-1.137999	-1.0916189
2.2	+0.4545455	-0.7018677	-1.119920	-1.0706422
2.4	+0.4166667	-0.6931046	-1.102084	-1.0493324
2.6	+0.3846154	-0.6814745	-1.085288	-1.0284347
2.8	+0.3571429	-0.6684156	-1.069956	-1.0083673
3.0	+0.3333333	-0.6548443	-1.056297	-0.9893529
3.2	+0.3125000	-0.6413228	-1.044395	-0.9714956
3.6	+0.2777778	-0.6156030	-1.025663	-0.9393347
3.8	+0.2631579	-0.6036960	-1.018506	-0.9249804
4.0	+0.2500000	-0.5925234	-1.007867	-0.9117103
4.2	+0.2380952	-0.5821281	-1.007867	-0.8994630
5.0	+0.2000000	-0.5486641		-0.8593936
6.0	+0.1666667	-0.5234549		-0.8248475
7.0	+0.1428571	-0.5108372		-0.8019376
8.0	+0.1250000	-0.5049567		-0.7864752
9.0	+0.1111111	-0.5023036		-0.7757476
10.0	+0.1000000	-0.5011162		-0.7680437
11.0	+0.0909091	-0.5005781		-0.7623010
12.0	+0.0833333	-0.5003261		-0.7578581
13.0	+0.0769231	-0.5002012		-0.7542987
14.0	+0.0714286	-0.5001346		-0.7513597
15.0	+0.0666667	-0.5000959		-0.7488739
16.0	+0.0625000	-0.5000715		-0.7467320
17.0	+0.0588235	-0.5000551		-0.7448601
18.0	+0.0555556	-0.5000434		-0.7432062
19.0	+0.0526316	-0.5000348		-0.7417322
20.0	+0.0500000	-0.5000283		-0.7404090
21.0	+0.0476190	-0.5000232		-0.7392138
22.0	+0.0454545	-0.5000193		-0.7381278
23.0	+0.0434783	-0.5000161		-0.7371383
24.0	+0.0416667	-0.5000136		-0.7362312

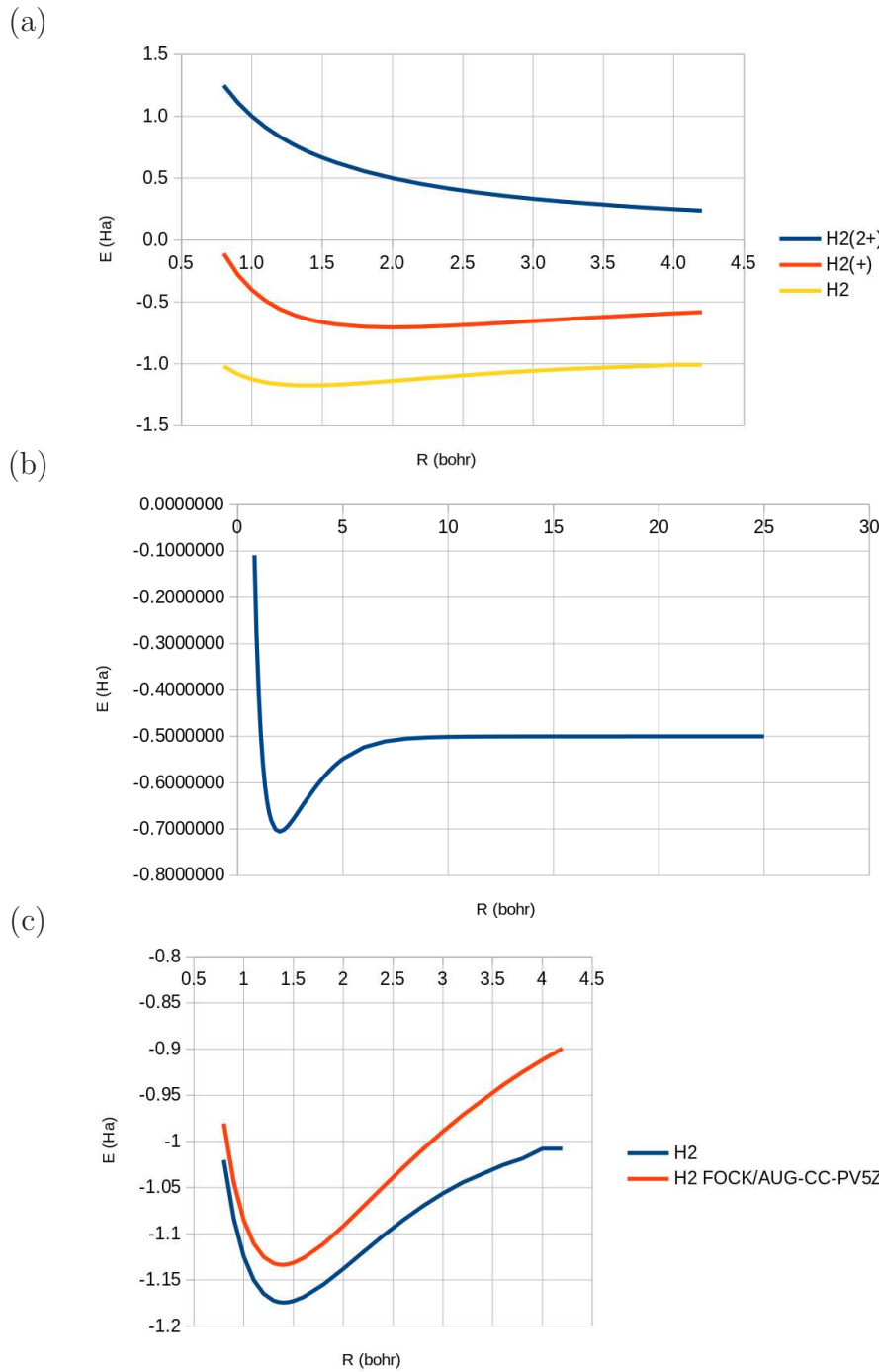


Figure 3.3: Potential energy curves for H_2^{2+} [$H_2(2^+)$], H_2^+ [$H_2(+)$], and for H_2 [H_2], plotted using the data in Table 3.1: (a) H_2^{2+} , H_2^+ , and H_2 ; (b) H_2^+ ; and (c) H_2 and RHF H_2 .

$$\epsilon_L = \epsilon_L^0 + 2[\rho_H || \rho_L] - [HL || LH]$$

$$\epsilon_H = \epsilon_H^0 + [\rho_H || \rho_H]$$

$$E = 2\epsilon_H^0 + [\rho_H || \rho_H] + 1/R = 2\epsilon_H - [\rho_H || \rho_H] + 1/R$$

Figure 3.4: Hartree-Fock formulae for a two-orbital two-electron model (TOTEM): $\epsilon_{H(L)}$, HOMO (LUMO) orbital energy including electron-electron repulsions; $\epsilon_{H(L)}^0$, HOMO (LUMO) orbital energy excluding electron-electron repulsions; $[\rho_H || \rho_H]$, Coulomb repulsion integral; $[HL || LH]$, exchange integral (included for completeness but not needed in this lesson); and total energy E including the repulsion $1/R$ between the nuclei separated by a distance R .

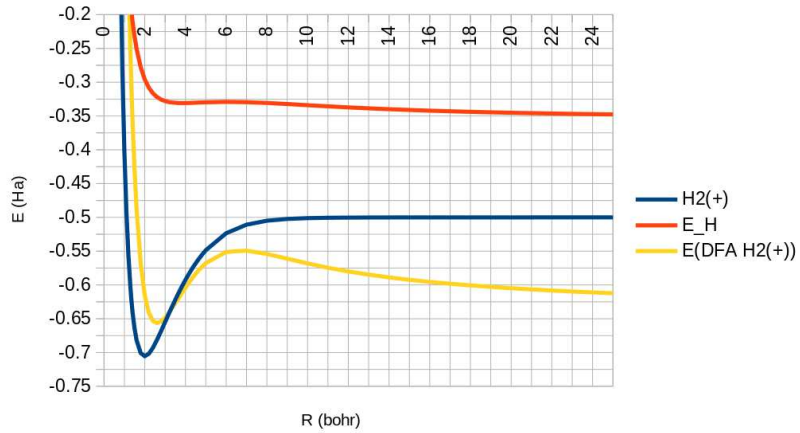


Figure 3.5: Potential energy curves for H_2^+ : exact, blue line; estimated DFA orbital energy [Eq. (3.20)], red line; estimated DFA potential energy curve [Eq. (3.25)], yellow line.

Hartree-Fock (RHF) results for H_2 calculated at the FOCK/AUG-CC-PV5Z level. The H_2^+ potential energy curve values in this table are calculated using the Padé approximant fits of Ref. [104, 105]. Finally, note that the potential energy curve for H_2^{2+} is just $V(R) = 1/R$.

Plots of the PECs for H_2^{2+} , H_2^+ , and H_2 are shown in Fig. 3.3. The H_2^{2+} curve is repulsive with a large R limit of $V = 0$. The H_2^+ has the shape of a generic PEC with a hard wall at small R , a minimum at the equilibrium bond distance, and goes to $V = -0.5$ Ha in the large R limit. The exact PEC for H_2 also has the shape of a generic PEC but goes to $V = -0.5$ Ha at large R . The RHF H_2 curve is qualitatively similar but dissociates to $V \approx -0.735$ Ha for reasons which will become clear in Lesson 4.

Let us now turn to the problem of what we expect when using a DFA with no PNDD. This problem will be approached by constructing a Hartree-Fock curve using classic Hartree-Fock formulae (Fig. 3.4) but *changing the value of the occupied orbital energy to reflect the behavior of a DFA without PNDD*. This will be referred to as our DFA model.

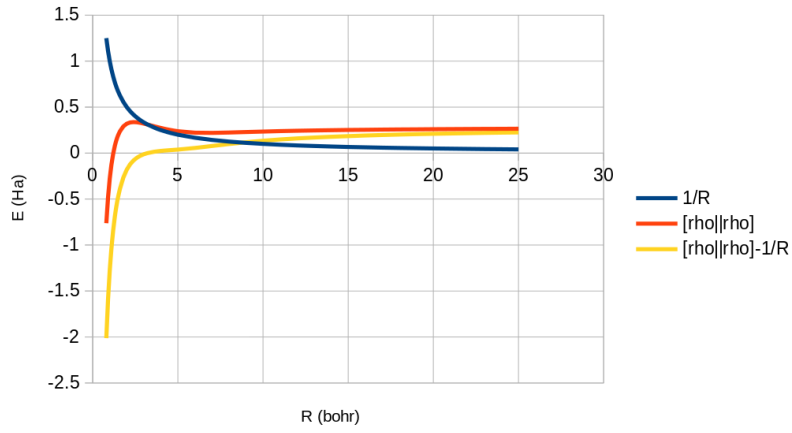


Figure 3.6: Variation of the term $[\rho||\rho] - 1/R$ as a function of R .

For our DFA model we have already established that,

$$\epsilon_H(H_2^{2+}) \approx -\frac{IP(H_2^{2+}) + EA(H_2^{2+})}{2} = \frac{E(H_2) - E(H_2^{2+})}{2}. \quad (3.20)$$

This gives us the red line shown in Fig. 3.5. Beyond $R = 3.5$ bohr it is very flat and slowly varying. We may estimate the limiting value at large R by using the Hartree-Fock model:

$$\begin{aligned} E(H_2) &= 2\epsilon_H^0 + [\rho||\rho] \\ E(H_2^{2+}) &= \frac{1}{R} \\ \epsilon_H(H_2^{2+}) &\approx \epsilon_H^0 + \frac{([\rho||\rho] - 1/R)}{2}, \end{aligned} \quad (3.21)$$

where $\epsilon_H^0 = -0.5$ Ha is the bare orbital energy and $[\rho||\rho]$ is the Coulomb repulsion integral of the σ bonding orbital with itself. Note that the second term on the last line of Eq. (3.21) gives us an explicit expression for the self-interaction error (SIE) in the orbital energy. In order to evaluate this SIE, we must estimate the $[\rho||\rho]$ integral which we may do using the formula,

$$[\rho||\rho] = E(H_2) - 2E(H_2^+), \quad (3.22)$$

and the RHF H_2 and H_2^+ PECs. Figure 3.6 shows how this integral varies with R . In order to estimate the large R limit, we need to realize that

$$\rho = \left[\frac{1}{\sqrt{2}} (s_A + s_B) \right]^2. \quad (3.23)$$

This gives that the large R limit is

$$[\rho||\rho] = \frac{1}{2}[(s_A)^2||(s_A)^2] \approx -\frac{1}{2} [\epsilon_H(H) + EA(H)] = \frac{0.5 \text{ Ha} - 0.0277 \text{ Ha}}{2} = 0.236 \text{ Ha}, \quad (3.24)$$

in good agreement with Fig. 3.6.

In order to obtain an estimate of the DFA total energy we may continue to use the Hartree-Fock theory as a model for estimating terms. The total DFA energy is thus,

$$\begin{aligned} E(\text{DFA } H_2^+) &= \epsilon_H(H_2^+) - [\rho||\rho] \\ &= \epsilon_H^0(H_2^+) + \frac{([\rho||\rho] - 1/R)}{2} - [\rho||\rho] \\ &= \epsilon_H^0(H_2^+) - \frac{([\rho||\rho] + 1/R)}{2}. \end{aligned} \quad (3.25)$$

The second term in the last line is the SIE in the energy. Equation (3.25) gives the yellow curve in Fig. 3.5 which is in curiously good agreement with, for example, Fig. 1 in Ref. [29]. In particular we see that the DFA H_2^+ energy should go through a maximum around 7 bohr (3.7 Å). According to Eq. (3.25) should be $-0.5 \text{ Ha} - (0.236 \text{ Ha}/2) = -0.618 \text{ Ha}$, in good agreement with the yellow curve in Fig. 3.5. We have seen how the predicted curious shape of the DFA H_2^+ comes from the lack of a PNDD. Other explanations given in the literature associate the shape with a delocalization error [29] or a self-interaction error [109]. We have tried to show that these are not really independent explanations but rather all closely interrelated failures of DFAs.

3.1.3 Exercise

Compute the total energy and occupied orbital energies with different functionals and the AUG-CC-PV5Z orbital basis set for the bond lengths given in Table 3.1 and plot the values along with the accurate PEC of H_2^+ whose data points are given in the table. Also shift the calculated PECs with different functionals to have the same minimum energy as does the accurate PEC in order to be able to better compare the shape of the PEC curves near the equilibrium geometry. As this requires quite a number of calculations for each value of R we will limit the number of functionals by choosing one functional from each rung of Jacob's ladder:

FOCK Hartree-Fock model, the exact answer in this case

NONE Hartree model

VWN LDA

BLYP GGA

B3LYP hybrid

Here is an input file with a recommended basis that you can modify and run Copy the following input file and run DEMON2K for VSCTYPE VWN and for the other functionals mentioned above:

```
TITLE H2(+)
MULTI 2
CHARGE 1
#
VXCTYPE VWN
#
PRINT MOS
#
# --- GEOMETRY ---
```

```

#
#
GEOMETRY CARTESIAN BOHR
H      0.000000    0.000000    0.000000
H      0.000000    0.000000    1.400000
#
AUXIS (GEN-A3*)
BASIS (AUG-CC-PV5Z)

```

Remember to always check that your calculations are converged. Some of your calculations will require tricks to make them converge. DEMON2K offers a variety of tricks such as DIIS, MIXING, LEVEL SHIFT, and SMEAR. Experiment to see what seems to work best for this problem! Also remember that

“It is never enough to just calculate; you must also analyse and discuss your results.” — paraphrasing from memory some remarks made by Roald Hoffmann about his approach to quantum chemistry

3.2 Lesson 4: Treating Multideterminantal Problems by Symmetry-Breaking

The Boyg told Peer Gynt to “*Go round*” in Henrik Ibsen’s play *Peer Gynt*

In this lesson we confront another one of the fundamental difficulties of DFT. As the only wave function in DFT is that of the fictitious system of noninteracting electrons, it must be a single determinant unless the ground state of the fictitious system happens to be degenerate. But, while single determinantal wave functions are reasonable first approximations to the wave function of closed-shell molecules at their equilibrium geometry, single-determinantal wave functions are often inappropriate for describing open-shell systems or the making and breaking of bonds in a closed-shell system. Nevertheless DFAs can do surprisingly well here provided we have a good understanding of the multideterminantal problem. In particular, we will see that DFAs do much better for describing the potential energy curve of H_2 than for describing the potential energy curve of H_2^+ provided we find an appropriate way to *go round* the multideterminantal problem (i.e., symmetry breaking.) Even here, as we shall see, there will be a price to pay for the trick we play.

Our focus here is on wave functions. Energy will be treated more qualitatively, until (of course) we get to the calculations. In principle, the theory in this lesson is a standard part of basic physical chemistry courses. However I have noticed that it tends more and more to be neglected or forgotten. This is a shame because we are here at the heart of chemistry—namely the making and breaking of chemical bonds.

3.2.1 Preliminaries

Consider an (x, y, z) -coordinate system and place the H_2 molecule along the z -axis with the origin at the center point between the two atoms. Then the (x, y) -plane forms a symmetry plane which exchanges the two atoms, which will be distinguished by the letters A and B. (See Fig. 3.7.) Also any wave functions that we will construct will be either even (g for the German *gerade*) or odd (u for the German *ungerade*) with respect to reflection through that symmetry plane. This gives us a very simple character table which will be quite adequate for our purposes:

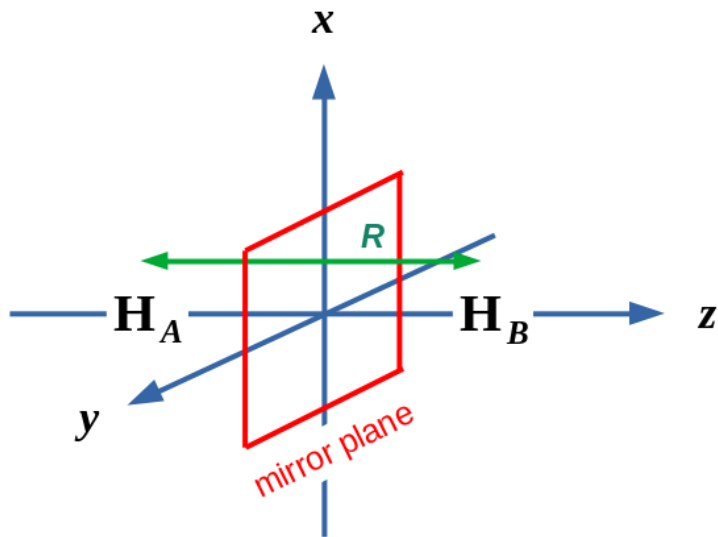


Figure 3.7: “Quantum chemistry” coordinate system chosen for studying H_2 .

	E	$\sigma_{(x,y)}$
g	1	1
u	1	-1

Here E is the identity symmetry operation which does nothing, while $\sigma_{(x,y)}$ is the symmetry operation corresponding to reflection in the (x, y) mirror plane ($H_A \leftrightarrow H_B$).

We will also make the usual LCAO approximation which says that we will take (as a first approximation) our molecular orbitals (MOs) to be linear combinations of the (valence) atomic orbitals (AOs), namely s_A on hydrogen atom A and s_B on hydrogen atom B. These MOs will be of σ type because they are cylindrically symmetric with respect to rotation around the internuclear axis. Including mirror symmetry we get the two MOs,

$$\begin{aligned}\sigma_g &= \frac{1}{\sqrt{2(1+S)}}(s_A + s_B) \\ \sigma_u &= \frac{1}{\sqrt{2(1-S)}}(s_A - s_B),\end{aligned}\tag{3.26}$$

where

$$\begin{aligned}\langle s_A | s_A \rangle &= \langle s_B | s_B \rangle = 1 \\ \langle s_A | s_B \rangle &= \langle s_B | s_A \rangle = S.\end{aligned}\tag{3.27}$$

The wave functions given by Eq. (3.26) are orthonormal:

$$\begin{aligned}\langle \sigma_g | \sigma_g \rangle &= \langle \sigma_u | \sigma_u \rangle = 1 \\ \langle \sigma_g | \sigma_u \rangle &= \langle \sigma_u | \sigma_g \rangle = 0,\end{aligned}\tag{3.28}$$

where normality follows directly from symmetry. Most chemistry students will know σ_g as the σ bonding MO while σ_u is the σ^* antibonding MO. The quantity $S = S(R)$ is the overlap integral and goes to zero in the limit of large internuclear separation, $R \rightarrow \infty$.

As we have a two-electron system, we must also build a basis of antisymmetric two-electron wave functions:

$$\begin{array}{ccccccc} \sigma_u & [\ ,\] & [\uparrow,\] & [\ ,\downarrow] & [\uparrow,\] & [\ ,\downarrow] & [\uparrow,\downarrow] \\ \sigma_g & [\uparrow,\downarrow] & [\ ,\downarrow] & [\uparrow,\] & [\uparrow,\] & [\ ,\downarrow] & [\ ,\] \\ |\sigma_g, \bar{\sigma}_g| & |\sigma_u, \bar{\sigma}_g| & |\sigma_g, \bar{\sigma}_u| & |\sigma_g, \sigma_u| & |\bar{\sigma}_g, \bar{\sigma}_u| & |\sigma_u, \bar{\sigma}_u| \end{array}$$

Here the overbar signifies $\beta = \downarrow$ spin while the absence of an overbar signifies $\alpha = \uparrow$. For example, the Slater determinant,

$$\begin{aligned} |\sigma_u, \bar{\sigma}_g| &= \frac{1}{\sqrt{2}} (\sigma_u(1)\alpha(1)\sigma_g(2)\beta(2) - \sigma_g(1)\beta(1)\sigma_u(2)\alpha(2)) \\ &= \frac{1}{\sqrt{2}} \det \begin{vmatrix} \sigma_u(1)\alpha(1) & \sigma_g(1)\beta(1) \\ \sigma_u(2)\alpha(2) & \sigma_g(2)\beta(2) \end{vmatrix} \end{aligned} \quad (3.29)$$

As we will be using the algebraic properties of Slater determinants quite a bit, let us note the following two properties for generic orbitals ϕ , φ , and ψ :

$$\begin{aligned} |\phi, \psi| &= -|\psi, \phi| \\ |a\phi + b\varphi, \psi| &= a|\phi, \psi| + b|\varphi, \psi|. \end{aligned} \quad (3.30)$$

All of the determinants that we have constructed out of σ_g and σ_u orbitals have Σ symmetry. (Note the well-established spectroscopic convention that many-electron quantities are designated by capital letters with lower-case letters being reserved for orbital quantities.) These determinants may also be divided according to their mirror symmetry and assigned as either *gerade* or *ungerade*. Hence,

$$\begin{aligned} |\sigma_g, \bar{\sigma}_g| &\text{ is } {}^{(1,0)}\Sigma_g = {}^1\Sigma_g(M_S = 0) \\ |\sigma_u, \bar{\sigma}_g| &\text{ is } {}^{(?,0)}\Sigma_u = {}^?\Sigma_u(M_S = 0) \\ |\sigma_g, \bar{\sigma}_u| &\text{ is } {}^{(?,0)}\Sigma_u = {}^?\Sigma_u(M_S = 0) \\ |\sigma_g, \sigma_u| &\text{ is } {}^{(3,1)}\Sigma_u = {}^3\Sigma_u(M_S = 1) \\ |\bar{\sigma}_g, \bar{\sigma}_u| &\text{ is } {}^{(3,-1)}\Sigma_u = {}^3\Sigma_u(M_S = -1) \\ |\sigma_u, \bar{\sigma}_u| &\text{ is } {}^{(1,0)}\Sigma_g = {}^1\Sigma_g(M_S = 0), \end{aligned} \quad (3.31)$$

because, for example,

$$\begin{aligned} \hat{E}|\sigma_u, \bar{\sigma}_g| &= |\sigma_u, \bar{\sigma}_g| \\ \hat{\sigma}_{(x,y)}|\sigma_u, \bar{\sigma}_g| &= |-\sigma_u, \bar{\sigma}_g| = -|\sigma_u, \bar{\sigma}_g|. \end{aligned} \quad (3.32)$$

Notice that I have also added the \hat{S}_z quantum number M_S which, in the case of single determinants is just the sum of the values of $m_S = \pm 1/2$ of the orbitals making up the determinant. In particular,

$$M_S = \frac{n_\uparrow - n_\downarrow}{2}, \quad (3.33)$$

where $n_{\uparrow(\downarrow)}$ denotes the number of spin $\uparrow(\downarrow)$ electrons in the determinant. It would also be desirable to assign the total spin quantum number S , but not all of the determinants are eigenfunctions of \hat{S} . When they are, the corresponding eigenvalue is $S(S+1)$ and the spin multiplicity is $2S+1$. In most of the cases, the value of the spin multiplicity is sufficiently obvious that I have included it as a pre-exponent ${}^{2S+1}\Sigma = {}^1\Sigma$ or ${}^3\Sigma$. However two of the determinants have neither singlet nor triplet symmetry. This is sorted out in the next subsection.

3.2.2 Excited States

Two-electron wave functions have the nice property that they always factor into a spatial times a spin part. We may use this property to discover how to make the missing singlet and triplet wave functions. However this will be followed by a more formal discussion of spin symmetry for many-electron systems using second quantization.

Let us begin by factoring the two $(^{1,0})\Sigma_g$ wave functions:

$$\begin{aligned} |\sigma_g, \bar{\sigma}_g| &= \frac{1}{\sqrt{2}} (\sigma_g(1)\alpha(1)\sigma_g(2)\beta(2) - \sigma_g(1)\beta(1)\sigma_g(2)\alpha(2)) \\ &= (\sigma_g(1)\sigma_g(2)) \left[\frac{1}{\sqrt{2}} (\alpha(1)\beta(2) - \beta(1)\alpha(2)) \right] \\ |\sigma_u, \bar{\sigma}_u| &= \frac{1}{\sqrt{2}} (\sigma_u(1)\alpha(1)\sigma_u(2)\beta(2) - \sigma_u(1)\beta(1)\sigma_u(2)\alpha(2)) \\ &= (\sigma_u(1)\sigma_u(2)) \left[\frac{1}{\sqrt{2}} (\alpha(1)\beta(2) - \beta(1)\alpha(2)) \right]. \end{aligned} \quad (3.34)$$

Notice how each wave function is expressed as the product of a spatial part (namely $\sigma_g(1)\sigma_g(2)$ or $\sigma_u(1)\sigma_u(2)$) and a spin part [namely $(1/\sqrt{2})(\alpha(1)\beta(2) - \beta(1)\alpha(2))$]. As the total wave function must be antisymmetric, exactly one (not both) of the two parts must be antisymmetric while the other is symmetric. In the case of singlet wave functions, the spatial part is symmetric and the spin part is antisymmetric. Also spin does not normally appear in most quantum chemistry model hamiltonians, so that the total energy is determined purely by the spatial part. This is why early molecular orbital (MO) theory just wrote the wave function as $\sigma_g(1)\sigma_g(2)$ (see, e.g., Ref. [110] pp. 687-688.) This is a good first approximation to the H_2 wave function near the equilibrium geometry, but (as we shall see) does not describe bond breaking very well.

It is also easy to factor the wave functions for the $(^{3,\pm 1})\Sigma_u$ states:

$$\begin{aligned} |\sigma_g, \sigma_u| &= \frac{1}{\sqrt{2}} (\sigma_g(1)\alpha(1)\sigma_u(2)\alpha(2) - \sigma_u(1)\alpha(1)\sigma_g(2)\alpha(2)) \\ &= \left[\frac{1}{\sqrt{2}} (\sigma_g(1)\sigma_u(2) - \sigma_u(1)\sigma_g(2)) \right] (\alpha(1)\alpha(2)) \\ |\bar{\sigma}_g, \bar{\sigma}_u| &= \frac{1}{\sqrt{2}} (\sigma_g(1)\beta(1)\sigma_u(2)\beta(2) - \sigma_u(1)\beta(1)\sigma_g(2)\beta(2)) \\ &= \left[\frac{1}{\sqrt{2}} (\sigma_g(1)\sigma_u(2) - \sigma_u(1)\sigma_g(2)) \right] (\beta(1)\beta(2)). \end{aligned} \quad (3.35)$$

This time it is the spatial part which is antisymmetric while the spin part is symmetric.

The reader is invited to try to factor the two mixed-symmetry wave functions $|\sigma_u, \bar{\sigma}_g|$ and $|\bar{\sigma}_g, \bar{\sigma}_u|$ into the product of a spatial and a spin part. It simply cannot be done! Instead we need to take the plus and minus combinations of the two mixed-symmetry wave functions in order to obtain symmetry-pure wave functions:

$$\begin{aligned} \frac{1}{\sqrt{2}} (|\sigma_u, \bar{\sigma}_g| \pm |\bar{\sigma}_g, \bar{\sigma}_u|) &= \frac{1}{2} (\sigma_u(1)\alpha(1)\sigma_g(2)\beta(2) - \sigma_g(1)\beta(1)\sigma_u(2)\alpha(2)) \\ &\quad \pm (\sigma_g(1)\alpha(1)\sigma_u(2)\beta(2) - \sigma_u(1)\beta(1)\sigma_g(2)\alpha(2)) \\ &= \left[\frac{1}{\sqrt{2}} (\sigma_u(1)\sigma_g(2) \pm \sigma_g(1)\sigma_u(2)) \right] \\ &\quad \times \left[\frac{1}{\sqrt{2}} (\alpha(1)\beta(2) \mp \beta(1)\alpha(2)) \right]. \end{aligned} \quad (3.36)$$

This gives us a $(^{1,0})\Sigma_u$ wave function,

$$\begin{aligned} \frac{1}{\sqrt{2}} (|\sigma_u, \bar{\sigma}_g| + |\sigma_g, \bar{\sigma}_u|) &= \left[\frac{1}{\sqrt{2}} (\sigma_u(1)\sigma_g(2) + \sigma_g(1)\sigma_u(2)) \right] \\ &\times \left[\frac{1}{\sqrt{2}} (\alpha(1)\beta(2) - \beta(1)\alpha(2)) \right], \end{aligned} \quad (3.37)$$

and a $(^{3,0})\Sigma_u$ wave function,

$$\begin{aligned} \frac{1}{\sqrt{2}} (|\sigma_u, \bar{\sigma}_g| - |\sigma_g, \bar{\sigma}_u|) &= \left[\frac{1}{\sqrt{2}} (\sigma_u(1)\sigma_g(2) - \sigma_g(1)\sigma_u(2)) \right] \\ &\times \left[\frac{1}{\sqrt{2}} (\alpha(1)\beta(2) + \beta(1)\alpha(2)) \right], \end{aligned} \quad (3.38)$$

Notice that the three triplet wave functions ($(^{3,-1})\Sigma_u$, $(^{3,0})\Sigma_u$, and $(^{3,+1})\Sigma_u$) have exactly the same spatial part. (And there are exactly three linearly-independent ways to make the symmetric spin part.) Therefore, as long as the hamiltonian is spin-free (i.e., no external magnetic fields or spin-orbit coupling terms), these three states must be rigorously energetically degenerate (which is why it is called a triplet state.)

We may also determine the relative ordering of the ${}^3\Sigma_u$ and ${}^1\Sigma_u$ states using the multiplet spin method [111, 112]. The goal is to reduce all energy expressions to single-determinantal expressions which we may then evaluate with our intuitive knowledge of how to write down Hartree-Fock energy expressions. We begin with the observation that

$$\begin{aligned} E({}^{(1,0)}\Sigma_u) &= \frac{1}{2} \langle |\sigma_u, \bar{\sigma}_g| + |\sigma_g, \bar{\sigma}_u| | \hat{H} | |\sigma_u, \bar{\sigma}_g| + |\sigma_g, \bar{\sigma}_u| \rangle \\ &= \langle |\sigma_u, \bar{\sigma}_g| | \hat{H} | |\sigma_u, \bar{\sigma}_g| \rangle + \langle |\sigma_u, \bar{\sigma}_g| | \hat{H} | |\sigma_g, \bar{\sigma}_u| \rangle \\ &= E(|\sigma_u, \bar{\sigma}_g|) + \langle |\sigma_u, \bar{\sigma}_g| | \hat{H} | |\sigma_g, \bar{\sigma}_u| \rangle \\ E({}^{(3,0)}\Sigma_u) &= \frac{1}{2} \langle |\sigma_u, \bar{\sigma}_g| - |\sigma_g, \bar{\sigma}_u| | \hat{H} | |\sigma_u, \bar{\sigma}_g| - |\sigma_g, \bar{\sigma}_u| \rangle \\ &= \langle |\sigma_u, \bar{\sigma}_g| | \hat{H} | |\sigma_u, \bar{\sigma}_g| \rangle - \langle |\sigma_u, \bar{\sigma}_g| | \hat{H} | |\sigma_g, \bar{\sigma}_u| \rangle \\ &= E(|\sigma_u, \bar{\sigma}_g|) - \langle |\sigma_u, \bar{\sigma}_g| | \hat{H} | |\sigma_g, \bar{\sigma}_u| \rangle, \end{aligned} \quad (3.39)$$

The cross term, $\langle |\sigma_u, \bar{\sigma}_g| | \hat{H} | |\sigma_g, \bar{\sigma}_u| \rangle$, is problematic but is easily eliminated because,

$$E({}^{(1,0)}\Sigma_u) + E({}^{(3,0)}\Sigma_u) = 2E(|\sigma_u, \bar{\sigma}_g|). \quad (3.40)$$

We now use the fact that,

$$E({}^{(3,0)}\Sigma_u) = E({}^{(3,1)}\Sigma_u), \quad (3.41)$$

to obtain the singlet and triplet energies in terms of expectation values of the hamiltonian with purely single-determinantal wave functions:

$$\begin{aligned} E({}^{(3,0)}\Sigma_u) &= E(|\sigma_u, \bar{\sigma}_g|) \\ E({}^{(1,0)}\Sigma_u) &= 2E(|\sigma_u, \bar{\sigma}_g|) - E(|\sigma_u, \bar{\sigma}_g|). \end{aligned} \quad (3.42)$$

As chemical intuition works very nicely at the single-determinantal level (Hartree-Fock approximation), we may now write out the various energies from highest to lowest in terms of the bare orbital energies (ϵ^0) and coulomb [$(\phi\phi||\psi\psi)$] and exchange integrals [$(\phi\psi||\psi\phi)$], just by counting same-spin and opposite-spin interactions:

$$\begin{array}{c} \sigma_u [\uparrow, \downarrow] \\ \sigma_g [,] \\ E^{(1,0)\Sigma_g} = 2\epsilon_u^0 + (\sigma_u \sigma_u || \sigma_u \sigma_u) \end{array}$$

$$\begin{array}{cc} \sigma_u [\uparrow,] & \sigma_u [, \downarrow] \\ + & \\ \sigma_g [, \downarrow] & \sigma_g [\uparrow,] \\ E^{(1,0)\Sigma_u} = \epsilon_g^0 + \epsilon_u^0 + (\sigma_u \sigma_u || \sigma_u \sigma_u) + (\sigma_g \sigma_u || \sigma_u \sigma_g) \end{array}$$

$$\begin{array}{c} \sigma_u [\uparrow,] \\ \sigma_g [\uparrow,] \\ E^{(3,1)\Sigma_u} = \epsilon_g^0 + \epsilon_u^0 + (\sigma_u \sigma_u || \sigma_g \sigma_g) - (\sigma_g \sigma_u || \sigma_u \sigma_g) \end{array}$$

$$\begin{array}{cc} \sigma_u [\uparrow,] & \sigma_u [, \downarrow] \\ - & \\ \sigma_g [, \downarrow] & \sigma_g [\uparrow,] \\ E^{(3,0)\Sigma_u} = \epsilon_g^0 + \epsilon_u^0 + (\sigma_u \sigma_u || \sigma_u \sigma_u) - (\sigma_g \sigma_u || \sigma_u \sigma_g) \end{array}$$

$$\begin{array}{c} \sigma_u [, \downarrow] \\ \sigma_g [, \downarrow] \\ E^{(3,-1)\Sigma_u} = \epsilon_g^0 + \epsilon_u^0 + (\sigma_u \sigma_u || \sigma_g \sigma_g) - (\sigma_g \sigma_u || \sigma_u \sigma_g) \end{array}$$

$$\begin{array}{c} \sigma_u [,] \\ \sigma_g [\uparrow, \downarrow] \\ E^{(1,0)\Sigma_g} = 2\epsilon_g^0 + (\sigma_g \sigma_g || \sigma_g \sigma_g) \end{array}$$

Physically, the ${}^1\Sigma_u$ state is higher in energy than the ${}^3\Sigma_u$ state is that electrons with the same spin avoid each other in space, thus reducing their electron repulsion (by the exchange integral) and hence leading to a lower energy than is the case with opposite spin electrons (which, we see, is raised in energy by the exchange integral.)

3.2.3 Spin-Coupling Theory

So far the treatment of spin has been kept as elementary as possible, but this limits us to two-electron wave functions. Let us now try to give a more advanced treatment of spin. This treatment can be generalized to more than two spins where wave functions no longer factor into the product of a spatial and a spin part. Even in the two-electron case, it may help to make the structure of the spin problem more evident. We will skip many details which may be found in advanced textbooks, but there should be enough detail that the reader can follow and apply the basic ideas. We consider the case where we have N unpaired spins to place in N orbitals. In our two-electron problem, this corresponds to the case of placing one electron in each of the σ_g and σ_u orbitals.

The spin-coupling problem is of fundamental importance in the few-body problem and is closely linked to the Lie algebra treatment of continuous groups. Under these conditions, it is perhaps not surprising that many different ways have been invented to handle spin-coupling (e.g., Clebsch-Gordon coefficients, Young diagrams based upon the symmetric group, graphical unitary group treatment, etc.) The approach presented here is based upon ladder operators. The ladder operator treatment of angular momentum is treated in most graduate-level textbooks on quantum physics.

In the case of a single electron, we have the three basic spin operators \hat{s}_x , \hat{s}_y , and \hat{s}_z which commute with our spin-less hamiltonian, but not with each other. Hence the three spin-components do *not* constitute a set of three simultaneous observables. They obey the cyclic commutation relations,

$$\begin{aligned} [\hat{s}_x, \hat{s}_y] &= i\hbar\hat{s}_z \\ [\hat{s}_z, \hat{s}_x] &= i\hbar\hat{s}_y \\ [\hat{s}_y, \hat{s}_z] &= i\hbar\hat{s}_x . \end{aligned} \quad (3.43)$$

In some sense, any set of three operators that obey these relations may be thought of as “angular momentum operators.” All three of the basic spin operators commute with the total spin operator,

$$\hat{s}^2 = \hat{s}_x^2 + \hat{s}_y^2 + \hat{s}_z^2 . \quad (3.44)$$

As $[\hat{H}, \hat{s}_z] = [\hat{H}, \hat{s}^2] = [\hat{s}^2, \hat{s}_z] = 0$, quantum mechanics tells us that we may chose the simultaneous eigenvalues of \hat{s}^2 and of \hat{s}_z as constants of motion,

$$\begin{aligned} \hat{s}^2\psi_{s,m_s} &= s(s+1)\hbar^2\psi_{s,m_s} \\ \hat{s}_z\psi_{s,m_s} &= m_s\hbar\psi_{s,m_s} . \end{aligned} \quad (3.45)$$

In particular, for a single electron, $s = 1/2$ and $m_s = \pm 1/2$, so we have

$$\begin{aligned} \hat{s}^2\psi &= \frac{3}{4}\hbar^2\psi \\ \hat{s}_z\psi &= +\frac{1}{2}\hbar\psi \\ \hat{s}^2\bar{\psi} &= \frac{3}{4}\hbar^2\bar{\psi} \\ \hat{s}_z\bar{\psi} &= -\frac{1}{2}\hbar\bar{\psi} . \end{aligned} \quad (3.46)$$

It is also useful to define the raising operator,

$$\hat{s}_+ = s_x + is_y , \quad (3.47)$$

and the lowering operator,

$$\hat{s}_- = s_x - is_y . \quad (3.48)$$

It can be shown that

$$\begin{aligned} \hat{s}_+\psi &= 0 \\ \hat{s}_+\bar{\psi} &= \hbar\psi \\ \hat{s}_-\psi &= \hbar\bar{\psi} \\ \hat{s}_-\bar{\psi} &= 0 . \end{aligned} \quad (3.49)$$

We say that each pair $(\psi, \bar{\psi})$ forms a spin ladder which can be climbed with \hat{s}_+ and descended with \hat{s}_- .

In the case of N electrons, the spin operators generalize to,

$$\begin{aligned} \hat{S}_x &= \sum_{i=1,N} \hat{s}_x(i) \\ \hat{S}_y &= \sum_{i=1,N} \hat{s}_y(i) \\ \hat{S}_z &= \sum_{i=1,N} \hat{s}_z(i) . \end{aligned} \quad (3.50)$$

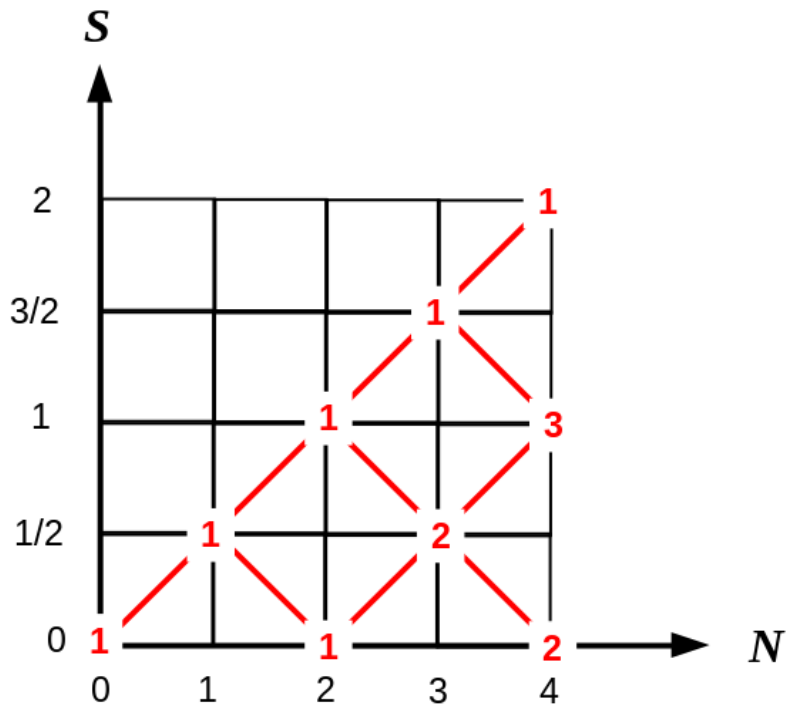


Figure 3.8: Spin-coupling diagram for counting the number of spin ladders as a function of the number of electrons. For example, for $N = 4$ electrons, there is one quintet ladder with $S = 2$, three triplet ladders with $S = 1$, and two singlet ladders with $S = 0$.

(Notice the use of capital letters since we are now dealing with many-electron quantities.) The definitions,

$$\begin{aligned}\hat{S}^2 &= \hat{S}_x^2 + \hat{S}_y^2 + \hat{S}_z^2 \\ \hat{S}_+ &= \hat{S}_x + i\hat{S}_y \\ \hat{S}_- &= \hat{S}_x - i\hat{S}_z,\end{aligned}\tag{3.51}$$

still hold, but

$$\hat{S}^2 \neq \sum_{i=1,N} \hat{s}^2(i).\tag{3.52}$$

This complicates the problem of constructing spin eigenfunctions. In general, for arbitrary N , there will be several spin ladders. The precise number can be read off the spin-coupling diagram 3.8.

We will explain one method for constructing spin eigenfunctions and illustrate the method by applying it to the case of $N = 2$ electrons placed in the orbitals ψ and ϕ . This consists in beginning with the head of the spin ladder with the largest value of S which is always single determinantal and descending, knowing the general relations,

$$\begin{aligned}\hat{S}_+ \Psi_{(S,M_S)} &= \hbar \sqrt{S(S+1) - M_S(M_S+1)} \Psi_{(S,M_S+1)} \\ \hat{S}_- \Psi_{(2S+1,M_S)} &= \hbar \sqrt{S(S+1) - M_S(M_S-1)} \Psi_{(S,M_S-1)},\end{aligned}\tag{3.53}$$

where the complicated prefactor preserves normalization. Although not strictly necessary, I will rewrite key operators in second-quantized form.

In order to introduce second-quantized operators, let us abandon the overbar notation and work directly with spin-orbitals *for this paragraph only!* We will assume a spin-orbital basis of orthonormal orbitals. The effect of a creation operator $r^\dagger = \hat{a}_r^\dagger$ on a single determinant wave function $|s, t, u, v, \dots|$ is to add another spin-orbital at the beginning of the determinant,

$$r^\dagger |s, t, u, v, \dots| = |r, s, t, u, v, \dots|. \quad (3.54)$$

The result is zero if r is already one of the spin-orbitals in the determinant. The adjoint of the creation operator is the corresponding annihilation operator $r = \hat{a}_r$ which undoes the operation of r^\dagger ,

$$r |r, s, t, u, v, \dots| = |s, t, u, v, \dots|. \quad (3.55)$$

If the spin-orbital r is not in the beginning of the determinant list, then use antisymmetry to permute r to the beginning of the determinant list, keeping track of any sign changes. If the spin-orbital r is not in the list, then the action of r on the determinant is zero. It is then possible to deduce the following *anticommutation* rules:

$$\begin{aligned} [r, s]_+ &= [r^\dagger, s^\dagger]_+ = 0 \\ [r, s^\dagger]_+ &= [r^\dagger, s]_+ = \delta_{r,s}. \end{aligned} \quad (3.56)$$

Writing operators in second-quantized form provides an easy machinery for working with antisymmetric wave functions without having to think too much (which is why I like to use it.)

Let us return now to our usual notation and denote spin α (\uparrow) orbitals by r and spin β (\downarrow) orbitals by \bar{r} . It is now easy to write the operators,

$$\begin{aligned} \hat{n}_\uparrow &= \sum_r r^\dagger r \\ \hat{n}_\downarrow &= \sum_r \bar{r}^\dagger \bar{r}, \end{aligned} \quad (3.57)$$

that count the number of each type of spin in a determinant or a linear combination of determinants all with the same number of orbitals of each spin-type. Let us call this wave function, Ψ , then

$$\begin{aligned} \hat{n}_\uparrow \Psi &= n_\uparrow \Psi \\ \hat{n}_\downarrow \Psi &= n_\downarrow \Psi. \end{aligned} \quad (3.58)$$

From Eq. (3.33), we have that

$$\hat{S}_z = \frac{\hbar}{2} (\hat{n}_\uparrow - \hat{n}_\downarrow). \quad (3.59)$$

Expressing \hat{S}^2 is aided by knowing that,

$$\begin{aligned} \hat{S}^2 &= \hat{S}_+ \hat{S}_- + \hat{S}_z (\hat{S}_z - \hbar \hat{1}) \\ \hat{S}^2 &= \hat{S}_- \hat{S}_+ + \hat{S}_z (\hat{S}_z + \hbar \hat{1}), \end{aligned} \quad (3.60)$$

which comes from the standard ladder operator treatment of angular momenta, and using the second-quantized forms of the raising and lowering operators,

$$\begin{aligned} \hat{S}_+ &= \hbar \sum_r r^\dagger \bar{r} \\ \hat{S}_- &= \hbar \sum_r \bar{r}^\dagger r. \end{aligned}$$

Then it is easy to derive that,

$$\hat{S}^2 = \hbar^2 \hat{\mathcal{P}} + \frac{\hbar^2}{4} (\hat{n}_\uparrow - \hat{n}_\downarrow)^2 + \frac{\hbar^2}{2} \hat{n}, \quad (3.61)$$

where

$$\hat{n} = \hat{n}_\uparrow + \hat{n}_\downarrow \quad (3.62)$$

is the number operator which just counts the number of electrons in the wave function and

$$\hat{\mathcal{P}} = \sum_{r,s} r^\dagger \bar{s}^\dagger s \bar{r} \quad (3.63)$$

is the spin transposition operator which sums over all possible exchanges of $\alpha = \uparrow$ and $\beta = \downarrow$ pairwise exchanges.

We are now all set to apply these formulae to obtain our spin-adapted functions for the two-electron problem. The spin-coupling diagram (Fig. 3.8) tells us that there will be one one triplet ladder with $(S, M_S) = (1, +1), (1, 0), (1, -1)$ and one singlet ladder with $(S, M_S) = (0, 0)$. To find the head of the triplet ladder, we only need to identify the wave function with $M_S = 1$, namely

$$\Psi_{(1,+1)} = |\psi, \phi|. \quad (3.64)$$

We can verify that this is indeed a spin eigenfunction with the correct quantum numbers:

$$\begin{aligned} \hat{S}_z \Psi_{(1,+1)} &= \frac{\hbar}{2} (\hat{n}_\uparrow - \hat{n}_\downarrow) |\psi, \phi| \\ &= \frac{\hbar}{2} (2 - 0) |\psi, \phi| \\ &= \hbar |\psi, \phi| \\ &\Rightarrow M_S = 1 \\ \hat{S}^2 \Psi_{(1,+1)} &= \left(\hbar^2 \hat{\mathcal{P}} + \frac{\hbar^2}{4} (\hat{n}_\uparrow - \hat{n}_\downarrow)^2 + \frac{\hbar^2}{2} \hat{n} \right) |\psi, \phi| \\ &= \left(0 + \frac{\hbar^2}{4} 2^2 + \frac{\hbar^2}{2} 2 \right) |\psi, \phi| \\ &= 2\hbar^2 |\psi, \phi| \\ &\Rightarrow S(S+1) = 2 \Rightarrow S = 1. \end{aligned} \quad (3.65)$$

Now we apply the spin lowering operator to find $\Psi_{(1,0)}$ by descending the ladder:

$$\begin{aligned} \hat{S}_- |\psi, \phi| &= \hbar \left(\sum_r \bar{r}^\dagger r \right) |\psi, \phi| \\ &= \hbar (|\bar{\psi}, \phi| + |\psi, \bar{\phi}|) \\ &= \hbar \sqrt{2} \Psi_{(1,0)}, \end{aligned} \quad (3.66)$$

according to Eq. (3.53). Hence,

$$\Psi_{(1,0)} = \frac{1}{\sqrt{2}} (|\bar{\psi}, \phi| + |\psi, \bar{\phi}|), \quad (3.67)$$

but this result could just as easily be obtained by using the orthonormality of the determinants directly. Let us check that this is indeed a simultaneous eigenfunction of \hat{S}_z and of \hat{S}^2 :

$$\begin{aligned}
\hat{S}_z \Psi_{(1,0)} &= \frac{\hbar}{2} (\hat{n}_\uparrow - \hat{n}_\downarrow) \frac{1}{\sqrt{2}} (|\bar{\psi}, \phi| + |\psi, \bar{\phi}|) \\
&= \frac{\hbar}{2} (1 - 1) \frac{1}{\sqrt{2}} (|\bar{\psi}, \phi| + |\psi, \bar{\phi}|) \\
&= 0\hbar \frac{1}{\sqrt{2}} (|\bar{\psi}, \phi| + |\psi, \bar{\phi}|) \\
\Rightarrow M_S &= 0 \\
\hat{S}^2 \Psi_{(1,0)} &= \left(\hbar^2 \hat{\mathcal{P}} + \frac{\hbar^2}{4} (\hat{n}_\uparrow - \hat{n}_\downarrow)^2 + \frac{\hbar^2}{2} \hat{n} \right) \frac{1}{\sqrt{2}} (|\bar{\psi}, \phi| + |\psi, \bar{\phi}|) \\
&= \hbar^2 \left(1 + \frac{0}{4} + \frac{2}{2} \right) \frac{1}{\sqrt{2}} (|\bar{\psi}, \phi| + |\psi, \bar{\phi}|) \\
&= 2\hbar^2 \Psi_{(1,0)} = S(S+1)\hbar^2 \Psi_{(1,0)} \\
\Rightarrow S &= 1. \tag{3.68}
\end{aligned}$$

So it does check! To obtain $\Psi_{(1,-1)}$, apply the spin-lowering operator once again:

$$\hat{S}_- \Psi_{(1,-1)} = \hbar \left(\sum_r \bar{r}^\dagger r \right) \frac{1}{\sqrt{2}} (|\bar{\psi}, \phi| + |\psi, \bar{\phi}|) = \sqrt{2} |\bar{\psi}, \bar{\phi}|. \tag{3.69}$$

So, after normalization,

$$\Psi_{(1,-1)} = |\bar{\psi}, \bar{\phi}|, \tag{3.70}$$

and we will leave it as an exercise to the reader to verify that this is a simultaneous eigenfunction of \hat{S}_z and of \hat{S}^2 with the correct eigenvalues. We have missed $\Psi_{(0,0)}$ but we know it must be a linear combination of the two determinants with $M_S = 0$ — namely $|\bar{\psi}, \phi|$ and $|\psi, \bar{\phi}|$ — and be orthogonal to $\Psi_{(1,0)}$. There is no choice left but

$$\Psi_{(0,0)} = \frac{1}{2} (|\bar{\psi}, \phi| - |\psi, \bar{\phi}|). \tag{3.71}$$

The reader is invited to verify that this is a simultaneous eigenfunction of \hat{S}_z and of \hat{S}^2 with the correct eigenvalues and that both the raising and the lower operators annihilate $\Psi_{(0,0)}$. This confirms the main results of the previous subsection and provides some powerful tools for treating the case of more than $N = 2$ singly-occupied orbitals.

3.2.4 Dissociation Limits

One (overly narrow) definition of chemistry is that it is all about chemical reactions, i.e., making and breaking bonds. The dissociation



has two possible products, namely ions (homolytic bond cleavage),



and radicals (heterolytic bond cleavage),



Note that thermal (i.e., ground-state) dissociation corresponds to dissociation into radicals. Other heterolytic outcomes are,

$$H^\uparrow + H^\uparrow, \quad (3.75)$$

and,

$$H^\downarrow + H^\downarrow, \quad (3.76)$$

Let us check the dissociation limits of our wave functions. To do so, we must re-express our wave functions in terms of atomic orbitals and then follow the old valence-bond practice [113] of associating wave functions with Lewis dot structures [114].

In the limit of $R = \infty$, then $S = 0$ and our orbitals become

$$\begin{aligned} \sigma_g &= \frac{1}{\sqrt{2}}(s_A + s_B) \\ \sigma_u &= \frac{1}{\sqrt{2}}(s_A - s_B), \end{aligned} \quad (3.77)$$

In this same limit,

$$\begin{aligned} \Psi_{(1,1)} &= |\sigma_g, \sigma_u| \\ &= \frac{1}{2}|s_A + s_B, s_A - s_B| \\ &= \frac{1}{2}(-|s_A, s_B| + |s_B, s_A|) \\ &= -|s_A, s_B|, \end{aligned} \quad (3.78)$$

which corresponds to the Lewis dot structure (3.75). Similarly,

$$\Psi_{(1,-1)} = |\bar{\sigma}_g, \bar{\sigma}_u| = -|\bar{s}_A, \bar{s}_B|, \quad (3.79)$$

which corresponds to the Lewis dot structure (3.76). We might expect that the dissociation limit of $\Psi_{(1,0)}$ is given by the Lewis dot structure (3.74) and this indeed is true:

$$\begin{aligned} \Psi_{(1,0)} &= \frac{1}{\sqrt{2}}(|\sigma_u, \bar{\sigma}_g| - |\sigma_g, \bar{\sigma}_u|) \\ &= \frac{1}{2\sqrt{2}}(|s_A - s_B, \bar{s}_A + \bar{s}_B| - |s_A + s_B, \bar{s}_A - \bar{s}_B|) \\ &= \frac{1}{2\sqrt{2}}[(|s_A, \bar{s}_A| + |s_A, \bar{s}_B| - |s_B, \bar{s}_A| - |s_B, \bar{s}_B|) - (|s_A, \bar{s}_A| - |s_A, \bar{s}_B| + |s_B, \bar{s}_A| - |s_B, \bar{s}_B|)] \\ &= \frac{1}{\sqrt{2}}(|s_A, \bar{s}_B| - |s_B, \bar{s}_A|). \end{aligned} \quad (3.80)$$

We now come to the famous problem of the dissociation of the ground-state wave function. According to naïve MO theory, the ground-state wave function is,

$$\begin{aligned} \Psi_{(0,0)}^1 &= |\sigma_g, \bar{\sigma}_g| \\ &= \frac{1}{2}|s_A + s_B, \bar{s}_A + \bar{s}_B| \\ &= \frac{1}{2}(|s_A, \bar{s}_A| + |s_B, \bar{s}_B|) + \frac{1}{2}(|s_A, \bar{s}_B| + |s_B, \bar{s}_A|). \end{aligned} \quad (3.81)$$

That is,

$$\Psi_{(0,0)}^1 = \frac{1}{\sqrt{2}} (\Psi_{(0,0)}^{\text{ionic}} + \Psi_{(0,0)}^{\text{covalent}}) , \quad (3.82)$$

is an equal mixture of a covalent wave function,

$$\Psi_{(0,0)}^{\text{covalent}} = \frac{1}{\sqrt{2}} (|s_A, \bar{s}_B| + |s_B, \bar{s}_A|) , \quad (3.83)$$

corresponding to the expected dissociation into radicals [Lewis dot structure (3.74)] and an ionic wave function,

$$\Psi_{(0,0)}^{\text{ionic}} = \frac{1}{\sqrt{2}} (|s_A, \bar{s}_A| + |s_B, \bar{s}_B|) , \quad (3.84)$$

corresponding to dissociation into ions [Lewis dot structure (3.73)]. The presence of the ionic term means that MO theory will not dissociate correctly, but rather will dissociate to too high an energy. In order to correct the problem, let us look at the $R \rightarrow \infty$ limit of the doubly-excited determinant,

$$\begin{aligned} \Psi_{(0,0)}^2 &= |\sigma_u, \bar{\sigma}_u| \\ &= \frac{1}{2} |s_A - s_B, \bar{s}_A - \bar{s}_B| \\ &= \frac{1}{2} (|s_A, \bar{s}_A| + |s_B, \bar{s}_B|) - \frac{1}{2} (|s_A, \bar{s}_B| + |s_B, \bar{s}_A|) \\ &= \frac{1}{\sqrt{2}} (\Psi_{(0,0)}^{\text{ionic}} - \Psi_{(0,0)}^{\text{covalent}}) . \end{aligned} \quad (3.85)$$

Apparently the correct dissociation limit requires the linear combination,

$$\frac{1}{\sqrt{2}} (\Psi_{(0,0)}^1 - \Psi_{(0,0)}^2) = \Psi_{(0,0)}^{\text{covalent}} , \quad (3.86)$$

as $R \rightarrow 0$. Note that ${}^{(0,0)}\Psi_{\text{covalent}}$ is the Heitler-London [valence-bond (VB)] wave function,

$$\Psi_{(0,0)}^{\text{covalent}} = \left[\frac{1}{\sqrt{2}} (s_A(1)s_B(2) + s_B(1)s_A(2)) \right] \left[\frac{1}{2} (\alpha(1)\beta(2) - \beta(1)\alpha(2)) \right] . \quad (3.87)$$

As neither the naïve MO wave function nor the naïve VB wave function are correct at all R , but the MO wave function is best near the equilibrium geometry and the VB wave function is best near dissociation, then the recommended choice is to take a linear combination,

$$\begin{aligned} \Psi_{(0,0)} &= C_1 \Psi_{(0,0)}^1 - C_2 \Psi_{(0,0)}^2 \\ &= C_{\text{ionic}} \Psi_{(0,0)}^{\text{ionic}} + C_{\text{covalent}} \Psi_{(0,0)}^{\text{covalent}} , \end{aligned} \quad (3.88)$$

with R -dependent coefficients whose values should be determined variationally. Equation (3.88) is an example of a configuration-interaction (CI) wave function. CI wave functions are often necessary for describing chemical reactions because, by taking a geometry-dependent linear combination of the product and reactant wave functions, the CI wave function provides a smooth interpolation along the chemical reaction pathway.

3.2.5 Symmetry Breaking and Spin Contamination

Up until now, we have considered only spin-restricted wave functions with the same orbitals for different spin (SODS.) Let us now consider spin-unrestricted wave functions with different orbitals for different spin (DODS.) Let us write the orbitals as,

$$\begin{aligned}\sigma_1 &= \sqrt{\frac{C_1}{C_1 + C_2}}\sigma_g + \sqrt{\frac{C_2}{C_1 + C_2}}\sigma_u \\ \sigma_2 &= \sqrt{\frac{C_1}{C_1 + C_2}}\sigma_g - \sqrt{\frac{C_2}{C_1 + C_2}}\sigma_u.\end{aligned}\quad (3.89)$$

Then

$$\begin{aligned}\Psi_{(0,0)}^{\text{CI}} &= \frac{C_1 + C_2}{2}(|\sigma_1, \bar{\sigma}_2| + |\sigma_2, \bar{\sigma}_1|) \\ &= \frac{1}{2}\left(|\sqrt{C_1}\sigma_g + \sqrt{C_2}\sigma_u, \sqrt{C_1}\bar{\sigma}_g - \sqrt{C_2}\bar{\sigma}_u| + |\sqrt{C_1}\sigma_g - \sqrt{C_2}\sigma_u, \sqrt{C_1}\bar{\sigma}_g + \sqrt{C_2}\bar{\sigma}_u|\right) \\ &= C_1|\sigma_g, \bar{\sigma}_g| - C_2|\sigma_u, \bar{\sigma}_u|,\end{aligned}\quad (3.90)$$

which is one of the forms of the CI wave function in Eq. (3.88). Around the equilibrium geometry, the lower energy determinant dominates,

$$R = R_{eq} : (C_1, C_2) \approx (1, 0), \quad (3.91)$$

while in the limit of ground-state dissociation,

$$R \rightarrow \infty : (C_1, C_2) = \left(\frac{1}{\sqrt{2}}, \frac{1}{\sqrt{2}}\right). \quad (3.92)$$

Symmetry breaking consists of using a single-determinantal DODS wave function which I will write as,

$$\begin{aligned}\Psi_{\text{broken}} &= |\sigma_1, \bar{\sigma}_2| \\ &= \frac{1}{C_1 + C_2}|\sqrt{C_1}\sigma_g + \sqrt{C_2}\sigma_u, \sqrt{C_1}\bar{\sigma}_g - \sqrt{C_2}\bar{\sigma}_u| \\ &= \frac{1}{C_1 + C_2}(C_1|\sigma_g, \bar{\sigma}_g| - C_2|\sigma_u, \bar{\sigma}_u|) \\ &\quad + \frac{\sqrt{2C_1C_2}}{C_1 + C_2} \left[\frac{1}{\sqrt{2}}(|\sigma_u, \bar{\sigma}_g| + |\sigma_g, \bar{\sigma}_u|)\right] \\ &= \frac{1}{C_1 + C_2}\Psi_{(0,0)}^{\text{CI}} + \frac{\sqrt{2C_1C_2}}{C_1 + C_2}\Psi_{(1,0)}.\end{aligned}\quad (3.93)$$

As long as the symmetry unbroken (SODS) solution is the lower variational solution, then $(C_1, C_2) = (1, 0)$ and $\Psi_{\text{broken}} = |\sigma_g, \bar{\sigma}_g|$. This happens for $R < R_{CF}$ where R_{CF} is the Coulson-Fischer point (or more exactly, bond distance). For $R > R_{CF}$, the broken-symmetry (DODS) solution is the lower energy variational solution. As can be seen in Eq. (3.93), the DODS solution is contaminated by a triplet component ($\Psi_{(1,0)}$). This has two consequences: For the energy,

$$E_{\text{broken}} = \frac{E_{(0,0)}^{\text{CI}} + 2C_1C_2E_{(1,0)}}{(C_1 + C_2)^2}. \quad (3.94)$$

We may also investigate *spin contamination* by calculating,

$$\langle \Psi_{\text{broken}} | \hat{S}^2 | \Psi_{\text{broken}} \rangle = \frac{4C_1 C_2}{(C_1 + C_2)^2}. \quad (3.95)$$

In the $R \rightarrow \infty$ limit, where $(C_1, C_2) = (1/\sqrt{2}, 1/\sqrt{2})$,

$$\begin{aligned} E_{\text{broken}} &= \frac{E_{(0,0)}^{\text{CI}} + E_{(1,0)}}{2} \\ \langle \Psi_{\text{broken}} | \hat{S}^2 | \Psi_{\text{broken}} \rangle &= 1. \end{aligned} \quad (3.96)$$

In practice the broken symmetry energy is better than this last equation may make it appear as both $E_{(0,0)}^{\text{CI}}$ and $E_{(1,0)}$ tend towards the energy of two separated hydrogen atoms (i.e., 2 Ha.) However $\langle \hat{S}^2 \rangle = 0$ for a true singlet. Hence spin contamination is a problem after the Coulson-Fischer point.

While the DFT wave function is generally assumed to be single determinantal, a broken symmetry single determinantal wave function is sometimes an eigenfunction of \hat{S}^2 or, at least, not very far from being one. This is why it is important to be able to calculate the expectation value of \hat{S}^2 for a DODS determinant. The basic equation for doing so was worked out by Löwdin in the text of Hartree-Fock theory [115] and is easily obtained using second quantization [116]. The result is,

$$\langle \hat{S}^2 \rangle = \left(\frac{n_\uparrow - n_\downarrow}{2} \right) \left(\frac{n_\uparrow - n_\downarrow}{2} + 1 \right) - \sum_{i,j}^{\text{occupied}} |\Delta_{i,j}|^2. \quad (3.97)$$

Here Δ is the spin-similarity matrix which is defined as the overlap between the *spatial* parts of the spin α and spin β orbitals which I will write as,

$$\Delta_{r,s} = \langle r | \hat{S}_+ | \bar{s} \rangle. \quad (3.98)$$

This is the same as

$$\Delta_{r,s} = \int \psi_r^*(\vec{r}) \psi_s(\vec{r}) d\vec{r}, \quad (3.99)$$

where ψ_r is the spatial part of the r th spin α orbital and ψ_s is the spatial part of the s th spin β orbital.

An approximate way to remove spin-contamination using $\langle \hat{S}^2 \rangle$ is given in Ref. [117]. In the present context this amounts to solving the equations,

$$\begin{aligned} \Psi_{\text{broken}} &= \sqrt{1 - C^2} \Psi_{(0,0)} + C \Psi_{(1,0)} \\ E_{\text{broken}} &= (1 - C^2) E_{(0,0)} + C^2 E_{(1,0)} \\ \langle \hat{S}^2 \rangle_{\text{broken}} &= (1 - C^2) \langle \hat{S}^2 \rangle_{(0,0)} + C^2 \langle \hat{S}^2 \rangle_{(1,0)} = 2C^2, \end{aligned} \quad (3.100)$$

to obtain,

$$E_{(0,0)} = \frac{2E_{\text{broken}} - \langle \hat{S}^2 \rangle_{\text{broken}} {}^3E}{2 - \langle \hat{S}^2 \rangle_{\text{broken}}}, \quad (3.101)$$

where ${}^3E = E_{(1,0)}$ is the triplet energy. While this seems like a very good idea, there is a serious problem — namely where to get the 3E energy! Ideally the $\Psi_{(0,0)}$ and $\Psi_{(1,0)}$ are close to being exact, which means that the value used for 3E should also be close to being exact. Usually however accessible values of 3E are upper limits to the exact value, which means that $E_{(0,0)}$ will be underestimated (i.e., too low in energy)! This actually prevents this type of spin projection from being very useful.

3.2.6 Exercise

Calculate the DODS and SODS $M_S = 0$ and $M_S = 1$ potential energy curves and spin-contamination for H_2 at the different bond distances given in Table 3.1 for the LDA, BLYP, B3LYP, and HF DFAs. Find the location of the Coulson-Fischer point for each functional. Use Eq. (3.101) to remove spin-contamination from the energy. Discuss.

There are a few complications which enter into this work, the biggest of which is that symmetric guesses lead to symmetric orbitals and so make symmetry breaking difficult to impossible. In order to surmount this problem, we will have to use some tricks. This involves using restart files. You will need to modify the run shell to be the following:

```
#!/bin/csh
# The previous line indicates that this is a C-shell file
# -----
# Program to run deMon in the present working directory.
# To use: Create an input file with the name xxx.inp where
# xxx can be anything. Execute with
# /home/mcasida/ENGINEERING/workbook/examples/run.csh xxx
# The job runs interactively in foreground.
# -----
set xxx = $1
echo "Input file \"$xxx.inp"
set PWD = `pwd`
echo "The present working directory is \"$PWD"
set deMon_root = /home/mcasida/ENGINEERING/workbook/deMon # location of deMon files
echo "Using directories and executables from \"$deMon_root"
#
# copy essential files to the present working directory
#
cp $deMon_root/BASIS $PWD # copy the BASIS file to the run directory
cp $deMon_root/AUXIS $PWD # copy the AUXIS file to the run directory
cp $deMon_root/binary $PWD/deMon.x # copy the executable to the run directory
cp $xxx.inp deMon.inp
if ( -f $xxx.rst ) then
    cp $xxx.rst deMon.rst
else
    echo No restart file
endif
#
# run deMon
#
./deMon.x
#
# clean up
\rm BASIS
\rm AUXIS
mv deMon.out $xxx.out
mv deMon.rst $xxx.rst
```

```
\rm deMon.*  
# -----  
# End of file  
# -----
```

The file with the “.rst” ending is the restart file.

Next, perform the following calculation:

```
TITLE H2  
MULTI 1  
CHARGE 0  
  
SCFTYPE UKS TOL=1.E-8  
# SCFTYPE UKS TOL=1.E-5  
MOMODIFY 0 2  
1 0.99  
2 0.01  
VXCTYPE VWN  
  
#  
DIIS OFF  
# SYMMETRY OFF  
#mec GUESS CORE  
# GRID FIXED COARSE  
  
#  
# PRINT MOS  
POPULATION MULLIKEN  
  
#  
# EFIELD 0.0 0.0 0.000000001  
  
#  
# --- GEOMETRY ---  
  
#  
#  
GEOMETRY CARTESIAN BOHR  
H 0.000000 0.000000 0.000000  
H 0.000000 0.000000 4.300000  
  
#  
AUXIS (GEN-A3*)  
BASIS (AUG-CC-PV5Z)
```

The MOMODIFY keyword is mixing 0.1 of the $\sigma^* = \sigma_u$ with the $\sigma = \sigma_g$ orbital in order to break symmetry. The answer does not make too much sense because of this mixing but provides the initial guess that we will use at 4.2 bohr using the input file:

```
TITLE H2  
MULTI 1  
CHARGE 0  
  
SCFTYPE UKS TOL=1.E-8  
# SCFTYPE UKS TOL=1.E-5
```

```

# MOMODIFY 0 2
# 1 0.99
# 2 0.01
VXCTYPE VWN
#
DIIS OFF
GUESS RESTART
#
POPULATION MULLIKEN
#
# EFIELD 0.0 0.0 0.000000001
#
# --- GEOMETRY ---
#
#
GEOMETRY CARTESIAN BOHR
H 0.000000 0.000000 0.000000
H 0.000000 0.000000 4.200000
#
AUXIS (GEN-A3*)
BASIS (AUG-CC-PV5Z)

```

This assumes that the file `4p3.rst` has first been copied to `4p2.rst` before running the job at 4.2 bohr. This should give a broken symmetry result and a new restart file `4p2.rst` which should be copied to `4p1.rst` before running the next job at 4.1 bohr. In this manner, by gradually shortening the bond, and using the restart file for the previous geometry where symmetry breaking has already occurred, there should be no particular difficulties carrying out the symmetry broken UKS calculation. Another thing to note is that the `ROKS` (restricted open-shell Kohn-Sham) keyword should be used to carry out the SODS triplet calculation. However the total energy will be the same as for the UKS triplet calculation.

It should be emphasized that `UKS` indicates spin-unrestricted DODS while replacing it with `RKS` (or `ROKS`) indicates spin-restricted SODS. Also `MULT 1` is a $M_S = 0$ calculation while `MULT 3` is a $M_S = 1$ calculation. Note that especially that the multiplicity keyword `MULT` does not always give pure singlets in this case when symmetry breaking occurs. Thus `UKS MULT 1` shows

```
REFERENCE VALUE OF S**2 FOR PURE SPIN STATE S(S+1):      0.0000
```

```
S**2 BEFORE SPIN PROJECTION:      0.7845
S**2 AFTER SPIN PROJECTION:     0.0000
```

The spin projection described here is that of Ref. [118] but it is *not* used by the program in the energy calculation.

Molecule	No. Atoms	No. Internal DOFs
H ₂	2	$3 \times 2 - 5 = 1$
H ₂ O	3	$3 \times 3 - 6 = 3$
NH ₃	4	$3 \times 4 - 6 = 6$
C ₆ H ₆ ^a	12	$3 \times 12 - 6 = 30$
C ₆ H ₁₂ O ₆ ^b	24	$3 \times 24 - 6 = 66$
C ₆₀ ^c	60	$3 \times 60 - 6 = 174$

^a Benzene. ^b Glucose. ^c Buckminsterfullerene.

Table 3.2: Number of internal degrees of freedom for different molecules.

3.3 Lesson 5: Analytic Gradients and Geometry Optimization

“May the force be with you.” — Star Wars

In the last few lessons, we have produced potential energy curves for H₂⁺ and for H₂. Finding the equilibrium geometry was a simple as finding the bond length that gave the minimum energy on the graph. That works because there is only one degree of freedom (DOF). For a molecule with N atoms, as each atom can be moved in three independent directions, there are $6N$ degrees of freedom in configuration space (i.e., the space describing all the possible geometries of the molecule.) Three of these are just trivial translations and another three (two for linear molecules) are rotations, so that the total number of internal degrees of freedom is thus $3N - 6$ ($3N - 5$ for a linear molecule.) As shown in Table 3.2, that leaves only one internal DOF for a linear diatomic (the bond length.) Also shown in the table is how fast the number of DOFs increases with the number of atoms. If you want to plot the potential energy surface of the molecule, you will need an energy axis and $3N - 6$ ($3N - 5$) other coordinates to plot a $3N - 6$ ($3N - 5$) dimensional hypersurface in a $3N - 5$ ($3N - 4$) hyperspace. For H₂⁺ and H₂, an ordinary (x, y)-plot suffices, but the problem rapidly gets out of hand for larger molecules and it is no longer practical to search for the minimum by hand. During the 1970s, quantum chemists developed analytic derivative methods [119, 120] for computing forces and finding energy minima for a wide variety of electronic structure methods. This now allows us to do routine calculations where stationary points on the potential energy surface are found from a guessed geometry by minimizing the energy. The calculation of second derivatives (vibrational frequencies) then allows the stationary point to be identified as a minimum (all real frequencies), a transition state (exactly one imaginary frequency), or some higher-order stationary state. Although none of these methods guarantees that a global minimum has been found, they do make it possible to find many molecular configurations of fundamental interest and, with a little chemical intuition and/or help from experiment, often do lead to accurate identification and characterization of a global minimum energy structure. This is a somewhat technical section whose objective is to try to help you understand what the program is doing when you ask it to optimize a geometry and hence to be able to use the program properly to perform this task and to figure out what is going wrong should something not go as expected. We will just focus on analytic derivatives with a little about geometry optimizations and leave other more technical aspects (such as calculating frequencies, finding transition states, and finding intrinsic reaction coordinates) for future lessons. Of course the connection between forces

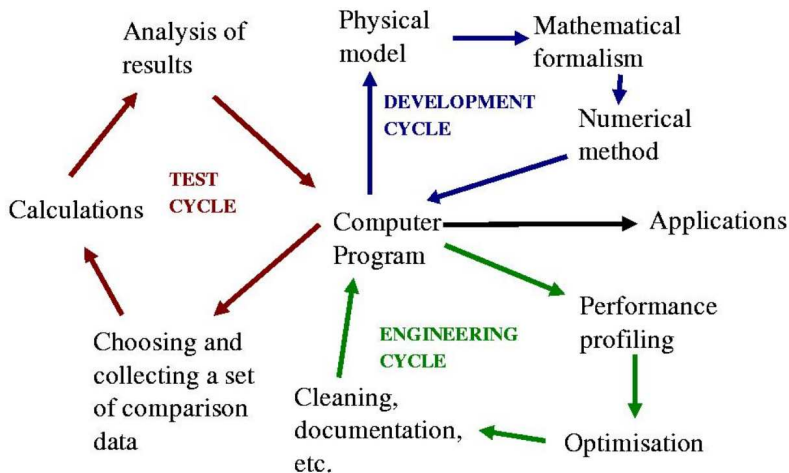


Figure 3.9: A model for methods development.

and geometry optimizations is that the q component of the force on the nuclei is

$$F_q = -\frac{\partial V}{\partial R_q}, \quad (3.102)$$

where $V = V(\mathbf{R})$ is the potential energy surface (PES) and R_q is the one of the (X, Y, Z) coordinates of the one the nuclei. This means that we have a stationary point on the PES when all of the forces are equal to zero.

At the risk of stating the obvious, I find the methods development model shown in Fig. 3.9 to be very useful. Put yourself in the place of a pure theoretician and suppose that you want to develop a method for calculating something, such as a new property needed to understand a new experimental method. These days the end result will often be a program which can then run applications useful for understanding the experiment. In practice, this involves at least three cycles to make an efficient and reliable method. The key cycle for us is the development cycle which, itself, has three steps. The first is our *physical model* which, in the case of finding minimum energy molecular structures, is the notion of a molecular energy which varies as a function of the relative position of the atoms (which makes sense provided we have made the Born-Oppenheimer approximation.) This has to be reduced to a *mathematical formalism* which tells us how to calculate this energy as a function of molecular position. For us, this follows from wave function theory and from density-functional theory. However, most of the time, the mathematical formalism will involve equations which must be solved numerically. Hence a choice of *numerical method* is needed. This involves approximations which are, in principle, purely numerical and which allow us to approach the exact mathematical formalism provided we are able to put in more numerical effort. An example is the use of a finite basis set expansion for the wave function. Once everything is worked out and programmed, the method must still be tested and, if found to be useful, optimized and documented. Of course, very often problems are found which can send us back to the development cycle. I find that Fig. 3.9, while somehow rather obvious, is also highly useful as a reminder that we need to be clear at every moment in what we are doing where we are on this diagram when developing a method.

3.3.1 Variational Calculus

Functional derivatives allow a compact and elegant way to discuss the analytic derivative problem. They were already introduced in Sec. 2.2. This is the topic of variational calculus about which entire books have been written (e.g., Ref. [33].) Fortunately we need not go into much detail beyond a little review of what was already introduced in Sec. 2.2.

The reader is undoubtedly familiar with regular derivatives dF/df of functions of a single variable $F(f)$ and has probably encountered the notion of a differential,

$$dF = \frac{dF}{df} df, \quad (3.103)$$

where dF and df refer to infinitesimal variations. Very often we encounter functions of more than one variable $F(\vec{f})$ where I have grouped all of the variables into a single vector $\vec{f} = (f_1, f_2, \dots, f_n)$. The differential is then,

$$dF = \sum_{i=1,n} \frac{\partial F}{\partial f_i} df_i. \quad (3.104)$$

The indices i are, of course, discrete. But suppose they were not! Suppose instead that they were continuous like the numbers x on the real number line. Then, instead of talking about $F(\vec{f})$, we would be talking about $F[f]$ where $f = f(x)$. The square bracket notation is a reminder that F is a *functional* — i.e., a function of a function. Note that it would actually be *incorrect* to write $F[f(x)]$ as this would imply that F depended only upon f evaluated at the single point x , whereas $F[f]$ tells us that F depends upon f at all values of x . (This incorrect notation is used far too often in the literature and should be strongly discouraged!) The corresponding differential form is written,

$$\delta F = \int \frac{\delta F}{\delta f(x)} dx. \quad (3.105)$$

The sum in Eq. (3.104) has been replaced by an integral as is expected for a continuous variable. Note the distinction between the three types of differentials d , ∂ , and δ . Nevertheless they often behave in very similar ways (albeit with occasional important differences [33].)

Now let us apply the calculus of variations to a practical problem. The variational principle tells us that,

$$E_0 \leq \langle \Psi | \hat{H} | \Psi \rangle = \int \Psi^* \hat{H} \Psi, \quad (3.106)$$

subject to the normalization condition,

$$1 = \langle \Psi | \Psi \rangle = \int \Psi^* \Psi. \quad (3.107)$$

(I have suppressed the differential in the integral as is often done in informal writing among theorists. I am trusting that this will not cause confusion. I will put it back in when it seems important.) We may solve the minimization problem with the method of Lagrange multipliers by minimizing,

$$L[\Psi, \Psi^*] = \langle \Psi | \hat{H} | \Psi \rangle - W (\langle \Psi | \Psi \rangle - 1) = \int \Psi^* \hat{H} \Psi - W \left(\int \Psi^* \Psi - 1 \right). \quad (3.108)$$

The corresponding differential

$$\begin{aligned} \delta L[\Psi, \Psi^*] &= L[\Psi + \delta\Psi, \Psi^* + \delta\Psi^*] - L[\Psi, \Psi^*] \\ &= \int \delta\Psi^* (\hat{H} - W) \Psi + \int \Psi^* (\hat{H} - W) \delta\Psi \\ &= \int \delta\Psi^* (\hat{H} - W) \Psi + \int [\hat{H} - W^*]^* \delta\Psi \end{aligned} \quad (3.109)$$

is zero at a minimum. As the two variations, $\delta\Psi$ and $\delta\Psi^*$, are independent, we have (over range of the integration) that,

$$\begin{aligned} (\hat{H} - W)\Psi &= 0 \\ (\hat{H} - W^*)\Psi &= 0, \end{aligned} \quad (3.110)$$

or just,

$$\begin{aligned} \hat{H}\Psi &= W\Psi \\ \hat{H}\Psi &= W^*\Psi. \end{aligned} \quad (3.111)$$

We recognize that these are just the time-independent Schrödinger equation and that W is the energy. Also $W = W^*$ must be real valued. Probably most readers will have seen this derivation without functional derivatives, so there is very little new here except the use of variational calculus instead of more familiar calculus.

The method becomes more powerful when we have a variational energy functional $E(\{\psi_i, \psi_i^*\})$ expressed in terms of orthonormal orbitals $\langle \psi_i | \psi_j \rangle$. This functional should be real valued, so that $E^*(\{\psi_i, \psi_i^*\}) = E(\{\psi_i, \psi_i^*\})$ and it should also be unitarily invariant. A unitary matrix \mathbf{U} is one whose adjoint is its inverse,

$$\begin{aligned} \mathbf{U}^\dagger &= \mathbf{U}^{-1} \\ \mathbf{1} &= \mathbf{U}\mathbf{U}^\dagger = \mathbf{U}^\dagger\mathbf{U} \\ \delta_{i,j} &= \sum_k U_{i,k} U_{k,j}^\dagger = \sum_k U_{i,k}^\dagger U_{k,j} \\ \delta_{i,j} &= \sum_k U_{i,k} U_{j,k}^* = \sum_k U_{k,i}^* U_{k,j}. \end{aligned} \quad (3.112)$$

We want $E(\{\psi_i, \psi_i^*\})$ to be invariant under a unitary transformation of the occupied orbitals. When this happens, we can normally rewrite $E(\{\psi_i, \psi_i^*\})$ as $E(\gamma)$, where

$$\gamma(1, 2) = \sum_i^{\text{occ}} \psi_i(1) \psi_i^*(2), \quad (3.113)$$

is called the density matrix and its diagonal element

$$\rho(1) = \gamma(1, 1) \quad (3.114)$$

is the density. These conditions are very general as almost all types of density-functional theory only depend upon the density-matrix.

[This terminology is confusing! It might be better to call

$$\hat{\gamma} = \sum_i |\psi_i\rangle n_i \langle \psi_i| \quad (3.115)$$

the density operator where n_i is the occupation number of the orbital ψ_i . Then $\gamma(1, 2)$ is the kernal of the density operator, defined by

$$\hat{\gamma}\varphi(1) = \int \gamma(1, 2)\varphi(2) d2, \quad (3.116)$$

for an arbitrary function φ . Given a (non-orthonormal) discrete basis set $\{\chi_\mu\}$, it might seem natural to define the density matrix as

$$\gamma_{\mu,\nu} = \langle \chi_\mu | \hat{\gamma} | \chi_\nu \rangle, \quad (3.117)$$

but quantum chemists generally prefer to define the density matrix in this basis as

$$\mathbf{P} = \mathbf{S}^{-1} \gamma \mathbf{S}^{-1}, \quad (3.118)$$

where

$$S_{\mu,\nu} = \langle \chi_\mu | \chi_\nu \rangle \quad (3.119)$$

is the overlap matrix for the basis set (and P is a capital ρ , for density.) Clearly $\mathbf{P} = \gamma$ for an orthonormal basis set ($\mathbf{S} = \mathbf{1}$.) For better or for worse, these three quantities (the operator $\hat{\gamma}$, the kernel $\gamma(1, 2)$, and the matrix \mathbf{P}) are traditionally (even if sloppily) all called “the density matrix.”]

Unitary invariance means that the density matrix is invariant under a unitary transformation of the occupied orbitals,

$$\tilde{\psi}_i = \sum_j \psi_j U_{j,i}. \quad (3.120)$$

It is then easy to show unitary invariance:

$$\begin{aligned} \gamma(1, 2) &= \sum_i \tilde{\psi}_i(1) \tilde{\psi}_i^*(2)_i \\ &= \sum_i \left(\sum_j \psi_j(1) U_{j,i} \right) \left(\sum_k \psi_k(2) U_{k,i} \right)^* \\ &= \sum_{j,k} \psi_j(1) \left(\sum_k U_{j,i} U_{k,i}^* \right) \psi_k^*(2) \\ &= \sum_{j,k} \psi_j(1) \delta_{j,k} \psi_k^*(2) \\ &= \sum_j \psi_j(1) \psi_j^*(2) \\ &= \sum_i \psi_i(1) \psi_i^*(2). \end{aligned} \quad (3.121)$$

Let us now return to the problem of minimizing the $E(\{\psi_i, \psi_i^*\})$ subject to the orthonormality constraint $\langle \psi_i | \psi_j \rangle = \delta_{i,j}$. This is typically done with the method of Lagrange multipliers and will lead to an orbital Schrödinger equation with hamiltonian \hat{h} defined by

$$n_i \hat{h} \psi_i(1) = \frac{\delta E}{\delta \psi_i^*(1)} = \frac{\delta E^*}{\delta \psi_i^*(1)} \quad (3.122)$$

(because $E = E^*$ is real valued.) [The reader will find a small exercise to do below which should help to clarify any mysteries surrounding Eq. (3.122).] The Lagrangian is

$$L(\{\psi_i, \psi_i^*\}) = E(\{\psi_i, \psi_i^*\}) - \sum_{k,j} \sqrt{n_j} \epsilon_{j,k} \sqrt{n_k} \left(\int \psi_k^*(1) \psi_j(1) d1 - \delta_{k,j} \right). \quad (3.123)$$

The corresponding differential is

$$\begin{aligned}
\delta L(\{\psi_i, \psi_i^*\}) &= \sum_j \int \left(\frac{\delta E(\{\psi_i, \psi_i^*\})}{\delta \psi_j(1)} - \sum_k \sqrt{n_j} \epsilon_{j,k} \sqrt{n_k} \psi_k^*(1) \right) \delta \psi_j(1) d1 \\
&+ \sum_k \int \left(\frac{\delta E(\{\psi_i, \psi_i^*\})}{\delta \psi_k^*(1)} - \sum_j \psi_j(1) \sqrt{n_j} \epsilon_{j,k} \sqrt{n_k} \right) \delta \psi_k^*(1) d1 \\
&= \sum_j \int \left(\frac{\delta E^*(\{\psi_i, \psi_i^*\})}{\delta \psi_j^*(1)} - \sum_k \psi_k(1) \sqrt{n_k} \epsilon_{k,j}^\dagger \sqrt{n_j} \right)^* \delta \psi_j(1) d1 \\
&+ \sum_k \int \left(\frac{\delta E(\{\psi_i, \psi_i^*\})}{\delta \psi_k^*(1)} - \sum_j \psi_j(1) \sqrt{n_j} \epsilon_{j,k} \sqrt{n_k} \right) \delta \psi_k^*(1) d1 \\
&= \sum_j \int \left(n_j \hat{h} \psi_j(1) - \sum_k \psi_k(1) \sqrt{n_k} \epsilon_{k,j}^\dagger \sqrt{n_j} \right) * \delta \psi_j(1) d1 \\
&+ \sum_k \int \left(n_k \hat{h} \psi_k(1) - \sum_j \psi_j(1) \sqrt{n_j} \epsilon_{j,k} \sqrt{n_k} \right) \delta \psi_k^*(1) . \tag{3.124}
\end{aligned}$$

As the variations over the $\delta \psi_j$ and over $\delta \psi_j^*$ are independent, we arrive at

$$\begin{aligned}
n_i \hat{h} \psi_i(1) &= \sum_j \psi_j(1) \sqrt{n_j} \epsilon_{j,i} \sqrt{n_i} \\
n_i \hat{h} \psi_i(1) &= \sum_j \psi_j(1) \sqrt{n_j} \epsilon_{j,i}^\dagger \sqrt{n_i} . \tag{3.125}
\end{aligned}$$

If we are only interested in occupied orbitals, then we can set the occupation numbers equal to unity to get

$$\begin{aligned}
\hat{h} \psi_i(1) &= \sum_j \psi_j(1) \epsilon_{j,i} \\
\hat{h} \psi_i(1) &= \sum_j \psi_j(1) \epsilon_{i,j}^\dagger , \tag{3.126}
\end{aligned}$$

which shows that

$$\begin{aligned}
\epsilon_{j,i} &= \epsilon_{i,j}^\dagger \\
\epsilon &= \epsilon^\dagger . \tag{3.127}
\end{aligned}$$

Since $E(\{\psi_i, \psi_i^*\})$ was chosen to be unitarily invariant, we may use this degree of freedom to choose *canonical* orbitals which diagonalize the ϵ matrix. This finally gives the sought-after orbital equation,

$$\hat{h} \psi_i(1) = \epsilon_i \psi_i(1) . \tag{3.128}$$

3.3.2 Mathematical Formalism and the Hellmann-Feynman Theorem

In order to calculate forces, we first need a mathematical formalism. This is provided by first making the Born-Oppenheimer separation of electronic and nuclear degrees of freedom and solving the Schrödinger equation for the many-electron problem within the field of the fixed nuclei,

$$\hat{H}(\mathbf{R}) \Psi(\mathbf{R}) = E(\mathbf{R}) \Psi(\mathbf{R}) , \tag{3.129}$$

where

$$\begin{aligned}\mathbf{R} &= (\vec{R}_1, \vec{R}_2, \dots, \vec{R}_N) \\ \vec{R}_q &= \begin{pmatrix} X_q \\ Y_q \\ Z_q \end{pmatrix}\end{aligned}\quad (3.130)$$

are the nuclear coordinates. (Note that \mathbf{R} is a $3 \times N$ matrix, consisting of N column vectors, each of length 3.) In addition, we will require that the wave function is normalized,

$$\langle \Psi(\mathbf{R}) | \Psi(\mathbf{R}) \rangle = 1. \quad (3.131)$$

Note that the notation $\langle \cdots \rangle$ refers *only* to integration over electron coordinates! Then

$$E(\mathbf{R}) = \langle \Psi(\mathbf{R}) | \hat{H}(\mathbf{R}) | \Psi(\mathbf{R}) \rangle, \quad (3.132)$$

and the potential energy surface (PES) $V(\mathbf{R})$ is,

$$V(\mathbf{R}) = E(\mathbf{R}) + V_{N,N}(\mathbf{R}), \quad (3.133)$$

where

$$V_{N,N}(\mathbf{R}) = \sum_{I,J} \frac{Z_I Z_J}{R_{I,J}} \quad (3.134)$$

is the potential energy in Hartree atomic units (i.e., Gaussian electromagnetic units with $m_e = e = \hbar = 1$) due to the repulsion between nuclei. The R_q component of the force is given by Eq. (3.102). So this is what we want to calculate. In order to make the formalism ever so slightly more general, I am going to replace R_q with ξ in order to include such things as the strength of an applied field, because the formalism that I am about to present may also be used to calculate not just forces but also such things as dipole moments which are derivatives of the energy with respect to the strength of an applied electric field.

Thus we want to calculate,

$$\frac{dV}{d\xi} = \left\langle \frac{d\Psi}{d\xi} \right| \hat{H} \left| \Psi \right\rangle + \left\langle \Psi \right| \frac{d\hat{H}}{d\xi} \left| \Psi \right\rangle + \left\langle \Psi \right| \hat{H} \left| \frac{d\Psi}{d\xi} \right\rangle + \frac{dV_{N,N}}{d\xi}. \quad (3.135)$$

We may now use Eq. (3.129) to rewrite this last equation as,

$$\begin{aligned}\frac{dV}{d\xi} &= \left\langle \Psi \right| \frac{d\hat{H}}{d\xi} \left| \Psi \right\rangle + \frac{dV_{N,N}}{d\xi} + E \left(\left\langle \frac{d\Psi}{d\xi} \right| \Psi \right\rangle + \left\langle \Psi \right| \frac{d\Psi}{d\xi} \right) \\ &= \left\langle \Psi \right| \frac{d\hat{H}}{d\xi} \left| \Psi \right\rangle + \frac{\partial V_{N,N}}{\partial \xi} + E \frac{d\langle \Psi | \Psi \rangle}{d\xi}.\end{aligned}\quad (3.136)$$

However, because the wave function is normalized [Eq. (3.131)], the last term vanishes and we arrive at just

$$\frac{dV}{d\xi} = \left\langle \Psi \right| \frac{d\hat{H}}{d\xi} \left| \Psi \right\rangle + \frac{dV_{N,N}}{d\xi}. \quad (3.137)$$

This is the celebrated Hellmann-Feynman theorem [121, 122, 123, 124]. In the case of forces, it becomes

$$\frac{\partial V}{\partial R_q} = \left\langle \Psi \right| \frac{\partial V_{N,e}}{\partial R_q} \left| \Psi \right\rangle + \frac{\partial V_{N,N}}{\partial R_q}, \quad (3.138)$$

where

$$V_{N,e} = - \sum_{I,i} \frac{Z_I}{|\vec{R}_I - \vec{r}_i|} \quad (3.139)$$

is the electron-nucleus attraction potential energy term. *Voilà* for the wave function case!

In DFT, the energy expression is $E(\{\psi_i, \psi_i^*\}, \eta)$. Let us introduce a special notation for the derivative of the PES when the orbitals are held constant,

$$V^{(\xi)} = \left(\frac{\partial V}{\partial \xi} \right)_{\{\psi_i, \psi_i^*\}} . \quad (3.140)$$

(Be careful! Later I will use the notation $V^\xi \neq V^{(\xi)}$. I have deliberately made the notations similar, but different, because they describe similar, but different, concepts.) Then

$$\begin{aligned} \frac{dV}{d\xi} &= V^{(\xi)} + \sum_i \int \frac{\delta E}{\delta \psi_i(1)} \frac{\partial \psi_i(1)}{\partial \xi} d1 + \sum_i \int \frac{\delta E}{\delta \psi_i^*(1)} \frac{\partial \psi_i^*(1)}{\partial \xi} d1 \\ &= V^{(\xi)} + \sum_i \int \left(\frac{\delta E}{\delta \psi_i^*(1)} \right)^* \frac{\partial \psi_i(1)}{\partial \xi} d1 + \sum_i \int \frac{\delta E}{\delta \psi_i^*(1)} \frac{\partial \psi_i^*(1)}{\partial \xi} d1 \\ &= V^{(\xi)} + \sum_i \int \left(n_i \hat{h} \psi_i(1) \right)^* \frac{\partial \psi_i(1)}{\partial \xi} d1 + \sum_i \int \left(n_i \hat{h} \psi_i(1) \right) \frac{\partial \psi_i^*(1)}{\partial \xi} d1 . \end{aligned} \quad (3.141)$$

Using the eigenfunction condition of Eq. (3.128) gives,

$$\begin{aligned} \frac{dV}{d\xi} &= V^{(\xi)} + \sum_i n_i \langle \psi_i | \hat{h} | \frac{\partial \psi_i}{\partial \xi} \rangle + \sum_i n_i \langle \frac{\partial \psi_i}{\partial \xi} | \hat{h} | \psi_i \rangle \\ &= V^{(\xi)} + \sum_i n_i \epsilon_i \left(\langle \langle \psi_i | \frac{\partial \psi_i}{\partial \xi} \rangle + \langle \frac{\partial \psi_i}{\partial \xi} | \psi_i \rangle \right) \\ &= V^{(\xi)} + \sum_i n_i \epsilon_i \frac{\partial \langle \psi_i | \psi_i \rangle}{\partial \xi_i} \\ &= V^{(\xi)} + \sum_i n_i \epsilon_i \frac{1}{\partial \xi_i} \\ &= V^{(\xi)} . \end{aligned} \quad (3.142)$$

This proves the Hellmann-Feynman theorem for DFT (and Hartree-Fock, which may be regarded as a particular DFA.) In particular, the force equation is

$$\frac{\partial V}{\partial R_q} = \sum_i n_i \langle \psi_i | \frac{\partial V_{N,e}}{\partial R_q} | \psi_i \rangle + \frac{\partial V_{N,N}}{\partial R_q} . \quad (3.143)$$

3.3.3 Numerical Method and Pulay Forces

Many quantum chemistry programs, including DEMON2K, are based upon expanding the molecular orbitals (MOs) ψ_i as a linear combination of atom-centered “atomic orbitals” (AOs) χ_μ ,

$$\psi_i(1) = \sum_\mu \chi_\mu(1) C_{\mu,i} . \quad (3.144)$$

This is sometimes called the LCAO approximation where LCAO stands for “linear combination of atomic orbitals.” However, as discussed in Sec. 2.1, these AOs are not really AOs but just atom-centered basis functions. (Note the use of the common convention that the MOs have Latin labels but the AOs have Greek labels.) The orbital Schrödinger equation [Eq. (3.128)] then becomes the matrix pseudo-eigenvalue problem,

$$\mathbf{H}\vec{C}_i = \epsilon_i \mathbf{S}\vec{C}_i, \quad (3.145)$$

and the energy expression involves the MO coefficients \vec{C}_i and integrals over (real) atomic orbitals such as the electron repulsion integral,

$$[\chi_\mu\chi_\nu||\chi_\kappa\chi_\lambda] = [\mu\nu||\kappa\lambda] = \int \int \chi_\mu(1)\chi_\nu(1) \frac{1}{r_{12}} \chi_\kappa(2)\chi_\lambda(2) d1d2 \quad (3.146)$$

(in Mulliken charge-cloud notation.) It is important to understand the paradigm shift: It is now the MO coefficients which play the role in this numerical method that the orbitals played in the mathematical formalism. This effectively creates a parallel but different formalism. We may now repeat the derivation of the analytic derivative of the PES in this formalism and we will see that a new term appears. This new term is called the Pulay force [120] and arises because the AOs move when the nuclei move.

Let us now turn to the problem of differentiating $E[\{C_{\mu,i}\}, \{C_{\mu,i}^*\}, \{\chi_\nu\}, \{\chi_\nu^*\}, \xi]$, which is just the same as $E[\{\psi_i, \psi_i^*\}, \xi]$, except that ψ_i is expanded in the LCAO approximation [Eq. 3.144]. It is usually the case that the AOs and MO coefficients are real valued in quantum chemical calculations, although there are exceptions. (NMR calculations involving magnetic fields are one case that springs to mind where complex-valued orbitals are often used.) So $E[\{C_{\mu,i}\}, \{C_{\mu,i}^*\}, \{\chi_\nu\}, \{\chi_\nu^*\}, \xi]$ reduces to $E[\{C_{\mu,i}\}, \{\chi_\nu\}, \xi]$. We will make this assumption because it leads to more compact equations without any fundamental loss of understanding. However there will also be some factors of two which come from the equivalence of derivatives with respect to the variable and its complex conjugate. The energy is thus an equation involving MO coefficients and integrals expressed over AOs.

Taking the derivative of the integrals only leads to so-called *skeleton terms*. Let us make this more precise. *We will introduce the notation V^ξ which means something different from the notation $V^{(\xi)}$ earlier introduced, but which provides a better reflection of the paradigm shift in our point of view.* Given an arbitrary quantity A , then

$$A^\xi = \left(\frac{\partial A}{\partial \xi} \right)_{\{C_{\mu,i}\}}. \quad (3.147)$$

This is a *skeleton term*. It means that include only derivatives of AO integrals with respect to ξ , including any constant terms (i.e., trivial “integrals.”) This is very convenient within the context of our numerical method. The relation with our previous notation is that,

$$\begin{aligned} \frac{dA}{d\xi} &= \underbrace{\left(\frac{\partial A}{\partial \xi} \right)_{\{C_{\mu,i}\}, \{\chi_\mu\}}}_{A^{(\xi)}} + \sum_\nu \int \left(\frac{\delta A}{\delta \chi_\nu(1)} \right)_{\{C_{\mu,i}\}} \frac{\partial \chi_\nu(1)}{\partial \xi} d1 + \sum_{\mu,i} \left(\frac{\partial A}{\partial C_{\mu,i}} \right)_{\{\chi_\nu\}} \frac{\partial C_{\mu,i}}{\partial \xi} \\ &= A^{(\xi)} + \underbrace{\sum_\nu \int \left(\frac{\delta A}{\delta \chi_\nu(1)} \right)_{\{C_{\mu,i}\}} \frac{\partial \chi_\nu(1)}{\partial \xi} d1}_{A^\xi} + \sum_{\mu,i} \left(\frac{\partial A}{\partial C_{\mu,i}} \right)_{\{\chi_\nu\}} \frac{\partial C_{\mu,i}}{\partial \xi} \\ &= A^\xi + \sum_{\mu,i} \left(\frac{\partial A}{\partial C_{\mu,i}} \right)_{\{\chi_\nu\}} \frac{\partial C_{\mu,i}}{\partial \xi}. \end{aligned} \quad (3.148)$$

Let us specialize to the case of the electronic energy. Then the last term may be transformed,

$$\begin{aligned} \sum_{\mu,i} \left(\frac{\partial E}{\partial \psi_i(1)} \right)_{\{\chi_\nu\}} \frac{\partial C_{\mu,i}}{\partial \xi} &= \sum_{\mu,i} \left(\int \frac{\delta E}{\delta \psi_i(1)} \frac{\partial \psi_i(1)}{\partial C_{\mu,i}} d1 \right)_{\{\chi_\nu\}} \frac{\partial C_{\mu,i}}{\partial \xi} \\ &= 2 \sum_{\mu,i} n_i \int \chi_\mu(1) \hat{h} \psi_i(1) \frac{\partial C_{\mu,i}}{\partial \xi} \\ &= 2 \sum_i n_i \int \left(\sum_\mu \chi_\mu(1) \frac{\partial C_{\mu,i}}{\partial \xi} \right) \hat{h} \psi_i(1) d1. \end{aligned} \quad (3.149)$$

(The factor of two is because the derivatives with respect to ψ_i^* and with respect to ψ_i are the same when working with real functions.) The last term in parentheses in Eq. (3.149) is usually rewritten as

$$\sum_\nu \chi_\nu(1) \frac{\partial C_{\nu,j}}{\partial \xi} = \sum_i \psi_i(1) U_{i,j}^\xi, \quad (3.150)$$

because it is often more convenient to work in the MO representation rather than in the AO representation. Note that the \mathbf{U}^ξ is *not* a skeleton term. Rather they are referred to as the *coupled perturbed coefficients*.

The coupled perturbed coefficients are important enough that they are worth studying in more detail. I will temporarily allow the wave functions to be complex-valued because it does not complicate the notation much and does increase the rigor. Left multiplying Eq. (3.150) by $\psi_k^*(1)$ and integrating (“multigrating”) gives

$$\sum_\nu \langle \psi_k | \chi_\nu \rangle \frac{\partial C_{\nu,j}}{\partial \xi} = U_{k,j}^\xi, \quad (3.151)$$

because of $\langle \psi_i | \psi_j \rangle = \delta_{i,j}$. But

$$\langle \psi_k | \chi_\nu \rangle = \sum_\mu C_{\mu,k}^* S_{\mu,\nu}. \quad (3.152)$$

Hence we finally obtain,

$$\begin{aligned} U_{k,j}^\xi &= \sum_{\mu,\nu} C_{\mu,k}^* S_{\mu,\nu} \frac{\partial C_{\nu,j}}{\partial \xi} \\ \mathbf{U}^\xi &= \mathbf{C}^\dagger \mathbf{S} \frac{\partial \mathbf{C}}{\partial \xi} \end{aligned} \quad (3.153)$$

Of course,

$$U_{k,j}^{\xi,*} = \sum_{\mu,\nu} C_{\mu,k} S_{\mu,\nu}^* \frac{\partial C_{\nu,j}^*}{\partial \xi} = \sum_{\mu,\nu} \frac{\partial C_{\nu,j}^*}{\partial \xi} S_{\nu,\mu} C_{\mu,k}. \quad (3.154)$$

Another important relation is something that I call the *turn-over rule*. ($A_{i,j}^\dagger = A_{j,i}^*$ which defines the adjoint of an operator is also known as the turn-over rule.) The turn-over rule is obtained by differentiating the orthonormality condition,

$$\delta_{i,j} = \langle \psi_i | \psi_j \rangle = \sum_{\mu,\nu} C_{\mu,i}^* S_{\mu,\nu} C_{\nu,j}. \quad (3.155)$$

Then

$$\begin{aligned}
0 &= \frac{\partial \delta_{i,j}}{\partial \xi} \\
&= \sum_{\mu,\nu} \frac{\partial C_{\mu,i}^*}{\partial \xi} S_{\mu,\nu} C_{\nu,j} + \sum_{\mu,\nu} C_{\mu,i}^* \frac{\partial S_{\mu,\nu}}{\partial \xi} C_{\nu,j} + \sum_{\mu,\nu} C_{\mu,i}^* S_{\mu,\nu} \frac{\partial C_{\nu,j}}{\partial \xi} \\
&= U_{j,i}^{\xi,*} + S_{i,j}^{\xi} + U_{i,j}^{\xi}.
\end{aligned} \tag{3.156}$$

So

$$U_{j,i}^{\xi,*} = -U_{i,j}^{\xi} - S_{i,j}^{\xi}, \tag{3.157}$$

which is the sought-after turn-over rule for the coupled perturbed coefficients. The diagonal case is particularly important,

$$\Re U_{i,i}^{\xi} = -\frac{1}{2} S_{i,i}^{\xi}. \tag{3.158}$$

We will now return to real functions, so

$$U_{i,i}^{\xi} = -\frac{1}{2} S_{i,i}^{\xi}. \tag{3.159}$$

We may now return to the energy derivative. Equation (3.149) now reads,

$$\begin{aligned}
V_P^{\xi} &= \sum_{\mu,i} \left(\frac{\partial E}{\partial \psi_i(1)} \right)_{\{\chi_{\nu}\}} \frac{\partial C_{\mu,i}}{\partial \xi} \\
&= 2 \sum_i n_i \int \left(\sum_j \psi_j(1) U_{j,i}^{\xi} \right) \hat{h} \psi_i(1) d1 \\
&= 2 \sum_i n_i \sum_j U_{j,i}^{\xi} \langle \psi_j | \hat{h} | \psi_i \rangle \\
&= 2 \sum_i n_i \epsilon_i U_{i,i}^{\xi} \\
&= - \sum_i n_i \epsilon_i S_{i,i}^{\xi} \\
&= - \sum_{\mu,\nu} \underbrace{\sum_i C_{\mu,i} n_i \epsilon_i C_{\nu,i}}_{W_{\mu,\nu}} S_{\nu,\mu}^{\xi} \\
&= -\text{tr}(\mathbf{WS}^{\xi}).
\end{aligned} \tag{3.160}$$

(Notice that \mathbf{S}^{ξ} could refer either to derivatives in the AO or MO representation. Here it refers to the AO representation.) V_P^{ξ} is the *Pulay force* V_P^{ξ} which must be added to V^{ξ} to get $dV/d\xi$. The quantity,

$$W_{\mu,\nu} = \sum_i C_{\mu,i} n_i \epsilon_i C_{\nu,i} \tag{3.161}$$

is the *energy-weighted density matrix*. Notice that this expression for V_P^{ξ} depends on having a well-converged self-consistent field (SCF) calculation so that the canonical MOs diagonalize the orbital hamiltonian matrix. The final force equation reads

$$\frac{\partial V}{\partial R_q} = V^{R_q} + V_P^{R_q}. \tag{3.162}$$

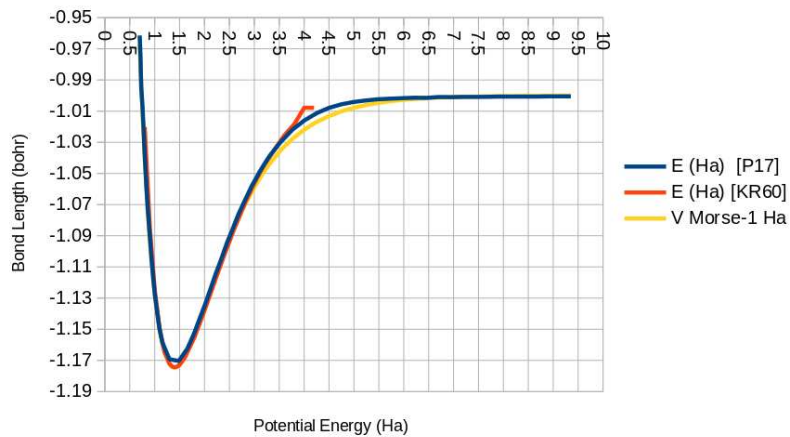


Figure 3.10: Comparison of the Morse potential (shifted down by 1 Ha) with the high-quality results of Refs. [106, 125]. Parameters: $R_e = 1.4$ bohr, $D_e = 0.174442$ Ha, and $a = 1.05103/\text{bohr}$.

We will explore the question of how well the SCF needs to be converged to have accurate forces in the exercise section below. Notice also that we never actually have to solve for the coupled perturbed coefficients, but rather we must take derivatives of the overlap matrix, a “simple” skeleton term. This is good because solving for the coupled perturbed coefficients can become quite involved.

3.3.4 Walking on the Potential Energy Surface

We know how the PES $V(R)$ is calculated and how its analytic derivatives $V'(R)$ are calculated. This means that we should be able to develop an algorithm for finding stationary points on the PES. In general this means starting from an initial *guess* for the structure of the molecule and then *walking* (this is a useful but nontechnical term) in a directed way towards the expected position of a stationary point, and back tracking if necessary if we accidentally walk past it. Such an algorithm is (at least informally) called a (PES) *walker*. We will discuss one possible walker in the context of searching for the minimum energy geometry R_e on the H_2 potential energy curve.

Let us start out with something concrete, namely the Morse potential approximation to the potential energy curve of a diatomic: [126]

$$\begin{aligned} V(R) &= D_e e^{-a(R-R_e)} (e^{-a(R-R_e)} - 2) \\ &= D_e [a^2(R-R_e)^2 - 1] + \text{HOT}, \end{aligned} \quad (3.163)$$

where “HOT” stands for “higher-order terms.” The Morse potential has several advantages, including that the vibrational Schrödinger equation is analytically solvable. Here we are only interested in the Morse potential as a convenient “generic” potential energy curve. The Taylor’s expansion around R_e shows that D_e is the binding energy. Also

$$\begin{aligned} V'(R) &= 2aD_e e^{-a(R-R_e)} (1 - e^{-a(R-R_e)}) \\ &= D_e 2a(R-R_e) + \text{HOT}, \end{aligned} \quad (3.164)$$

and

$$\begin{aligned} V''(R) &= 2a^2 D_e e^{-a(R-R_e)} (2e^{-a(R-R_e)} - 1) \\ &= 2a^2 D_e + \text{HOT}. \end{aligned} \quad (3.165)$$

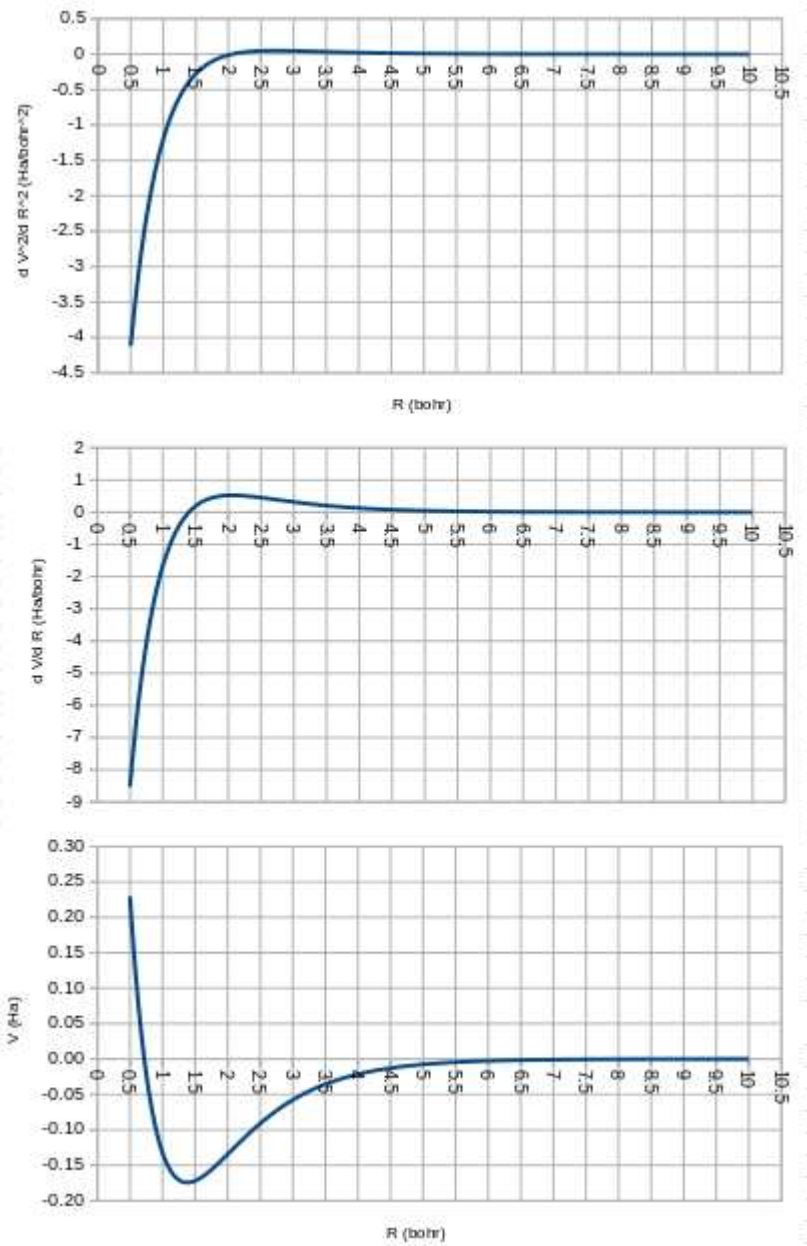


Figure 3.11: Morse potential and its first two derivatives. Parameters: $R_e = 1.4$ bohr, $D_e = 0.174442$ Ha, and $a = 1.05103$ /bohr.

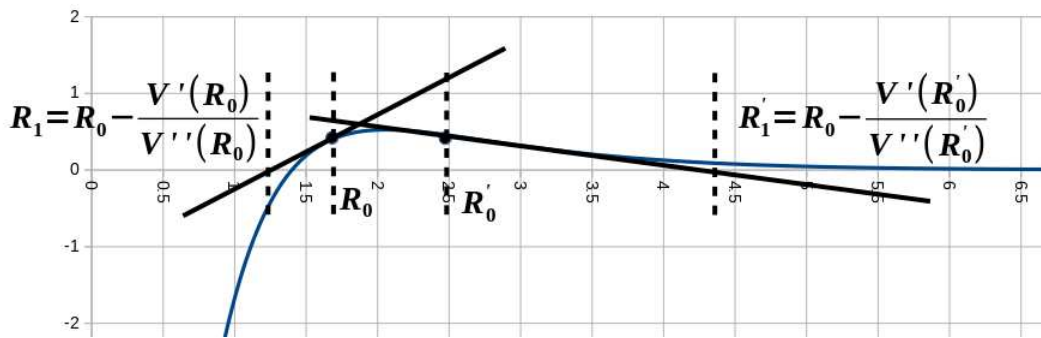


Figure 3.12: Newton’s algorithm for finding stationary points of $V(R)$ by finding zeros of $V'(R)$.

Figure 3.10 shows how well the Morse potential fits high-quality potential energy curves for H_2 .

Figure 3.11 shows the Morse potential $V(R)$, its first derivative $V'(R)$, and its second derivative $V''(R)$. As expected, $V'(R) = 0$ where $V(R)$ is a minimum. Also $V''(R) = 0$ where $V'(R)$ has a maximum.

In general in quantum chemistry, second derivatives are more costly to compute than first derivatives so many walkers often restrict themselves to using first derivatives (and approximate second derivatives.) Our strategy will be to create an algorithm that begins with an initial value $R = R_0$ and then goes through a succession of values R_1, R_2, \dots to find where $V'(R) = 0$ to within some predetermined convergence factor. Newton’s method is a well-known numerical algorithm to find the zeros of a function. In this case we would need the second derivative $V''(R)$, but it is still worth thinking about. So suppose we have an initial value of the geometry R_0 . We can approximate $V'(R)$ by the tangent line,

$$V'(R) \approx V'(R_0) + V''(R_0)(R - R_0). \quad (3.166)$$

When this expression is set equal to zero, we have an equation whose solution provides a guess R_1 as to the location of the root:

$$R_1 = R_0 - \frac{V'(R_0)}{V''(R_0)}. \quad (3.167)$$

Once R_1 is found, then the same algorithm is used to find the next value R_2 , etc. Figure 3.12 gives an idea of how this works. The initial guess is quite important as it can determine whether we converge towards the minimum of $V(R)$ or towards a maximum! We may also overstep the zero of $V'(R)$ which is not a problem as long as we come back again to closer to the zero. But sometimes the algorithm will take us farther and farther from the zero. In general, it is best not to extrapolate too far so that we should actually use,

$$R_{i+1} = R_i - \min \left[\frac{V'(R_i)}{V''(R_i)}, \operatorname{sgn} \left(\frac{V'(R_i)}{V''(R_i)} \right) R_{\max} \right], \quad (3.168)$$

where $\operatorname{sgn}(f) = f/|f|$ is the sign function and R_{\max} is a maximum step size to make sure that we do not go too far.

To be more realistic, we should *not* use the second derivative $V''(R)$. Instead we begin with a guess R_0 and take a step $R_1 = R_0 + \Delta R$ for some arbitrary but predetermined step size ΔR so that we have two values of R to start our iterations: $R_i = R_0$ and $R_{i+1} = R_1$. We may then solve the

linear equations,

$$\begin{aligned} V'(R_i) &= mR_i + b \\ V'(R_{i+1}) &= mR_{i+1} + b, \end{aligned} \quad (3.169)$$

to obtain

$$\begin{aligned} m &= \frac{V'(R_{i+1}) - V'(R_i)}{R_{i+1} - R_i} \\ b &= (V'(R_i) - V'(R_{i+1})) R_0. \end{aligned} \quad (3.170)$$

Solving gives,

$$R_{i+1} = \frac{V'(R_{i+1})R_i - V'(R_i)R_{i+1}}{V'(R_{i+1}) - V'(R_i)}, \quad (3.171)$$

which is equivalent to Newton's method with

$$V''(R_i) \approx \frac{V'(R_{i+1}) - V'(R_i)}{R_{i+1} - R_i}. \quad (3.172)$$

A little thought will show that, once we have at least three points, we can fit a parabola and have a better approximation to the second derivative than the most primitive one given in Eq. (3.172). But the objective here is not to present a complete and perfect algorithm for geometry optimizations but rather to help the reader think through some of the considerations that go into building a walker. In our simple-minded approach, Eq. (3.171) is then iterated until

$$|R_{i+1} - R_i| < \epsilon, \quad (3.173)$$

where ϵ is some predetermined convergence criterion. Alternatively the the convergence criterion may be directly on the force:

$$|V'(R_i)| < \epsilon. \quad (3.174)$$

This completes our small discussion of walkers. We may now pass on to the exercises.

3.3.5 Exercises

These exercises are intended to remove some of the abstraction from the mathematical treatment given above.

1. Functional Derivatives

It was promised after Eq. (3.122) to give you an exercise aimed at clarifying the hamiltonian definition,

$$n_i \hat{h} \psi_i(1) = \frac{\delta E}{\delta \psi_i^*(1)}. \quad (3.175)$$

Here then is that exercise. It is a pencil-and-paper exercicise. Please use the functional derivative formalism to take the functional derivatives $\delta/\delta\psi_i^*$ and $\delta/\delta\psi_i^*$ of the generic global hybrid DFA energy expression,

$$E = \sum_i n_i \langle \psi_i | \hat{t} + v | \psi_i \rangle + \frac{1}{2} \int \frac{\rho(1)\rho(2)}{r_{1,2}} d1d2 - a \frac{1}{2} \int \frac{|\gamma(1,2)|^2}{r_{1,2}} d1d2 + b E_x[\rho] + c E_c[\rho]. \quad (3.176)$$

Here a , b , and c are constants (ideally $b = 1 - a$ but this is not always true in practice), $\hat{t} = -\frac{1}{2}\nabla^2$ is the one-electron kinetic energy operator, v is the external potential (i.e., the potential energy of attraction of the electrons to the nuclei and interaction with any applied electric fields). Also the density,

$$\rho(1) = \sum_i n_i |\psi_i(1)|^2, \quad (3.177)$$

and the density matrix,

$$\gamma(1, 2) = \sum_i \psi_i(1) n_i \psi_i^*(2). \quad (3.178)$$

Note that Eq. (3.176) includes the Hartree-Fock approximation. What happens if we use a Thomas-Fermi (like) expression where the kinetic energy term is replaced by a local functional:

$$T_{TF} = \frac{3}{10} (3\pi^2)^{2/3} \int \rho^{5/3}(\vec{r}) d\vec{r}, \quad (3.179)$$

instead of,

$$T_s = \sum_i n_i \langle \psi_i | \hat{t} | \psi_i \rangle ? \quad (3.180)$$

2. SCF Convergence and Forces

When we are learning, the first thing we want to do is to make things work. However we are not really done until we have pushed them to the breaking point and see how and when they can fail¹. The object of this exercise is to make graphs of both the potential energy curve and the forces for H_2 around the equilibrium bond length and to really zoom in on this region to see how the correspondance works between the minimum of the potential energy curve and the position of the zero of the gradient. Use the following input and vary the bond distance and the convergence factor:

```
TITLE H2
#
# --- CHARGE AND MULTILICITY ---
CHARGE 0
MULTI 1
#
# --- CONTROL OPTIONS ---
#
SCFTYPE RKS TOL=1.E-5
OPTIMIZATION MAX=1
VXCTYPE BLYP
#
# --- GEOMETRY ---
#
GEOMETRY CARTESIAN BOHR
H 0.000000 0.000000 0.000000
```

¹One of my doctoral students once remarked that, given a computer game, I would not just play it, but I would always also try to make it fail!

```
H 0.000000 0.000000 1.409800
#
# --- BASIS SETS ---
AUXIS (GEN-A3*)
BASIS (AUG-CC-PV5Z)
```

This asks for a single geometry optimisation step which is adequate to get the program to print out the gradient:

```
RMSQ FORCE : 0.0001611 MAXIMUM : 0.0003000 CONVERGED :YES
MAX FORCE : 0.0001611 MAXIMUM : 0.0004500 CONVERGED :YES
```

The number you want is MAX FORCE = RMSQ FORCE (which are generally different, but which are the same for H₂.) What are the units? What about the sign?

Rather than tell you exactly what to do, I would like you to explore and discuss what you have learned. However I will ask one question to think about: “How tight a convergence do you need to get the bond distance accurate to, say, 5 significant figures?”

3. How Good a Guess Do We Need?

The very crude walker described above suggests that a geometry optimization that begins in a region where $V''(R) > 0$ will diverge towards $R = +\infty$. The walkers used in quantum chemistry programs, such as DEMON2K, are much more sophisticated than this and actually do converge to the proper minimum. Please run the following job to see for yourself:

```
TITLE H2
#
# --- CHARGE AND MULTILICITY ---
CHARGE 0
MULTI 1
#
# --- CONTROL OPTIONS ---
#
SCFTYPE RKS TOL=1.E-8
OPTIMIZATION
VXCTYPE BLYP
#
# --- GEOMETRY ---
#
GEOMETRY CARTESIAN BOHR
H 0.000000 0.000000 0.000000
H 0.000000 0.000000 3.600000
#
# --- BASIS SETS ---
AUXIS (GEN-A3*)
BASIS (AUG-CC-PV5Z)
```


Chapter 4

Lesson 6: Singlet Oxygen, $^1\Delta$ O₂

This lesson is dedicated to Abraham Ponra, without whose thesis project on reactive oxygen species this lesson would not have been here.

Our atmosphere is about 80% N₂ and 20% O₂, both of which are important for life. Our focus here is on oxygen — a very famous molecule! Until late in the 1700s, chemists still spoke of the four elements — earth, fire, air, and water (and sometimes added the aether as a fifth element.) This all changed with the discovery of “fixed air” (CO₂) by Joseph Black in the 1750s, proving that air was not an element because there are different types of “airs” (i.e., gases.) This opened a veritable flood gate to the discovery of different gases during the era termed “pneumatic chemistry” by historians of chemistry. Major among the new “airs” that were discovered was oxygen. While assigning the priority of a discovery (what constitutes a “discovery” — an accidental synthesis without the discoverer recognizing what he found? a full description of the significance of a new find? actually making others aware of the find?) is always a tricky matter, most sources agree that oxygen was first discovered in 1772 by the Swedish chemist Carl Wilhelm Scheele. It was independently discovered by the English (later American) chemist Joseph Priestley in 1774 who was apparently the first to note the physiological effect of O₂.

“I have procured air ... between five and six times as good as the best common air that I have ever met with.” — Joseph Priestley

Perhaps surprisingly to modern readers, chemistry was not yet a quantitative science. This was changed by a contemporary of Priestley, namely the French chemist Antoine Laurent Lavoisier, who famously said,

“Nothing is lost, nothing is created, everything is transformed.” — Antoine Lavoisier

Lavoisier used his very accurate scale (possibly the most accurate one in the world at that time) and his mass conservation law to give birth to what historians of chemistry now call “modern chemistry.” In particular, Lavoisier took it upon himself to re-examine Priestley’s discovery *quantitatively*. Now we will take it upon ourselves to re-examine the electronic structure of O₂ both qualitatively and quantitatively using DFT.

4.0.1 Different Types of Oxygen

The lowest three potential energy curves for O₂ are shown in Fig. 4.1. (See also Refs. [129, 130, 131].) These are the $^3\Sigma_g^-$ ground state, the lowest $^1\Delta_g$ singlet state, and a higher $^1\Sigma_g^+$ excited state. We want to work out the minimal configurations needed to describe these three states. Notice how these

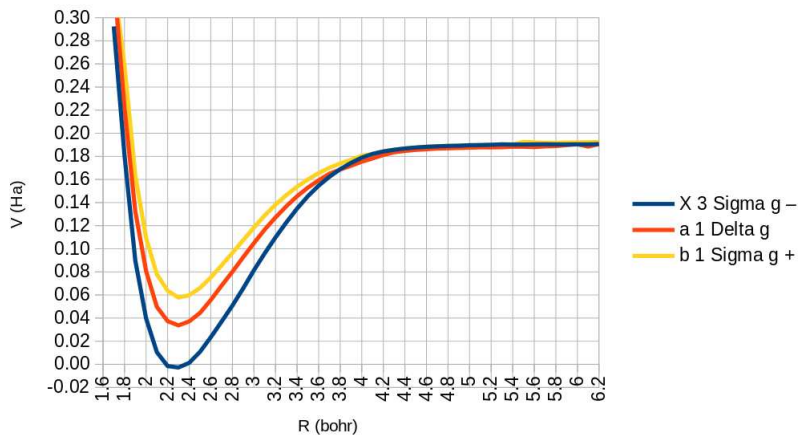
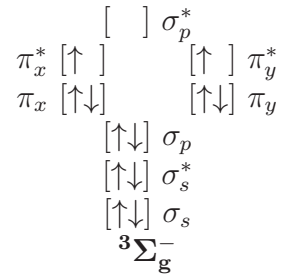


Figure 4.1: O_2 potential energy curves from Fig. 1 of Ref. [127] digitized with WEBPLOTDIGITIZER [128] and redrawn. The zero of energy is the vibrational zero-point energy of the ground state.

states are labeled with group theoretic term symbols. Like other homonuclear diatomics, O_2 belongs to the $D_{\infty h}$ point group whose character table is shown in Table 4.1. Let us consider each of the three states one at a time.

Triplet (${}^3\Sigma_g^-$) Oxygen The most common form of oxygen is the oxygen molecule, O_2 , in its triplet state. Whether this is referred to as a diradical or not is a matter of taste. Whatever the terminology that is used, it is important to realize that O_2 is not especially reactive as radicals go. In particular, it is kinetically rather stable [132]. Figure 4.2 summarizes what we learn in our first-year University chemistry course about the electronic structure of O_2 . Although the Lewis dot structure seems to indicate that all electrons are paired, molecular orbital theory shows that the ground state of O_2 is, in fact, a triplet (3O_2). Nevertheless, the calculation of the bond order index still shows a double bond. As I would like to avoid having to make a new figure each time I want to write a configuration, I will type the electron configuration of triplet oxygen as



This term symbol should be determined by the symmetry point group of the molecule, which is $D_{\infty h}$ and whose character table is shown in Table 4.1, and by the part of the wave function outside of the closed shell—hence by the determinant $|\pi_x^*, \pi_y^*|$. The character table says that this wave function should have the same symmetry as a rotation around the z axis (R_z). Let us check this. In order to do so, we will need two symmetry operations, namely rotation by an angle ϕ around and reflection through a vertical plane passing through the two nuclei and at an angle of ϕ to the x -axis. As for R_z , the rotation should leave the wave function invariant (character +1) while the reflection should change the sign of the wave function (character -1).

Table 4.1: Character table for the $D_{\infty h}$ point group of homonuclear diatomic molecules. The molecule is assumed to lie along the z -axis.

$D_{\infty h}$	E	$2C_\infty$...	$\infty\sigma_v$	i	$2S_\infty$...	$\infty C'_2$	functions
$A_{1g} = \Sigma_g^+$	+1	+1	...	+1	+1	+1	...	+1	$x^2 + y^2, z^2$
$A_{2g} = \Sigma_g^-$	+1	+1	...	-1	+1	+1	...	-1	R_z
$E_{1g} = \Pi_g$	+2	$+2 \cos(\phi)$...	0	+2	$-2 \cos(\phi)$...	0	$(R_x, R_y), (xy, yz)$
$E_{2g} = \Delta_g$	+2	$+2 \cos(2\phi)$...	0	+2	$+2 \cos(2\phi)$...	0	$(x^2 - y^2, xy)$
$E_{3g} = \Phi_g$	+2	$+2 \cos(3\phi)$...	0	+2	$-2 \cos(3\phi)$...	0	
E_{ng}	+2	$+2 \cos(n\phi)$...	0	+2	$(-1)^n 2 \cos(n\phi)$...	0	
⋮	⋮	⋮	⋮	⋮	⋮	⋮	⋮	⋮	⋮
$A_{1u} = \Sigma_u^+$	+1	+1	...	+1	-1	-1	...	-1	$z, z^3, z(x^2 + y^2)$
$A_{2u} = \Sigma_u^-$	+1	+1	...	-1	-1	-1	...	+1	
$E_{1u} = \Pi_u$	+2	$+2 \cos(\phi)$...	0	-2	$+2 \cos(\phi)$...	0	$(x, y), (xz^2, yz^2),$
$E_{2u} = \Delta_u$	+2	$+2 \cos(2\phi)$...	0	-2	$-2 \cos(2\phi)$...	0	$[xyz, z(x^2 - y^2)]$
$E_{3u} = \Phi_u$	+2	$+2 \cos(3\phi)$...	0	-2	$+2 \cos(3\phi)$...	0	$[y(3x^2 - y^2), x(x^2 - 3y^2)]$
E_{nu}	+2	$+2 \cos(n\phi)$...	0	-2	$(-1)^{n+1} 2 \cos(n\phi)$...	0	
⋮	⋮	⋮	⋮	⋮	⋮	⋮	⋮	⋮	⋮

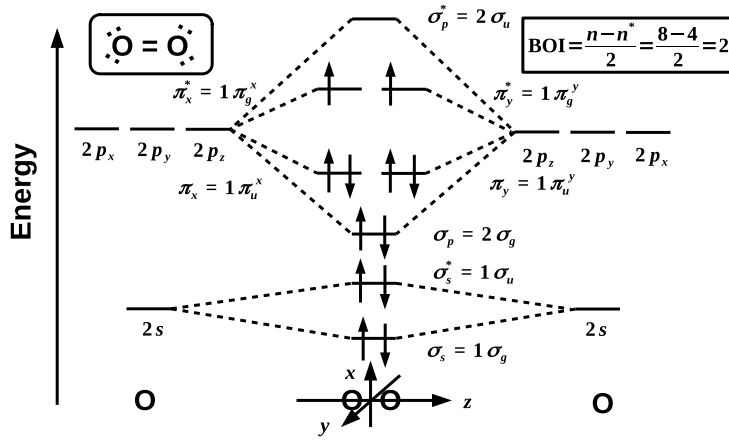


Figure 4.2: First-year University description of the electronic structure of O_2 : atomic orbital/molecular orbital correlation diagram, Lewis dot structure (upper left inset), and calculation of the bond order index (BOI, upper right inset.)

Let us begin with the rotation. Rotating the orbitals by ϕ in the positive (i.e., counter clockwise) direction is equivalent to rotating the (x, y) coordinate system by ϕ in the negative (i.e., clockwise) direction. Before rotation, we have

$$\begin{aligned} x &= r \cos \theta \\ y &= r \sin \theta. \end{aligned} \quad (4.1)$$

After rotation, we have

$$\begin{aligned} x' &= r \cos(\theta + \phi) = r \cos \theta \cos \phi - r \sin \theta \sin \phi \\ &= x \cos \phi - y \sin \phi \\ y' &= r \sin(\theta + \phi) = r \cos \theta \sin \phi + r \sin \theta \cos \phi \\ &= x \sin \phi + y \cos \phi. \end{aligned} \quad (4.2)$$

It is convenient to write this as

$$\begin{pmatrix} x' \\ y' \end{pmatrix} = \mathbf{R}(\phi) \begin{pmatrix} x \\ y \end{pmatrix} \quad (4.3)$$

where the rotation matrix

$$\mathbf{R}(\phi) = \begin{bmatrix} \cos \phi & -\sin \phi \\ \sin \phi & \cos \phi \end{bmatrix}. \quad (4.4)$$

The inverse rotation is given by

$$\mathbf{R}(-\phi) = \begin{bmatrix} \cos \phi & \sin \phi \\ -\sin \phi & \cos \phi \end{bmatrix}, \quad (4.5)$$

as is easily checked by verifying that

$$\mathbf{R}(\phi)\mathbf{R}(-\phi) = \mathbf{1}. \quad (4.6)$$

Let us turn now to reflection through a line at a positive angle ϕ in the (x, y) -plane. If $\phi = 0$, then the line is just the x -axis and the transformation is,

$$\begin{aligned} x' &= x \\ y' &= -y. \end{aligned} \quad (4.7)$$

Let us write this as

$$\begin{pmatrix} x' \\ y' \end{pmatrix} = \sigma_v(0) \begin{pmatrix} x \\ y \end{pmatrix}, \quad (4.8)$$

where

$$\sigma_v(0) = \begin{bmatrix} 1 & 0 \\ 0 & -1 \end{bmatrix}. \quad (4.9)$$

To find the reflection matrix at an arbitrary angle, we can do an old group theoretician's trick called conjugation: we will first rotate by $-\phi$ to move the reflection line onto the x -axis, then we will reflect through the x -axis, and finally we will undo the rotation to place the reflection line in its original position. The new matrix is,

$$\begin{aligned} \sigma_v(\phi) &= \mathbf{R}(\phi)\sigma_v(0)\mathbf{R}(-\phi) \\ &= \begin{bmatrix} \cos \phi & -\sin \phi \\ \sin \phi & \cos \phi \end{bmatrix} \begin{bmatrix} 1 & 0 \\ 0 & -1 \end{bmatrix} \begin{bmatrix} \cos \phi & \sin \phi \\ -\sin \phi & \cos \phi \end{bmatrix} \\ &= \begin{bmatrix} \cos^2 \phi - \sin^2 \phi & 2 \cos \phi \sin \phi \\ 2 \cos \phi \sin \phi & \sin^2 \phi - \cos^2 \phi \end{bmatrix} \\ &= \begin{bmatrix} \cos(2\phi) & \sin(2\phi) \\ \sin(2\phi) & -\cos(2\phi) \end{bmatrix}. \end{aligned} \quad (4.10)$$

Hence reflection through an arbitrary σ_v plane gives,

$$\begin{aligned} x' &= x \cos(2\phi) + y \sin(2\phi) \\ y' &= x \sin(2\phi) - y \cos(2\phi). \end{aligned} \quad (4.11)$$

We may see how the wave function $|\pi_x^*, \pi_y^*|$ transforms under rotation around the bond axis:

$$\begin{aligned} |\pi_{x'}^*, \pi_{y'}^*| &= |\pi_x^* \cos \phi - \pi_y^* \sin \phi, \pi_x^* \sin \phi + \pi_y^* \cos \phi| \\ &= |\pi_x^*, \pi_x^*| \cos \phi \sin \phi + |\pi_x^*, \pi_y^*| \cos^2 \phi - |\pi_y^*, \pi_x^*| \sin^2 \phi + |\pi_y^*, \pi_y^*| \sin \phi \cos \phi \\ &= 0 + |\pi_x^*, \pi_y^*| \cos^2 \phi + |\pi_x^*, \pi_y^*| \sin^2 \phi + 0 \\ &= |\pi_x^*, \pi_y^*| (\cos^2 \phi + \sin^2 \phi) \\ &= |\pi_x^*, \pi_y^*|. \end{aligned} \quad (4.12)$$

The wave function is indeed invariant with respect to a rotation around the z axis, consistent with the +1 character in the $2C_\infty$ column.

We may now see how the wave function $|\bar{\pi}_x^*, \bar{\pi}_y^*|$ changes upon reflection through an arbitrary σ_v axis:

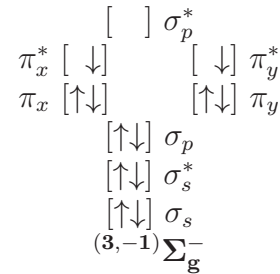
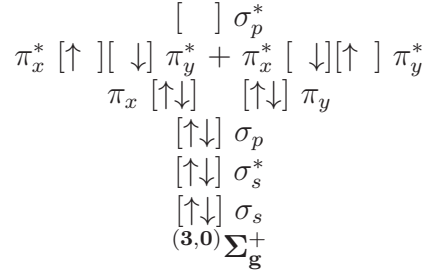
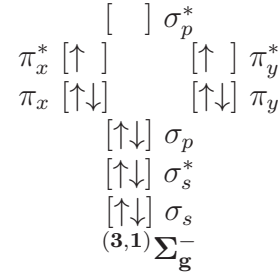
$$\begin{aligned} |\pi_{x'}^*, \pi_{y'}^*| &= |\pi_x^* \cos(2\phi) + \pi_y^* \sin(2\phi), \pi_x^* \sin(2\phi) - \pi_y^* \cos(2\phi)| \\ &= |\pi_x^*, \pi_x^*| \cos(2\phi) \sin(2\phi) - |\pi_x^*, \pi_y^*| \cos^2(2\phi) + |\pi_y^*, \pi_x^*| \sin^2(2\phi) - |\pi_y^*, \pi_y^*| \sin(2\phi) \cos(2\phi) \\ &= 0 - |\pi_x^*, \pi_y^*| \cos^2(2\phi) - |\pi_x^*, \pi_y^*| \sin^2(2\phi) + 0 \\ &= -|\pi_x^*, \pi_y^*| (\cos^2(2\phi) + \sin^2(2\phi)) \\ &= -|\pi_x^*, \pi_y^*|, \end{aligned} \quad (4.13)$$

so the wave function changes sign upon arbitrary reflection through a mirror plane containing the two nuclei. This is why there is a -1 character in the $\infty\sigma_v$ column of the character table.

As everything seems to work fine for the spatial wave function, we now only need to recall that every triplet is three-fold spin degenerate. That is, there are three wave functions, differing only by the value of $M_S = -1, 0, +1$ which have the same energy if we neglect any magnetic field effects. These three Ψ_{S,M_S} wave functions are energetically degenerate because they factor into the same antisymmetric spatial part times one of the three different possible symmetric spin parts:

$$\begin{aligned} \Psi_{1,1} &= |\pi_x^*, \pi_y^*| \\ &= \left[\frac{1}{\sqrt{2}} (\pi_x^*(\vec{r}_1) \pi_y^*(\vec{r}_2) - \pi_y^*(\vec{r}_1) \pi_x^*(\vec{r}_2)) \right] (\alpha_1 \alpha_2) \\ \Psi_{1,0} &= \frac{1}{\sqrt{2}} (|\pi_x^*, \bar{\pi}_y^*| + |\bar{\pi}_x^*, \pi_y^*|) \\ &= \left[\frac{1}{\sqrt{2}} (\pi_x^*(\vec{r}_1) \pi_y^*(\vec{r}_2) - \pi_y^*(\vec{r}_1) \pi_x^*(\vec{r}_2)) \right] \left[\frac{1}{\sqrt{2}} (\alpha_1 \beta_2 + \beta_1 \alpha_2) \right] \\ &= \left[\frac{1}{\sqrt{2}} (\pi_x^*(\vec{r}_1) \pi_y^*(\vec{r}_2) - \pi_y^*(\vec{r}_1) \pi_x^*(\vec{r}_2)) \right] (\alpha_1 \alpha_2) \\ \Psi_{1,-1} &= |\bar{\pi}_x^*, \bar{\pi}_y^*| \\ &= \left[\frac{1}{\sqrt{2}} (\pi_x^*(\vec{r}_1) \pi_y^*(\vec{r}_2) - \pi_y^*(\vec{r}_1) \pi_x^*(\vec{r}_2)) \right] (\beta_1 \beta_2). \end{aligned} \quad (4.14)$$

Here the overbar indicates spin $\beta = \downarrow$ otherwise the spin function associated with the orbital is $\alpha = \uparrow$. It is a bit of a puzzle how to represent these in MO diagrams. I suggest supplementing the multiplicity $2S + 1 = 3$ with the value of M_S , $(2S + 1, M_S)$:



This emphasizes the multideterminantal nature of the $(3,0)\Sigma_g^-$ state.

For completeness we should verify what happens to $\Psi_{1,0}$ under rotation and reflection. Rotation:

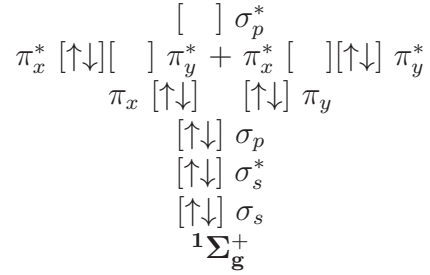
$$\begin{aligned}
 \hat{R}(\phi)\Psi_{1,0} &= \frac{1}{\sqrt{2}} (|\pi_{x'}^* \bar{\pi}_{y'}^*| + |\bar{\pi}_{x'}^* \pi_{y'}^*|) \\
 &= \frac{1}{\sqrt{2}} (|\pi_x^* \cos \phi - \pi_y^* \sin \phi, \bar{\pi}_x^* \sin \phi + \bar{\pi}_y^* \cos \phi| + |\bar{\pi}_x^* \cos \phi - \bar{\pi}_y^* \sin \phi, \pi_x^* \sin \phi + \pi_y^* \cos \phi|) \\
 &= \frac{1}{\sqrt{2}} (|\pi_x^*, \bar{\pi}_x^*| \cos \phi \sin \phi + |\pi_x^*, \bar{\pi}_y^*| \cos^2 \phi - |\pi_y^*, \bar{\pi}_x^*| \sin^2 \phi - |\pi_y^*, \bar{\pi}_y^*| \sin \phi \cos \phi) \\
 &+ \frac{1}{\sqrt{2}} (|\bar{\pi}_x^*, \pi_x^*| \cos \phi \sin \phi + |\bar{\pi}_x^*, \pi_y^*| \cos^2 \phi - |\bar{\pi}_y^*, \pi_x^*| \sin^2 \phi - |\bar{\pi}_y^*, \pi_y^*| \cos \phi \sin \phi) \\
 &= \frac{1}{\sqrt{2}} (|\pi_x^* \bar{\pi}_y^*| + |\bar{\pi}_x^* \pi_y^*|) \\
 &= \Psi_{1,0}
 \end{aligned} \tag{4.15}$$

Reflection:

$$\begin{aligned}
\hat{\sigma}_v(\phi)\Psi_{1,0} &= \frac{1}{\sqrt{2}}(|\pi_x^* \bar{\pi}_{y'}^*| + |\bar{\pi}_x^* \pi_{y'}^*|) \\
&= \frac{1}{\sqrt{2}}|\pi_x^* \cos(2\phi) + \pi_y^* \sin(2\phi), \bar{\pi}_x^* \sin(2\phi) - \bar{\pi}_y^* \cos(2\phi)| \\
&+ \frac{1}{\sqrt{2}}|\bar{\pi}_x^* \cos(2\phi) + \bar{\pi}_y^* \sin(2\phi), \pi_x^* \sin(2\phi) - \pi_y^* \cos(2\phi)| \\
&= \frac{1}{\sqrt{2}}(|\pi_x^*, \bar{\pi}_x^*| \cos(2\phi) \sin(2\phi) - |\pi_x^*, \bar{\pi}_y^*| \cos^2(2\phi) + |\pi_y^*, \bar{\pi}_x^*| \sin^2(2\phi) - |\pi_y^*, \bar{\pi}_y^*| \cos(2\phi) \sin(2\phi)) \\
&+ \frac{1}{\sqrt{2}}(|\bar{\pi}_x^* \pi_x^*| \cos(2\phi) \sin(2\phi) - |\bar{\pi}_x^*, \pi_y^*| \cos^2(2\phi) + |\bar{\pi}_y^*, \pi_x^*| \sin^2(2\phi) - |\bar{\pi}_y^*, \pi_y^*| \cos(2\phi) \sin(2\phi)) \\
&= -\frac{1}{\sqrt{2}}(|\pi_x^*, \bar{\pi}_y^*| + |\bar{\pi}_x^*, \pi_y^*|) \\
&= -\Psi_{1,0}
\end{aligned} \tag{4.16}$$

So the $\Psi_{1,0}$ wave function does indeed transform according to the Σ_g^- representation.

Singlet Sigma Oxygen There are two low-lying singlet excited states of oxygen, namely ${}^1\Delta_g$ and ${}^1\Sigma_g^+$ (Fig. 4.1.) Singlet oxygen usually refers to the lower-energy ${}^1\Delta_g$ state. However we will start with the mathematically-simpler ${}^1\Sigma_g^+$ state here whose configuration is



Notice that I have written this as a linear combination of two determinants. According to the character table, this wave function should transform like $x^2 + y^2$. Its wave function is

$$\Psi = \frac{1}{\sqrt{2}}(|\pi_x^*, \bar{\pi}_x^*| + |\pi_y^*, \bar{\pi}_y^*|) . \tag{4.17}$$

Let us check that it transforms correctly under rotation and reflection.

Rotation:

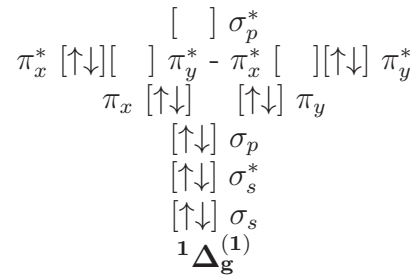
$$\begin{aligned}
 \hat{R}(\phi)\Psi &= \frac{1}{\sqrt{2}} (|\pi_{x'}^*, \bar{\pi}_{x'}^*| + |\pi_{y'}^*, \bar{\pi}_{y'}^*|) \\
 &= \frac{1}{\sqrt{2}} |\pi_x^* \cos \phi - \pi_y^* \sin \phi, \bar{\pi}_x^* \cos \phi - \bar{\pi}_y^* \sin \phi| \\
 &+ \frac{1}{\sqrt{2}} |\pi_x^* \sin \phi + \pi_y^* \cos \phi, \bar{\pi}_x^* \sin \phi + \bar{\pi}_y^* \cos \phi| \\
 &= \frac{1}{\sqrt{2}} (|\pi_x^*, \bar{\pi}_x^*| \cos^2 \phi - |\pi_x^*, \bar{\pi}_y^*| \cos \phi \sin \phi - |\pi_y^*, \bar{\pi}_x^*| \cos \phi \sin \phi + |\pi_y^*, \bar{\pi}_y^*| \sin^2 \phi) \\
 &+ \frac{1}{\sqrt{2}} (|\pi_x^*, \bar{\pi}_x^*| \sin^2 \phi + |\pi_x^*, \bar{\pi}_y^*| \cos \phi \sin \phi + |\pi_y^*, \bar{\pi}_x^*| \cos \phi \sin \phi + |\pi_y^*, \bar{\pi}_y^*| \cos^2 \phi) \\
 &= \frac{1}{\sqrt{2}} (|\pi_x^*, \bar{\pi}_x^*| + |\pi_y^*, \bar{\pi}_y^*|) \\
 &= \Psi
 \end{aligned} \tag{4.18}$$

Reflection:

$$\begin{aligned}
 \hat{\sigma}_v(\phi)\Psi &= \frac{1}{\sqrt{2}} (|\pi_{x'}^*, \bar{\pi}_{x'}^*| + |\pi_{y'}^*, \bar{\pi}_{y'}^*|) \\
 &= \frac{1}{\sqrt{2}} |\pi_x^* \cos(2\phi) + \pi_y^* \sin(2\phi), \bar{\pi}_x^* \cos(2\phi) + \bar{\pi}_y^* \sin(2\phi)| \\
 &+ \frac{1}{\sqrt{2}} |\pi_x^* \sin(2\phi) - \pi_y^* \cos(2\phi), \bar{\pi}_x^* \sin(2\phi) - \bar{\pi}_y^* \cos(2\phi)| \\
 &= \frac{1}{\sqrt{2}} (|\pi_x^*, \bar{\pi}_x^*| \cos^2(2\phi) + |\pi_x^*, \bar{\pi}_y^*| \cos(2\phi) \sin(2\phi) + |\pi_y^*, \bar{\pi}_x^*| \cos(2\phi) \sin(2\phi) + |\pi_y^*, \bar{\pi}_y^*| \sin^2(2\phi)) \\
 &+ \frac{1}{\sqrt{2}} (|\pi_x^*, \bar{\pi}_x^*| \sin^2(2\phi) - |\pi_x^*, \bar{\pi}_y^*| \cos(2\phi) \sin(2\phi) - |\pi_y^*, \bar{\pi}_x^*| \cos(2\phi) \sin(2\phi) + |\pi_y^*, \bar{\pi}_y^*| \cos^2(2\phi)) \\
 &= \frac{1}{\sqrt{2}} (|\pi_x^*, \bar{\pi}_x^*| + |\pi_y^*, \bar{\pi}_y^*|) \\
 &= \Psi
 \end{aligned} \tag{4.19}$$

Hence Ψ belongs to the representation with the character +1 for both $2C_\infty$ and $\infty\sigma_v$, i.e., Σ_g^+ .

Singlet Delta Oxygen (Normal Singlet Oxygen) Normal singlet oxygen is the $^1\Delta_g$ state. Δ_g is a doubly degenerate representation. That means that it has two components which I shall write as,



i.e.,

$$^1\Delta_g^{(1)} = \frac{1}{\sqrt{2}} (|\pi_x^*, \bar{\pi}_x^*| - |\pi_y^*, \bar{\pi}_y^*|) , \tag{4.20}$$

and

$$\begin{array}{c}
 [\sigma_p^*] \\
 \pi_x^* [\uparrow][\downarrow] \pi_y^* - \pi_x^* [\downarrow][\uparrow] \pi_y^* \\
 \pi_x [\uparrow\downarrow] [\uparrow\downarrow] \pi_y \\
 [\uparrow\downarrow] \sigma_p \\
 [\uparrow\downarrow] \sigma_s^* \\
 [\uparrow\downarrow] \sigma_s \\
 {}^1\Delta_g^{(2)}
 \end{array}$$

i.e.,

$${}^1\Delta_g^{(2)} = \frac{1}{\sqrt{2}} (|\pi_x^*, \bar{\pi}_y^*| - |\bar{\pi}_x^*, \pi_y^*|), \quad (4.21)$$

will transform into linear combinations of each other under rotations and reflections. Let us check this.

Rotation:

$$\begin{aligned}
 \hat{R}(\phi) {}^1\Delta_g^{(1)} &= \frac{1}{\sqrt{2}} (|\pi_{x'}^*, \bar{\pi}_{x'}^*| - |\bar{\pi}_{y'}^*, \pi_{y'}^*|) \\
 &= \frac{1}{\sqrt{2}} |\pi_x^* \cos \phi - \pi_y^* \sin \phi, \bar{\pi}_x^* \cos \phi - \bar{\pi}_y^* \sin \phi| \\
 &- \frac{1}{\sqrt{2}} |\pi_x^* \sin \phi + \pi_y^* \cos \phi, \bar{\pi}_x^* \sin \phi + \bar{\pi}_y^* \cos \phi| \\
 &= \frac{1}{\sqrt{2}} (|\pi_x^*, \bar{\pi}_x^*| \cos^2 \phi - |\pi_x^*, \bar{\pi}_y^*| \cos \phi \sin \phi - |\pi_y^*, \bar{\pi}_x^*| \cos \phi \sin \phi + |\pi_y^*, \bar{\pi}_y^*| \sin^2 \phi) \\
 &- \frac{1}{\sqrt{2}} (|\pi_x^*, \bar{\pi}_x^*| \sin^2 \phi - |\pi_x^*, \bar{\pi}_y^*| \cos \phi \sin \phi - |\pi_y^*, \bar{\pi}_x^*| \cos \phi \sin \phi - |\pi_y^*, \bar{\pi}_y^*| \cos^2 \phi) \\
 &= \frac{1}{\sqrt{2}} (|\pi_x^*, \bar{\pi}_x^*| - |\pi_y^*, \bar{\pi}_y^*|) \cos(2\phi) - \frac{1}{\sqrt{2}} (|\pi_x^*, \bar{\pi}_y^*| - |\bar{\pi}_x^*, \pi_y^*|) \sin(2\pi) \\
 &= {}^1\Delta_g^{(1)} \cos(2\phi) - {}^1\Delta_g^{(2)} \sin(2\phi)
 \end{aligned} \quad (4.22)$$

$$\begin{aligned}
 \hat{R}(\phi) {}^1\Delta_g^{(2)} &= \frac{1}{\sqrt{2}} (|\pi_{x'}^*, \bar{\pi}_{y'}^*| - |\bar{\pi}_{x'}^*, \pi_{y'}^*|) \\
 &= \frac{1}{\sqrt{2}} |\pi_x^* \cos \phi - \pi_y^* \sin \phi, \bar{\pi}_x^* \sin \phi + \bar{\pi}_y^* \cos \phi| \\
 &- \frac{1}{\sqrt{2}} |\bar{\pi}_x^* \cos \phi - \bar{\pi}_y^* \sin \phi, \pi_x^* \sin \phi + \pi_y^* \cos \phi| \\
 &= \frac{1}{\sqrt{2}} (|\pi_x^*, \bar{\pi}_x^*| \cos \phi \sin \phi + |\pi_x^*, \bar{\pi}_y^*| \cos^2 \phi - |\pi_y^*, \bar{\pi}_x^*| \sin^2 \phi - |\pi_y^*, \bar{\pi}_y^*| \cos \phi \sin \phi) \\
 &- \frac{1}{\sqrt{2}} (|\bar{\pi}_x^*, \pi_x^*| \cos \phi \sin \phi + |\bar{\pi}_x^*, \pi_y^*| \cos^2 \phi - |\bar{\pi}_y^*, \pi_x^*| \sin^2 \phi - |\bar{\pi}_y^*, \pi_y^*| \cos \phi \sin \phi) \\
 &= \frac{1}{\sqrt{2}} (|\pi_x^*, \bar{\pi}_x^*| - |\pi_y^*, \bar{\pi}_y^*|) \sin(2\phi) + \frac{1}{\sqrt{2}} (|\pi_x^*, \bar{\pi}_y^*| + |\bar{\pi}_x^*, \pi_y^*|) \cos(2\phi) \\
 &= {}^1\Delta_g^{(1)} \sin(2\phi) + {}^1\Delta_g^{(2)} \cos(2\phi)
 \end{aligned} \quad (4.23)$$

Hence

$$\hat{R}(\phi) \begin{pmatrix} {}^1\Delta_g^{(1)} & {}^1\Delta_g^{(2)} \end{pmatrix} = \begin{pmatrix} {}^1\Delta_g^{(1)} & {}^1\Delta_g^{(2)} \end{pmatrix} \begin{bmatrix} R_{1,1} & R_{1,2} \\ R_{2,1} & R_{2,2} \end{bmatrix} = \begin{pmatrix} {}^1\Delta_g^{(1)} & {}^1\Delta_g^{(2)} \end{pmatrix} \begin{bmatrix} \cos(2\phi) & \sin(2\phi) \\ -\sin(2\phi) & \cos(2\phi) \end{bmatrix} \quad (4.24)$$

The character for the rotation is $\chi(R) = R_{1,1} + R_{2,2} = 2\cos(2\phi)$, in perfect agreement with the Δ_g character for $2C_\infty$.

Reflection:

$$\begin{aligned} \hat{\sigma}_v(\phi) {}^1\Delta_g^{(1)} &= \frac{1}{\sqrt{2}} (|\pi_x^*, \bar{\pi}_{x'}^*| - |\bar{\pi}_{y'}^*, \pi_y^*|) \\ &= \frac{1}{\sqrt{2}} |\pi_x^* \cos(2\phi) + \pi_y^* \sin(2\phi), \bar{\pi}_x^* \cos(2\phi) + \bar{\pi}_y^* \sin(2\phi)| \\ &- \frac{1}{\sqrt{2}} |\pi_x^* \sin(2\phi) - \pi_y^* \cos(2\phi), \bar{\pi}_x^* \sin(2\phi) - \bar{\pi}_y^* \cos(2\phi)| \\ &= \frac{1}{\sqrt{2}} (|\pi_x^*, \bar{\pi}_x^*| \cos^2(2\phi) + |\pi_x^*, \bar{\pi}_y^*| \cos(2\phi) \sin(2\phi) + |\pi_y^*, \bar{\pi}_x^*| \cos(2\phi) \sin(2\phi) + |\pi_y^*, \bar{\pi}_y^*| \sin^2(2\phi)) \\ &- \frac{1}{\sqrt{2}} (|\pi_x^*, \bar{\pi}_x^*| \sin^2(2\phi) - |\pi_x^*, \bar{\pi}_y^*| \cos(2\phi) \sin(2\phi) - |\pi_y^*, \bar{\pi}_x^*| \cos(2\phi) \sin(2\phi) + |\pi_y^*, \bar{\pi}_y^*| \cos^2(2\phi)) \\ &= \frac{1}{\sqrt{2}} (|\pi_x^*, \bar{\pi}_x^*| - |\pi_y^*, \bar{\pi}_y^*|) \cos(4\phi) + \frac{1}{\sqrt{2}} (|\pi_x^*, \bar{\pi}_y^*| - |\bar{\pi}_x^*, \pi_y^*|) \sin(4\phi) \\ &= {}^1\Delta_g^{(1)} \cos(4\phi) + {}^1\Delta_g^{(2)} \sin(4\phi) \end{aligned} \quad (4.25)$$

$$\begin{aligned} \hat{\sigma}_v(\phi) {}^1\Delta_g^{(2)} &= \frac{1}{\sqrt{2}} (|\pi_{x'}^*, \bar{\pi}_{y'}^*| - |\bar{\pi}_{x'}^*, \pi_{y'}^*|) \\ &= \frac{1}{\sqrt{2}} |\pi_x^* \cos(2\phi) + \pi_y^* \sin(2\phi), \bar{\pi}_x^* \sin(2\phi) - \bar{\pi}_y^* \cos(2\phi)| \\ &- \frac{1}{\sqrt{2}} |\bar{\pi}_x^* \cos(2\phi) + \bar{\pi}_y^* \sin(2\phi), \pi_x^* \sin(2\phi) - \pi_y^* \cos(2\phi)| \\ &= \frac{1}{\sqrt{2}} (|\pi_x^*, \bar{\pi}_x^*| \cos(2\phi) \sin(2\phi) - |\pi_x^*, \bar{\pi}_y^*| \cos^2(2\phi) + |\pi_y^*, \bar{\pi}_x^*| \sin^2(2\phi) - |\pi_y^*, \bar{\pi}_y^*| \cos(2\phi) \sin(2\phi)) \\ &- \frac{1}{\sqrt{2}} (|\bar{\pi}_x^*, \pi_x^*| \cos(2\phi) \sin(2\phi) - |\bar{\pi}_x^*, \pi_y^*| \cos^2(2\phi) + |\bar{\pi}_y^*, \pi_x^*| \sin^2(2\phi) - |\bar{\pi}_y^*, \pi_y^*| \cos(2\phi) \sin(2\phi)) \\ &= \frac{1}{\sqrt{2}} (|\pi_x^*, \bar{\pi}_x^*| - |\pi_y^*, \bar{\pi}_y^*|) \sin(4\phi) - \frac{1}{\sqrt{2}} (|\pi_x^*, \bar{\pi}_y^*| - |\bar{\pi}_x^*, \pi_y^*|) \cos(4\phi) \\ &= {}^1\Delta_g^{(1)} \sin(4\phi) - {}^1\Delta_g^{(2)} \cos(4\phi) \end{aligned} \quad (4.26)$$

Hence

$$\hat{\sigma}_v(\phi) \begin{pmatrix} {}^1\Delta_g^{(1)} & {}^1\Delta_g^{(2)} \end{pmatrix} = \begin{pmatrix} {}^1\Delta_g^{(1)} & {}^1\Delta_g^{(2)} \end{pmatrix} \begin{bmatrix} \cos(4\phi) & \sin(4\phi) \\ \sin(4\phi) & -\cos(4\phi) \end{bmatrix} \quad (4.27)$$

and the corresponding character, which is the trace of the matrix, is zero in perfect agreement with the Δ_g character for $\infty\sigma_v$.

Caveat The above treatment is adequate for our purposes, but a more elegant treatment would have been to construct the projectors onto each representation (which should involve some integrals for these infinite groups) and apply them to project out the wave functions for each representation. This was not judged necessary.

4.0.2 Oxygen Electronic States from DFT

$^3\Sigma_g^-$ State The question arises as to how to calculate the energy of the various electronic states of O_2 using DFT. Strictly speaking Kohn-Sham theory applies only to the ground state of the molecule. So handling the $^3\Sigma_g^-$ ground state is not a formal problem (as long as it is non-interacting v -representable.) It should suffice to do a ground state calculation with multiplicity three.

Even here we have a choice of whether to do a spin-unrestricted Kohn-Sham (UKS) calculation [different-orbitals-for-different-spin (DODS)] or a spin-restricted open-shell Kohn-Sham (ROKS) calculation [same-orbitals-for-different-spin (SODS).] There are arguments in favor of both approaches. The UKS approach is conceptually simpler and is consistent with the variational basis of DFT. However having the SODS simplifies analysis which may be desirable. Roothaan's spin-restricted open-shell Hartree-Fock (ROHF) method [133] has been adopted to make several variants on ROKS [134, 135, 136]. The **DEMON2K** uses the approach of Ref. [135] but has several different parameterizations which allow different treatments of open-shell problems [133, 137, 138, 139, 140, 141].

Whether UKS or ROKS is used, there is another difficulty, namely that of dissociating the diatomic into two oxygen atoms in definite electronic states. The oxygen atom has $n = 4$ electrons in $2(2l + 1) = 6$ degenerate p orbitals. This leads to

$$\binom{4l+2}{n} = \binom{6}{4} = 15 \quad (4.28)$$

possible ways to place the electrons. These 15 microstates are:

- (1) : $\begin{array}{c} [\uparrow\downarrow] \quad [\uparrow \quad] \quad [\uparrow \quad] \\ \hline 2p_{-1} \quad 2p_0 \quad 2p_{+1} \end{array} M_L = -1, M_S = +1$
- (2) : $\begin{array}{c} [\uparrow\downarrow] \quad [\uparrow \quad] \quad [\downarrow \quad] \\ \hline 2p_{-1} \quad 2p_0 \quad 2p_{+1} \end{array} M_L = -1, M_S = 0$
- (3) : $\begin{array}{c} [\uparrow\downarrow] \quad [\downarrow \quad] \quad [\uparrow \quad] \\ \hline 2p_{-1} \quad 2p_0 \quad 2p_{+1} \end{array} M_L = -1, M_S = 0$
- (4) : $\begin{array}{c} [\uparrow\downarrow] \quad [\downarrow \quad] \quad [\downarrow \quad] \\ \hline 2p_{-1} \quad 2p_0 \quad 2p_{+1} \end{array} M_L = -1, M_S = -1$
- (5) : $\begin{array}{c} [\uparrow \quad] \quad [\uparrow\downarrow] \quad [\uparrow \quad] \\ \hline 2p_{-1} \quad 2p_0 \quad 2p_{+1} \end{array} M_L = 0, M_S = +1$
- (6) : $\begin{array}{c} [\uparrow \quad] \quad [\uparrow\downarrow] \quad [\downarrow \quad] \\ \hline 2p_{-1} \quad 2p_0 \quad 2p_{+1} \end{array} M_L = 0, M_S = 0$
- (7) : $\begin{array}{c} [\downarrow \quad] \quad [\uparrow\downarrow] \quad [\uparrow \quad] \\ \hline 2p_{-1} \quad 2p_0 \quad 2p_{+1} \end{array} M_L = 0, M_S = 0$
- (8) : $\begin{array}{c} [\downarrow \quad] \quad [\uparrow\downarrow] \quad [\downarrow \quad] \\ \hline 2p_{-1} \quad 2p_0 \quad 2p_{+1} \end{array} M_L = 0, M_S = -1$
- (9) : $\begin{array}{c} [\uparrow \quad] \quad [\uparrow \quad] \quad [\uparrow\downarrow] \\ \hline 2p_{-1} \quad 2p_0 \quad 2p_{+1} \end{array} M_L = +1, M_S = +1$
- (10) : $\begin{array}{c} [\uparrow \quad] \quad [\downarrow \quad] \quad [\uparrow\downarrow] \\ \hline 2p_{-1} \quad 2p_0 \quad 2p_{+1} \end{array} M_L = +1, M_S = 0$
- (11) : $\begin{array}{c} [\downarrow \quad] \quad [\uparrow \quad] \quad [\uparrow\downarrow] \\ \hline 2p_{-1} \quad 2p_0 \quad 2p_{+1} \end{array} M_L = +1, M_S = 0$
- (12) : $\begin{array}{c} [\downarrow \quad] \quad [\downarrow \quad] \quad [\uparrow\downarrow] \\ \hline 2p_{-1} \quad 2p_0 \quad 2p_{+1} \end{array} M_L = +1, M_S = -1$
- (13) : $\begin{array}{c} [\uparrow\downarrow] \quad [\uparrow\downarrow] \quad [\quad \quad] \\ \hline 2p_{-1} \quad 2p_0 \quad 2p_{+1} \end{array} M_L = -2, M_S = 0$
- (14) : $\begin{array}{c} [\uparrow\downarrow] \quad [\quad \quad] \quad [\uparrow\downarrow] \\ \hline 2p_{-1} \quad 2p_0 \quad 2p_{+1} \end{array} M_L = 0, M_S = 0$
- (15) : $\begin{array}{c} [\quad \quad] \quad [\uparrow\downarrow] \quad [\uparrow\downarrow] \\ \hline 2p_{-1} \quad 2p_0 \quad 2p_{+1} \end{array} M_L = +2, M_S = 0.$ (4.29)

Note that not every microstate corresponds to a wave function because not every symmetry may be represented by a single determinant.

We can work out the possible term symbols using various methods, but I rather like the double ladder method of Hyde [142]. This requires us to make a table of how many times each (M_L, M_S) combination occurs:

$M_L \setminus M_S$	-1	0	+1
+2		1	
+1	1	2	1
0	1	3	1
-1	1	2	1
-2		1	

This decomposes into the sum of three double ladders—namely,

1D Double Ladder			
$M_L \setminus M_S$	-1	0	+1
+2		1	
+1		1	
0		1	
-1		1	
-2		1	

3P Double Ladder			
$M_L \setminus M_S$	-1	0	+1
+2			
+1	1	1	1
0	1	1	1
-1	1	1	1
-2			

1S Double Ladder			
$M_L \setminus M_S$	-1	0	+1
+2			
+1			
0		1	
-1			
-2			

Here we are using Russell-Saunders coupling of the spin and orbital magnetic moments. The term symbol takes the form $^{2S+1}L_J$ where

$$J = L + S, L + S - 1, \dots, |L - S|, \quad (4.30)$$

is a new label used to distinguish the different levels with the same L and S . Hund's rules tell us which state should have the lowest energy. There are three rules:

1. Levels with larger S are lower in energy than levels with smaller S .
2. For a given value of S , levels with larger L are lower in energy than levels with smaller L .
3. For the same values of S and L , maximizing J minimizes the energy if the shell is more than half-filled minimizing J minimizes the energy if the shell is half-filled or less.

This tells us that the ground state of the oxygen atom is 3P . These correspond to the $3 \times 3 = 9$ microstates (1)-(9) above. As the shell is more than half full, maximizing J minimizes the energy.

Hund's rules work well for the ground state but not necessarily for excited states. The Atomic Spectra Database of the American National Institute of Standards and Technology [143] gives the following data for the $2p^4$ term symbols ("multiplets") of the oxygen atom:

Term	J	Energy	
		cm^{-1}	eV
1S	0	33 792.483	4.1897359
1D	2	15 867.862	1.9673651
3P	0	226.977	0.0281416
	1	158.265	0.0196224
	2	0.000	0.0000000

In this particular case, Hund's rules actually also work for the excited states, but this should be taken as purely coincidental.

Let us now consider the problem of dissociating O_2 . According to Ref. [127] (and other sources) the $^3\Sigma_g^-$, $^1\Delta_g$, and $^1\Sigma_g^+$ states all dissociate into two 3P atoms. Let us try to figure out how this works for the $^3\Sigma_g^-$ state. This is basically an exercise in how molecular orbital theory is connected with valence bond theory which can be represented by Lewis representations. As I will be putting linear combinations of Slater determinants inside Slater determinants, I should take a moment to clarify what I mean by a determinant of a determinant. As the determinant of a matrix and the determinant of the transpose of a determinant are the same, we could define a Slater determinant either by,

$$|\psi_1, \psi_2, \dots, \psi_N| = \frac{1}{\sqrt{N!}} \sum_{\sigma \in \mathcal{S}_N} (-1)^\sigma \psi_{\sigma(1)}(1) \psi_{\sigma(2)}(2) \cdots \psi_{\sigma(N)}(N), \quad (4.31)$$

or by,

$$|\psi_1, \psi_2, \dots, \psi_N| = \frac{1}{\sqrt{N!}} \sum_{\sigma \in \mathcal{S}_N} (-1)^\sigma \psi_1(\sigma(1)) \psi_2(\sigma(2)) \cdots \psi_N(\sigma(N)), \quad (4.32)$$

where \mathcal{S}_N is the symmetric group for (i.e., the group of permutation of) the numbers $1, 2, \dots, N$ and $(-1)^\sigma$ is the sign of the permutation. Only the second definition of the Slater determinant is suitable for a general function. Thus we may write that,

$$|f(1, 2, \dots, N)| = \frac{1}{\sqrt{N!}} \sum_{\sigma \in \mathcal{S}_N} (-1)^\sigma f(\sigma(1), \sigma(2), \dots, \sigma(N)). \quad (4.33)$$

It is then a relatively simple exercise in group theory to show that,

$$||\psi_1, \psi_2, \dots, \psi_P|, \psi_{P+1}, \psi_N| = \sqrt{P!} |\psi_1, \psi_2, \dots, \psi_N|. \quad (4.34)$$

We also need that determinants are linear so that, for example,

$$|\psi_1, \psi_2, \dots, C_a \psi_a + C_b \psi_b, \dots, \psi_N| = C_a |\psi_1, \psi_2, \dots, \psi_a, \dots, \psi_N| + C_b |\psi_1, \psi_2, \dots, \psi_b, \dots, \psi_N|. \quad (4.35)$$

This latter allows us to replace $p_{\pm 1}$ with p_x and p_y using the relations,

$$\begin{aligned} p_x &= \frac{1}{\sqrt{2}} (p_{+1} + p_{-1}) \\ p_y &= \frac{1}{i\sqrt{2}} (p_{+1} - p_{-1}). \end{aligned} \quad (4.36)$$

In particular,

$$|p_x, p_y| = +i|p_{+1}, p_{-1}| \quad (4.37)$$

differ only by a phase factor. Recall also that $p_0 = p_z$.

We may now make a connection with chemical bonding and in particular with chemical bond breaking. Orbitals χ_A and χ_B on two different centers A and B may form bonding and antibonding combinations,

$$\psi_{\pm} = \frac{1}{\sqrt{2}} (\chi_A \pm \chi_B) . \quad (4.38)$$

Here I have assumed that we are only interested in the dissociation limit when the two centers are so far apart that any overlap between χ_A and χ_B is large enough to be able to define what is meant between bonding and antibonding but small enough to be neglected in the normalization. Note also that which of the plus and minus combinations is bonding and which is antibonding depends upon the precise nature of the orbitals χ_A and χ_B . Filling both the bonding and antibonding combinations is equivalent to bond breaking because,

$$|\psi_+, \psi_-| = -|\chi_A, \chi_B| . \quad (4.39)$$

This is why these terms cancel when calculating the bond order index ($\text{BOI} = (n - n^*)/2$, where n is the number of electrons in bonding orbitals and n^* is the number of electrons in antibonding orbitals.) Referring back to Fig. 4.2, we see that we already have in the dissociation limit that, dropping unimportant phase factors,

$$|\sigma, \bar{\sigma}, \sigma^*, \bar{\sigma}^*, \sigma_p, \bar{\sigma}_p, \pi_x, \bar{\pi}_x, \pi_y, \bar{\pi}_y, \pi_x^*, \pi_y^*| \rightarrow |s_A, \bar{s}_A, s_B, \bar{s}_B, \sigma_p, \bar{\sigma}_p, p_x^A, p_y^A, p_x^B, p_y^B, \bar{\pi}_x, \bar{\pi}_y| . \quad (4.40)$$

Dissociating the σ_p bond is a bit more complicated. As the diatomic traditionally lies along the z -axis, we have that

$$\begin{aligned} \sigma_p &= \frac{1}{\sqrt{2}} (p_z^A - p_z^B) \\ \sigma_p^* &= \frac{1}{\sqrt{2}} (p_z^A + p_z^B) . \end{aligned} \quad (4.41)$$

This leads to

$$\frac{1}{\sqrt{2}} (-|\sigma_p, \bar{\sigma}_p| + |\sigma_p^*, \bar{\sigma}_p^*|) = \frac{1}{\sqrt{2}} (|p_z^A, \bar{p}_z^B| - |\bar{p}_z^A, p_z^B|) , \quad (4.42)$$

which is proper dissociation. Hence (dropping phase factors)

$$\begin{aligned} &\frac{1}{\sqrt{2}} |\sigma, \bar{\sigma}, \sigma^*, \bar{\sigma}^*, \frac{1}{\sqrt{2}} (-|\sigma_p, \bar{\sigma}_p| + |\sigma_p^*, \bar{\sigma}_p^*|), \pi_x, \bar{\pi}_x, \pi_y, \bar{\pi}_y, \pi_x^*, \pi_y^*| \\ &\rightarrow \frac{1}{\sqrt{2}} |s_A, \bar{s}_A, s_B, \bar{s}_B, p_z^A, \bar{p}_z^B, p_x^A, p_y^A, p_x^B, p_y^B, \bar{\pi}_x, \bar{\pi}_y| \\ &- \frac{1}{\sqrt{2}} |s_A, \bar{s}_A, s_B, \bar{s}_B, \bar{p}_z^A, p_z^B, p_x^A, p_y^A, p_x^B, p_y^B, \bar{\pi}_x, \bar{\pi}_y| . \end{aligned} \quad (4.43)$$

Getting proper atomic dissociation into 3P components requires us to use that,

$$\begin{aligned} \bar{\pi}_x &= \bar{p}_x^A + \bar{p}_x^B \\ \bar{\pi}_x^* &= \bar{p}_x^A - \bar{p}_x^B \\ \bar{\pi}_y &= \bar{p}_y^A + \bar{p}_y^B \\ \bar{\pi}_y^* &= \bar{p}_y^A - \bar{p}_y^B . \end{aligned} \quad (4.44)$$

Then

$$\frac{1}{\sqrt{2}} (|\bar{\pi}_x, \bar{\pi}_y| - |\bar{\pi}_x^*, \bar{\pi}_y^*|) = \frac{1}{\sqrt{2}} (|\bar{p}_x^A, \bar{p}_y^B| + |\bar{p}_y^A, \bar{p}_x^B|) . \quad (4.45)$$

Hence

$$\begin{aligned} & \frac{1}{2} |\sigma, \bar{\sigma}, \sigma^*, \bar{\sigma}^*, \frac{1}{\sqrt{2}} (-|\sigma_p, \bar{\sigma}_p| + |\sigma_p^*, \bar{\sigma}_p^*|), \pi_x, \bar{\pi}_x, \pi_y, \bar{\pi}_y, \frac{1}{\sqrt{2}} (|\bar{\pi}_x, \bar{\pi}_y| - |\bar{\pi}_x^*, \bar{\pi}_y^*|)| \\ \rightarrow & \frac{1}{2} |s_A, \bar{s}_A, s_B, \bar{s}_B, p_z^A, \bar{p}_z^B, p_x^A, p_x^B, p_y^A, p_y^B, \bar{p}_x^A, \bar{p}_y^B| \\ + & \frac{1}{2} |s_A, \bar{s}_A, s_B, \bar{s}_B, p_z^A, \bar{p}_z^B, p_x^A, p_x^B, p_y^A, p_y^B, \bar{p}_y^A, \bar{p}_x^B| \\ - & \frac{1}{2} |s_A, \bar{s}_A, s_B, \bar{s}_B, \bar{p}_z^A, p_z^B, p_x^A, p_x^B, p_y^A, p_y^B, \bar{p}_x^A, \bar{p}_y^B| \\ - & \frac{1}{2} |s_A, \bar{s}_A, s_B, \bar{s}_B, \bar{p}_z^A, p_z^B, p_x^A, p_x^B, p_y^A, p_y^B, \bar{p}_y^A, \bar{p}_x^B| , \end{aligned} \quad (4.46)$$

which is a sum of four terms each corresponding to two 3P oxygen atoms. We cannot do this in ordinary DFT calculations but we can imagine trying to make a $|s_A, \bar{s}_A, s_B, \bar{s}_B, p_z^A, \bar{p}_z^B, p_x^A, p_x^B, p_y^A, p_y^B, \bar{p}_y^A, \bar{p}_x^B|$ (i.e., $|s_A, \bar{s}_A, p_x^A, p_y^A, \bar{p}_y^A, p_z^A|$ and $|s_B, \bar{s}_B, p_x^B, \bar{p}_x^B, p_y^B, \bar{p}_z^B|$) by symmetry breaking. Note that it is not enough to break the σ_p or π_x or π_y symmetries but that we have to break them all simultaneously in the right way, which is not at all an obvious thing to do.

Reference State Problem Let us now turn our attention to singlet oxygen. The result of specifying a spin multiplicity of one and running a calculation is that most programs will try to pair up electrons to put two electrons in a single π^* orbital. Such a doubly-occupied π^* orbital will no longer be energetically degenerate with the other (empty) π^* orbital. In fact, the occupied π^* orbital will have a higher energy than the unoccupied π^* orbital because of self-interaction errors. Formal DFT predicts that this can happen in open-shell systems even for the exact functional when noninteracting v -representability (NVR) fails. We call this an effective failure of NVR when it occurs for an approximate functional [144]. In either case, the result is that most programs will try to satisfy the *Aufbau* principle at each iteration by transferring electrons from the higher-energy occupied π^* orbital to the lower-energy unoccupied π^* orbital. As this then raises the energy of the newly occupied orbital and lowers the energy of the newly unoccupied orbital, we have an unstable situation and the calculations will typically no longer converge.

This problem may be solved by creating a reference state with each π^* orbital having half a spin-up and half spin-down electron. Most programs have an option which allows the user to create this fractionally-occupied state easily. In **DEMON2K**, it suffices to use the keyword combination **SMEAR 0.1 UNIFORM** where the number 0.1 is an adjustable number in eV which controls how close orbitals are in energy before they are uniformly occupied. *A priori* this type of fractionally-occupied state corresponds to some sort of ensemble electronic state, where the ensemble average has been carried out over several multiplet states. However deeper thought indicates that this conclusion is far from obvious. Another possibility (not tried) would be to use a carefully-selected ROKS calculation as a reference state.

Once such a reference state is created, electrons may be displaced to create different occupation states without additional iterations. In **DEMON2K**, this is done with the keywords **SCFTYPE UKS MAX=0** and **MOMODIFY**. It should be emphasized that this is not just needed in order to converge the calculation, but also to guarantee that the different determinants which are created are properly orthogonal to each other so as to avoid variational collapse. The same problem is addressed in

complete active state self-consistent field (CAS-SCF) calculations by using state averaging. Of course, the price that has to be paid is that orbital relaxation is neglected, which is not always a good thing. Thus the ${}^3\Sigma_g^-$ state created in this manner will be higher in energy than the fully-relaxed ${}^3\Sigma_g^-$ state from a UKS calculation.

Singlet States from the Multiplet Sum Method Although DFT is only giving us access to states with a single-determinant reference, we may obtain the energies of other states using the Ziegler-Rauk-Baerends (Daul) multiplet sum method (MSM) [111, 112]. (There are also some relevant papers by Noddleman, e.g., [145].) This works for single-point (i.e., at a single geometry) calculations but I am only aware of one implementation of analytic gradients which would allow geometry optimizations with this method (Friedrichs and Frank used such a method in the CPMD program to do excited-state dynamics [146].)

To see how to apply the MSM, we will consider the three ${}^3\Sigma_g^-$ wavefunctions,

$$\begin{aligned} {}^{(3,1)}\Sigma_g^- &= |\pi_x^*, \pi_y^*| \\ {}^{(3,0)}\Sigma_g^- &= \frac{1}{\sqrt{2}} (|\pi_x^*, \bar{\pi}_y^*| + |\bar{\pi}_x^*, \pi_y^*|) \\ {}^{(3,-1)}\Sigma_g^- &= |\bar{\pi}_x^*, \bar{\pi}_y^*|, \end{aligned} \quad (4.47)$$

and the two ${}^1\Delta_g$ wavefunctions,

$$\begin{aligned} {}^1\Delta_g^{(1)} &= \frac{1}{\sqrt{2}} (|\pi_x^*, \bar{\pi}_x^*| - |\bar{\pi}_y^*, \pi_y^*|) \\ {}^1\Delta_g^{(2)} &= \frac{1}{\sqrt{2}} (|\pi_x^*, \bar{\pi}_y^*| - |\bar{\pi}_x^*, \pi_y^*|). \end{aligned} \quad (4.48)$$

Then

$$\begin{aligned} E[{}^3\Sigma_g^-] &= E[{}^{(3,0)}\Sigma_g^-] = E[|\pi_x^*, \bar{\pi}_y^*|] + \langle |\pi_x^*, \bar{\pi}_y^*| \hat{H} | \bar{\pi}_x^*, \pi_y^* \rangle \\ E[{}^1\Delta_g] &= E[{}^1\Delta_g^{(2)}] = E[|\pi_x^*, \bar{\pi}_y^*|] - \langle |\pi_x^*, \bar{\pi}_y^*| \hat{H} | \bar{\pi}_x^*, \pi_y^* \rangle. \end{aligned} \quad (4.49)$$

Hence,

$$E[{}^3\Sigma_g^-] + E[{}^1\Delta_g] = 2E[|\pi_x^*, \bar{\pi}_y^*|], \quad (4.50)$$

and,

$$\begin{aligned} E[{}^1\Delta_g] &= 2E[|\pi_x^*, \bar{\pi}_y^*|] - E[{}^3\Sigma_g^-] \\ &= 2E[|\pi_x^*, \bar{\pi}_y^*|] - E[{}^{(3,0)}\Sigma_g^-] \\ &= 2E[|\pi_x^*, \bar{\pi}_y^*|] - E[|\pi_x^*, \pi_y^*|]. \end{aligned} \quad (4.51)$$

Thus the ${}^1\Delta_g$ energy has been expressed purely in terms of the energies of two single-determinantal states—namely the fictitious mixed-symmetry $|\pi_x^*, \bar{\pi}_y^*|$ state and the triplet state $|\pi_x^*, \pi_y^*|$. Formally these should be calculated using the same orbitals. However it may be advantageous to using a relaxed triplet determinant.

In principle the extension of the MSM to the

$${}^1\Sigma_g^+ = \frac{1}{\sqrt{2}} (|\pi_x^*, \bar{\pi}_x^*| + |\pi_y^*, \bar{\pi}_y^*|) \quad (4.52)$$

is just as straightforward as

$$\begin{aligned} E[{}^1\Sigma_g^+] &= E[|\pi_x^*, \bar{\pi}_x^*|] + \langle |\pi_x^*, \bar{\pi}_x^*| \hat{H} | \pi_y^*, \bar{\pi}_y^* \rangle \\ E[{}^1\Delta_g] &= E[{}^1\Delta_g^{(1)}] = E[|\pi_x^*, \bar{\pi}_x^*|] - \langle |\pi_x^*, \bar{\pi}_x^*| \hat{H} | \pi_y^*, \bar{\pi}_y^* \rangle. \end{aligned} \quad (4.53)$$

So,

$$E[{}^1\Sigma_g^+] + E[{}^1\Delta_g] = 2E[|\pi_x^*, \bar{\pi}_x^*|], \quad (4.54)$$

and

$$E[{}^1\Sigma_g^+] = 2E[|\pi_x^*, \bar{\pi}_x^*|] - E[{}^1\Delta_g]. \quad (4.55)$$

Although we will not consider it here, time-depedent (TD) DFT provides an alternative and intrinsically multideterminantal way to access excited states and many programs include analytic gradients for TD-DFT which allow geometry optimizations. We will not pursue this further here but we note that applications of TD-DFT are not always straightforward for open-shell systems either and may, for example, require special techniques such as TD spin-flip DFT [147].

4.0.3 Exercises

We wish to calculate the potential energy curves (PECs) for the ${}^3\Sigma_g^-$, ${}^1\Delta_g$, and ${}^1\Sigma_g^+$ states and compare them with the accurate curves tabulated in Table 4.2.

Without Symmetry Breaking

We will do this at the BLYP/DEF2-TZVPP lvl of calculation with the GEN-A3* auxiliary basis set and we will ignore the problem of symmetry breaking, at least in the first instance.

The input file for calculating the ${}^3\Sigma_g^-$ PEC is:

```
TITLE 02
MULTI 3
CHARGE 0
VXCTYPE BLYP
SCFTYPE UKS
#
PRINT MOS = 8-9
#
# --- GEOMETRY ---
#
#
GEOMETRY CARTESIAN BOHR
0 0.000000 0.000000 0.000000
0 0.000000 0.000000 1.700000
#
AUXIS (GEN-A3*)
BASIS (DEF2-TZVPP)
```

Only the 1.7 bohr bond distance needs to be varied. This produces the relaxed ${}^3\Sigma_g^-$ PEC.

We need to create the fractional occupation reference state. This can be done using the SMEAR 0.05 UNIFORM keywords. Here 0.05 is the window in eV within which all of the orbitals will have the same occupation number. Some adjusting of the size of this window may be necessary for different bond distances. A suitable input file is:

Table 4.2: O₂ potential energy curves from Fig. 1 of Ref. [127] digitized with WEBPLOTDIGITIZER [128]. The zero of energy is the vibrational zero-point energy of the ground state.

R (bohr)	Energy (Ha)			R (bohr)	Energy (Ha)		
	$X\ ^3\Sigma_g^-$	$a\ ^1\Delta_g$	$b\ ^1\Sigma_g^+$		$X\ ^3\Sigma_g^-$	$a\ ^1\Delta_g$	$b\ ^1\Sigma_g^+$
1.7	0.29247	0.33467	0.33185	4.2	0.18426	0.18120	0.18426
1.8	0.18075	0.22188	0.25813	4.3	0.18571	0.18353	0.18578
1.9	0.08980	0.13237	0.16356	4.4	0.18681	0.18466	0.18681
2.0	0.03976	0.08080	0.10942	4.5	0.18766	0.18557	0.18766
2.1	0.01050	0.04976	0.07790	4.6	0.18829	0.18616	0.18829
2.2	-0.00157	0.03736	0.06365	4.7	0.18869	0.18674	0.18869
2.3	-0.00276	0.03367	0.05777	4.8	0.18905	0.18696	0.18905
2.4	0.00125	0.03717	0.05979	4.9	0.18924	0.18725	0.18924
2.5	0.01083	0.04452	0.06617	5.0	0.18963	0.18747	0.18963
2.6	0.02345	0.05571	0.07520	5.1	0.18974	0.18778	0.18974
2.7	0.03699	0.06810	0.08565	5.2	0.19001	0.18775	0.19001
2.8	0.05081	0.08012	0.09644	5.3	0.19040	0.18788	0.19040
2.9	0.06570	0.09264	0.10734	5.4	0.19025	0.18831	0.19025
3.0	0.08143	0.10494	0.11840	5.5	0.19027	0.18828	0.19250
3.1	0.09608	0.11663	0.12890	5.6	0.19037	0.18804	0.19214
3.2	0.10986	0.12714	0.13814	5.7	0.19045	0.18858	0.19181
3.3	0.12276	0.13678	0.14644	5.8	0.19033	0.18885	0.19178
3.4	0.13480	0.14545	0.15365	5.9	0.19034	0.18966	0.19196
3.5	0.14550	0.15296	0.15999	6.0	0.19036	0.19045	0.19206
3.6	0.15459	0.15927	0.16552	6.1	0.19039	0.18840	0.19228
3.7	0.16234	0.16498	0.17007	6.2	0.19061	0.19061	0.19233
3.8	0.16889	0.16858	0.17387	6.3	0.19065	0.19065	0.19237
3.9	0.17434	0.17189	0.17698	6.4	0.19067	0.19067	0.19262
4.0	0.17892	0.17540	0.18056	6.5	0.19068	0.19068	0.19262
4.1	0.18210	0.17821	0.18210	6.6	0.19059	0.19060	0.19264

```

TITLE 02
CHARGE 0
VXCTYPE BLYP
# ----- uncomment for step 1 -----
MULTI 1
SCFTYPE UKS MAX=200
MIXING OMA
SMEAR 0.05 UNIFORM
# ----- end step 1 commands-----
# ----- uncomment for step 2 -----
# MULTI 3
# SCFTYPE UKS MAX=0
# MOMODIFY 2 2
# 8 1
# 9 1
# 8 0
# 9 0
# ----- end step 2 commands-----
PRINT MOS = 8-9
#
# --- GEOMETRY ---
#
#
GEOMETRY CARTESIAN BOHR
0 0.000000 0.000000 0.000000
0 0.000000 0.000000 1.800000
#
AUXIS (GEN-A3*)
BASIS (DEF2-TZVPP)

```

The `MIXING OMA` is a special type of mixing that uses fractional occupation and improves the changes of finding the lowest energy solution of the SCF problem by passing through the interior of the space of N -representable density matrices[148]. This input creates a restart file. Then commenting out *step 1* and uncommenting *step 2* provides us with a file that will begin with the restart and do a single iteration with the orbital occupancy of our choice, in this case one spin up electron in each of orbitals 8 and 9 and no spin down electrons in these orbitals:

```

TITLE 02
CHARGE 0
VXCTYPE BLYP
# ----- uncomment for step 1 -----
# MULTI 1
# SCFTYPE UKS MAX=200
# MIXING OMA
# SMEAR 0.1 UNIFORM
# ----- end step 1 commands-----
# ----- uncomment for step 2 -----
MULTI 3

```

```

SCFTYPE UKS MAX=0
MOMODIFY 2 2
8 1
9 1
8 0
9 0
# ----- end step 2 commands-----
PRINT MOS = 8-9
#
# --- GEOMETRY ---
#
#
GEOMETRY CARTESIAN BOHR
0 0.000000 0.000000 0.000000
0 0.000000 0.000000 1.800000
#
AUXIS (GEN-A3*)
BASIS (DEF2-TZVPP)

```

This allows us to calculate the energy of the ${}^3\Sigma_g^-$ without relaxation from the fractionally occupied reference state.

The energies of the mixed states needed to calculate the MSM energies of the ${}^1\Delta_g$ and ${}^1\Sigma_g^+$ PECs may be obtained by a similar strategy using this input file:

```

TITLE 02
MULTI 1
CHARGE 0
VXCTYPE BLYP
# ----- uncomment for step 1 -----
SCFTYPE UKS MAX=200
MIXING OMA
SMEAR 0.05 UNIFORM
# ----- end step 1 commands-----
# ----- uncomment for step 2a -----
# SCFTYPE UKS MAX=0
# MOMODIFY 2 2
# 8 1
# 9 0
# 8 0
# 9 1
# ----- end step 2a commands-----
# ----- uncomment for step 2b -----
# SCFTYPE UKS MAX=0
# MOMODIFY 2 2
# 8 1
# 9 0
# 8 1
# 9 0

```

```
# ----- end step 2b commands-----
#
PRINT MOS = 8-9
#
# --- GEOMETRY ---
#
#
GEOMETRY CARTESIAN BOHR
0 0.000000 0.000000 0.000000
0 0.000000 0.000000 2.600000
```

Step 1 provides the initial restart file while *step 2a* provides the mixed state $\pi_x^*[\uparrow\downarrow][\downarrow\uparrow]\pi_y^*$ and *step 2b* provides the mixed state $\pi_x^*[\uparrow\downarrow][\downarrow\uparrow]\pi_y^*$.

With Symmetry Breaking

As we saw previously with the calculation of the H_2 potential energy curve (PEC, Sec. 3.2), symmetry breaking is essential for capturing at least some of the intrinsically multideterminantal aspects of bond breaking. However symmetry breaking for any molecule can be a difficult business both because symmetric initial guesses mean that it can be hard to make the molecule break symmetry but also because there may be multiple ways to break symmetry and we are not guaranteed to find the one that we really want. Diatomic oxygen is already fairly complicated. Nevertheless it can be a good learning lesson to try to break symmetry for the ground and excited states. Expect a little frustration with this part but also expect to learn something by overcoming your frustration!

An important first step is to first calculate the BLYP/DEF2-TZVPP energy of atomic oxygen with configuration



This may be accomplished with the following input:

```
TITLE 02
MULTI 3
CHARGE 0
VXCTYPE BLYP
SCFTYPE UKS MAX=200
MIXING OMA
#
# --- GEOMETRY ---
#
#
GEOMETRY CARTESIAN BOHR
0 0.000000 0.000000 0.000000
#
AUXIS (GEN-A3*)
BASIS (DEF2-TZVPP)
```

This provides a useful energy zero for calculating the PEC for the diatomic:

$$V(R) = E[O_2](R) - 2E[O]. \quad (4.57)$$

After much experimentation, I found that I could use the *atomic* restart file as an intial guess for the *diatomic* (something that I did not think should work):

```
TITLE 02
MULTI 3
CHARGE 0
VXCTYPE BLYP
SCFTYPE UKS MAX=200
MIXING OMA
GUESS RESTART
#
PRINT MOS = 5-10
#
# --- GEOMETRY ---
#
#
GEOMETRY CARTESIAN BOHR
0 0.000000 0.000000 0.000000
0 0.000000 0.000000 6.600000
#
AUXIS (GEN-A3*)
BASIS (DEF2-TZVPP)
```

I could then keep the symmetry broken by for the ground state by gradually shortening the bond length while using the restart file from the previous (longer) bond length. Occasionally I had to play a few tricks (such as shortening the bond length less quickly) in order to keep the PEC calculations converging. In this way I obtained a classic (Morse or Lennard-Jones shaped) potential energy curve for the $^3\Sigma_g^-$ ground state.

Getting broken-symmetry excited states proved to be much more difficult. In the end, I noticed that the broken-symmetry $^3\Sigma_g^-$ restart file could be used to converge the $\pi_x^*[\downarrow][\uparrow]\pi_y^*$ mixed-symmetry reference configuration

```
TITLE 02
MULTI 1
CHARGE 0
VXCTYPE BLYP
# -----
SCFTYPE UKS MAX=200
MIXING OMA
GUESS RESTART
# -----
#
PRINT MOS = 8-9
#
# --- GEOMETRY ---
#
#
GEOMETRY CARTESIAN BOHR
```

```
0 0.000000 0.000000 0.000000
0 0.000000 0.000000 6.600000
#
AUXIS (GEN-A3*)
BASIS (DEF2-TZVPP)
```

Note that it is very easy to misread the output because (at least in my calculations) the spin \uparrow orbitals 8 and 9 are *switched* for spin \downarrow . (It is also possible that the orbitals are not simply switched but mixed in a more complicated way, but this seemed to be at worst only a minor problem in my calculations.)

To get the energy of the configuration $\pi_x^*[\quad][\uparrow\downarrow]\pi_y^*$ use the restart from the previous calculation and this input:

```
TITLE 02
MULTI 1
CHARGE 0
VXCTYPE BLYP
# -----
SCFTYPE UKS MAX=0
MOMODIFY 2 2
8 1
9 0
8 0
9 1
# -----
# 
PRINT MOS = 8-9
#
# --- GEOMETRY ---
#
#
GEOMETRY CARTESIAN BOHR
0 0.000000 0.000000 0.000000
0 0.000000 0.000000 6.600000
#
AUXIS (GEN-A3*)
BASIS (DEF2-TZVPP)
```

Give it a try and have fun!

Chapter 5

Answers

5.1 Lesson 1 Answers

5.1.1 Raw Results

We should always look out for (i) failure of the SCF convergence and (ii) indications that basis functions have been removed due to near-linear dependence problems. Neither seems to have occurred here.

DEMON2K is using spherical GTOs. *s*-, *p*-, *d*-, *f*-, and *g*-type orbitals are easily distinguished by the $2l+1$ degeneracy of their orbital energies (and by looking at the corresponding MO coefficients.) In order to retain a certain objectivity when analyzing the results, I have decided to use a notation where the lowest energy orbital of *p* type is labeled $1p$, rather than $2p$, the lowest energy orbital of *d* type is labeled $1d$, rather than $3d$, etc. It is hoped that this will avoid confusion caused by trying to assign too much physical meaning to results which are not necessarily good physical approximations to anything.

Results have been ordered by total energy. The size of the basis set is the total number of contracted GTOs. I have given the number of *sets* of each type of contracted GTO in parentheses.

Whenever possible orbital energies are also ordered by energy. However exceptions are marked in **bold** where the spin- α and spin- β orbitals follow a slightly different energetic order.

Basis	Size	Energy (Ha)	MO energies (Ha)		
				↑	↓
STO-3G	1 (1s)	-0.435508095618	1s [↑]	-0.1625	+0.1130
LANL2DZ	2 (2s)	-0.474566071191	2s []	+0.7591	+0.9963
			1s [↑]	-0.2532	-0.0576
EPR	10 (4s2p)	-0.474658227199	4s []	36.2537	36.7491
			3s []	+4.5424	+4.8865
			2p []	+3.4550	+3.7323
			2s []	+0.5893	+0.7823
			1p []	+0.5350	+0.6815
			1s [↑]	-0.2539	-0.0609
6-31G**	5 (2s1p)	-0.476223308988	1p []	+1.8919	+2.1568
			2s []	+0.6857	+0.9181
			1s [↑]	-0.2597	-0.0703

Basis	Size	Energy (Ha)	MO energies (Ha)		
				↑	↓
TZVP-FIP2	13 (2s2p1d)	-0.476532343353	2p []	+1.4199	+1.6324
			2s []	+0.6364	+0.8638
			3d []	+0.1949	+0.2070
			1p []	+0.1246	+0.1782
			1s [↑]	-0.2616	-0.0746
DZV	2 (2s)	-0.476548931869	2s []	+0.6379	+0.8651
			1s [↑]	-0.2615	-0.0742
DZVP	5 (2s1p)	-0.476548931869	1p []	+1.2046	+1.4275
			2s []	+0.6379	+0.8651
			1s [↑]	-0.2615	-0.0742
TZVP	8 (2s2p)	-0.476587919472	2p []	+1.4214	+1.6338
			2s []	+0.6374	+0.8648
			1p []	+0.1268	+0.1804
			1s [↑]	-0.2616	-0.0744
TZVP-FIP1	8 (2s2p)	-0.476587919472	2p []	+1.4214	+1.6338
			2s []	+0.6374	+0.8648
			1p []	+0.1268	+0.1804
			1s [↑]	-0.2616	-0.0744

Basis	Size	Energy (Ha)	MO energies (Ha)		
				↑	↓
DZV-GGA	2 (2s)	-0.476781268721	2s []	+0.6194	+0.8433
			1s [↑]	-0.2607	+0.6194
DZVP-GGA	5 (2s1p)	-0.476781268721	1p []	+1.2053	+1.4290
			2s []	+0.6194	+0.8433
			1s [↑]	-0.2607	-0.0727

Basis	Size	Energy (Ha)	MO energies (Ha)		
				↑	↓
AUG-PCJ-0	4 (4s)	-0.477158407949	4s []	+6.2855	+6.6716
			3s []	+0.5694	+0.7480
			2s []	+0.0283	+0.0623
			1s [↑]	-0.2692	-0.1009
AUG-CC-PVDZ	9 (3s2p)	-0.478013390837	2p []	+1.4512	+1.6581
			3s []	+0.5197	+0.6956
			1p []	+0.1525	+0.2172
			2s []	+0.0314	+0.0663
			1s [↑]	-0.2683	-0.0994
AUG-PCJ-1	14 (5s2p)	-0.478215200122	5s []	21.3469	+21.8066
			3p []	20.9480	+21.3855
			4s []	+2.6785	+2.9701
			2p []	+1.7632	+2.0098
			3s []	+0.3701	+0.4986
			1p []	+0.0733	+0.1070
			2s []	+0.0247	+0.0524
			1s [↑]	-0.2691	-0.1006

Basis	Size	Energy (Ha)	MO energies (Ha)			
				↑	↓	
SAD	9 (3s2p)	-0.478495254602	2p []	+0.7971	+0.9528	
			3s []	+0.4346	+0.5919	
			1p []	+0.1010	+0.1441	
			2s []	+0.0318	+0.0648	
			1s [↑]	-0.2687	-0.0998	
DEF2-TZVPP	14 (3s2p1d)	-0.478523349354	2p []	+3.4420	+3.7150	
			1d []	+3.0716	+3.2875	
			3s []	+2.1195	+2.4013	
			1p []	+0.5280	+0.6717	
			2s []	+0.2277	+0.3484	
			1s [↑]	-0.2678	-0.0932	
6-311G**	6 (3s1p)	-0.478526032411	3s []	+2.1078	+2.3892	
			1p []	+1.1997	+1.4214	
			2s []	+0.2264	+0.3467	
			1s [↑]	-0.2678	-0.0932	
cc-pVTZ	14 (3s2p1d)	-0.478526581011	2p []	+3.4420	+3.7150	
			1d []	+3.0716	+3.2875	
			3s []	+2.1076	+2.3889	
			1p []	+0.5280	+0.6717	
			2s []	+0.2263	+0.3465	
			1s [↑]	-0.2678	-0.0932	
IGLO-II	6 (3s1p)	-0.478538678025	3s []	+2.0706	+2.3505	
			1p []	+1.0109	+1.2172	
			2s []	+0.2212	+0.3400	
			1s [↑]	-0.2679	-0.0936	

Basis	Size	Energy (Ha)	MO energies (Ha)		
				↑	↓
AUG-CC-PVTZ	23 (4s3p2d)	-0.478556529112	3p []	+3.6446	+3.9123
			2d []	+3.4802	+3.6919
			4s []	+2.2039	+2.4823
			2p []	+0.7776	+0.9128
			1d []	+0.6392	+0.7090
			3s []	+0.3244	+0.4366
			1p []	+0.1027	+0.1463
			2s []	+0.0227	+0.0489
			1s [↑]	-0.2689	-0.1000
DZ-ANO	9 (3s2p)	-0.478584935851	2p []	+1.5802	+1.7989
			3s []	+0.9139	+1.1454
			1p []	+0.1586	+0.2280
			2s []	+0.0374	+0.0868
			1s [↑]	-0.2681	-0.0985
AUG-PCJ-2	33 (6s4p3d)	-0.478638545287	6s []	26.8033	27.2601
			3d []	25.6063	26.0085
			4p []	24.6743	25.1102
			5s []	+4.9664	+5.2842
			3p []	+4.0671	+4.3464
			2d []	+3.6788	+3.9097
			4s []	+1.1220	+1.3041
			2p []	+0.7554	+0.9056
			1d []	+0.2280	+0.2477
			3s []	+0.2156	+0.2924
			1p []	+0.0634	+0.0921
			2s []	+0.0173	+0.0370
			1s [↑]	-0.2690	-0.1002
AUG-CC-PVQZ	46 (5s3p3d2f)	-0.478665974013	3d []	+7.9271	+8.2063
			4p []	+7.4415	+7.7525
			5s []	+6.8584	+7.2210
			2f []	+6.1674	+6.3806
			3p []	+2.2361	+2.4329
			2d []	+2.1685	+2.3201
			1f []	+1.3706	+1.4463
			4s []	+1.3119	+1.5094
			2p []	+0.5704	+0.6741
			1d []	+0.4781	+0.5271
			3s []	+0.2607	+0.3483
			1p []	+0.0826	+0.1168
			2s []	+0.0203	+0.0430
			1s [↑]	-0.2690	-0.1001

Basis	Size	Energy (Ha)	MO energies (Ha)		
				↑	↓
AUG-PCJ-3	61 (9s6p4d2f)	-0.478678491280	9s []	316.1227	316.6702
			6p []	106.2487	106.7586
			8s []	65.2161	65.7009
			4d []	41.1240	41.5577
			5p []	18.7322	19.1300
			7s []	18.5835	18.9808
			2f []	+9.0720	+9.3366
			3d []	+7.3085	+7.5818
			6s []	+5.8099	+6.1036
			4p []	+4.7623	+5.0262
			5s []	+1.8494	+2.0393
			2d []	+1.7992	+1.9490
			3p []	+1.4287	+1.5852
			4s []	+0.5535	+0.6570
			2p []	+0.3560	+0.4403
			1f []	+0.3609	+0.3727
			1d []	+0.1934	+0.2081
			3s []	+0.1345	+0.1799
			1p []	+0.0534	+0.0747
			2s []	+0.0128	+0.0270
			1s [↑]	-0.2690	-0.1002

Basis	Size	Energy (Ha)	MO energies (Ha)		
				↑	↓
AUG-PCJ-4	99 (11s8p5d3f2g)	-0.478679881242	11s []	1295.3479	1295.9104
			8p []	504.2247	504.7784
			10s []	272.4493	272.9869
			7p []	89.5868	90.0788
			9s []	80.4120	80.8955
			5d []	44.6374	45.0753
			8s []	26.7114	27.1212
			6p []	22.8657	23.2553
			2g []	16.6930	16.9745
			2f []	12.1613	12.4375
			7s []	+9.4810	+9.8020
			4d []	+8.5163	+8.7931
			5p []	+8.0131	+8.2957
			1f []	+3.4595	+3.6155
			6s []	+3.4567	+3.6834
			4p []	+3.0843	+3.2809
			3d []	+2.7283	+2.8856
			5s []	+1.2377	+1.3801
			3p []	+1.0624	+1.1866
			2d []	+0.8473	+0.9197
			1f []	+0.5145	+0.5227
			4s []	+0.4088	+0.4862
			1f []	+0.3302	+0.3400
			2p []	+0.2893	+0.3478
			1d []	+0.1760	+0.1870
			3s []	+0.1079	+0.1439
			1p []	+0.0486	+0.0667
			2s []	+0.0105	+0.0225
			1s [↑]	-0.2690	-0.1001

Basis	Size	Energy (Ha)	MO energies (Ha)		
				↑	↓
AUG-CC-PV5Z	80 (6s5p4d3f2g)	-0.478696304484	5p []	16.3297	16.5007
			4d []	13.3297	13.6430
			2g []	12.6824	12.9295
			3f []	12.3776	12.6525
			6s []	12.2082	12.6030
			4p []	+5.3953	+5.6572
			3d []	+4.7656	+4.9710
			2f []	+3.8388	+3.9923
			5s []	+2.8146	+3.0578
			1g []	+2.7065	+2.7992
			3p []	+1.7409	+1.9084
			2d []	+1.5748	+1.6892
			1f []	+1.0184	+1.0711
			4s []	+0.8071	+0.9410
			2p []	+0.4732	+0.5613
			1d []	+0.3838	+0.4197
			3s []	+0.1867	+0.2496
			1p []	+0.0713	+0.1002
			2s []	+0.0153	+0.0331
			1s [↑]	-0.2690	-0.1001

Basis	Size	Energy (Ha)	MO energies (Ha)		
				↑	↓
IGLO-III	10 (4s2p)	-0.478715109266	4s []	+5.5700	+5.9174
			2p []	+3.0597	+3.3244
			3s []	+1.0276	+1.2117
			1p []	+0.4350	+0.5646
			2s []	+0.1408	+0.2243
			1s [↑]	-0.2688	-0.0973
LIC	11 (5s2p)	-0.478715642643	5s []	12.1268	12.5219
			2p []	+2.9876	+3.2619
			4s []	+2.7444	+2.9895
			3s []	+0.7299	+0.8680
			1p []	+0.3112	+0.4200
			2s []	+0.1060	+0.1730
			1s [↑]	-0.2689	-0.0985

5.1.2 Analysis

What Should We Expect?

It is always useful to anticipate what we should find so that we are surprised (and learn something!) when things are not as we expected. As Louis Pasteur famously said,

Dans les champs de l'observation le hasard ne favorise que les esprits préparés.
 (In the field of observation, chance favors the prepared mind.)

The exact solution is, of course, known for the hydrogen atom. In particular, the ground state energy is,

$$E = -\frac{1}{2}, \quad (5.1)$$

in Hartree atomic units. Orbital energies depend only on the principle quantum number n and are given by,

$$\epsilon_n = -\frac{1}{2} \frac{1}{n^2}. \quad (5.2)$$

Neither of these exact results is observed in our calculations, even with the largest basis set! Why?

Those familiar with density-functional theory (DFT) will recognize that the problem comes from the self-interaction error (SIE) in the local (spin) density approximation (LDA). In particular, the total energy DFT energy is given by,

$$E = \langle \psi | \left(-\frac{1}{2} \nabla^2 - \frac{1}{r} \right) | \psi \rangle + E_H[\rho] + E_{xc}[\rho], \quad (5.3)$$

where the Coulomb (also called the Hartree) energy is given in terms of the density,

$$\rho(\vec{r}) = |\psi(\vec{r})|^2, \quad (5.4)$$

as,

$$E_H = \frac{1}{2} \int \int \frac{\rho(\vec{r}_1)\rho(\vec{r}_2)}{r_{1,2}} d\vec{r}_1 d\vec{r}_2. \quad (5.5)$$

In principle, had we the exact DFT exchange-correlation (xc) energy functional then we should have $E_H + E_{xc} = 0$. However usually we have the SIE, $E_H + E_{xc} > 0$, with the result that for the hydrogen atom, $E > -1/2$.

Let us also look at how the SIE affects orbital energies. The dominant part of the LDA exchange-correlation (xc) energy is the exchange part which is known exactly,

$$E_x = C_x \left(\int \rho_{\uparrow}^{4/3}(\vec{r}) d\vec{r} + \int \rho_{\downarrow}^{4/3}(\vec{r}) d\vec{r} \right), \quad (5.6)$$

where,

$$C_x = -\frac{3}{4} \left(\frac{6}{\pi} \right)^{1/3}. \quad (5.7)$$

The fact that this depends on spin tells us something important, namely that,

$$\begin{aligned} \epsilon_{\uparrow} &= \langle \psi | \left(-\frac{1}{2} \nabla^2 + \frac{1}{r} \right) | \psi \rangle + \int \int \frac{\rho(\vec{r}_1)\rho(\vec{r}_2)}{r_{1,2}} d\vec{r}_1 d\vec{r}_2 + \frac{4}{3} C_x \int \int \rho^{4/3}(\vec{r}) d\vec{r} \\ \epsilon_{\downarrow} &= \langle \psi | \left(-\frac{1}{2} \nabla^2 + \frac{1}{r} \right) | \psi \rangle + \frac{\rho(\vec{r}_1)\rho(\vec{r}_2)}{r_{1,2}} d\vec{r}_1 d\vec{r}_2, \end{aligned} \quad (5.8)$$

assuming the lone electron has spin \uparrow . As $C_x < 0$, then we should have

$$\epsilon_{\uparrow} < \epsilon_{\downarrow} \quad (5.9)$$

for corresponding orbital energies, exactly as observed. Moreover the SIE is actually larger for the orbital energy than for the total energy because, in going from the total energy expression to the orbital energy expression, the Hartree part has doubled but the (partially) compensating xc part has only increased by a factor of $4/3$ for spin \uparrow and is totally lacking for spin \downarrow . Thus we actually expect (and have) that,

$$E < \epsilon_{\uparrow} < \epsilon_{\downarrow} \quad (5.10)$$

The Variational Principle

A numerical method to solve a mathematical equation is by definition an approximation. As such it is complemented by having a criterion that tells us when we have improved or degraded the approximation. In much of quantum chemistry, this criterion is the variational principle:

Wave Function Variational Principle

Consider the Schrödinger equation,

$$\hat{H}\Psi_I = E_I\Psi_I, \quad (5.11)$$

where the indices I have been chosen so that $E_0 \leq E_1 \leq E_2 \leq \dots$, and let Φ be a function which satisfies all of the boundary conditions of the boundary-value problem (5.11). Then

$$E_0 \leq E[\Phi] = \frac{\langle \Phi | \hat{H} | \Phi \rangle}{\langle \Phi | \Phi \rangle}. \quad (5.12)$$

Φ is called the trial wave function and $E[\Phi]$ is the variational integral. Note that the variational integral is a functional (i.e., a function of a function) of Φ .

The boundary conditions include any symmetry constraints so that a corollary is that a trial wave function belonging to an irreducible representation (irrep) of the symmetry group of the system is an upper bound to the energy of the lowest state of the same irrep. In the event that the trial wave function is expressed as a linear combination of basis functions, then the variational principle leads to the generalized eigenvalue problem,

$$\mathbf{H}\vec{C}_I = E_I \mathbf{S}\vec{C}_I. \quad (5.13)$$

This leads to another important result, namely:

Hylleraas-Undheim-MacDonald or Cayley Interleaving Theorem

(The first name is used by physicists and the second by mathematicians.) As basis functions are added to the basis set in a linear variational problem the solutions E_I to the variational problem interleave each other as shown in Fig. 5.1. A corollary is that the I th solution is an upper bound to the true energy of the I th state (though it may not be a very good upper bound.)

We use a different, but related, variational principle in DFT, namely

Hohenberg-Kohn DFT

(Levy-Lieb constrained search.) The ground state energy and charge density with external potential v may be found by minimizing a functional of N -representable charge densities ρ ,

$$E_0 \leq E_v[\rho] = F[\rho] + \int v(\vec{r})\rho(\vec{r}) d\vec{r}, \quad (5.14)$$

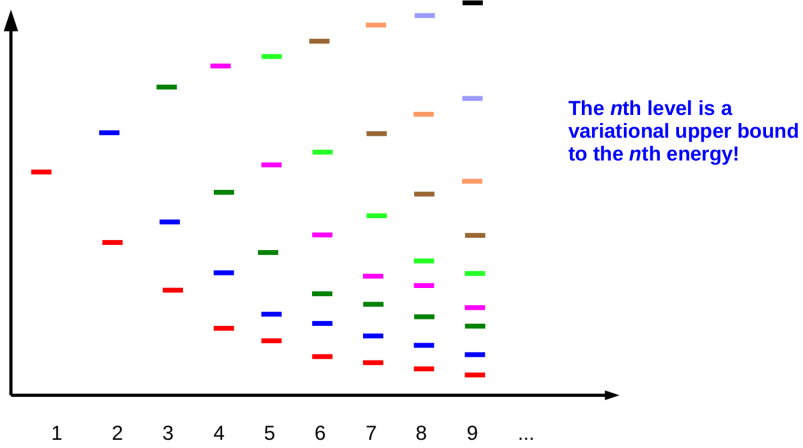


Figure 5.1: Illustration of the Hylleraas-Undheim-MacDonald/Cayley interleaving theorem for the linear variational principle.

where the quantity,

$$F[\rho] = \min_{\Psi \rightarrow \rho} \frac{\langle \Psi | \hat{T} + \hat{V}_{ee} | \Psi \rangle}{\langle \Psi | \Psi \rangle}, \quad (5.15)$$

is universal in the sense of being independent of v . The condition of N -representability means that a wave function Ψ exists whose density is ρ . Fortunately just about any non-negative function that integrates to N electrons can be shown to be an N -representable density.

In practice, we do not have any convenient exact expression for the universal functional $F[\rho]$ so it must be approximated.

Kohn-Sham DFT

It turns out that the kinetic energy part T is the most difficult part to approximate so Kohn and Sham proposed replacing the kinetic energy of a fictitious system of non-interacting electrons whose ground-state density is ρ . This last condition is known as the requirement of non-interacting v -representability (NIVR) and it fails whenever the lowest energy state has the LUMO lower in energy than the HOMO which is a familiar situation for open-shell atoms, transition metal complexes, and near transition states. Nevertheless for systems with NIVR, we may minimize the energy using the orbitals ψ_i of the non-interacting system,

$$E = \sum_i n_i \langle \psi_i | (\hat{t} + v) | \psi_i \rangle + \frac{1}{2} \int \int \frac{\rho(\vec{r}_1)\rho(\vec{r}_2)}{r_{1,2}} d\vec{r}_1 d\vec{r}_2 + E_{xc}[\rho], \quad (5.16)$$

subject to the constraint of orthonormal orbitals, to obtain the Kohn-Sham orbital equation,

$$\left(\hat{t} + v(\vec{r}_1) + \int \frac{\rho(\vec{r}_2)}{r_{1,2}} d\vec{r}_2 + v_{xc}[\rho](\vec{r}_1) \right) \psi_i(\vec{r}_1) = \epsilon_i \psi_i(\vec{r}_1), \quad (5.17)$$

where the xc potential,

$$v_{xc}[\rho](\vec{r}) = \frac{\delta E_{xc}[\rho]}{\delta \rho(\vec{r})}. \quad (5.18)$$

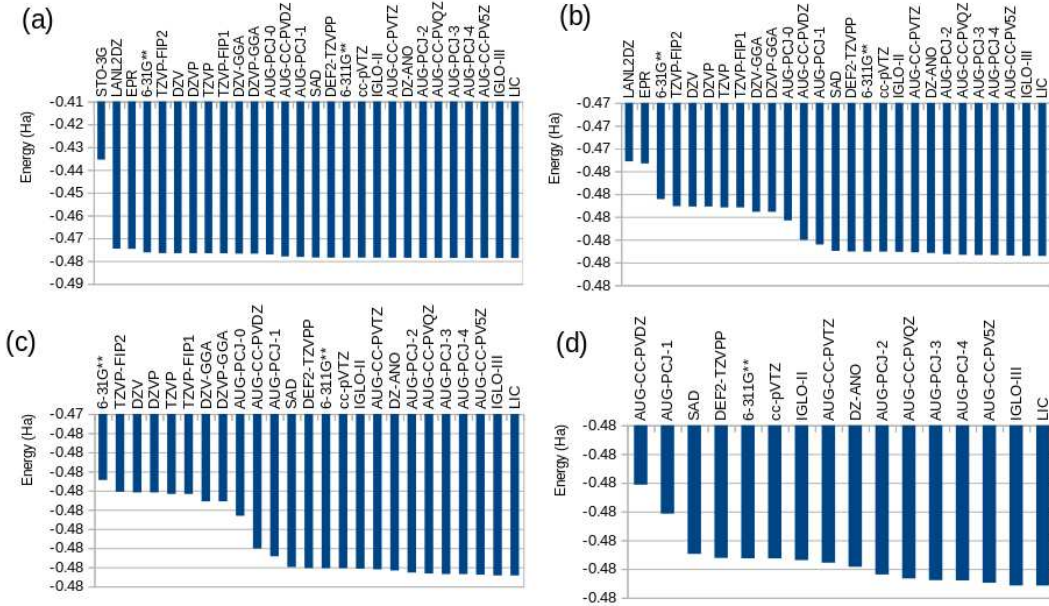


Figure 5.2: Convergence of energies with respect to basis set.

In some sense, the problem of finding a practical accurate form for F has just been transferred to the problem of finding a practical accurate form for E_{xc} . Nevertheless as E_{xc} makes a smaller magnitude contribution to the total energy, better results may be obtained with Kohn-Sham DFT than with the original Hohenberg-Kohn DFT by using approximate functionals. It is to be emphasized that *even more so than with wave function theory*, the variational principle is really at the heart of DFT.

If, in addition, we approximate the Kohn-Sham orbitals as a linear combination of basis functions, then we arrive at Eq. (5.13) for which we may expect the interleaving theorem to apply. There is a caveat however which is that the interleaving theorem was not derived for a self-consistent theory such as Kohn-Sham theory. Thus we should be wary that the interleaving theorem might fail because \mathbf{H} depends upon the \vec{C}_i .

With this preamble, let us now look at the results of our calculations with different basis sets from a variational point of view. Figure 5.2 shows how the basis set converges as the basis set is varied. If we take the lowest energy (i.e., the one obtained using the LIC basis set) as the LDA limit E_{LDA} (with this grid and this choice of auxiliary basis set), then we may define an error measure familiar to chemists who are used to using pH and pK_a :

$$p\Delta E = -\log(E - E_{\text{LDA}}). \quad (5.19)$$

To put this in perspective, “chemical accuracy” 1 kcal/mol = 0.0016 Ha, which corresponds to $p\Delta E = 2.80$. Figure 5.3 shows this quantity as a function of the basis set. Chemical accuracy is apparently obtained beginning with the AUG-CC-PVDZ basis set. Notice though that many basis sets have exactly the same value of $p\Delta E$.

Figure 5.4 explores how the size of the basis set affects the accuracy of the calculated result. Part (a) of the figure shows that there is no particular correlation between the total number of functions in the basis set. In particular, the total number of CGTOs goes up and down quite a bit on the left-hand side of the graph, rises quite a bit towards the right-hand side, only to crash down at the very right. Part (c) of the figure analyses how the number of sets of each type of CGTO correlates

with the accuracy of the calculated result. A little thought shows that this is a case where symmetry imposes a boundary condition so that only *s*-type CGTOs should be able to affect the accuracy of the calculation. This is most clearly seen in comparing parts (b) and (d) of the figure. Many basis sets share the same *s*-type CGTOs and hence have both the same number of *s*-type CGTOs and the same accuracy.

So you might say that, “A bigger basis is *often* better,” at least if you pay attention to the boundary constraints of the problem. But the choice of a basis set is not so simple. For one thing, it depends upon whether (i) you want to do the best possible calculation for a single molecule or (ii) you want to keep the basis set small but balanced and accurate for exploring many molecules or many geometries of the same molecule. Often chemists want (ii) and so keep the basis set small. In deciding how to reduce a larger basis set to make an efficient smaller basis set, it also has to be kept in mind that tight functions (GTOs with large exponents) may improve the energetically-dominant region near the nucleus but most chemistry is happening in regions of the electron cloud away from the nucleus in the bonding region. This is why a low total energy obtained from the presence of many tight functions may not be the best criterion for describing chemical bonding or reaction mechanisms. And this is also why we have many different types of basis sets here. Some are optimized to be efficient for describing hydrogen atoms in typical organic molecules where we may expect the atom to be more compressed than the free hydrogen atom. Some include polarization functions. Others, such as the EPR basis set, have even more tight functions than usual because they are designed to calculate electron pair resonance parameters which are sensitive to the quality of the wave function near the nucleus. Still others, such as the SAD and FIP basis sets, add diffuse polarization functions to describe how molecular orbitals are polarized in the presence of an applied electric field. The very largest basis sets are important primarily when you do not know what type of basis functions are needed to describe the property that interests you or you need to prove that your calculations are well-converged with respect to basis set. Most calculations will be done with basis sets from the left-hand side of the graphs, except when absolutely necessary to do otherwise.

Let us now turn to the orbital energies. Traditionally more attention is paid to getting an accurate total energy than to getting accurate orbital energies. This shows up in the fact that the orbital energies are printed out with fewer significant figures. Nevertheless we should expect some correlation between the accuracy of the energy of the $1s$ orbital and that of the total energy for the hydrogen atom. This correlation is shown in Fig. 5.5. There is a remarkably good correlation between the two quantities up to a value of about 3. A correlation limit of about 4 might have been expected given the number of significant figures printed out for the orbital energies, but the limit seems to be 3. As a general rule it seems fair to say that the total energy is usually more accurate than the individual orbital energies that enter into the calculation of the total energy. (Remember that errors cancel out!)

Figure 5.6 shows how the lowest $s \uparrow$ energies vary as a function of basis size. Note that the interleaving theorem should only apply if successive basis sets are constructed by adding functions to the previous basis sets. Nevertheless there is some indication of some interleaving-like behavior. This is even more the case when we look at the results for a specific family of basis functions. Results are shown for the AUG-PCJ-X basis sets in Fig. 5.7. This section ends with a tabulation of just the *s*-functions in the AUG-PCJ-X basis sets to emphasize that they are not constructed by successively adding basis functions to the previous basis set in the series. Although these basis sets do not fulfill the conditions of the interleaving theorem, the orbital energies do have a remarkable job of interleaving each other as the series of basis sets progresses.

#

O-HYDROGEN H (AUG-PCJ-0)

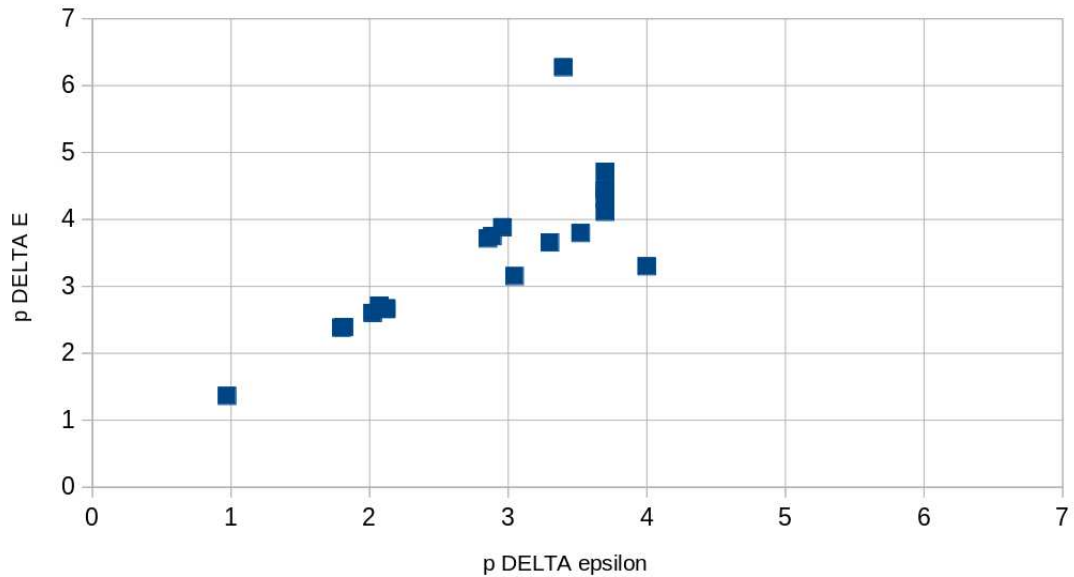


Figure 5.5: Correlation diagram between $p\Delta E$ (the error in the total energy) and $p\Delta\epsilon$ (the error in the 1s orbital energy). Results for the AUG-PCJ-0 (used as the reference for $p\Delta\epsilon$) and for the LIC (used as the reference for $p\Delta E$) have been omitted to avoid infinities.

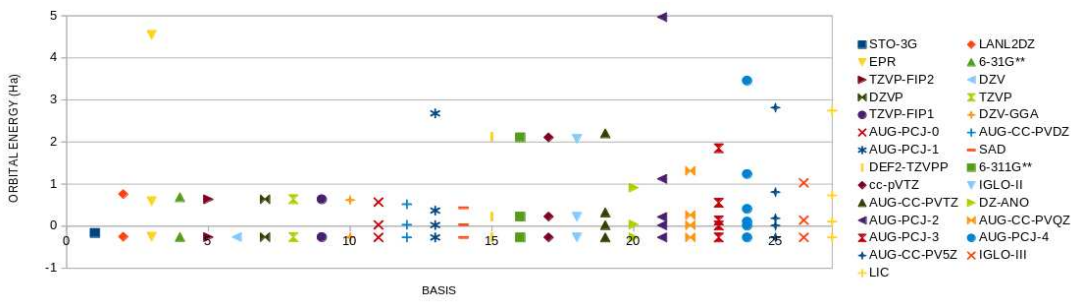
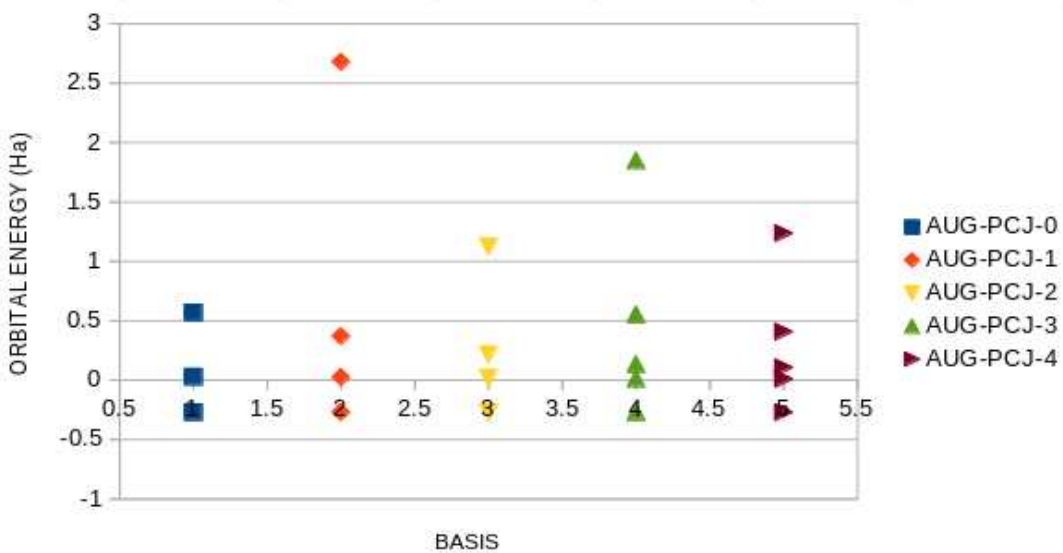


Figure 5.6: How the lowest $s\uparrow$ energies vary as a function of basis size.

Figure 5.7: How the lowest $s \uparrow$ energies vary as a function of basis size.

```

4
1 0 3
  0.135775E+04      0.662272E-03
  0.543100E+02      0.301414E-01
  0.434480E+01      0.500000E+00
2 0 1
  0.660491E+00      1.0000000000
3 0 1
  0.136687E+00      1.0000000000
4 0 1
  0.271740E-01      1.0000000000
#
#
# O-HYDROGEN H (AUG-PCJ-1)
8
1 0 3
  0.382870E+04      0.636372E-03
  0.153148E+03      0.286776E-01
  0.122519E+02      0.500000E+00
2 0 1
  0.186872E+01      1.0000000000
3 0 1
  0.418210E+00      1.0000000000
4 0 1
  0.106100E+00      1.0000000000
5 0 1
  0.256280E-01      1.0000000000
#

```

#

0-HYDROGEN H (AUG-PCJ-2)

13

1	0	4	
	0.235696E+05	0.783660E-04	
	0.942782E+03	0.352323E-02	
	0.754226E+02	0.623968E-01	
	0.113499E+02	0.500000E+00	
2	0	1	
	0.259926E+01	1.0000000000	
3	0	1	
	0.735130E+00	1.0000000000	
4	0	1	
	0.231669E+00	1.0000000000	
5	0	1	
	0.741474E-01	1.0000000000	
6	0	1	
	0.223340E-01	1.0000000000	

#

#

0-HYDROGEN H (AUG-PCJ-3)

21

1	0	4	
	0.242090E+06	0.768560E-04	
	0.968361E+04	0.345606E-02	
	0.774689E+03	0.613071E-01	
	0.116159E+03	0.500000E+00	
2	0	1	
	0.264490E+02	1.0000000000	
3	0	1	
	0.750149E+01	1.0000000000	
4	0	1	
	0.245685E+01	1.0000000000	
5	0	1	
	0.887743E+00	1.0000000000	
6	0	1	
	0.340847E+00	1.0000000000	
7	0	1	
	0.134773E+00	1.0000000000	
8	0	1	
	0.522633E-01	1.0000000000	
9	0	1	
	0.188000E-01	1.0000000000	

#

#

0-HYDROGEN H (AUG-PCJ-4)

29

1	0	3	
	0.615934E+05	0.244497E-02	
	0.307967E+04	0.627032E-01	
	0.461515E+03	0.500000E+00	
2	0	1	
	0.105058E+03	1.0000000000	
3	0	1	
	0.297641E+02	1.0000000000	
4	0	1	
	0.971826E+01	1.0000000000	
5	0	1	
	0.351795E+01	1.0000000000	
6	0	1	
	0.137696E+01	1.0000000000	
7	0	1	
	0.568306E+00	1.0000000000	
8	0	1	
	0.243407E+00	1.0000000000	
9	0	1	
	0.105053E+00	1.0000000000	
10	0	1	
	0.441983E-01	1.0000000000	
11	0	1	
	0.171310E-01	1.0000000000	

#

5.2 Lesson 2 Answers

5.2.1 Hartree-Fock

Because Hartree-Fock is self-interaction free, this is the closest thing that we have to an exact answer. For the total energy we expect to get $E = -0.5 \text{ Ha}$, the exact answer for the hydrogen atom. Similarly the potential seen by the $1s \uparrow$ electron is

$$v = -1/r, \quad (5.20)$$

the potential for the hydrogen atom, so we also expect to see

$$\epsilon_{1s}^{\uparrow} = -0.5 \text{ Ha}. \quad (5.21)$$

However the electrons in an unoccupied orbital $a \uparrow$ will see

$$\hat{v}_a^{\uparrow} = v + v_H[\rho_{1s}] + \hat{\Sigma}_x^{\uparrow} \quad (5.22)$$

while the electrons in an unoccupied orbital $a \downarrow$ will see

$$\hat{v}_a^{\downarrow} = v + v_H[\rho_{1s}], \quad (5.23)$$

the same as in the Hartree approximation to the extent that the ρ_{1s} density is the same. Hence we expect to see that

$$\epsilon_a^\uparrow < \epsilon_a^\downarrow. \quad (5.24)$$

For the $1s \downarrow$ virtual orbital, Koopmans' theorem tells us to expect an orbital energy close to the negative of the corresponding electron affinity.

Functional	Energy (Ha)	MO energies (Ha)		
			↑	↓
FOCK	-0.499994534955	5s []	12.7160	12.7757
		2p []	+3.3816	+3.4819
		4s []	+3.1011	+3.1920
		3s []	+0.9106	+1.0179
		1p []	+0.4855	+0.5630
		2s []	+0.1803	+0.2805
		1s [↑]	-0.5000	+0.0377

The predictions are pretty much as expected. In fact, the agreement is remarkable given that a finite orbital basis set and a finite auxiliary basis set is used. As the electron affinity of the hydrogen atom is 0.0278 Ha, we predicted a $1s \downarrow$ orbital energy of -0.0278 Ha which is in reasonable agreement with the calculated spin $1s \downarrow$ energy of +0.0377 Ha. That is both numbers are close to zero. This also permits us to estimate that

$$[\rho_{1s} || \rho_{1s}] \approx +0.5 \text{ Ha}. \quad (5.25)$$

5.2.2 Hartree

The Hartree approximation suffers from a substantial self-interaction error so that the total energy should be too high by about

$$\frac{1}{2}[\rho_{1s} || \rho_{1s}] \approx +0.25 \text{ Ha}. \quad (5.26)$$

Both occupied and virtual orbitals see the same potential irrespective of spin, namely

$$\hat{v} = v_H[\rho_{1s}], \quad (5.27)$$

Comparing with Eq. (5.23), the Hartree orbital energies should be roughly the same as the spin \uparrow Hartree-Fock orbital energies. This is confirmed in the following table, as is the expectation that the $1s$ orbital energy should be about,

$$\epsilon_{1s} \approx -0.5 \text{ Ha} + [\rho_{1s} || \rho_{1s}] \approx 0. \quad (5.28)$$

The $1s$ orbital is only *barely bound*!

Functional	Energy (Ha)	MO energies (Ha)		
			↑	↓
NONE	-0.240286508677	5s []	12.5551	12.5551
		2p []	+3.3157	+3.3157
		4s []	+3.0469	+3.0469
		3s []	+0.9311	+0.9311
		1p []	+0.5049	+0.5049
		2s []	+0.2237	+0.2237
		1s [↑]	-0.0274	-0.0274

Another thing that can be seen in these numbers has to do with the density-fitting procedure used by DEMON2K. In order to eliminate 4-center integrals, the true charge density ρ is often replaced by a fitted charge density,

$$\tilde{\rho}(\vec{r}) = \sum_I f_I(\vec{r}) a_I . \quad (5.29)$$

The a_I coefficients are obtained by minimizing

$$[\rho - \tilde{\rho}] [\rho - \tilde{\rho}] = [\rho] [\rho] - 2[\rho] [\tilde{\rho}] + [\tilde{\rho}] [\tilde{\rho}] \geq 0 . \quad (5.30)$$

The *antivariational* quantity $2[\rho] [\tilde{\rho}] - [\tilde{\rho}] [\tilde{\rho}]$ which is always a *lower bound* to the exact $[\rho] [\rho]$,

$$2[\rho] [\tilde{\rho}] - [\tilde{\rho}] [\tilde{\rho}] \leq [\rho] [\rho] , \quad (5.31)$$

is used in evaluating the total energy while $[\rho] [\tilde{\rho}]$ is used in the orbital energy calculation. From the numbers in the table, we see that

$$\begin{aligned} 2[\rho_{1s}] [\tilde{\rho}_{1s}] - [\tilde{\rho}_{1s}] [\tilde{\rho}_{1s}] &= +0.5194 \text{ Ha} \\ [\rho_{1s}] [\tilde{\rho}_{1s}] &= +0.4725 \text{ Ha} \\ [\tilde{\rho}_{1s}] [\tilde{\rho}_{1s}] &= +0.4256 \text{ Ha} . \end{aligned} \quad (5.32)$$

5.2.3 X α

Before looking at the LDA, it is useful to look just at the exchange part of the LDA. This has come to be known as the Dirac exchange and takes the form

$$E_x = C_x \left(\int \rho_{\uparrow}^{4/3}(\vec{r}) d\vec{r} + \int \rho_{\downarrow}^{4/3}(\vec{r}) d\vec{r} \right) , \quad (5.33)$$

where,

$$C_x = -\frac{3}{4} \left(\frac{6}{\pi} \right)^{1/3} . \quad (5.34)$$

At that time, closed shell systems were typically assumed with

$$\rho_{\sigma} = \frac{\rho}{2} . \quad (5.35)$$

Consequently,

$$\begin{aligned} E_x &= -\frac{3}{4} \left(\frac{3}{\pi} \right)^{1/3} \int \rho^{4/3}(\vec{r}) d\vec{r} \\ v_x(\vec{r}) &= -\left(\frac{3}{\pi} \right)^{1/3} \rho^{1/3}(\vec{r}) . \end{aligned} \quad (5.36)$$

Slater made the “mistake” of identifying the potential term with half the corresponding exchange energy — something which is valid in Hartree-Fock theory. (“Mistake” is in quotes because his arguments seemed logical at the time.) He thus arrived at

$$v_x(\vec{r}) = -\frac{3}{2} \left(\frac{3}{\pi} \right)^{1/3} \rho^{1/3}(\vec{r}) . \quad (5.37)$$

The Kohn-Sham paper made it clear that this was a mistake and led to a period of disagreement between Slater and Kohn which ended up with Slater proposing to replace Eq. (5.34) with

$$C_x = - \left(\alpha \frac{3}{2} \right) \frac{3}{4} \left(\frac{6}{\pi} \right)^{1/3}, \quad (5.38)$$

where α is an adjustable parameter. When $\alpha = 1$, we have the original Slater theory. When $\alpha = 2/3$, we recover the original Kohn-Sham theory. Schwartz obtained optimized values of α by fitting to Hartree-Fock energies for atoms [149]. It is remarkable that, though he found different values for different atoms, they were all roughly equal to $2/3$. However $\alpha = 0.75$ was found to be a typical good choice for molecular calculations aiming to reproduce Hartree-Fock energies. We may use the XALPHA keyword with $X = 0.75$ (XALPHA default) and $X = 0.66666667$ (DIRAC) to explore the sizes of key integrals.

Functional	Energy (Ha)	MO energies (Ha)		
			↑	↓
DIRAC	-0.457100711453	5s []	12.1542	12.7416
		2p []	+3.0126	+3.4562
		4s []	+2.7675	+3.1697
		3s []	+0.7470	+1.0043
		1p []	+0.3302	+0.5548
		2s []	+0.1172	+0.2709
		1s [↑]	-0.2467	+0.0299
XALPHA	-0.489405255903	5s []	12.0916	12.7663
		2p []	+2.9668	+3.4737
		4s []	+2.7270	+3.1852
		3s []	+0.7242	+1.0135
		1p []	+0.3085	+0.5598
		2s []	+0.1074	+0.2773
		1s [↑]	-0.2816	+0.0350

For the total energy,

$$\begin{aligned} 0.042899 &= E_H + E_x^{\text{Dirac}} \\ 0.010595 &= E_H + E_x^{X_\alpha} = E_H + 1.12499 E_x^{\text{Dirac}}. \end{aligned} \quad (5.39)$$

So

$$\begin{aligned} E_x^{\text{Dirac}} &= \frac{0.010595 - 0.042899}{0.12499} = -0.258452 \\ E_H &= 0.042899 + 0.258452 = 0.30135. \end{aligned} \quad (5.40)$$

(For comparison purposes, the output actually gives the value of E_x^{Dirac} and it is -0.2535 Ha.) For the $1s \uparrow$ orbital energy,

$$\begin{aligned} 0.2532 &= \epsilon_H + \epsilon_x^{\text{Dirac}} \\ 0.2183 &= \epsilon_H + \epsilon_x^{X_\alpha} = \epsilon_H + 1.12499 \epsilon_x^{\text{Dirac}} \end{aligned} \quad (5.41)$$

So

$$\begin{aligned}\epsilon_x^{\text{Dirac}} &= \frac{0.2183 - 0.2532}{0.12499} = -0.2792 \\ \epsilon_H &= 0.2532 + 0.2792 = 0.5324.\end{aligned}\quad (5.42)$$

As expected,

$$\epsilon_H \approx \frac{E_H}{2}. \quad (5.43)$$

As

$$E_x^{\text{Dirac}} \approx -E_H, \quad (5.44)$$

the exchange energy does roughly cancel the spurious self-interaction error in the total energy and this is even more true with the Xα than with the Dirac exchange. However such a cancellation is clearly not the case for the $1s^\uparrow$ orbital energy whose value is much closer to the approximation,

$$\epsilon_{1s}^\uparrow \approx -\frac{\text{IP} + \text{EA}}{2} = 0.2639 \text{ Ha} \quad (5.45)$$

predicted on the basis of particle number derivative discontinuity (PNDD) arguments.

5.2.4 LDA

For molecules, the dominant part of the xc energy and potential is the exchange part. However for the hydrogen atom, there should not be any correlation part.

Functional	Energy (Ha)	MO energies (Ha)		
			↑	↓
VWN	-0.478715642643	5s []	12.1268	12.5219
		2p []	+2.9876	+3.2619
		4s []	+2.7444	+2.9895
		3s []	+0.7299	+0.8680
		1p []	+0.3112	+0.4200
		2s []	+0.1060	+0.1730
		1s [↑]	-0.2689	-0.0985
PZ81	-0.478830327877	5s []	12.1542	12.7416
		2p []	+3.0126	+3.4562
		4s []	+2.7675	+3.1697
		3s []	+0.7470	+1.0043
		1p []	+0.3302	+0.5548
		2s []	+0.1172	+0.2709
		1s [↑]	-0.2467	+0.0299
PW92	-0.478755555490	5s []	12.1268	12.5285
		2p []	+2.9876	+3.2679
		4s []	+2.7444	+2.9952
		3s []	+0.7299	+0.8724
		1p []	+0.3111	+0.4246
		2s []	+0.1061	+0.1760
		1s [↑]	-0.2689	-0.0939

As these are all different parameterizations of the xc energy density of the homogeneous electron gas (HEG), we might have expected them to be even closer than they are. The VWN parameterization has long been favored by chemists while solid-state physicists have found better results for solids with the PZ81 parameterization. The PW92 parameterization is more modern and was designed to go with a GGA correction. The PW92 results are closer to the VWN results than to the PZ81 results. I am not sure where the differences come from, but it may be from the spin-dependence of the correlation part of the functional as this part is less well known than is the case where there is no spin polarization.

We may use the VWN numbers together with the Dirac numbers to estimate the size of the correlation part of the VWN energy. From the total energy,

$$\begin{aligned} E_{Hxc} &= -0.478715642643 + 0.5 = +0.02128 \\ E_{xc} &= E_{Hxc} - E_H = +0.02128 - 0.30135 = -0.28007 \\ E_c &= E_{xc} - E_x = -0.28007 + 0.25845 = -0.02162 . \end{aligned} \quad (5.46)$$

(The output gives $E_{xc} = -0.2783$ Ha.) From the orbital energy,

$$\begin{aligned} \epsilon_{Hxc} &= -0.2689 + 0.5 = +0.23110 \\ \epsilon_{xc} &= \epsilon_{Hxc} - \epsilon_H = 0.2311 - 0.5324 = -0.3013 \\ \epsilon_c &= \epsilon_{xc} - \epsilon_x = -0.3013 + 0.2792 = -0.0221 . \end{aligned} \quad (5.47)$$

The “correlation energy” (there is no correlation in the hydrogen atom!) is less than a tenth the magnitude of the exchange but of the same sign. Nevertheless, for the total energy, the erroneous correlation energy is correcting the erroneous exchange energy to give an improved xc energy. This emphasizes an important principle of DFAs:

The LDA works by cancellation of errors between the exchange and correlation parts.

This is why it is usually a bad idea to mix 100% exact exchange with DFA correlation.

5.2.5 GGAs

GGAs improve the total energy. In general they reduce the overbinding of the LDA and improve bond lengths (usually by making them longer.)

Functional	Energy (Ha)	MO energies (Ha)		
			↑	↓
PW86	-0.502012085529	5s []	12.0195	12.6435
		2p []	+2.9688	+3.3335
		4s []	+2.7135	+3.0651
		3s []	+0.7138	+0.9267
		1p []	+0.3088	+0.4778
		2s []	+0.0970	+0.2128
		1s [↑]	-0.2823	-0.0410

Functional	Energy (Ha)	MO energies (Ha)		
			↑	↓
BLYP	-0.497978305125	5s []	12.0130	12.7278
		2p []	+2.9780	+3.3710
		4s []	+2.7237	+3.1037
		3s []	+0.7240	+0.9483
		1p []	+0.3228	+0.4897
		2s []	+0.1026	+0.2266
		1s [↑]	-0.2720	-0.0258
		5s []	12.0852	12.7272
		2p []	+2.9725	+3.3733
OLYP	-0.498786265116	4s []	+2.7335	+3.1052
		3s []	+0.7350	+0.9491
		1p []	+0.3300	+0.4904
		2s []	+0.0984	+0.2274
		1s [↑]	-0.2711	-0.0250

The spin-pairing energy is the energetic cost of pairing electrons. Our studies of spin-crossover iron complexes show that the spin-pairing energy is too high in the HF method, leading to too much destabilization of low-spin states compared to high-spin states, and too low in the LDA and GGA, leading to too much stabilization of low-spin states compared to high-spin states [150, 151, 152, 153, 154, 155]. OLYP has a different parameterization of the spin part of the functional which we found helpful for our problem [152] though the best solution is to seek out functional-independent quantities [154].

Functional	Energy (Ha)	MO energies (Ha)		
			↑	↓
PW91	-0.501709458186	5s []	12.0377	12.6085
		2p []	+2.9674	+3.3166
		4s []	+2.7186	+3.0575
		3s []	+0.7209	+0.9377
		1p []	+0.3150	+0.5029
		2s []	+0.0959	+0.2247
		1s [↑]	-0.2809	-0.0274
		5s []	12.0377	16.2157
		2p []	+2.9674	+6.8816
PW91SSF	-0.501709458186	4s []	+2.7186	+6.1649
		3s []	+0.7209	+3.6635
		1p []	+0.3150	+1.7466
		2s []	+0.0959	+1.2593
		1s [↑]	-0.2809	+0.1956

Note that the PW91 and PW91SSF differ only in the spin ↓ energies in this case.

Functional	Energy (Ha)	MO energies (Ha)		
			↑	↓
PBE	-0.500096631914	5s []	12.0492	12.6205
		2p []	+2.9679	+3.3272
		4s []	+2.7218	+3.0673
		3s []	+0.7225	+0.9433
		1p []	+0.3163	+0.5101
		2s []	+0.0968	+0.2284
		1s [↑]	-0.2791	-0.0203
		5s []	12.0492	15.9124
		2p []	+2.9679	+6.4435
		4s []	+2.7218	+5.8147
PBESSF	-0.500096631915	3s []	+0.7225	+3.2070
		1p []	+0.3163	+1.4938
		2s []	+0.0968	+1.1062
		1s [↑]	-0.2791	+0.1835
		5s []	12.0982	12.5966
		2p []	+2.9800	+3.3056
		4s []	+2.7367	+3.0455
		3s []	+0.7300	+0.9289
		1p []	+0.3171	+0.4904
		2s []	+0.1049	+0.2203
PBESOL	-0.488800939153	1s [↑]	-0.2715	-0.0378

Functional	Energy (Ha)	MO energies (Ha)		
			↑	↓
KT1	-0.503232109232	5s []	11.9631	12.5627
		2p []	+2.9626	+3.2901
		4s []	+2.6983	+3.0144
		3s []	+0.7064	+0.8813
		1p []	+0.2989	+0.4283
		2s []	+0.0924	+0.1791
		1s [↑]	-0.2931	-0.0868
		5s []	11.9555	12.6468
		2p []	+2.9652	+3.3651
		4s []	+2.7024	+3.0848
KT2	-0.495143472381	3s []	+0.7158	+0.9362
		1p []	+0.3117	+0.4832
		2s []	+0.1041	+0.2197
		1s [↑]	-0.2862	-0.0332
		5s []	11.9814	12.7469
		2p []	+2.9602	3.3952
		4s []	+2.7071	+3.1237
		3s []	+0.7229	+0.9623
		1p []	+0.3235	+0.5021
		2s []	+0.0988	+0.2368
KT3	-0.504241654511	1s [↑]	-0.2836	-0.0135

Functional	Energy (Ha)	MO energies (Ha)		
			↑	↓
SO11	-0.506405023441	5s []	12.0016	9.5795
		2p []	+2.9824	-1.7955
		4s []	+2.6582	-0.6286
		3s []	+0.7314	-2.4455
		1p []	+0.3198	-3.3459
		2s []	+0.0343	-4.4832
		1s [↑]	-0.2900	-4.5591
N12	-0.495539166790	5s []	12.0313	12.5389
		2p []	+2.9588	+3.2811
		4s []	+2.7110	+3.0181
		3s []	+0.7258	+0.9179
		1p []	+0.3369	+0.5118
		2s []	+0.0688	+0.1178
		1s [↑]	-0.2759	-0.0591
GAM	-0.501238932629	5s []	12.0447	12.6141
		2p []	+2.9754	+3.3383
		4s []	+2.7228	+3.0847
		3s []	+0.7155	+0.9709
		1p []	+0.3152	+0.4599
		2s []	+0.1299	+0.4072
		1s [↑]	-0.2757	-0.0220
CAP	-0.499119321907	5s []	12.0751	15.9038
		2p []	+2.9747	+6.4409
		4s []	+2.7322	+5.8063
		3s []	+0.7285	+3.2171
		1p []	+0.3172	+1.4942
		2s []	+0.1140	+1.1014
		1s [↑]	-0.2745	+0.1791

I am really surprised that the spin ↓ orbital energies are lower than the spin ↑ orbital energies for the SO11 functional.

5.2.6 mGGAs

Meta-GGAs that have a kinetic-energy-density dependence become orbital dependent. Such functionals are an example of *generalized* Kohn-Sham theory.

Here we also get a surprise if we forget to add the BASIS keyword on the VXCTYPE line which is

```
*** META-GGAS NOT AVAILABLE FOR VXCTYPE OPTION AUXIS ***
```

The way to fix this is (to use the example of the VS98 calculation) to change the line

```
VXCTYPE VS98
```

to

```
VXCTYPE BASIS VS98
```

According to the manual,

“The option **BASIS** invokes the Kohn-Sham methodology. Note that this choice may slow down the calculation significantly. For meta-GGAs the option **BASIS** must be specified.”

This somewhat cryptic phrase means that the calculations make less use of the auxiliary functions and do more calculations of integrals via numerical integration. As this can affect accuracy, let us do an LDA calculation with and without the **BASIS** keyword.

Functional	Energy (Ha)	MO energies (Ha)		
			↑	↓
VWN	-0.478715642643	5s []	12.1268	12.5219
		2p []	+2.9876	+3.2619
		4s []	+2.7444	+2.9895
		3s []	+0.7299	+0.8680
		1p []	+0.3112	+0.4200
		2s []	+0.1060	+0.1730
		1s [↑]	-0.2689	-0.0985
BASIS VWN	-0.478648455671	5s []	12.1264	12.5217
		2p []	+2.9874	+3.2617
		4s []	+2.7453	+2.9903
		3s []	+0.7288	+0.8671
		1p []	+0.3111	+0.4199
		2s []	+0.1049	+0.1715
		1s [↑]	-0.2688	-0.0985

The changes in the orbital energies are on the order of $0.0015 \text{ Ha} = 0.41 \text{ eV}$ or (typically) much less. The changes difference in the calculation of the total energy is $6.18 \times 10^{-5} \text{ Ha} = 0.176 \text{ kcal/mol}$. It looks like there is not too much of a problem with the total energies but that some caution may be in order when orbital energies are important.

Functional	Energy (Ha)	MO energies (Ha)		
			↑	↓
VS98	-0.502876321650	5s []	11.3580	12.6263
		2p []	+2.8145	+3.3301
		4s []	+2.6080	+3.0643
		3s []	+0.7072	+0.9487
		1p []	+0.3003	+0.4902
		2s []	+0.0773	+0.2453
		1s [↑]	-0.2827	-0.0270
PKZB	-0.496427961330	5s []	12.2098	12.7699
		2p []	+3.0431	+3.4749
		4s []	+2.8039	+3.1864
		3s []	+0.7602	+1.0139
		1p []	+0.3468	+0.5591
		2s []	+0.0995	+0.2774
		1s [↑]	-0.2709	+0.0348
TPSS	-0.500214506138	5s []	13.2832	12.7747
		2p []	+3.1600	+3.4799
		4s []	+2.8467	+3.1905
		3s []	+0.7401	+1.0166
		1p []	+0.3292	+0.5614
		2s []	+0.0987	+0.2795
		1s [↑]	-0.2856	+0.0367
M06L	-0.503645248883	5s []	14.1623	12.5946
		2p []	+3.1699	+3.3248
		4s []	+2.8216	+3.0637
		3s []	+0.6773	+0.9728
		1p []	+0.3080	+0.4843
		2s []	+0.0995	+0.4125
		1s [↑]	-0.2932	-0.0169
M11L	-0.506362774397	5s []	13.4160	15.9590
		2p []	+2.9863	11.5222
		4s []	+2.5564	13.6111
		3s []	+0.6834	+8.0899
		1p []	+0.3079	+5.2408
		2s []	+0.0582	+0.2661
		1s [↑]	-0.2811	-1.1903
MN12	-0.491794626275	5s []	11.7326	15.0979
		2p []	+3.0868	+7.4963
		4s []	+2.8840	+9.3385
		3s []	+0.7283	+4.4421
		1p []	+0.3411	+6.3423
		2s []	+0.0768	+2.3333
		1s [↑]	-0.2848	+0.1970

The first spin ↑ orbital energy is oddly low for the M11L functional.

5.2.7 Hybrids

These are clearly examples of *generalized* Kohn-Sham theory and the interpretation of the orbital energies must be entirely different than that of normal Kohn-Sham theory.

Functional	Energy (Ha)	MO energies (Ha)		
			↑	↓
BH&H	-0.498826123629	5s []	12.3659	12.7278
		2p []	+3.1796	+3.3740
		4s []	+2.9119	+3.1060
		3s []	+0.8179	+0.9503
		1p []	+0.4043	+0.4919
		2s []	+0.1431	+0.2282
		1s [↑]	-0.3848	-0.0239
B3LYP	-0.502507438970	5s []	12.1569	12.6961
		2p []	+3.0530	+3.3567
		4s []	+2.7945	+3.0875
		3s []	+0.7573	+0.9363
		1p []	+0.3492	+0.4790
		2s []	+0.1158	+0.2181
		1s [↑]	-0.3225	-0.0364
PBE0	-0.501410762739	5s []	12.2241	12.6224
		2p []	+3.0685	+3.3285
		4s []	+2.8155	+3.0686
		3s []	+0.7691	+0.9445
		1p []	+0.3567	+0.5114
		2s []	+0.1187	+0.2289
		1s [↑]	-0.3356	-0.0192

The following are hybrids involving mGGAs, so you have to use VXCTYPE BASIS.

Functional	Energy (Ha)	MO energies (Ha)		
			↑	↓
M062X	-0.498768168660	5s []	11.2521	12.4845
		2p []	+3.0276	+3.2511
		4s []	+2.7539	+2.9928
		3s []	+0.8224	+0.9056
		1p []	+0.4075	+0.4559
		2s []	+0.1569	+0.2697
		1s [↑]	-0.3789	-0.0673
M06HF	-0.497579308751	5s []	+9.4923	12.4078
		2p []	+2.9095	+3.1890
		4s []	+2.7127	+2.9403
		3s []	+0.9664	+0.8702
		1p []	+0.5054	+0.4815
		2s []	+0.1818	+0.1198
		1s [↑]	-0.4503	-0.0953
M06	-0.500136455255	5s []	12.1841	12.4846
		2p []	+3.0858	+3.2539
		4s []	+2.7512	+2.9966
		3s []	+0.6740	+0.9129
		1p []	+0.3393	+0.4809
		2s []	+0.0648	+0.2428
		1s [↑]	-0.3263	-0.0566

The orbital energies may be used to estimate the fraction of exact exchange via the formula,

$$xx = \frac{\epsilon_{1s\uparrow} - \epsilon_{1s\uparrow}^{\text{LDA}}}{\epsilon_{1s\uparrow}^{\text{HF}} - \epsilon_{1s\uparrow}^{\text{LDA}}} = \frac{\epsilon_{1s\uparrow} + 0.2689}{-0.4999 + 0.2689} = -\frac{\epsilon_{1s\uparrow} + 0.2689}{0.2310}. \quad (5.48)$$

Here are the results:

Functional	Fraction Exact Exchange
BH&H	0.50
B3LYP	0.23
PBE0	0.29
M062X	0.48
M06HF	0.79
M06	0.25

Remember that these are only rough estimates, not necessarily the actual fraction of exact exchange appearing in the functional itself. Perdew, Ernzerhof, and Burke have argued on the basis of comparisons with second-order Møller-Plesset theory (MP2) that the fraction of exact exchange should be exactly 0.25 [94] and this is the exact fraction of exact exchange used in the PBE0 functional.

5.2.8 Trends

“It is often claimed that error cancellation plays an essential role in quantum chemistry and first-principle simulation for condensed matter physics and materials science. Indeed,

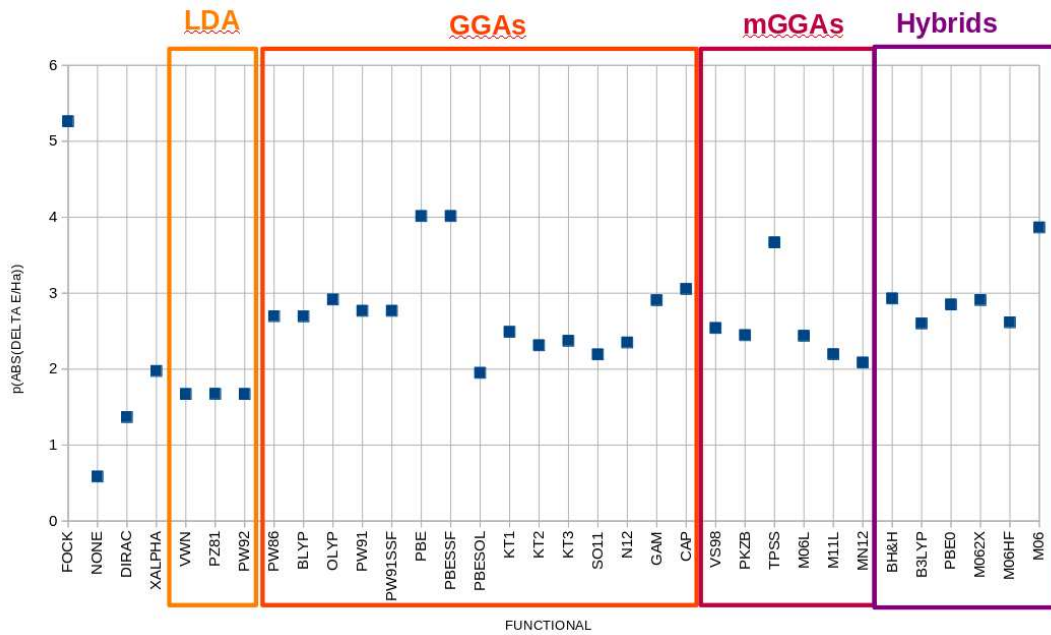


Figure 5.8: A graph of the self-interaction error (SIE) for different functionals. The y -axis is $p|\text{SIE}/\text{Ha}| = -\log_{10} |\text{SIE}/\text{Ha}|$. A *larger* value of $p|\text{SIE}/\text{Ha}|$ corresponds to a *smaller* SIE.

while the energy of a large, or even medium-size, molecular system cannot be estimated numerically within chemical accuracy (typically 1 kcal/mol or 1 mHa), it is considered that the energy difference between two configurations of the same system can be computed in practice within the desired accuracy.”

— from the abstract of Ref. [156] (Eric Cancès is a mathematician at the *École des Ponts et Chausées* in Paris who has contributed to improving quantum chemical methods.)

It is interesting but problematic to look at trends across different families of functionals. It is problematic because electronic structure calculations in chemistry and solid-state physics often rely on error cancellation in the sense that errors in the description of the core electrons tend to cancel out when examining properties which depend primarily on the valence electrons. Thus total energies are rarely as important as energy differences. Nevertheless it is interesting to calculate the self-interaction error (SIE)

$$\text{SIE} = E - (-0.5 \text{ Ha}) . \quad (5.49)$$

As this may be either positive or negative and varies quite a bit in magnitude I have actually calculated

$$p|\text{SIE}/\text{Ha}| = -\log_{10} |\text{SIE}/\text{Ha}| . \quad (5.50)$$

This quantity is shown in Fig. 5.8. The larger the value of $p|\text{SIE}/\text{Ha}|$, the smaller the self-interaction error. Not surprisingly, the largest SIE (smallest $p|\text{SIE}/\text{Ha}|$) is found for the Hartree method (NONE) and the smallest SIE (largest $p|\text{SIE}/\text{Ha}|$) is found for the auxiliary-function Hartree-Fock method (FOCK). The LDA is a definite improvement over the Hartree method and the GGAs further reduce the SIE (increase $p|\text{SIE}/\text{Ha}|$). Thereafter it is not so clear whether mGGAs and hybrid functionals reduce the SIE (increase $p|\text{SIE}/\text{Ha}|$) more than the GGAs have already done.

Other interesting quantities that we can examine are the Koopmans’ ionization potential,

$$\text{IP} = -\epsilon_{1s\uparrow} , \quad (5.51)$$

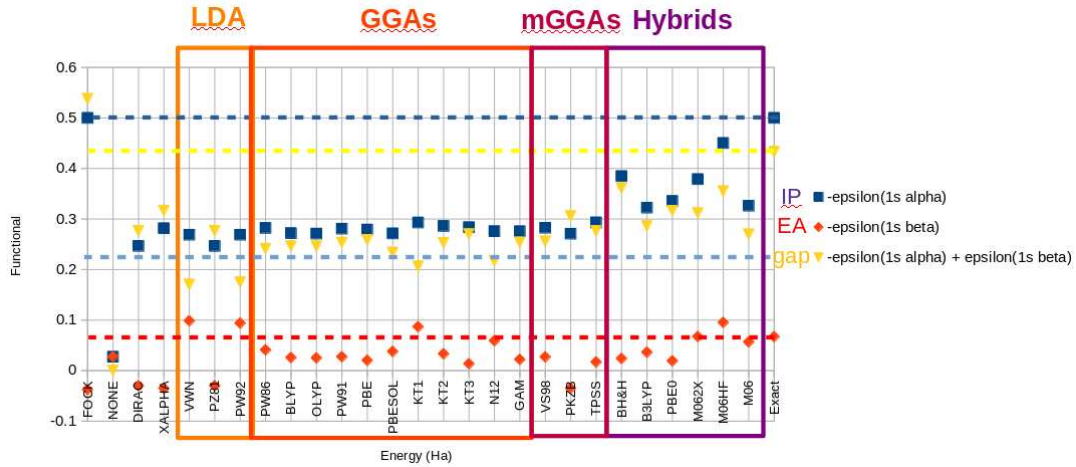


Figure 5.9: Koopmans' ionization potential (IP), electron affinity (EA), and band gap (gap = IP - EA) in Ha for different functionals. The dashed lines are exact values except for the light blue line which is the average of the exact IP and EA.

the Koopmans' electron affinity,

$$\text{EA} = -\epsilon_{1s\downarrow}, \quad (5.52)$$

and the band gap,

$$\text{gap} = \text{IP} - \text{EA}. \quad (5.53)$$

DFT tells us that the Koopmans' IP is the true ionization potential (0.5 Ha in this case) when the xc functional is exact. The experimental EA of the hydrogen atom is 0.0277161 Ha [39]. The band gap has been the subject of much discussion in the literature as the difference between the HOMO and LUMO energies is often calculated as an approximation to the band gap but DFT tells us that this is incorrect because of the particle number derivative discontinuity (PNDD). Nevertheless it is more correct in generalized Kohn-Sham theory than in the original Kohn-Sham theory. These quantities are shown in Fig. 5.9 for the various functionals. Note, however, that some functionals are not shown because they gave clearly absurd values. (The SO11 and M11L functionals gave negative gaps. The PW91SSF, PBESSF, CAP, M06L, and MN12 functionals had EA ≈ -0.19 Ha, though *this does result in a rather good value of the gap*. However negative EAs are likely to be subject to variational collapse as the basis set is expanded.) The LDA, GGAs, and mGGAs give IPs which are close to the average of the exact IP and EA as expected from PNDD arguments and far from the exact value of the IP. The hybrids are a marked improvement for the IP, but still contain large errors. Hartree-Fock (FOCK) gives the exact IP. All the functionals kept here give small values of the EA with the three hybrid mGGAs giving the closest values of the EA to the exact EA. As the EA is small the trends in the band gap follow those of the IP.

5.3 Lesson 3 Answers

5.3.1 Raw Data

Raw data may be found in Tables 5.1 and 5.2.

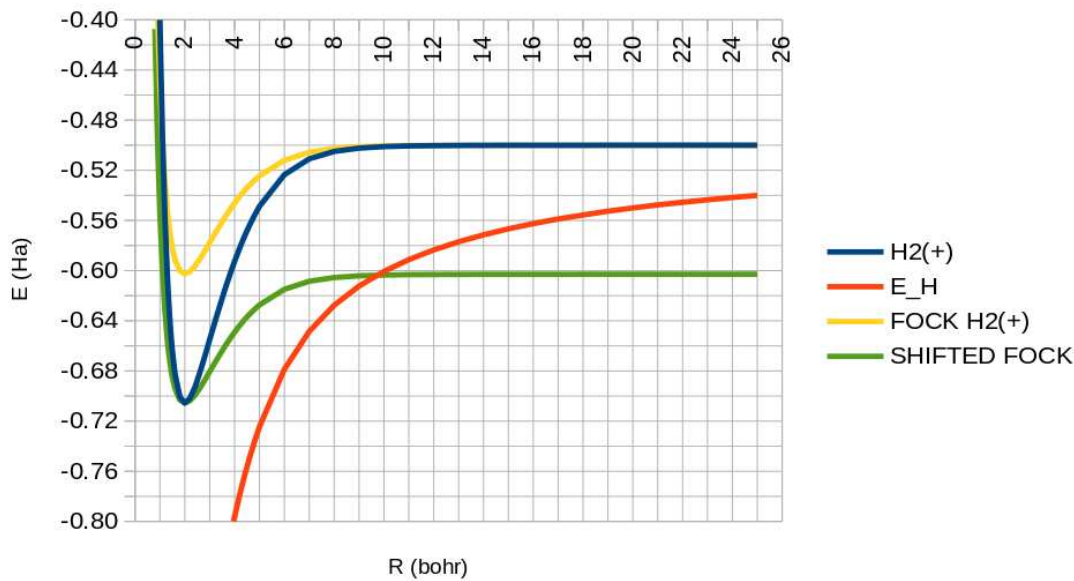
Table 5.1: Calculated H_2^+ HOMO energy curves using different functionals. All values are in atomic units (distances are bohr and energies are Ha.)

R (bohr)	Energy (Ha)					
	DFA	NONE	VWN	BLYP	B3LYP	FOCK
0.8	+0.1346	-0.7164	-1.1815	-1.1988	-1.2750	-1.5544
0.9	+0.0334	-0.6924	-1.1427	-1.1588	-1.2325	-1.5014
1.0	-0.0426	-0.6700	-1.1064	-1.1216	-1.1928	-1.4518
1.1	-0.1007	-0.6491	-1.0727	-1.0871	-1.1560	-1.4055
1.2	-0.1458	-0.6297	-1.0414	-1.0551	-1.1218	-1.3623
1.3	-0.1814	-0.6116	-1.0122	-1.0252	-1.0899	-1.3220
1.35	-0.1963	-0.6030	-0.9983	-1.0111	-1.0748	-1.3028
1.39	-0.2071	-0.5963	-0.9876	-1.0002	-1.0631	-1.2879
1.40	-0.2097	-0.5946	-0.9850	-0.9975	-1.0602	-1.2843
1.41	-0.2122	-0.5930	-0.9823	-0.9947	-1.0573	-1.2806
1.45	-0.2216	-0.5866	-0.9721	-0.9843	-1.0461	-1.2663
1.5	-0.2323	-0.5788	-0.9596	-0.9715	-1.0325	-1.2490
1.6	-0.2507	-0.5641	-0.9360	-0.9475	-1.0066	-1.2159
1.8	-0.2777	-0.5373	-0.8931	-0.9042	-0.9598	-1.1558
2.0	-0.2958	-0.5138	-0.8556	-0.8661	-0.9189	-1.1026
2.2	-0.3080	-0.4930	-0.8226	-0.8328	-0.8828	-1.0554
2.4	-0.3163	-0.4745	-0.4893	-0.8035	-0.8510	-1.0132
2.6	-0.3219	-0.4580	-0.7677	-0.7779	-0.8227	-0.9754
2.8	-0.3256	-0.4432	-0.7448	-0.7551	-0.7976	-0.9415
3.0	-0.3280	-0.4299	-0.7245	-0.7349	-0.7753	-0.9109
3.2	-0.3295	-0.4179	-0.7064	-0.7171	-0.7554	-0.8832
3.6	-0.3308	-0.3972	-0.6759	-0.6872	-0.7218	-0.8355
3.8	-0.3309	-0.3882	-0.6630	-0.6746	-0.7076	-0.8148
4.0	-0.3309	-0.3799	-0.6514	-0.6634	-0.6949	-0.7961
4.2	-0.3307	-0.3724	-0.6411	-0.6534	-0.6834	-0.7790
5.0	-0.3297	-0.3477	-0.6089	-0.6223	-0.6478	-0.7244
6.0	-0.3291	-0.3256	-0.5826	-0.5974	-0.6188	-0.6786
7.0	-0.3295	-0.3097	-0.5651	-0.5807*	-0.6001	-0.6484
8.0	-0.3307	-0.2978	-0.5545	-0.5690*	-0.5879	-0.6276
9.0	-0.3323	-0.2888	-0.5479	-0.5642*	-0.5799	-0.6123
10.0	-0.3340	-0.2807*	-0.5441	-0.5616*	-0.5648*	-0.6006
11.0	-0.3357	-0.2755*	-0.5487	-0.5661*	-0.5669*	-0.5912
12.0	-0.3373	-0.2714*	-0.5346	-0.5523*	-0.5555*	-0.5835
13.0	-0.3387	-0.2681*	-0.5411	-0.5593*	-0.5705*	-0.5770
14.0	-0.3400	-0.2652*	-0.5427	-0.5821*	-0.5741*	-0.5715
15.0	-0.3411	-0.2628*	-0.5242	-0.5407*	-0.5446*	-0.5667
16.0	-0.3421	-0.2607*	-0.5220	-0.5387*	-0.5425*	-0.5625
17.0	-0.3430	-0.2589*	-0.5283	-0.5478*	-0.5489*	-0.5588
18.0	-0.3438	-0.2572*	-0.5210	-0.5394*	-0.5423*	-0.5556
19.0	-0.3446	-0.2557*	-0.5213	-0.5945*	-0.5417*	-0.5526
20.0	-0.3452	-0.2544*	-0.5155	-0.5393*	-0.5413*	-0.5500
21.0	-0.3458	-0.2532*	-0.5143	-0.5305*	-0.5346*	-0.5476
22.0	-0.3463	-0.2522*	-0.5194	-0.5367*	-0.5388*	-0.5455
23.0	-0.3468	-0.2512*	-0.5130	-0.5302*	-0.5338*	-0.5435
24.0	-0.3473	-0.2503*	-0.5116	-0.5282*	-0.5321*	-0.5417

Table 5.2: Calculated H_2^+ potential energy curves using different functionals. All values are in atomic units (distances are bohr and energies are Ha.)

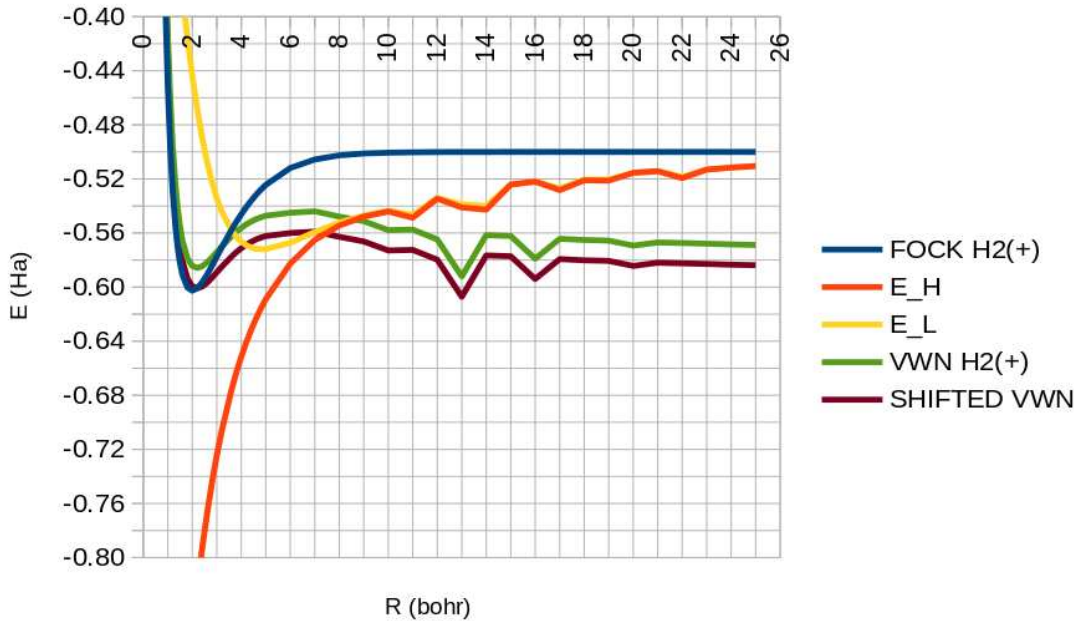
R (bohr)	Energy (Ha)					
	DFA	NONE	VWN	BLYP	B3LYP	FOCK
0.8	+0.8973504	+0.1346436	-0.2629462	-0.2981554	-0.3030816	-0.3044456
0.9	+0.5167050	+0.0333998	-0.3510191	-0.3844101	-0.3893343	-0.3902414
1.0	+0.2356733	-0.0425572	-0.4147360	-0.4465342	-0.4514071	-0.4517608
1.1	+0.0245328	-0.1006714	-0.4615067	-0.4919165	-0.4966969	-0.4963895
1.2	-0.1362266	-0.1458372	-0.4961552	-0.5253642	-0.5300112	-0.5289548
1.3	-0.2598560	-0.1813890	-0.5219501	-0.5501120	-0.5545917	-0.5527230
1.35	-0.3107530	-0.1963191	-0.5322630	-0.5599469	-0.5643363	-0.5620471
1.39	-0.3470817	-0.2071133	-0.5394831	-0.5668070	-0.5711188	-0.5684865
1.40	-0.3556068	-0.2096655	-0.5411579	-0.5683944	-0.5726867	-0.5699676
1.41	-0.3639207	-0.2121622	-0.5427827	-0.5699318	-0.5742045	-0.5714000
1.45	-0.3951705	-0.2216202	-0.5488166	-0.5756328	-0.5798246	-0.5766689
1.5	-0.4300872	-0.2323479	-0.5553981	-0.5818199	-0.5859067	-0.5823085
1.6	-0.4881108	-0.2506699	-0.5658501	-0.5915578	-0.5954209	-0.5909234
1.8	-0.5681885	-0.2776993	-0.5786792	-0.6032331	-0.6066006	-0.6002410
2.0	-0.6152906	-0.2958094	-0.5844092	-0.6081523	-0.6109560	-0.6026223
2.2	-0.6411415	-0.3080484	-0.5858306	-0.6090045	-0.6112030	-0.6008283
2.4	-0.6532097	-0.3163329	-0.5846095	-0.6073340	-0.6089182	-0.5965429
2.6	-0.6564241	-0.3219096	-0.5817922	-0.6042109	-0.6051651	-0.5908224
2.8	-0.6540761	-0.3256122	-0.5781077	-0.6003544	-0.6006670	-0.5843445
3.0	-0.6483454	-0.3280098	-0.5740684	-0.5963426	-0.5959701	-0.5775502
3.2	-0.6406478	-0.3294978	-0.5699931	-0.5924402	-0.5913533	-0.5707285
3.6	-0.6226498	-0.3307785	-0.5624272	-0.5855121	-0.5829353	-0.5576918
3.8	-0.6133228	-0.3309112	-0.5591234	-0.5826126	-0.5792899	-0.5516750
4.0	-0.6041916	-0.3308552	-0.5562041	-0.5801407	-0.5760812	-0.5460626
4.2	-0.5954770	-0.3306839	-0.5536796	-0.5780941	-0.5733086	-0.5408772
5.0	-0.5676313	-0.3296968	-0.5472329	-0.5735255	-0.5660900	-0.5243868
6.0	-0.5511527	-0.3290904	-0.5449962	-0.5727918	-0.5629142	-0.5119371
7.0	-0.5492770	-0.3295402	-0.5439532*	-0.5727096*	-0.5632526	-0.5055699
8.0	-0.5541758	-0.3307376	-0.5478204*	-0.5769225*	-0.5650712	-0.5025537
9.0	-0.5611778	-0.3323182	-0.5512310*	-0.5806171*	-0.5673661	-0.5011838
10.0	-0.5682105	-0.3328929*	-0.5578618*	-0.5881586*	-0.5680307*	-0.5005699
11.0	-0.5745513	-0.3350736*	-0.5574796*	-0.6026511*	-0.5792177*	-0.5002918
12.0	-0.5800564	-0.3369274*	-0.5647210*	-0.5958426*	-0.5750696*	-0.5001617
13.0	-0.5847915	-0.3385093*	-0.5920525*	-0.6211236*	-0.5897443*	-0.5000973
14.0	-0.5888750	-0.3398708*	-0.5615636*	-0.5962412*	-0.5758407*	-0.5000631
15.0	-0.5924215	-0.3410532*	-0.5622047*	-0.5915818*	-0.5723485*	-0.5000433
16.0	-0.5955271	-0.3420892*	-0.5789653*	-0.6140520*	-0.5892681*	-0.5000309
17.0	-0.5982684	-0.3430042*	-0.5642845*	-0.5938071*	-0.5745304*	-0.5000225
18.0	-0.6007059	-0.3438181*	-0.5651295*	-0.5946451*	-0.5753727*	-0.5000166
19.0	-0.6028877	-0.3445468*	-0.5656131*	-0.5949683*	-0.5757451*	-0.5000123
20.0	-0.6048521	-0.3452029*	-0.5693190*	-0.6001031*	-0.5798820*	-0.5000090
21.0	-0.6066300	-0.3457968*	-0.5669879*	-0.5963991*	-0.5771514*	-0.5000064
22.0	-0.6082474	-0.3463368*	-0.5673828*	-0.5966886*	-0.5774780*	-0.5000044
23.0	-0.6097250	-0.3468300*	-0.5678700*	-0.5971472*	-0.5779416*	-0.5000029
24.0	-0.6110783	-0.3472822*	-0.5684209*	-0.5979264*	-0.5786386*	-0.5000016

FOCK



The FOCK/AUG-CC-PV5Z calculations with DEMON2K are the closest thing that we have to the exact answer *in this orbital basis set*. The figure appears to show that FOCK/AUG-CC-PV5Z is not very exact compared to the “exact” results from the literature. In fact, the opposite is true: It is the FOCK/AUG-CC-PV5Z calculations which are more exact as very accurate calculations show that the minimum of the H_2^+ potential energy curve is at -0.597139 Ha (see Table 1 of Ref. [157]. *In the rest of this section, I will be taking the FOCK curve as the exact one!*

VWN



One of the most striking things about the VWN curves are that they are jagged, rather than smooth, for $R > 6$ bohr. The reason for this is that as R increases the HOMO and LUMO energies get closer and closer together which makes SCF convergence more and more difficult. In order to get

Table 5.3: VWN values of the HOMO and LUMO as a function of internuclear distance R as long as SMEAR values. All values are in atomic units (distances are bohr and energies are Ha.)

R (bohr)	Energy (Ha)		SMEAR value ^a
	HOMO	LUMO	
0.8	-1.1815	-0.2488	none
0.9	-1.1427	-0.2637	none
1.0	-1.1064	-0.2796	none
1.1	-1.0727	-0.2965	none
1.2	-1.0414	-0.3138	none
1.3	-1.0122	-0.3315	none
1.35	-0.9983	-0.3404	none
1.39	-0.9876	-0.3474	none
1.40	-0.9850	-0.3492	none
1.41	-0.9823	-0.3509	none
1.45	-0.9721	-0.3579	none
1.5	-0.9596	-0.3666	none
1.6	-0.9360	-0.3836	none
1.8	-0.8931	-0.4154	none
2.0	-0.8556	-0.4438	none
2.2	-0.8226	-0.4683	none
2.4	-0.7935	-0.4893	none
2.6	-0.7677	-0.5071	none
2.8	-0.7448	-0.5220	none
3.0	-0.7245	-0.5342	none
3.2	-0.7064	-0.5441	none
3.6	-0.6759	-0.5581	none
3.8	-0.6630	-0.5629	none
4.0	-0.6514	-0.5664	none
4.2	-0.6411	-0.5690	none
5.0	-0.6089	-0.5719	none
6.0	-0.5826	-0.5673	none
7.0	-0.5651	-0.5593	0.03
8.0	-0.5545	-0.5523	0.03
9.0	-0.5479	-0.5471	0.03
10.0	-0.5441	-0.5435	0.03
11.0	-0.5487	-0.5465	0.04
12.0	-0.5346	-0.5341	0.04
13.0	-0.5411	-0.5387	0.05
14.0	-0.5427	-0.5400	0.04
15.0	-0.5242	-0.5241	0.04
16.0	-0.5220	-0.5220	0.04
17.0	-0.5283	-0.5269	0.04
18.0	-0.5210	-0.5205	0.04
19.0	-0.5213	-0.5205	0.04
20.0	-0.5155	-0.5155	0.03
21.0	-0.5143	-0.5142	0.03
22.0	-0.5194	-0.5184	0.04
23.0	-0.5131	-0.5130	0.03
24.0	-0.5116	-0.5116	0.03

convergence I used the **SMEAR** option which displaces a fraction of an electron from the HOMO to the LUMO. The values of the **SMEAR** option that I used are shown in Table 5.3. It is not clear to me if the kinks in the curves correspond to changes in the value of **SMEAR**, but the remark about *variational principle violation* in the *deMon2k Users' Guide* explanation of this keyword is pertinent:

Keyword SMEAR

This keyword specifies a certain kind of fractional occupation at the Fermi level. Note two things: This smearing is not necessarily the same as Fermi-level smearing in other codes. *The variational principle may be violated if SMEAR is used.*

Options:

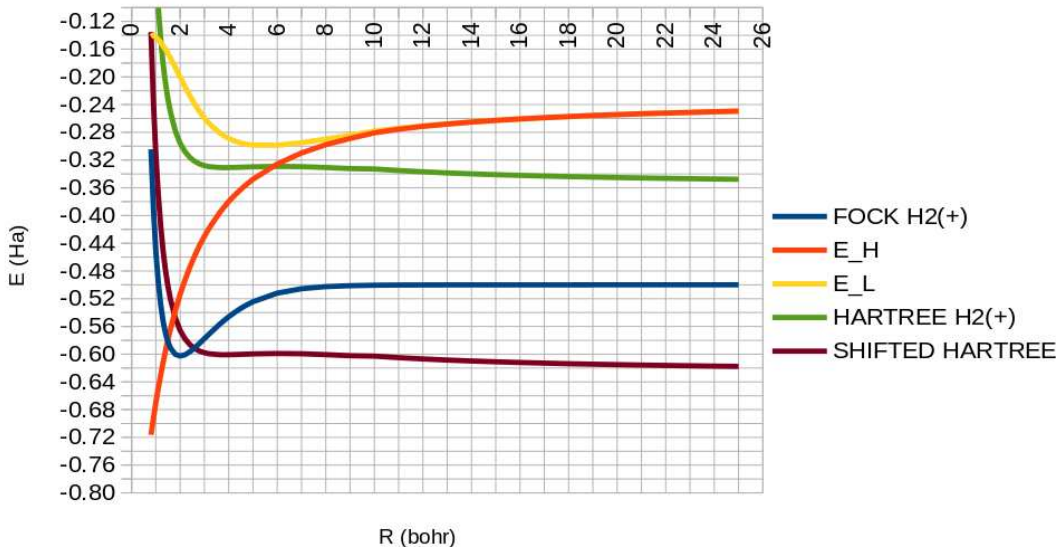
<Real> Energy range ΔE [in a.u.] around the HOMO energy in which orbitals are fractionally occupied.

UNIFORM Specifies uniform fractional occupation within ΔE [in a.u.] around the HOMO level.

Description:

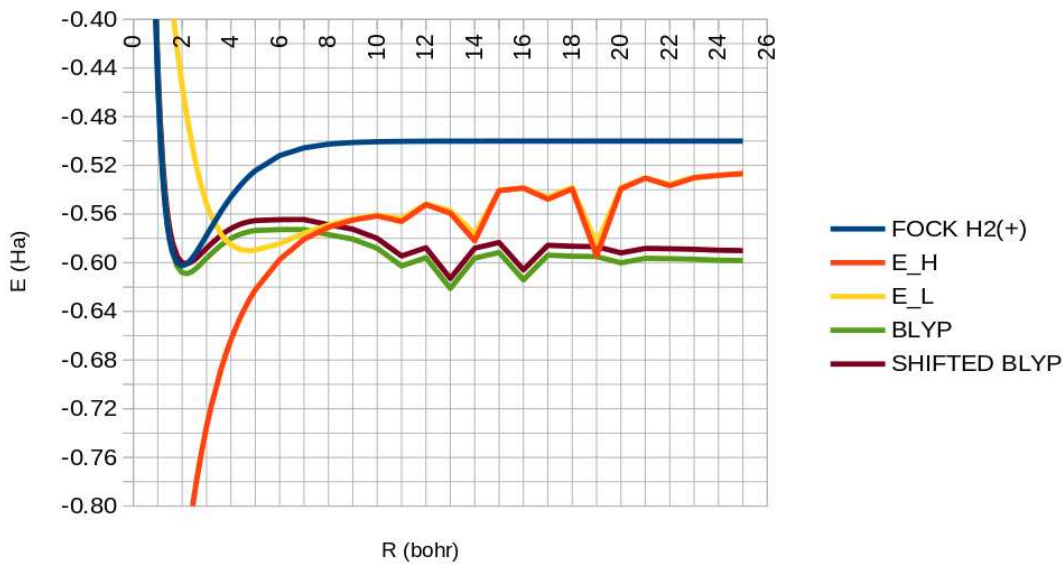
The **SMEAR** keyword affects only the molecular orbitals within the specified energy interval $[E_{\text{HOMO}} - \Delta E/2, E_{\text{HOMO}} + \Delta E/2]$. Therefore, the ΔE value should be selected based on the orbital energy spectrum (see MOS option of PRINT). The smearing is done by inverse proportionality to the energy interval of a given orbital energy to the reference energy $E_{\text{HOMO}} - \Delta E/2$. The closer the MO energy is to this reference energy, the larger will its occupation number be set. To enforce uniform occupation of the orbitals within the ΔE interval, the option **UNIFORM** should be used. In either case, the converged fractional orbital occupation is used in any further step of the calculation (optimization, frequencies, properties etc.).

NONE



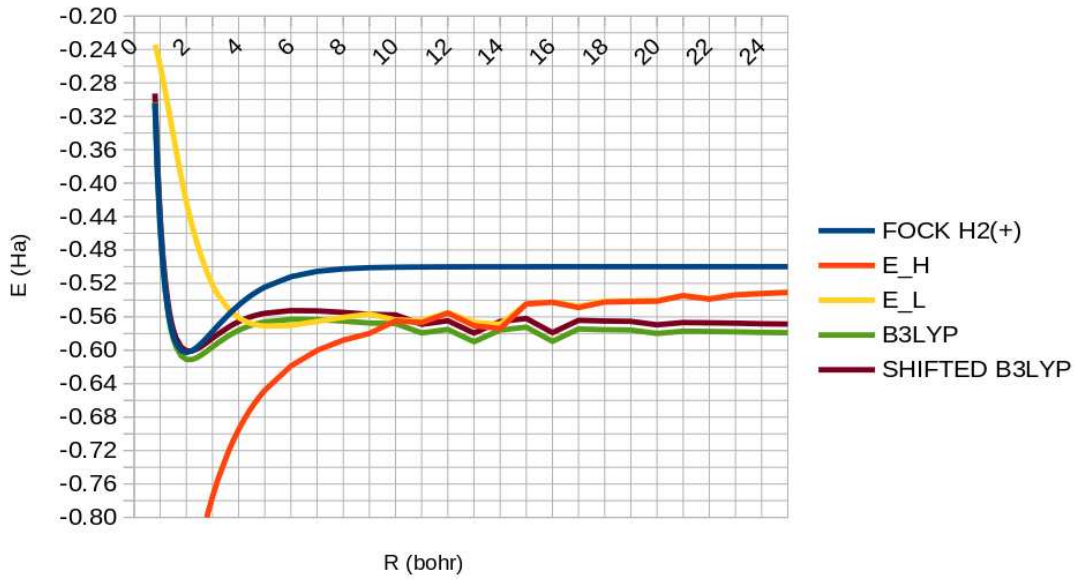
The keywords **VXCTYPE** **NONE** corresponds to the Hartree model or, to be more specific, a DFT calculation with no xc part. It is nearly not bound at all, though there is a shallow minimum around $R = 3.8$ bohr which has been shifted to match the energy of the minimum in the Hartree-Fock curve. The curve appears smooth. However I have used **SMEAR** 0.04 for $R \geq 10$ bohr.

BLYP



Very similar to the VWN case. I used SMEAR 0.04 for $R \geq 7$ bohr except that SMEAR 0.05 was used for $R = 19$ bohr.

B3LYP



This is only a mild improvement over the BLYP case. I used SMEAR 0.04 for $R \geq 10$ bohr.

5.3.2 Concluding Discussion

Here are the potential energy curves for all the calculations on a single graph:

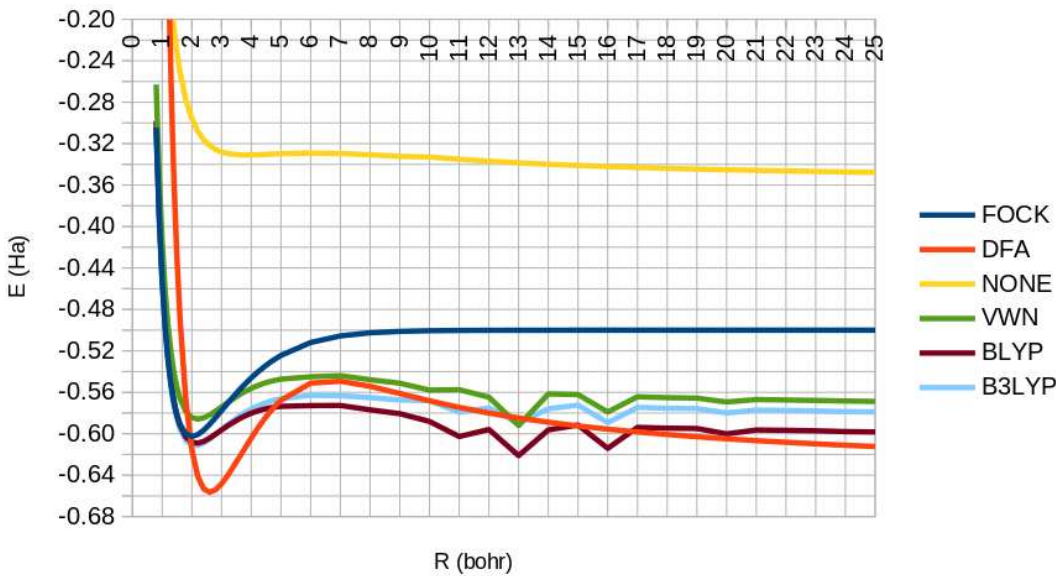
Table 5.4: An indication of the curvature of the hydrogen atom energy as a function of occupation number: Comparison of the asymptotic H_2^+ energy (twice the energy of a hydrogen atom having only half an electron) and the energy of the hydrogen atom (with an entire electron) with the same functional.

Functional	Energy (Ha)		
	H^a	H^b	H_2^{+c}
NONE	-0.2402865	-0.3576952	-0.3476983
DFT	-0.5000000	-0.6123247	-0.6123247
VWN	-0.4787156	-0.5787286	-0.5687823
BLYP	-0.4979783	-0.6080431	-0.5982572
B3LYP	-0.5025074	-0.5888330	-0.5789887
FOCK	-0.4999945	-0.4999948	-0.5000006

^a Calculations with one entire electron.

^b Twice the energy of the hydrogen atom with half an electron.

^c $R = 25$ bohr



We see that the theoretical DFA model constructed for learning purposes is not very accurate but captures the main qualitative features of the failings of real DFA calculations. Coincidentally, the energy of the DFA model at large R is not very far from that of the BLYP calculation (Table 5.4.)

The large R value should be equal to twice the value of the energy of a hydrogen atom calculated with half an electron, which makes a nice connection with the assertion of Ref. [29] that the form of the curve is related to curvature of the total energy of the hydrogen atom as a function of occupation number. DEMON2K allows calculations with a fractional total number of electrons only for atoms, so this calculation can be done using the following input:

```
TITLE H half-occupancy
CONFIGURE OCCUPY
1 ! put some electrons into the 1s alpha orbital
0 ! put nothing into the 1s beta orbital
```

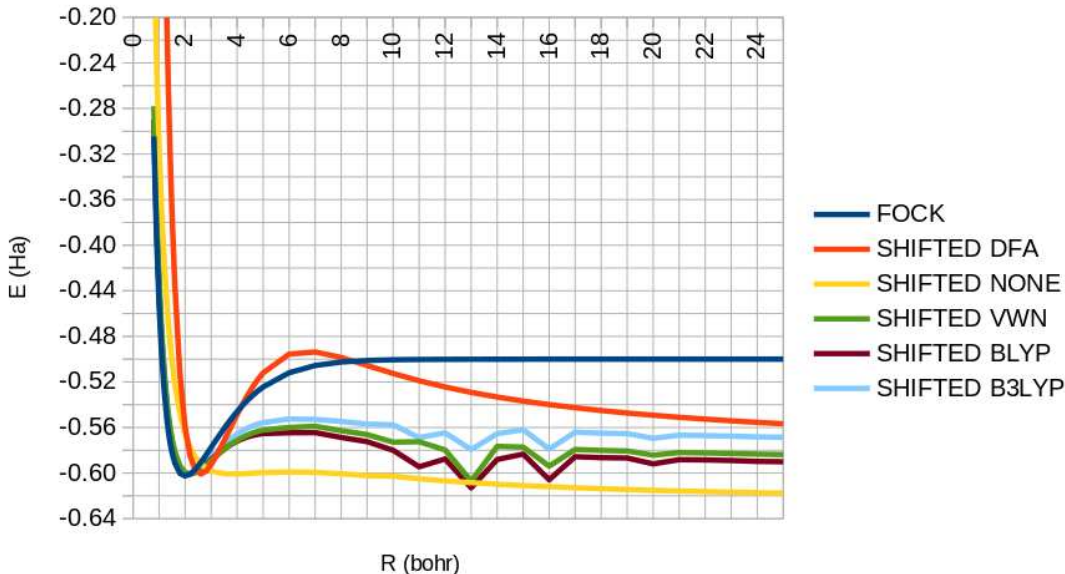
```

0.5 ! the total number of electrons is 0.5
0.5 ! put 0.5 electrons into the 1s alpha orbital
0. ! put 0. electrons into the 1s beta orbital
#
VXCTYPE VWN
#
PRINT MOS
#
# --- GEOMETRY ---
#
#
GEOMETRY CARTESIAN BOHR
H      0.000000    0.000000    0.000000
#
AUXIS (GEN-A3*)
BASIS (AUG-CC-PV5Z)

```

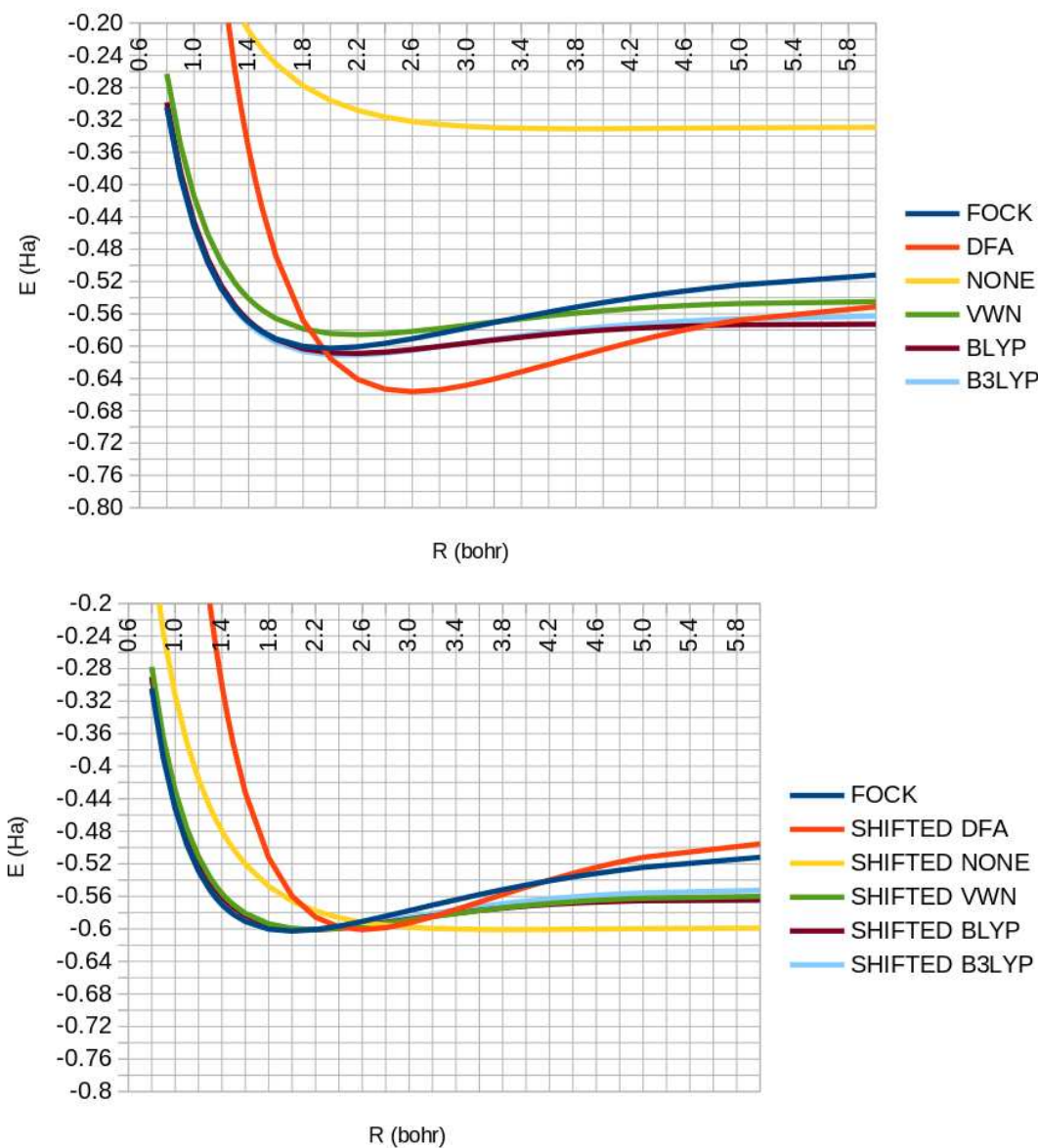
Note that the comment lines beginning with an explanation mark must be removed before running this input and (of course) the keyword VXCTYPE is to be varied. Table 5.4 shows that the value of the H_2^+ energy at $R = 25$ bohr is indeed close to twice the energy of hydrogen with only half an electron. Indeed, the later value is better as it is the $R = \infty$ value calculated without using SMEAR!

For most applications, it is not the total energy that matters but rather the shape of the potential energy curve. Here is a replotting of the previous data with curves shifted to have the same minimum:



Notice how the VWN and BLYP curves now look nearly identical.

It is also useful to look at the same two plots in the region where all calculations could be converged without the SMEAR option:



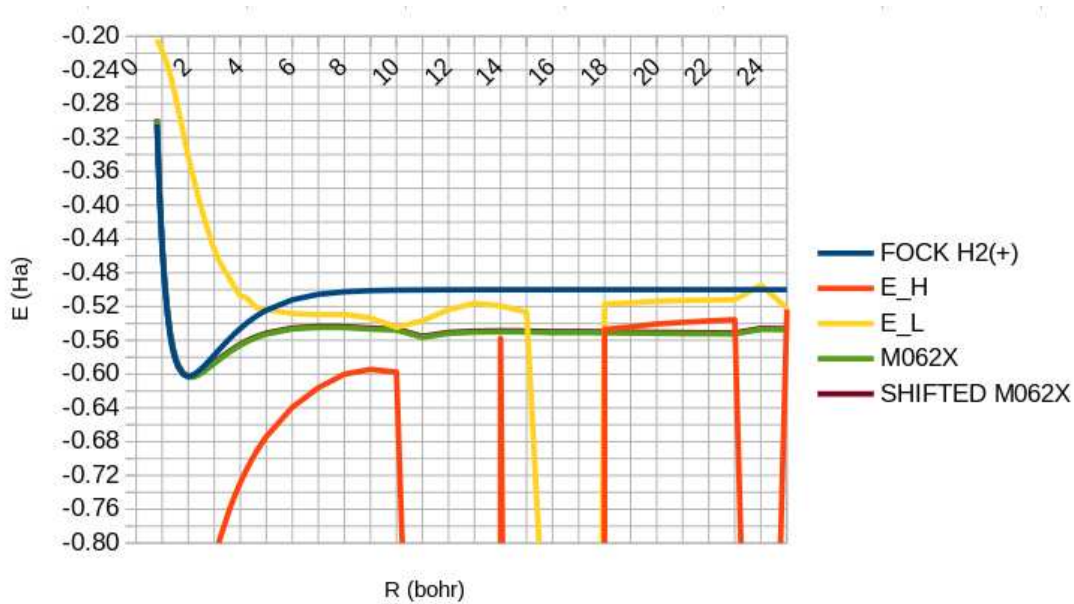
Notice how none of the conclusions really change. Remember that the **FOCK** curve is exact. Hence the shape of the potential energy curves remain quite wrong with all of the common functionals.

To summarize, several things have been learned, including:

1. The danger of the **SMEAR** option which can violate the variational principle.
2. The inability of current DFAs to give the correct description of the potential energy curve for breaking (this) one-electron/two-center bond.
3. Caution is in order when using DFT to study reactions between radicals or when using DFT to study reactions that produce radicals.
4. That the ultimate solution is to design a functional giving a total energy which is as nearly as possible a linear function of the total number of electrons.

5.3.3 M062X

In view of recommendations of which functionals are best for radical + molecule reactions [158], I decided it that it would be good to revisit the M062X functional [96] and also see how it works for H_2^+ dissociation.



This functional has numerical problems. For example, I had a division by zero at $R = 2.000$ bohr which I got around by using $R = 2.001$ bohr. Most of the calculations were converged either without any tricks or just using GUESS RESTART and the restart file from a previously converged geometry. Only for two geometries ($R = 24.0$ bohr and $R = 25.0$ bohr) did I have to use SMEAR 0.05 UNIFORM. Nevertheless the spin α orbital energies jump around all over the place in a very disturbing way even though I succeeded in obtaining a much smoother potential energy curve.

5.4 Lesson 4 Answers

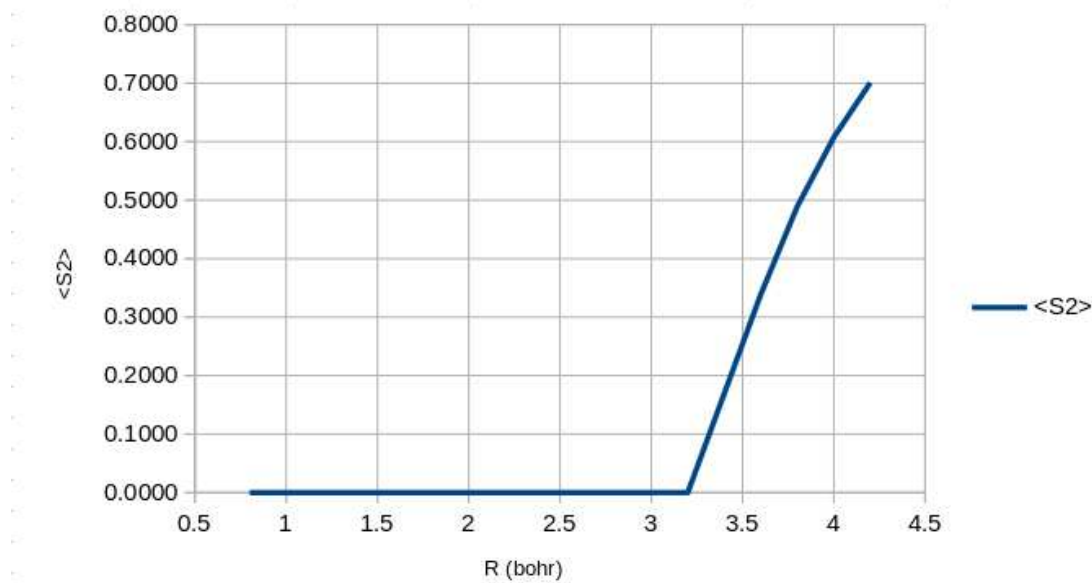
5.4.1 Raw Data

The “shifted” energy curves have been shifted so that the dissociation energy is exactly -1 bohr according to the prescription,

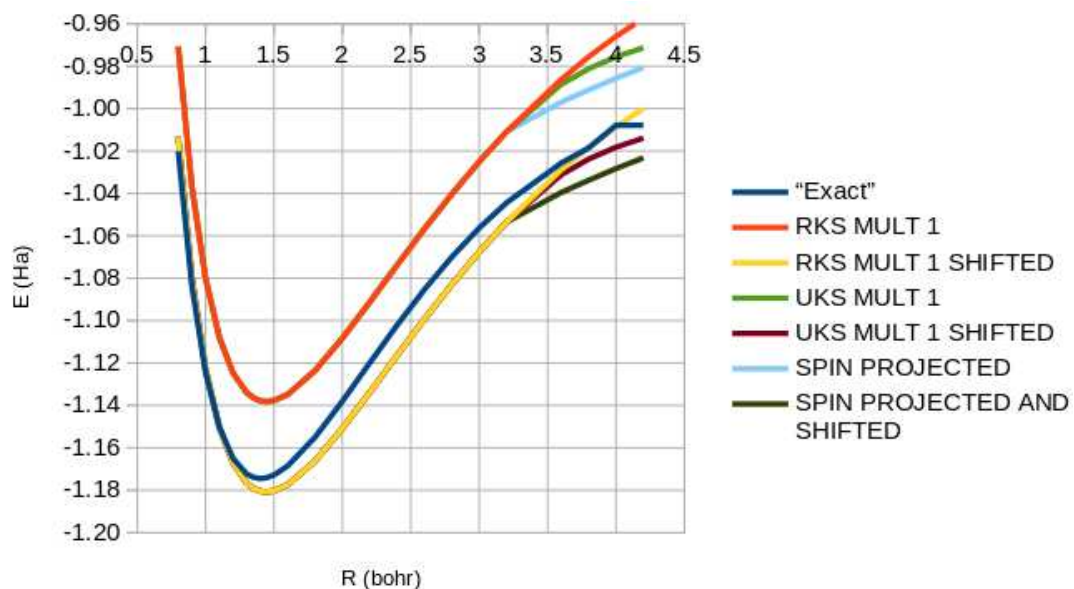
$$E_{\text{shifted}}(\text{H}_2) = E(\text{H}_2) - 2E(\text{H}) - 1 \text{ bohr}, \quad (5.54)$$

where the value of $E(\text{H})$ is taken from the answer to Lesson 2 (Sec. 5.2.)

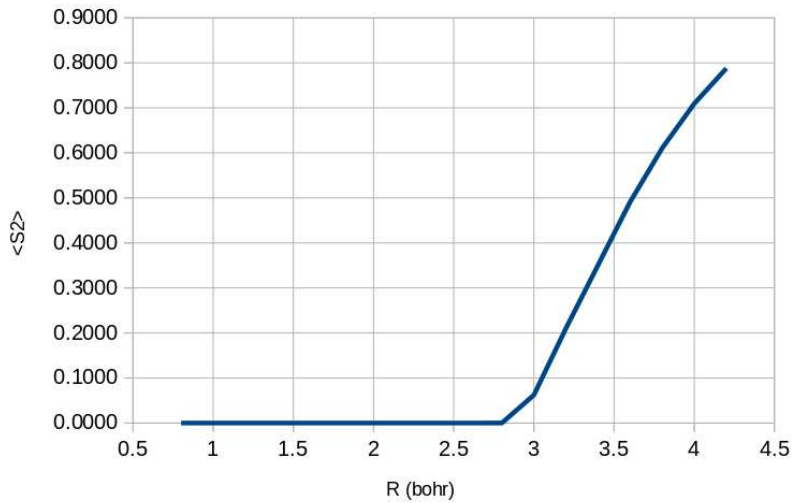
LDA



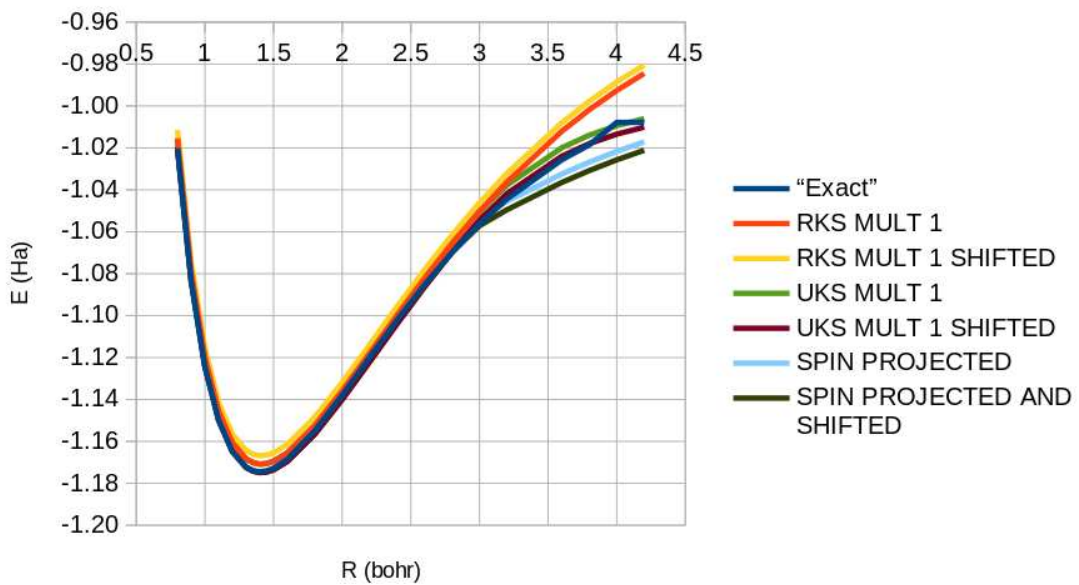
“Singlet” (MULT 1) spin-contamination $\langle \hat{S}^2 \rangle$ as a function of bond distance.



“Singlet” (MULT 1) energy as a function of bond length.

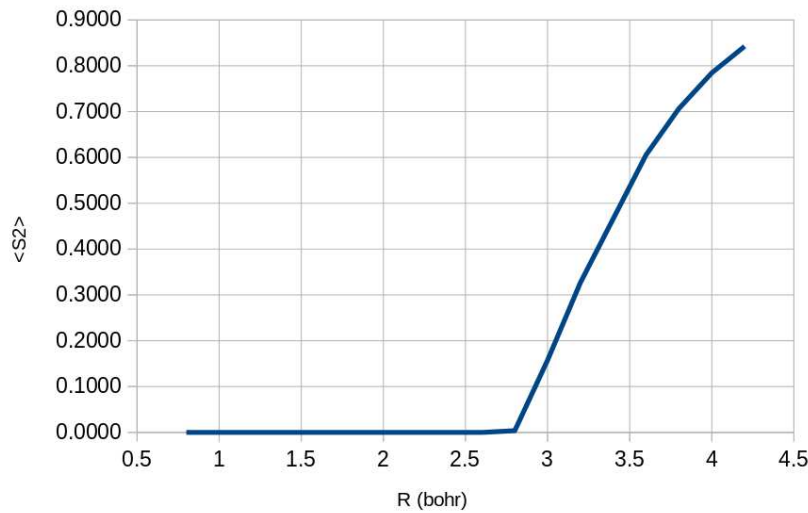
BLYP

“Singlet” (MULT 1) spin-contamination $\langle \hat{S}^2 \rangle$ as a function of bond distance.

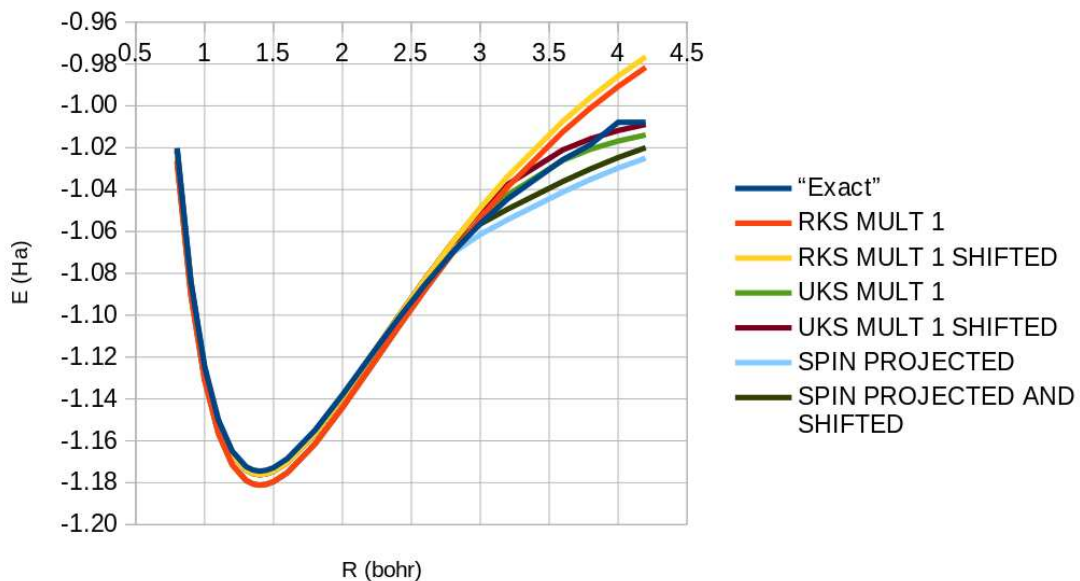


“Singlet” (MULT 1) energy as a function of bond length.

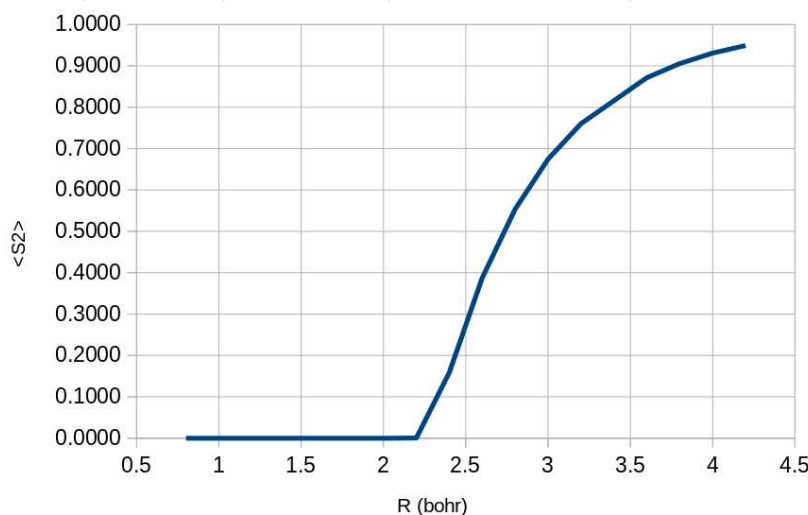
B3LYP



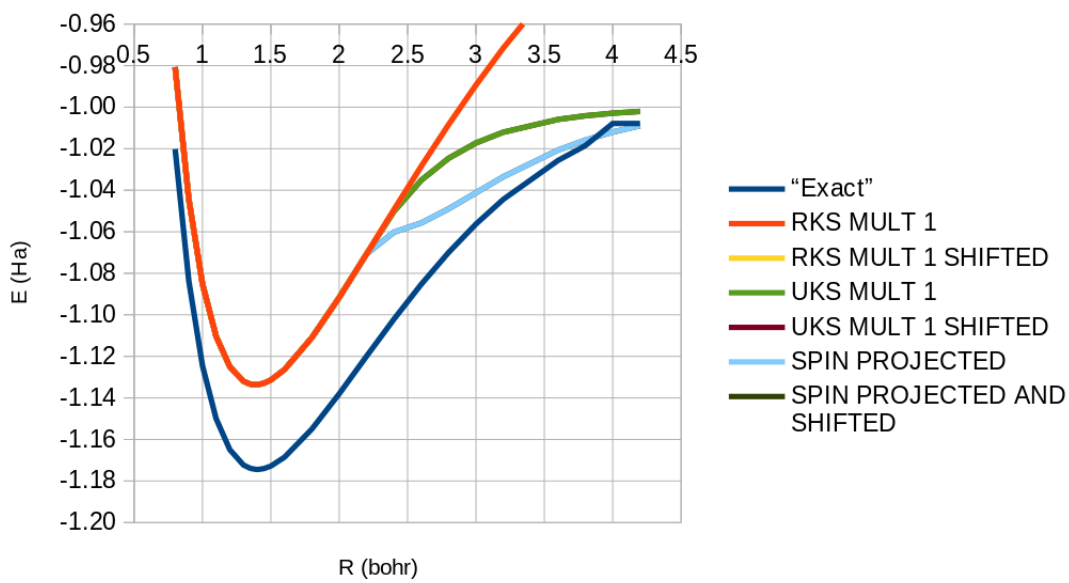
“Singlet” (MULT 1) spin-contamination $\langle \hat{S}^2 \rangle$ as a function of bond distance.



“Singlet” (MULT 1) energy as a function of bond length.

HF

“Singlet” (MULT 1) spin-contamination $\langle \hat{S}^2 \rangle$ as a function of bond distance.

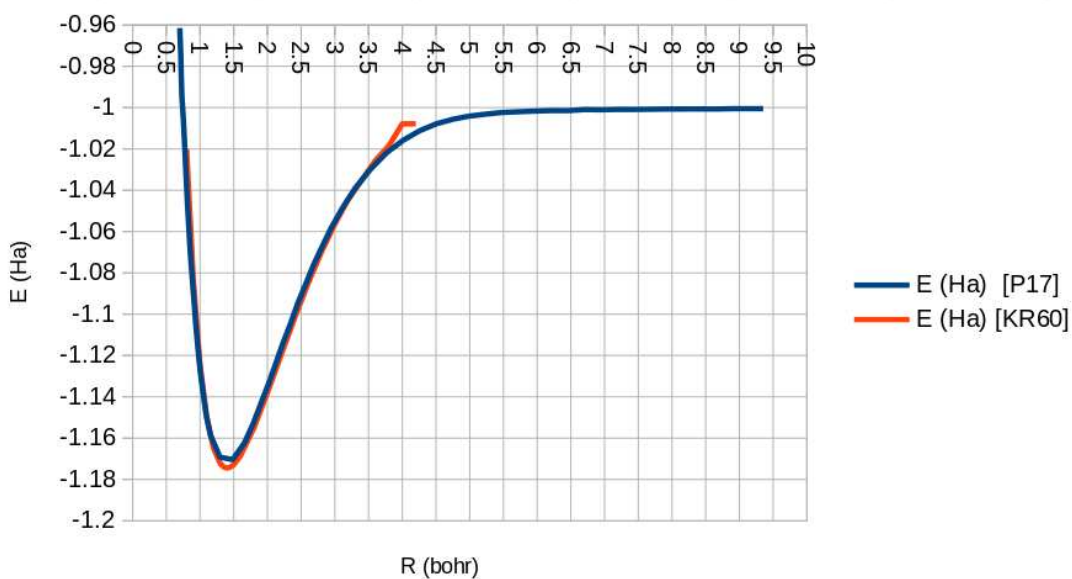


“Singlet” (MULT 1) energy as a function of bond length.

5.4.2 Concluding Discussion

One thing that emerges right away is that MULT 3 ROKS and UKS calculations give exactly the same energies.

As predicted, the spin-projected results *underestimate* the true results. While this looks like it may lead to increasingly correct energies at large R in the Hartree-Fock (HF) case, it is in general a disaster. Just to be sure I compare accurate potential energy curves from two different sources:

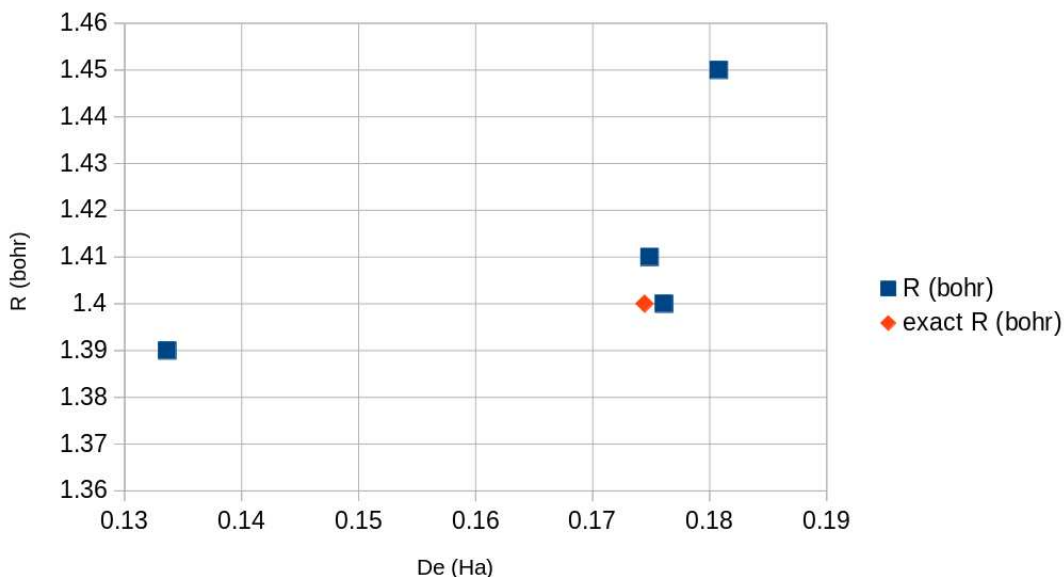


Comparison of accurate potential energy curves from Refs. [106] and [125].

To the extent that these are variational calculations, the potential energy curve from Ref. [106] is more correct around the minimum because it has the lower energy. However for $R > 3.5$ bohr, the data taken from Ref. [106] look a little erratic while the data from Ref. [125] remains well-behaved. Nevertheless the comparison data from Ref. [106] is quite adequate for present purposes and we can see that the proposed spin-projection is useless in practice.

The best way to use DFT to approximate the exact potential energy curve is to use the spin-unrestricted different-orbitals-for-different-spin (SODS) method. This method has the advantage of dissociating to $\text{H}^\uparrow + \text{H}^\downarrow$ or $\text{H}^\downarrow + \text{H}^\uparrow$, which is at least in some sense qualitatively correct. Thus RHF dissociates to too high an energy by UHF dissociates to the expected -1 Ha. limit as expected from chemical arguments. UHF dissociates correctly but is underbound. Symmetry-broken SODS calculations with DFT do much better than does UHF with, of the functionals tested, BLYP giving the best potential energy curve. It is interesting to note that HF is exact for H_2^+ but fails for H_2 because HF includes no electron correlation. It is a strength of DFT that it does include electron correlation.

Key data for the computed symmetry-broken curves is shown in Table 5.5. The following graphic summarizes the relation ship between the equilibrium bond length $R = R_e$ and the binding energy D_e :



As is frequently seen, there is a rough correlation between stronger bonds and shorter bond lengths. The best agreement with the exact values is obtained here using the BLYP functional.

The picture is different when we look at spin contamination in the symmetry-broken solutions. No symmetry-breaking should occur for the exact functional. The easiest way to see this is to note that in the exact case $\rho_{\uparrow} = \rho_{\downarrow} = \rho/2$ and that $\psi_{\uparrow} = \psi_{\downarrow} = \sqrt{\rho/2}$. The exact Kohn-Sham potential may then be calculated from a high-quality calculation of the charge density, showing that there is no non-interacting v -representability problem. The situation is very different for approximate functionals. At equilibrium there is no symmetry breaking. However when going to longer bond lengths, a point comes when the symmetry-broken solution gives a lower energy than the symmetry unbroken solution. This bond length is called the Coulson-Fischer point. It is farthest out for the LDA, closer in for the BLYP functional, and still closer in for the B3LYP functional. It is at a particularly small value of R for the HF functional. (HF may be viewed as a hybrid functional without correlation and with 100% exchange.) Note that a larger value of the Coulson-Fischer bond length does not correspond to a better bond energy. At values of R exceeding the Coulson-Fischer point, $\langle \hat{S}^2 \rangle$ is no longer zero but starts to increase until it reaches the limiting value of unity, indicating a 50/50 mixture of the singlet ($\langle \hat{S}^2 \rangle = 0$) and the triplet ($\langle \hat{S}^2 \rangle = 2$). Clearly extreme caution must be used with symmetry-broken solutions for magnetic and other properties depending upon spin.

Functional	Coulson-Fischer Point ^a	R_e^b	D_e^b
LDA	3.15 bohr	1.45 bohr	0.180780 Ha
BLYP	2.96 bohr	1.41 bohr	0.174860 Ha
B3LYP	2.81 bohr	1.40 bohr	0.176099 Ha
HF	2.26 bohr	1.39 bohr	0.133653 Ha
Exact	$+\infty$	1.40 bohr	0.174442 Ha

^a (x_1, y_1) and (x_2, y_2) satisfying $y = mx + b$ implies that $y = 0$ when $x = (x_1y_2 - x_2y_1)/(y_2 - y_1)$.

^b Obtained by a parabolic fit to three points: (x_1, y_1) , (x_2, y_2) , and (x_3, y_3) .

Table 5.5: Summary of key data obtained from the computational results. Here R_e is the equilibrium bond length, i.e., the bond length at the minimum of the potential energy curve while D_e is the traditional notation for the binding energy (D_0 is the notation used for the binding energy if the zero-point vibrational energy is included in the calculation.)

The formula for finding the minimum from a parabolic fit to three points is a little complicated, so I wrote a small python script:

```
# =====
# FILE: findmin.py
# Read three points on a parabola
# and find the coordinates of the
# minimum (maximum).
# LAST MODIFIED: 25 April 2021
# =====
from math import *
#
# input
#
print("Give the coordinates of three points")
x1bar=float(input("x1bar: "))
y1bar=float(input("y1bar: "))
print ("(",x1bar,",",y1bar,")")
x2bar=float(input("x2bar: "))
y2bar=float(input("y2bar: "))
print ("(",x2bar,",",y2bar,")")
x3bar=float(input("x3bar: "))
y3bar=float(input("y3bar: "))
print ("(",x3bar,",",y3bar,")")
#
# coordinate shift
#
x1=x1bar-x2bar
# print ("x1: ",x1)
y1=y1bar-y2bar
# print ("y1: ",y1)
x3=x3bar-x2bar
```

```

# print ("x3: ",x3)
y3=y3bar-y2bar
# print ("y3: ",y3)
#
# calculate (x0,y0)
#
# m=2.*(x1*y3-y1*x3)/(x1*x3*(x3-x1))
# print ("m: ",m)
x0=((x1**2)*y3-y1*(x3**2))/(2.* (x1*y3-y1*x3))
y0=0.25*((x1**2)*y3-y1*(x3**2))**2/(x1*x3*(x3-x1)*(y1*x3-x1*y3))
#
# unshift coordinate
#
x0bar=x0+x2bar
y0bar=y0+y2bar
#
# output
#
print("The minimum is at:")
print ("(",x0bar,",",y0bar,")")
#####
# EOF #
#####

```

5.5 Lesson 5 Answers

5.5.1 Functional Derivatives

We must differentiate

$$E = \sum_i n_i \langle \psi_i | \hat{t} + v | \psi_i \rangle + \frac{1}{2} \int \frac{\rho(1)\rho(2)}{r_{1,2}} d1d2 - a \frac{1}{2} \int \frac{|\gamma(1,2)|^2}{r_{1,2}} d1d2 + bE_x[\rho] + cE_c[\rho]. \quad (5.55)$$

Let us do this term by term, but not necessarily in the order of terms given.

Given a functional $F[f]$, we recall that the definition of the functional derivative $\delta F/\delta f(1)$ is that

$$\delta F[f] = F[f + \delta] - F[f] = \int \frac{\delta F}{\delta f(1)} \delta f(1) d1 \quad (5.56)$$

for an infinitesimal but arbitrary variation $\delta f(1)$. We may apply this directly to find $\delta/\delta\psi_i^*(1)$ for the one-electron contribution,

$$E_{t+v} = \sum_i n_i \langle \psi_i | \hat{t} + v | \psi_i \rangle. \quad (5.57)$$

Then,

$$\begin{aligned}
\delta E_{t+v}[\psi_i^*] &= E_{t+v}[\psi_i^* + \delta\psi_i^*] - E_{t+v}[\psi_i^*] \\
&= n_i \langle \delta\psi_i | \hat{t} + v | \psi_i \rangle \\
&= \int [n_i (\hat{t} + v(1)) \psi_i(1)] \delta\psi_i^*(1) d1.
\end{aligned} \quad (5.58)$$

Hence

$$\frac{\delta E_{t+v}}{\delta \psi_i^*(1)} = n_i (\hat{t} + v(1)) \psi_i(1). \quad (5.59)$$

Let us now turn to terms involving $\rho(1)$. For these we will need to use the chain rule,

$$\frac{\delta F}{\delta \psi_i^*(1)} = \int \frac{\delta F}{\delta \rho(2)} \frac{\delta \rho(2)}{\delta \psi_i^*(1)} d2. \quad (5.60)$$

A tricky point is the evaluation of $\delta \rho(2)/\delta \psi_i^*(1)$:

$$\begin{aligned} \delta \rho &= \rho[\psi_i^*(1) + \delta \psi_i^*(1)] - \rho[\psi_i(1)] \\ &= n_i \psi_i(1) \delta \psi_i^*(1) \\ &= \int (n_i \psi_i(2) \delta(2-1)) \delta_i^*(1) d1. \end{aligned} \quad (5.61)$$

Hence,

$$\frac{\delta \rho(2)}{\delta \psi_i^*(1)} = n_i \psi_i(2) \delta(2-1), \quad (5.62)$$

and

$$\begin{aligned} \frac{\delta F}{\delta \psi_i^*(1)} &= \int \frac{\delta F}{\delta \rho(2)} n_i \psi_i(2) \delta(2-1) d2 \\ &= n_i \frac{\delta F}{\delta \rho(1)} \psi_i(1). \end{aligned} \quad (5.63)$$

We immediately have the derivative of the terms,

$$E_{xc}[\rho] = b E_x[\rho] + c E_c[\rho], \quad (5.64)$$

namely

$$\begin{aligned} \frac{\delta E_{xc}[\rho]}{\delta \psi_i^*(1)} &= n_i \left(a \frac{\delta E_x[\rho]}{\delta \rho(1)} + c \frac{\delta E_c[\rho]}{\delta \rho(1)} \right) \psi_i(1) \\ &= n_i (av_x[\rho](1) + cv_c[\rho](1)) \psi_i(1). \end{aligned} \quad (5.65)$$

Let us now take the derivative of the classical Coulomb repulsion (also called the Hartree term),

$$E_H[\rho] = \frac{1}{2} \int \frac{\rho(1)\rho(2)}{r_{1,2}} d1d2. \quad (5.66)$$

We need $\delta E_H[\rho]/\delta \rho(1)$:

$$\begin{aligned} E_H[\rho + \delta \rho] - E_H[\rho] &= \frac{1}{2} \int \frac{(\rho(1) + \delta \rho(1))(\rho(2) + \delta \rho(2))}{r_{1,2}} d1d2 - \frac{1}{2} \int \frac{\rho(1)\rho(2)}{r_{1,2}} d1d2 \\ &= \frac{1}{2} \int \delta \rho(1) \frac{\rho(2)}{r_{1,2}} d1d2 + \frac{1}{2} \int \frac{\rho(1)}{r_{1,2}} \delta \rho(2) d1d2 + \frac{1}{2} \int \frac{\delta \rho(1)\delta \rho(2)}{r_{1,2}} d1d2 \\ &= \int \frac{\rho(2)}{r_{1,2}} \delta \rho(1) d1d2 + \text{HOT}, \end{aligned} \quad (5.67)$$

where ‘‘HOT’’ stands for ‘‘higher order terms’’ (i.e., the term with $\delta\rho(1)\delta\rho(2)$) which are to be neglected. Thus,

$$\frac{\delta E_H[\rho]}{\delta\rho(1)} = \int \frac{\rho(2)}{r_{1,2}} d2 = v_H[\rho](1), \quad (5.68)$$

the classical Coulomb (Hartree) potential. So the chain rule gives us,

$$\frac{\delta E_H}{\delta\psi_i^*(1)} = n_i v_H(1) \psi_i(1). \quad (5.69)$$

We are left with one last term to differentiate, namely the ‘‘Hartree-Fock’’ (really just the Fock part) or ‘‘exact exchange’’ term,

$$\begin{aligned} E_F[\gamma] &= -a\frac{1}{2} \int \frac{|\gamma(1,2)|^2}{r_{1,2}} d1d2 \\ &= -a\frac{1}{2} \int \frac{\gamma(1,2)\gamma(2,1)}{r_{1,2}} d1d2. \end{aligned} \quad (5.70)$$

Once again we need to use the chain rule,

$$\frac{\delta E_F[\gamma]}{\delta\psi_i^*(1)} = \int \frac{\delta E_F[\gamma]}{\delta\gamma(2,3)} \frac{\delta\gamma(2,3)}{\delta\psi_i^*(1)} d2d3. \quad (5.71)$$

We need to find each of the two functional derivatives, $\delta E_F/\delta\gamma(2,3)$ and $\delta\gamma(2,3)/\delta\psi_i^*(1)$. Let us start with the second one:

$$\begin{aligned} \delta\gamma(2,3)[\psi_i^*] &= \delta\gamma(2,3)[\psi_i^* + \delta\psi_i] - \gamma(2,3)[\psi_i^*] \\ &= \psi_i(2)n_i(\psi_i^*(3) + \delta\psi_i^*(3)) - \psi_i(2)n_i\psi_i^*(3) \\ &= \psi_i(2)n_i\delta\psi_i^*(3) \\ &= \int (\psi_i(2)n_i\delta(3-1)) \psi_i^*(1) d1. \end{aligned} \quad (5.72)$$

So,

$$\frac{\delta\gamma(2,3)}{\delta\psi_i^*(1)} = \psi_i(2)n_i\delta(3-1). \quad (5.73)$$

For the first derivative,

$$\begin{aligned} \delta E_F[\gamma] &= E_F[\gamma + \delta\gamma] - E_F[\gamma] \\ &= -a\frac{1}{2} \int \frac{(\gamma(2,3) + \delta\gamma(2,3))(\gamma(3,2) + \delta\gamma(3,2))}{r_{2,3}} d2d3 + a\frac{1}{2} \int \frac{\gamma(2,3)\gamma(3,2)}{r_{1,2}} d1d2 \\ &= -a\frac{1}{2} \int \frac{\gamma(3,2)}{r_{2,3}} \delta\gamma(2,3) d2d3 - a\frac{1}{2} \int \frac{\gamma(2,3)}{r_{2,3}} \delta\gamma(3,2) d2d3 + \text{HOT} \\ &= -a \int \int \frac{\gamma(3,2)}{r_{2,3}} \delta\gamma(2,3) d2d3 + \text{HOT}. \end{aligned} \quad (5.74)$$

So,

$$\frac{\delta E_F[\gamma]}{\delta\gamma(2,3)} = -a \frac{\gamma(3,2)}{r_{2,3}}. \quad (5.75)$$

Putting it altogether gives,

$$\begin{aligned} \frac{\delta E_F}{\delta \psi_i^*(1)} &= -a \int \frac{\gamma(3, 2)}{r_{2,3}} \psi_i(2) n_i \delta(3-1) d2d3 \\ &= -an_i \int \frac{\gamma(1, 2)}{r_{1,2}} \psi_i(2) d2 \\ &= an_i \hat{\Sigma}_x \psi_i(1), \end{aligned} \quad (5.76)$$

where I have renamed the integral operator the exchange self energy $\hat{\Sigma}_x = -\hat{K}$ which is equivalent to the chemist's exchange operator \hat{K} up to a sign.

We now see that,

$$\frac{\delta E}{\delta \psi_i^*(1)} = n_i \left(\hat{t} + v(1) + v_H(1) - a\hat{\Sigma}_x + bv_x[\rho](1) + cv_c[\rho](1) \right) \psi_i(1). \quad (5.77)$$

Thus the orbital hamiltonian,

$$\hat{h} = \hat{t} + v(1) + v_H(1) - a\hat{\Sigma}_x + bv_x[\rho](1) + cv_c[\rho](1), \quad (5.78)$$

which is the expected result.

Finally, if the kinetic energy is approximated as it is in Thomas-Fermi theory, then $n_i \hat{t} \psi_i(1)$ must be replaced by

$$\begin{aligned} \frac{\delta T_{\text{TF}}}{\delta \psi_i^*(1)} &= \int \frac{\delta T_{\text{TF}}}{\delta \rho(2)} \frac{\delta \rho(2)}{\delta \psi_i^*(1)} d2 \\ &= n_i \frac{\delta T_{\text{TF}}}{\delta \rho(1)} \psi_i(1) \\ &= n_i \frac{1}{2} (3\pi^2)^{2/3} \rho^{2/3}(1) \psi_i(1) \\ &= n_i v_{\text{TF}}(1) \psi_i(1), \end{aligned} \quad (5.79)$$

and \hat{h} is given by,

$$\hat{h} = v_{\text{TF}}(1) + v(1) + v_H(1) - a\hat{\Sigma}_x + bv_x[\rho](1) + cv_c[\rho](1). \quad (5.80)$$

We are left with an orbital eigenvalue equation,

$$\left(v_{\text{TF}}(1) + v(1) + v_H(1) - a\hat{\Sigma}_x + bv_x[\rho](1) + cv_c[\rho](1) \right) \psi_i(1) = \epsilon_i \psi_i(1). \quad (5.81)$$

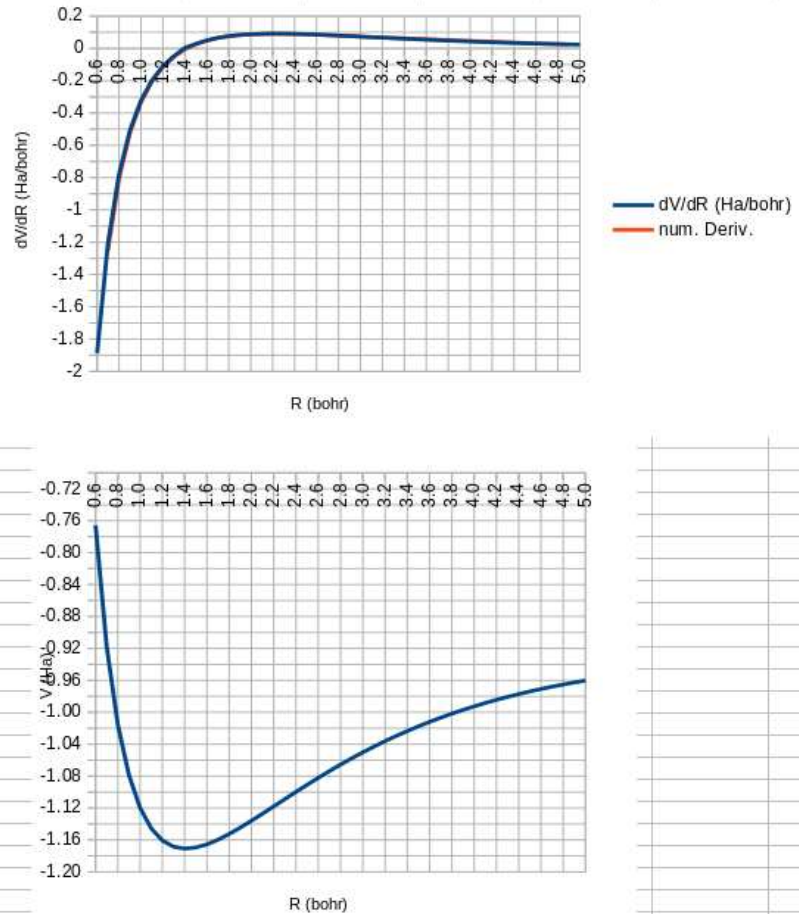
If $a = 0$, then we can divide out $\psi(1)$ (where it is nonzero!) and we are left with the very strange result that

$$v_{\text{TF}}(1) + v(1) + v_H(1) + bv_x[\rho](1) + cv_c[\rho](1) = \epsilon_i, \quad (5.82)$$

for all i which is indeed strange as (i) we have no way to determine the ψ_i , (ii) all the ϵ_i seem to be equal, and (iii) $v_{\text{TF}}(1) + v(1) + v_H(1) + bv_x[\rho](1) + cv_c[\rho](1)$ should be a constant function. The situation can hardly be expected to improve for $a \neq 0$. The answer to this paradoxical situation is, of course, that the Thomas-Fermi approximation is an *orbital-free* theory (i.e., justified by the original Hohenberg-Kohn paper [159]) whose fundamental parameter is only the charge density.

5.5.2 SCF Convergence and Forces

The convergence criterion is set to SCFTYPE RKS TOL=1.E-5. I first calculated the potential energy curve (PEC) and its derivative over a wide range of bond lengths, just to have a look at it:

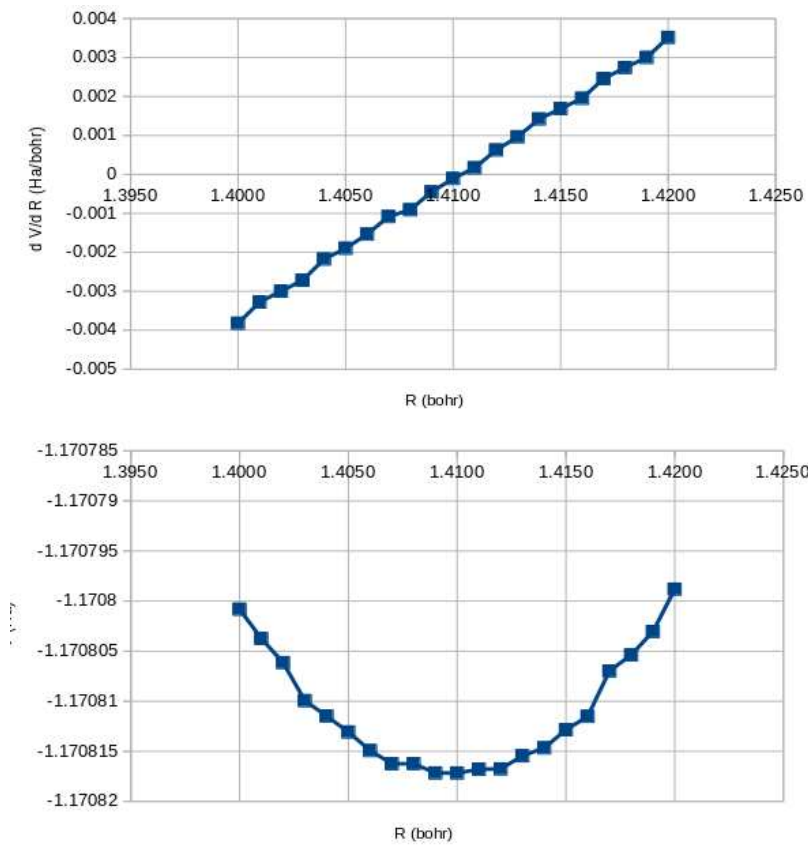


I also calculated the numerical derivative in the usual way as,

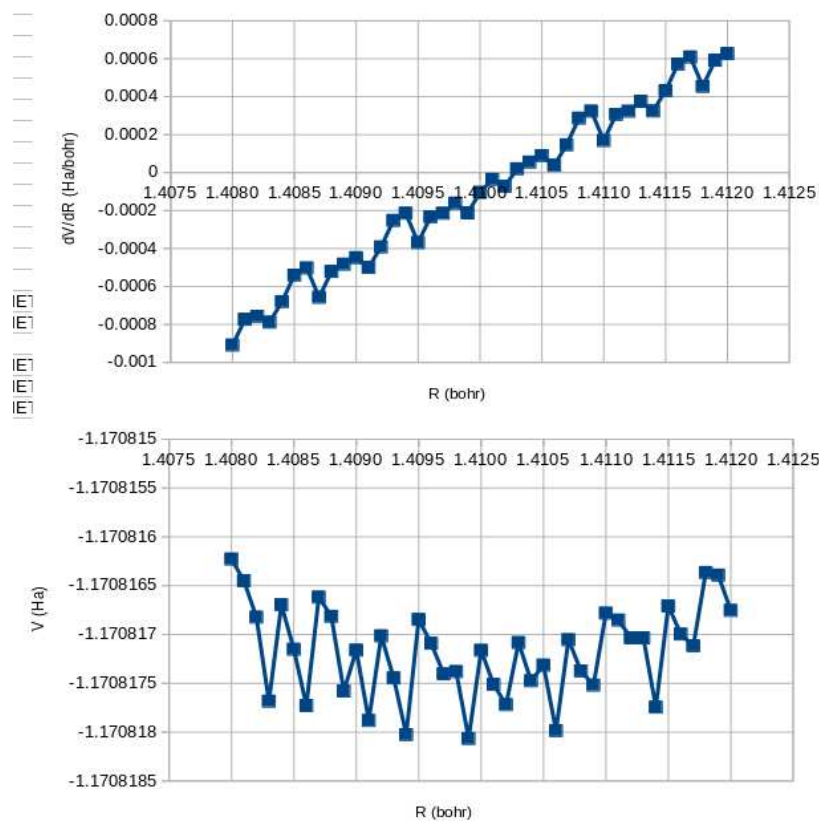
$$V'(R) \approx \frac{V(R + h) - V(R - h)}{2h} . \quad (5.83)$$

The graph shows that the numerical derivative and the analytical derivative agree, after changing signs. The change of sign is needed because the output only gave the absolute value of the analytical derivative. Hence the units of the FORCE printed in the output is really just Ha/bohr and it is a direct derivative without, for example, any mass weighting.

We are using the program defaults. Defaults are usually set a bit too loosely so that most calculations converge. While this makes most users happy, it is often necessary to tighten the convergence criteria for specific applications. For now, we leave them as is and zoom in on the minimum of the PEC:



Now we are beginning to see that the PEC is less smooth and there are wiggles in the force curve, but it still looks as though the zero of $V'(R)$ is at the minimum of the $V(R)$. But we have not yet seen the limits of the method, so let us zoom in still further:

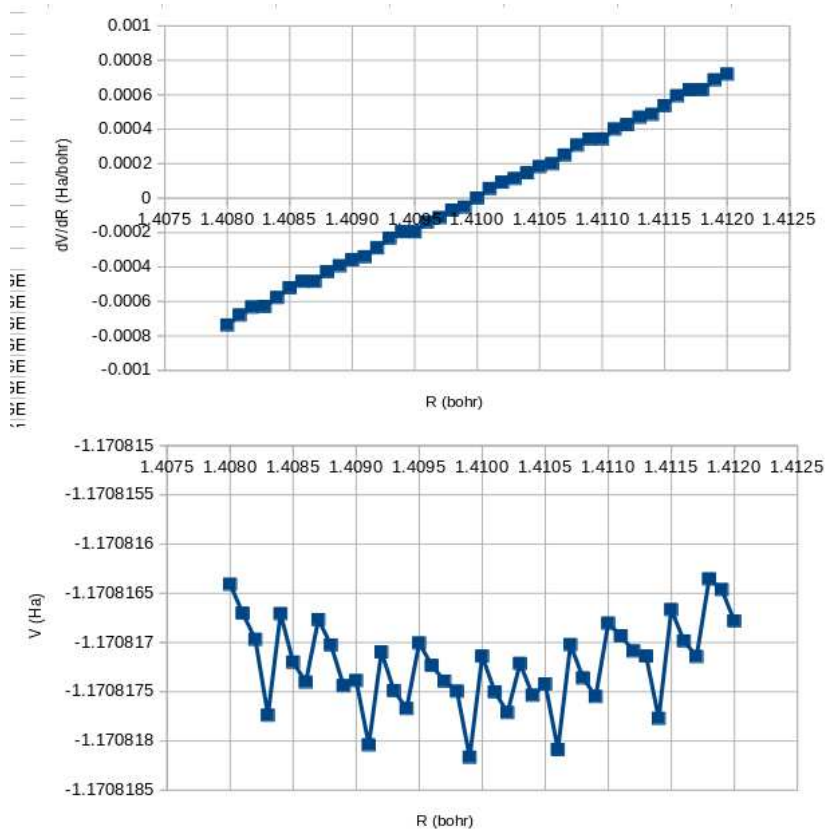


The oscillations are on the order of 10^{-6} which is an order of magnitude less than the requested convergence criterion 10^{-5} . It is much easier to locate the zero of $V'(R)$ (which is at about 4.125 bohr) than the minimum of $V(R)$, but with a little imagination you might think that the minimum of $V(R)$ is slightly displaced (towards smaller R) from the zero of $V'(R)$.

1.4091	-1.170817881	-0.0004996	0.00073
1.4092	-1.170817015	-0.0003917	0.00218
1.4093	-1.170817445	-0.0002520	-0.00505 *** THE GEOMETRY IS OPTIMIZED ***
1.4094	-1.170818025	-0.0002139	0.00299 *** THE GEOMETRY IS OPTIMIZED ***
1.4095	-1.170816847	-0.0003689	0.00467
1.4096	-1.170817091	-0.0002328	-0.00278 *** THE GEOMETRY IS OPTIMIZED ***
1.4097	-1.170817403	-0.0002145	-0.001445 *** THE GEOMETRY IS OPTIMIZED ***
1.4098	-1.170817380	-0.0001611	-0.00331 *** THE GEOMETRY IS OPTIMIZED ***
1.4099	-1.170818065	-0.0002124	0.001085 *** THE GEOMETRY IS OPTIMIZED ***
1.4100	-1.170817163	-0.0001045	0.002765 *** THE GEOMETRY IS OPTIMIZED ***
1.4101	-1.170817512	-3.600E-05	-0.00278 *** THE GEOMETRY IS OPTIMIZED ***
1.4102	-1.170817719	-7.3E-05	0.002145 *** THE GEOMETRY IS OPTIMIZED ***
1.4103	-1.170817083	2.02E-05	0.001225 *** THE GEOMETRY IS OPTIMIZED ***
1.4104	-1.170817474	5.53E-05	-0.001155 *** THE GEOMETRY IS OPTIMIZED ***
1.4105	-1.170817314	8.94E-05	-0.00255 *** THE GEOMETRY IS OPTIMIZED ***
1.4106	-1.170817984	3.84E-05	0.0013 *** THE GEOMETRY IS OPTIMIZED ***
1.4107	-1.170817054	0.0001463	0.003055 *** THE GEOMETRY IS OPTIMIZED ***
1.4108	-1.170817373	0.0002864	-0.002325 *** THE GEOMETRY IS OPTIMIZED ***
1.4109	-1.170817519	0.0003233	0.002955
1.4110	-1.170816782	0.0001684	0.00333 *** THE GEOMETRY IS OPTIMIZED ***
1.4111	-1.170816853	0.0003062	
1.4112	-1.170817035	0.0003229	

The program indicates an optimized geometry from roughly $R = 1.04093$ bohr to $R = 1.4110$ bohr with some places inbetween where the geometry is not indicated as converged. This corresponds to the geometry indicated as optimized roughly when $V'(R) < 0.0003$ Ha/bohr.

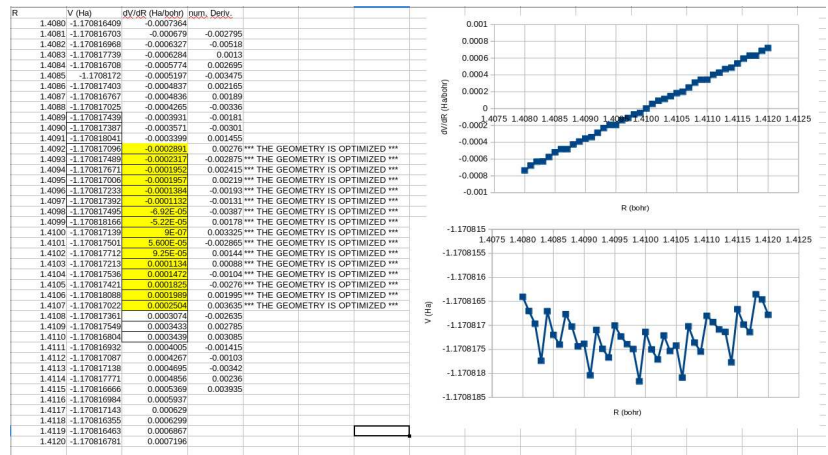
Here are the results obtained with SCFTYPE RKS TOL=1.E-8:



There are still large oscillations in $V(R)$ for $\text{TOL}=1.\text{E}-8$ but there also appear to be fewer oscillations than for $\text{TOL}=1.\text{E}-5$. Most importantly the numerical oscillations in $V'(R)$ seen for $\text{TOL}=1.\text{E}-5$ are nearly invisible on the scale of the plot for $\text{TOL}=1.\text{E}-8$.

5.5.3 How Good a Guess Do We Need?

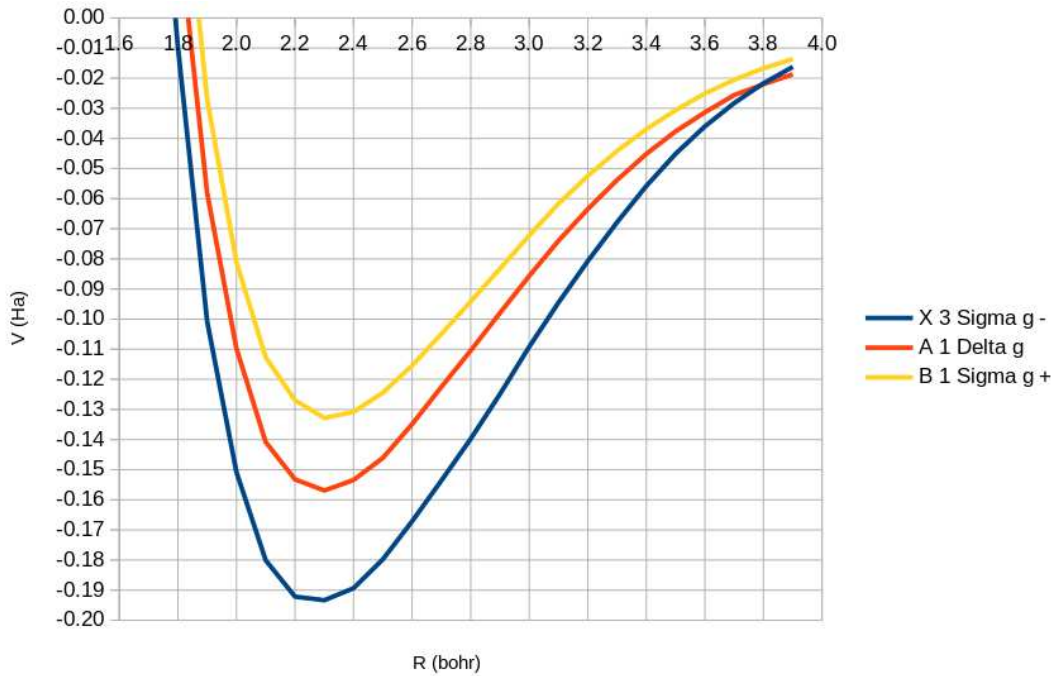
The initial guess $R = 4.6$ bohr is indeed in a region where the naïve walker algorithm described in the lesson will converge to a minimum. However running the job indicates that it converges to a minimum at $R = 1.408724$ bohr.



Some further playing with the geometry optimization parameters should yield an answer closer to the zero of $V(R)$ which we see is actually at $R = 1.4100$ bohr.

5.6 Lesson 6 Answers

Our objective is to use DFT at the BLYP/DEF2-TZVPP level to get as close as possible to the exact answers from Ref. [127]:

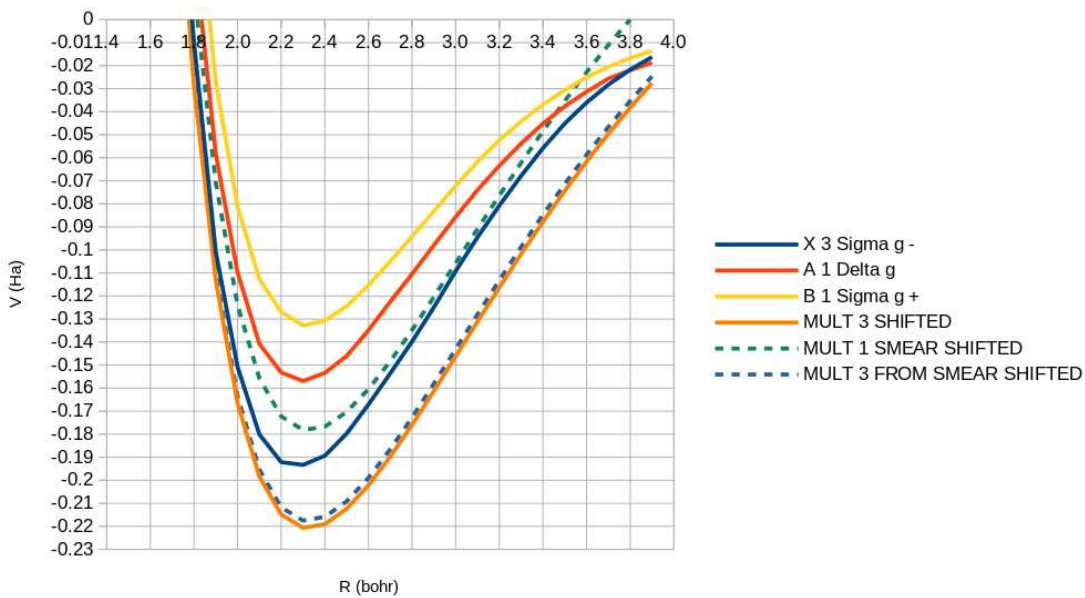


5.6.1 No Symmetry Breaking

Symmetry breaking is necessary to get properly shaped dissociation curves. Without symmetry breaking our DFT curves are not going to dissociate correctly. However proper symmetry breaking is quite challenging for this system. *Under the circumstances, the energy zero of the DFT calculations has been chosen to be that of twice the BLYP/DEF2-TZVPP atomic energy, namely $2E(O) = -150.165964758 \text{ Ha}$. Any basis-set-superposition error has been ignored.*

$^3\Sigma_g^-$ Ground State and Fractionally-Occupied Reference State

There are two ways to calculate the $^3\Sigma_g^-$ PEC. One is to do a fully-relaxed UKS calculation. This is indicated in orange on the following graph (labeled MULT 3 SHIFTED):



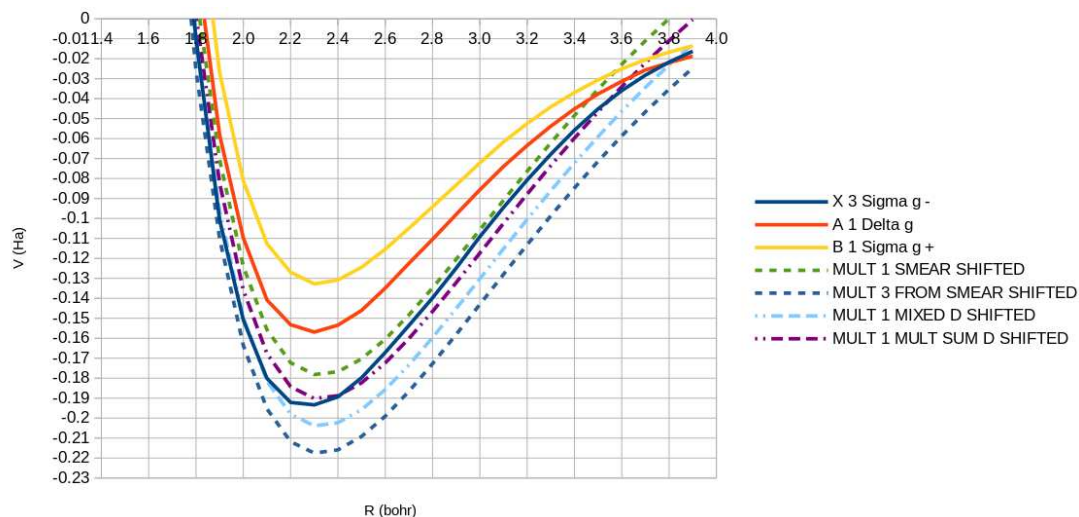
The BLYP curve is clearly overbound.

The other way to calculate the $^3\Sigma_g^-$ PEC is to first create a reference state with equal fractional occupation number (one half spin up and one half spin down electron in each π^* orbital.) This is the green dashed line on the curve (labeled MULT 1 SMEAR SHIFTED.)

We can use this reference state as a restart file to do a single iteration calculation where the orbital occupations have been readjusted to correspond to the $^3\Sigma_g^-$ state. This gives the blue dashed curve (labeled MULT 3 FROM SMEAR SHIFTED.) It is almost the same as the fully relaxed UKS result (orange curve) but is slightly higher in energy as should be expected on the basis of the variational principle. This blue dashed $^3\Sigma_g^-$ PEC will be used in our MSM calculations in order to maintain orbital orthogonality requirements.

$^1\Delta_g$ State

This is what is usually meant by singlet oxygen!



This is the same as the previous graph except that two new dashed-dot curves have been added. The light blue one (labeled MULT 1 MIXED D SHIFTED) is the $\pi_x^*[\uparrow][\downarrow]\pi_y^*$ reference configuration.

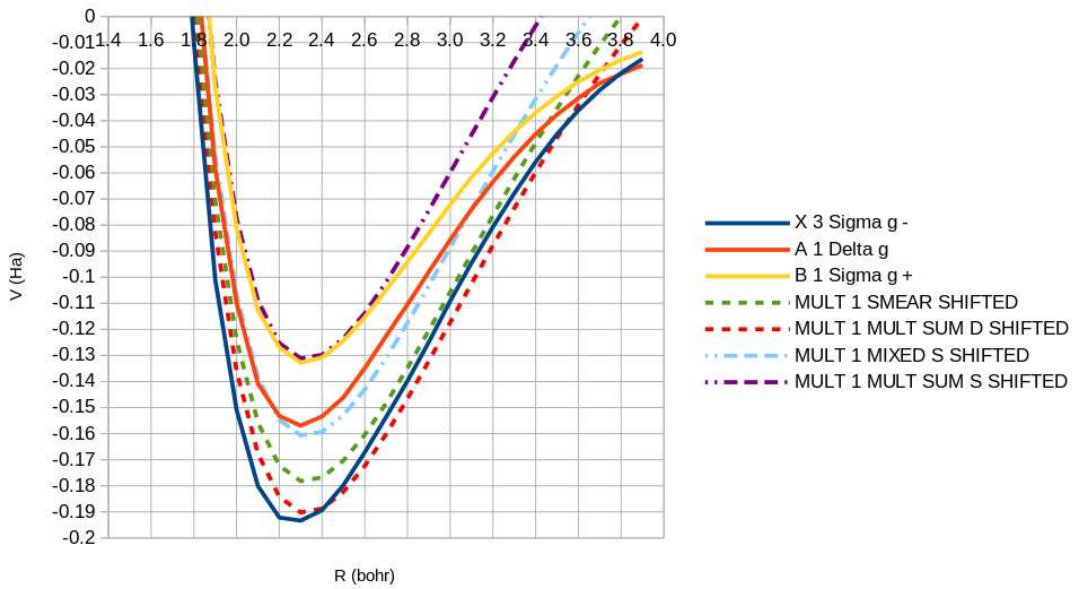
This is the one listed in the MO diagram of the Wikipedia entry for the ${}^1\Sigma_g^+$ state of singlet oxygen [160]. The excitation energy of the light blue dashed-dot curve with respect to that of the dashed blue curve is clearly too low to be that of the ${}^1\Sigma_g^+$ state. It is even too low to be the excitation energy of the ${}^1\Delta_g$ state. In contrast, the purple dashed-dot curve (labeled MULT 1 MULT SUM D SHIFTED) obtained from the MSM formula,

$$E[{}^1\Delta_g] = 2E[|\pi_x^*, \bar{\pi}_y^*|] - E[|\pi_x^*, \pi_y^*|], \quad (5.84)$$

is a reasonable description of the ${}^1\Delta_g$ PEC *relative to* the B3LYP ${}^3\Sigma_g^-$ PEC (even though the absolute energy is wrong.)

${}^1\Sigma_g^+$ State

Very often the higher the excited state, the more difficult it is to get a satisfying description. However the absolute energy of the MSM ${}^1\Sigma_g^+$ state is actually rather good. Here is a new graph, similar to the previous graph, but some of the colors have been changed:

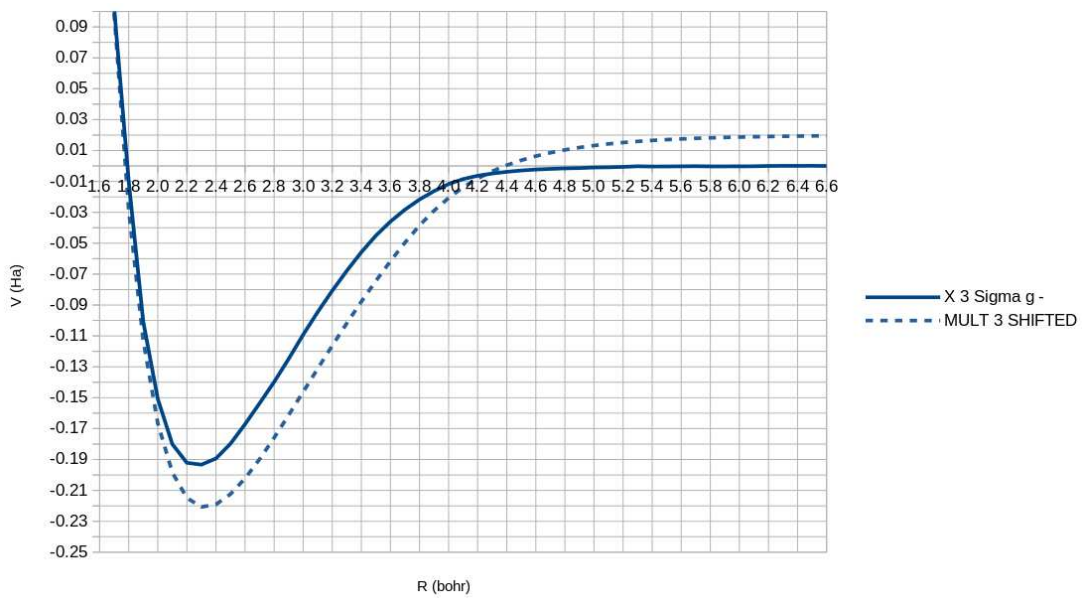


The purple dashed-dot line in the previous graph (labeled MULT 1 MULT SUM D SHIFT) is our best MSM answer for the ${}^1\Delta_g$ PEC. It is represented here a red dashed line (still labeled MULT 1 MULT SUM D SHIFT.) There is a new mixed state (labeled MULT 1 MIXED S SHIFTED) which corresponds to the configuration $\pi_x^*[\uparrow\downarrow][\quad]\pi_y^*$ and whose PEC is given by a light blue dashed-dotted line. Oddly enough this is exactly the configuration that the Wikipedia [160] gives for the ${}^1\Delta_g$ state. Coïncidentally its absolute energy is close to that of the exact ${}^1\Delta_g$ PEC. However its BLYP excitation energy is much closer to the BLYP ${}^1\Sigma_g^+$ excitation energy in our calculations. The final MSM ${}^1\Sigma_g^+$ PEC is given by a purple dashed-dot line (labeled MULT 1 MULT SUM S SHIFTED) which is in remarkably good agreement with the exact ${}^1\Sigma_g^+$ PEC curve.

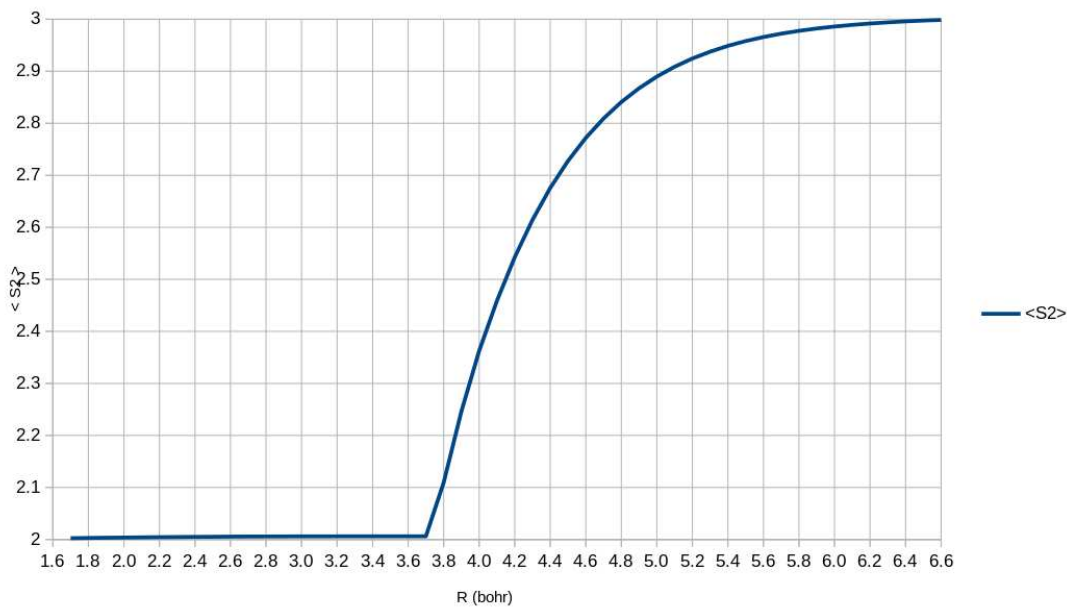
5.6.2 With Symmetry Breaking

${}^3\Sigma_g^-$ Ground State

Following the procedure given in the lesson gives

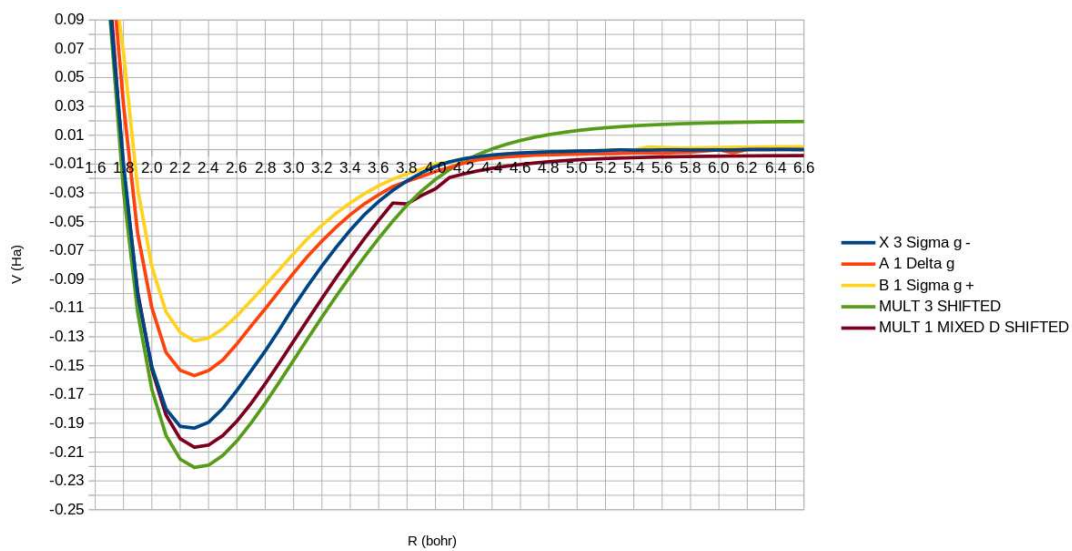


The general shape of the BLYP PEC is correct but it dissociates to a higher energy than twice the energy of two oxygen atoms, suggesting that further symmetry breaking might be possible. (Or perhaps this is simply the best that can be done without resorting to a multideterminantal approach?) It is also clear that BLYP overbinds the molecule. As in the case of H₂, there is a bond distance beyond which spin contamination sets in:

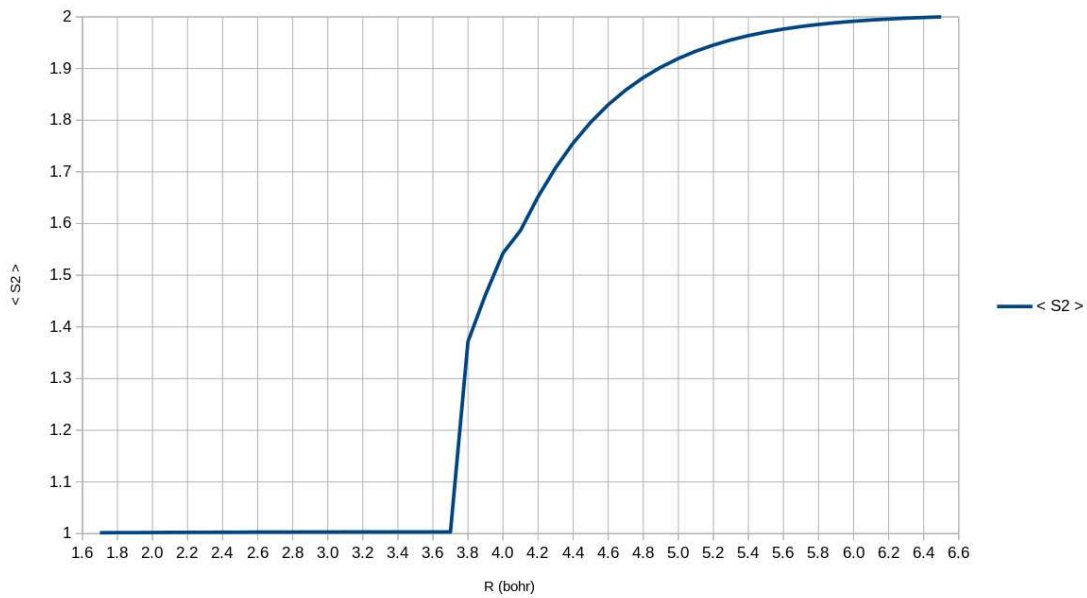


$\pi_x^* [\quad] [\uparrow\downarrow] \pi_y^*$ Reference State

This was obtained with MULTI 1 and a restart from the triplet:



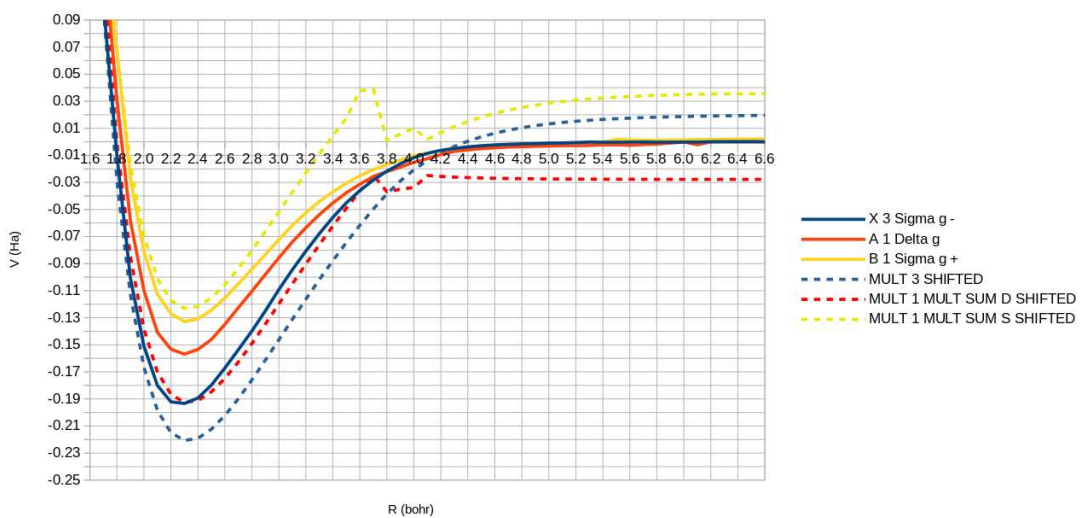
There are some problems in the shape of the curve noted between 3.7 bohr and 4.1 bohr. $R = 3.7$ bohr was where spin contamination set in for the triplet state. We may also calculate spin contamination for the MULT 1 reference state:



$\langle \hat{S}^2 \rangle = S(S + 1)$ should be zero for a singlet and two for a triplet. The value of $\langle \hat{S}^2 \rangle$ is constant up to the same bond length where spin contamination set in for the triplet state. It then seems to converge to a triplet state at very large values of R .

${}^1\Delta_g$ and ${}^1\Sigma_g^+$ States

The dashed lines are the BLYP MSM approximation to the accurate curves of the same color.



5.6.3 Conclusion

The two calculations above (symmetry unbroken and with symmetry breaking) give very similar results in the region where no symmetry breaking occurs even though different reference states have been used in the two cases. This is reassuring. However the MSM method breaks down badly for describing excited states once symmetry breaking occurs. There are several reasons this could happen including the possibility of more than one way to break symmetry and the problem of identifying spin \uparrow and spin \downarrow orbitals once symmetry breaking has occurred. However the most important difficulty and *the most important reason to avoid symmetry breaking when treating excited states* is that it is nearly impossible to construct excited states with well-defined symmetries unless the molecular orbitals belong to well-defined irreducible representations of the molecular point group, which is certainly not the case in broken-symmetry calculations.

Appendix A

Installing LINUX on a Mac Notebook

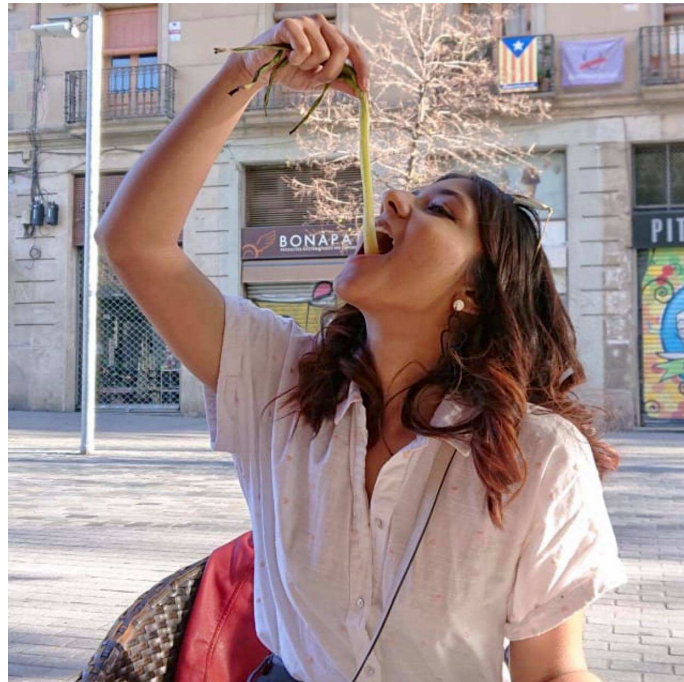


Figure A.1: Nabila Oozeer (shown here enjoying the culinary pleasures of Barcelona) did a *stage de L3 chimie physique* with MEC in January 2022. This appendix is one result of her stage.

This appendix is based upon work done by Nabila Oozeer (Fig. A.1) during a short research internship in 2022. The object of this stage was to test the reaction of a third-year University undergraduate to this workbook. We decided that she would work with DEMON2K on her Macintosh (Mac) Notebook computer. However the Mac Notebook uses the Mac operating system and not LINUX. So Nabila first installed Oracle's VIRTUALBOX [161] which allows multiple operating systems to be run on the same computer and then she installed the UBUNTU version of LINUX. What follows are Nabila's detailed instructions for duplicating her installation:

A.1 Step 1: VIRTUALBOX Installation

VIRTUALBOX allows you to run multiple operating systems (OSs) at the same time.

1. Go to [//www.virtualbox.org/](http://www.virtualbox.org/).
2. Click on Download VIRTUALBOX 6.1 (big blue button). You will be redirected to the “Downloads” section of the website.
3. Click on the type of OS of your computer (e.g., click on “OX hosts” if you have a Macbook or on “Windows hosts” if your computer runs on WINDOWS). *A pop-up might appear here if you have a Macbook requiring you to authorize the download.* If so, then go to System Preferences → Security and Preferences → Allow apps downloaded from Oracle America and save changes.
4. Now that the file has been downloaded, open the VIRTUALBOX file and click on install.

You may now go to the Launchpad and open VIRTUALBOX.

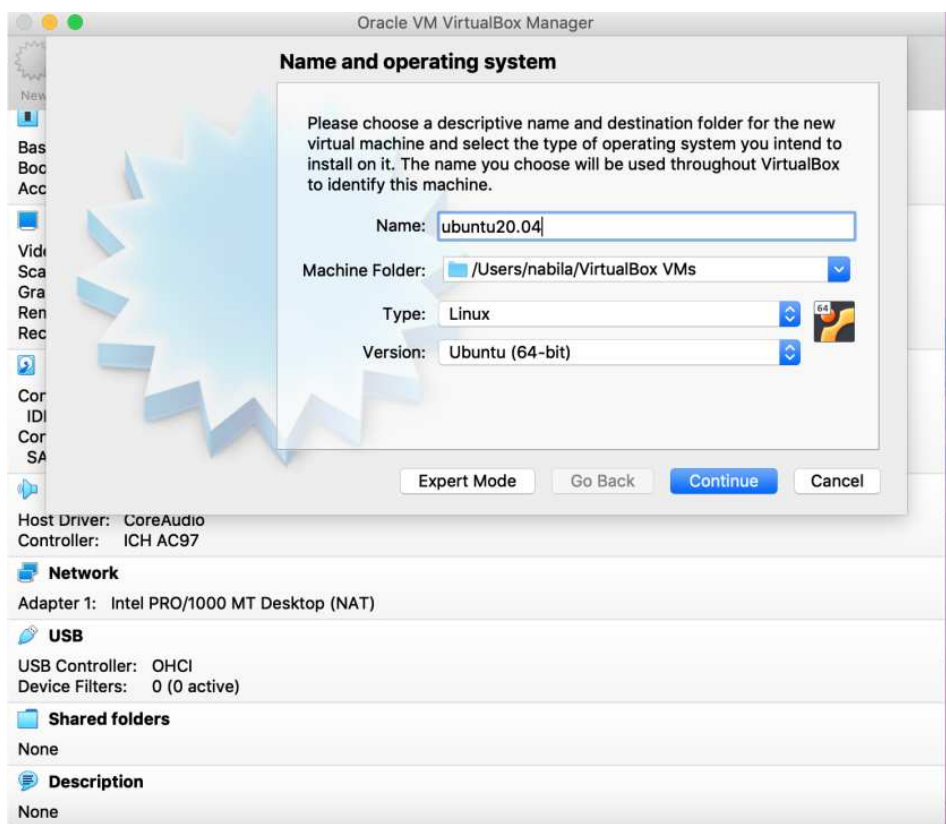
A.2 Step 2: LINUX Installation

Nabila decided to install UBUNTU but you can install another flavor of LINUX (such as MINT).

1. Go to <https://ubuntu.com/#download>. Click on Ubuntu Desktop 20.04 LTS.
2. The file is now downloaded as ubuntu_20.04.3-...iso.

A.3 Step 3: Creation of a Virtual Machine

Go to VIRTUALBOX and open a new window. It should look something like this:

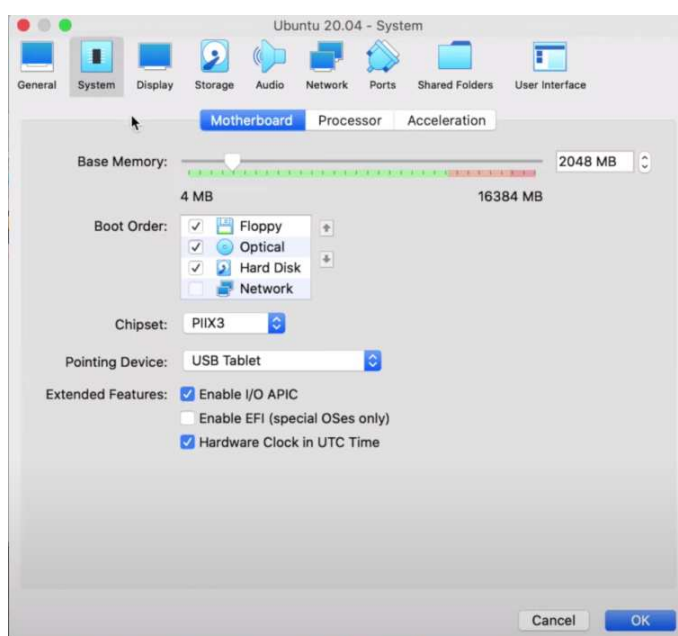


1. Click on **New** (top left corner).
2. Give the file a name (such as `ubuntu20.04`). Note the file destination so that you will be able to locate it later on.
3. Click on **Continue**.
4. Select the amount of RAM (i.e., random access memory) that you want to allocate for the virtual machine (2 GB of RAM is recommended but you can change this later on).
5. Go to **Hard Disk** → **Create** → **VDI** (Virtual box disk image) → **Dynamically allocated**. (The latter option allocates memory as needed. In contrast, the **Fixed size** option allocates all the memory at the beginning.)
6. **File size** → 50 GB. (You can choose more if you want to but 50 GB is fine for running UBUNTU with DEMON2K.) *Note that this disk size cannot be changed.*
7. **Create**.

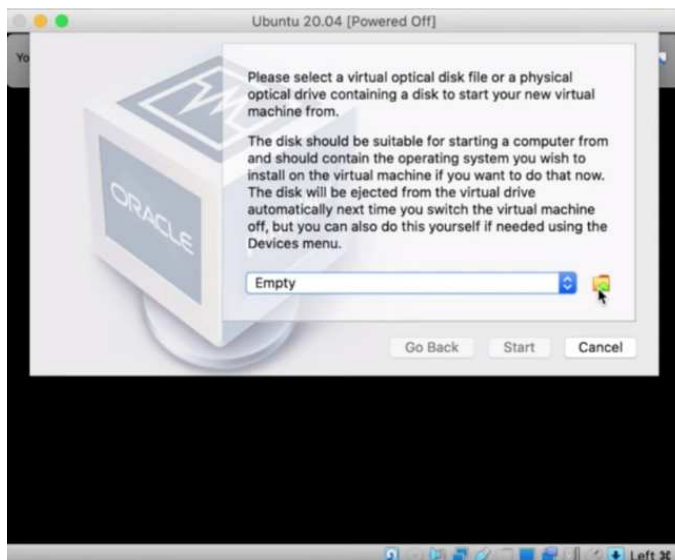
If all goes well, UBUNTU 20.04 has now been created. Before starting it up, we will click on the **Settings** button to check on a few things.



This menu will appear:



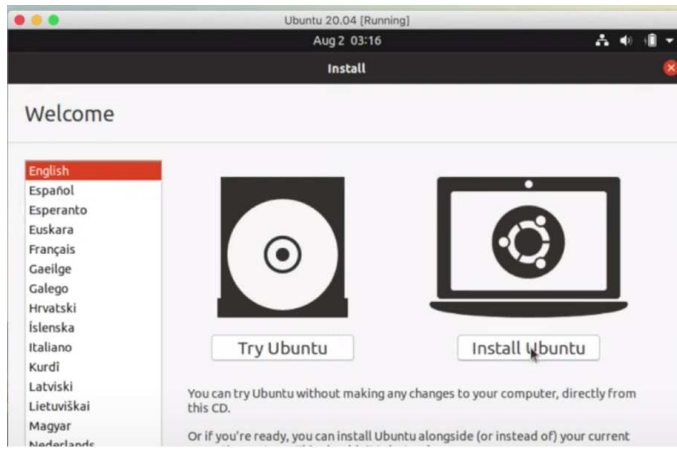
1. Go to **System**. First we have the **Motherboard** tab. This is where the RAM may be changed. Next there is the **Processor** tab. This is where more of the CPUs may be allocated to the virtual machine. (For our purpose, one CPU is enough. However, if the machine is performing poorly, we may need to add more processors to it.)
2. Go to **Display**. The **Screen** tab opens. The **Video Memory** should be set to its maximum value.
3. We can now click **OK** and then the **Start** button.
4. A menu asking you to insert the installation file will pop up:



5. Click on the **folder** icon.

We will now insert the `ubuntu.iso` file that we initially downloaded from the UBUNTU website. A menu will appear.

1. Click on the **Add** icon.
2. Locate your **.iso** file and open it.
3. The file will appear on the menu. Select the file and hit **choose**.
4. Click on the **Start** button. This means that the UBUNTU installation is booted up.
5. A welcome screen appears.



6. Choose your preferred language and click on **Install Ubuntu**.
7. Choose your desired keyboard layout.
8. Make sure to choose **Normal Installation**; this step gives you a full version of UBUNTU.
9. Click **Continue**.

The next step regards the installation type.

1. Click on **Erase disk and install Ubuntu**. (*Note that this step will not actually erase your disk!*)
2. Hit the *Install button*.
3. Create an account

UBUNTU is now installed.

Once the installation is complete, then you should click on *Restart now*.

You may now connect to your online accounts.

To get the most of your UBUNTU experience, you will need to install the UBUNTU guest edition. This improves the screen resolution and allows you to use UBUNTU in full-screen mode. (Nabila reports that it took her a few hours until she figured out why she could not use UBUNTU in full-screen mode.)

1. Go on the menu bar on the Mac and on the top left corner of the screen hit **Devices → Insert Guest Additions CD Image**.
2. A pop up will appear and click on run.
3. A terminal showing the installation of the guest addition will appear.
4. When the terminal is done, restart UBUNTU.

Enjoy your virtual operating system!

Acknowledgement

Nabila is grateful to Pierre Girard for valuable help with the installation process.

Bibliography

- [1] G. Geudtner, P. Calaminici, J. Carmona-Espindola, J. M. del Campo, V. D. Dominguez-Soria, R. Flores-Moreno, G. U. Gamboa, A. Goursot, A. M. Köster, J. U. Reveles, T. Mineva, J. M. Vasquez-Perez, A. Vela, B. Zuñiga-Gutierrez, and D. Salahub, **DEMON2K**, WIREs: Comput. Mol. Sci. **2**, 548 (2012).
- [2] A. Ponra, A. J. Etindele, O. Motapon, and M. E. Casida, **Practical treatment of singlet oxygen with density-functional theory and the multiplet-sum method**, Theo. Chem. Acc. **140**, 154 (2021).
- [3] E. R. Davidson and D. Feller, **Basis set selection for molecular calculations**, Chem. Rev. **86**, 681 (1986).
- [4] J. G. Hill, **Gaussian basis sets for molecular applications**, Int. J. Quant. Chem. **113**, 21 (2013).
- [5] B. Delley, **An allelectron numerical method for solving the local density functional for polyatomic molecules**, J. Chem. Phys. **92**, 508 (1990).
- [6] J. C. Slater, **Atomic shielding constants**, Phys. Rev. **36**, 57 (1930).
- [7] G. te Velde, F. M. Bickelhaupt, E. J. Baerends, C. F. Guerra, S. J. A. van Gisbergen, J. G. Snijders, and T. Ziegler, **Chemistry with ADF**, J. Comput. Chem. **22**, 931 (2001).
- [8] N. Godbout, D. R. Salahub, J. Andzelm, and E. Wimmer, **Optimization of Gaussian-type basis sets for local spin density functional calculations. Part I. Boron through neon, optimization technique and validation**, Can. J. Phys. **70**, 560 (1992).
- [9] P. Calaminici, F. Janetzko, A. M. Köster, R. Mejia-Olvera, and B. Zuniga-Gutierrez, **Density functional theory optimized basis sets for gradient corrected functionals: 3d transition metal systems**, J. Chem. Phys. **126**, 044108 (2007).
- [10] W. J. Hehre, R. Ditchfield, R. F. Stewart, and J. A. Pople, **Selfconsistent molecular orbital methods. IV. Use of Gaussian expansions of Slater-type orbitals. Extension to secondrow molecules**, J. Chem. Phys. **52**, 2769 (1970).
- [11] P. C. Hariharan and J. A. Pople, **The influence of polarization functions on molecular orbital hydrogenation energies**, Theor. Chim. Acta **28**, 213 (1973).
- [12] M. M. Franci, W. J. Pietro, and W. J. Hehre, **Selfconsistent molecular orbital methods. XXIII. A polarization-type basis set for secondrow elements**, J. Chem. Phys. **77**, 3654 (1982).
- [13] R. Krishnan, J. S. Binkley, R. Seeger, and J. A. Pople, **Selfconsistent molecular orbital methods. XX. A basis set for correlated wave functions**, J. Chem. Phys. **72**, 650 (1980).

- [14] F. Weigend and R. Ahlrichs, [Balanced basis sets of split valence, triple zeta valence and quadruple zeta valence quality for H to Rn: Design and assessment of accuracy](#), Phys. Chem. Chem. Phys. **7**, 3297 (2005).
- [15] N. Rega, M. Cossi, and V. Barone, [Development and validation of reliable quantum mechanical approaches for the study of free radicals in solution](#), J. Chem. Phys. **105**, 11060 (1996).
- [16] S. Huzinaga, [Gaussian-type functions for polyatomic systems. I](#), J. Chem. Phys. **42**, 1293 (1965).
- [17] G. C. Lie and E. Clementi, [Study of the electronic structure of molecules. XXI. Correlation energy corrections as a functional of the Hartree-Fock density and its application to the hydrides of the second row atoms](#), J. Chem. Phys. **60**, 1275 (1974).
- [18] A. J. Sadlej, [Medium-size polarized basis sets for high-level correlated calculations of molecular electric properties](#), Collection Czech. Chem. Commun. **53**, 1995 (1988).
- [19] J. Guan, P. Duffy, J. T. Carter, D. P. Chong, K. C. Casida, M. E. Casida, and M. Wrinn, [Comparison of local-density and Hartree-Fock calculations of molecular polarizabilities and hyperpolarizabilities](#), J. Chem. Phys. **98**, 4753 (1993).
- [20] R. Pu-Amérigo, M. Merchán, I. Nebot-Gil, P. Widmark, and B. O. Roos, [Density matrix averaged atomic natural orbital \(ANO\) basis sets for correlated molecular wave functions. III. First row transition metal atoms](#), Theor. Chim. Acta **92**, 149 (1995).
- [21] D. E. Woon and T. H. D. Jr., [Gaussian basis sets for use in correlated molecular calculations. V. Core-valence basis sets for boron through neon](#), J. Chem. Phys. **103**, 4572 (1995).
- [22] T. H. D. Jr., [Gaussian basis sets for use in correlated molecular calculations. I. The atoms boron through neon and hydrogen](#), J. Chem. Phys. **90**, 1007 (1989).
- [23] F. Jensen, [The basis set convergence of spin-spin coupling constants calculated by density functional methods](#), J. Chem. Theo. Comp. **2**, 1360 (2006).
- [24] T. H. Dunning and P. J. Hay, [Gaussian basis sets for molecular calculations](#), in *Methods of Electronic Structure Theory*, edited by H. F. S. III, volume 3 of *Modern Theoretical Chemistry*, page 1, Springer, 1977.
- [25] I. Cherkes, S. Klaiman, and N. Moiseyev, [Spanning the Hilbert space with an even tempered gaussian basis set](#), Int. J. Quant. Chem. **109**, 2996 (2009).
- [26] J. P. Perdew and A. Zunger, [Self-interaction correction to density-functional approximations for many-electron systems](#), Phys. Rev. B **23**, 5048 (1981).
- [27] J. P. Perdew and M. Levy, [Physical content of the exact Kohn-Sham orbital energies: band gaps and derivative discontinuities](#), Phys. Rev. Lett. **51** (1983).
- [28] L. J. Sham and M. Schlüter, [Density-functional theory of the energy gap](#), Phys. Rev. Lett. **51** (1983).
- [29] A. J. Cohen, P. Mori-Sánchez, and W. Yang, [Insights into current limitations of density functional theory](#), Science **321**, 792 (2008).

- [30] W. Kohn and L. J. Sham, [Self-consistent equations including exchange and correlation effects](#), Phys. Rev. **140**, A1133 (1965).
- [31] M. Levy, [Universal variational functionals of electron densities, first-order density matrices, and natural spin-orbitals and solution of the \$v\$ -representability problem](#), Proc. Natl. Acad. Sci. USA **76**, 6062 (1979).
- [32] M. Levy, [Electron densities in search of Hamiltonians](#), Phys. Rev. A **26**, 1200 (1982).
- [33] I. M. Gelfand and S. V. Fomin, *Calculus of Variations*, Prentice-Hall, 1963, translated and edited by R. A. Silverman.
- [34] J. F. Janak, [Proof that \$\partial e/\partial n_i = \epsilon_i\$ in density-functional theory](#), Phys. Rev. B **18**, 7165 (1978).
- [35] M. E. Casida and D. P. Chong, [Large \$r\$ approximation for spherically averaged momentum distributions](#), Chem. Phys. **132**, 391 (1989).
- [36] M. E. Casida, [Correlated optimized effective potential treatment of the derivative discontinuity and of the highest occupied Kohn-Sham eigenvalue: A Janak-type theorem for the optimized effective potential method](#), Phys. Rev. B **59**, 4694 (1999).
- [37] A. A. M. H. M. Darghouth, M. E. Casida, W. Taouali, K. Alimi, M. P. Ljungberg, P. Koval, D. Sánchez-Portal, and D. Foerster, [Assessment of density-functional tight-binding ionization potentials and electron affinities of molecules of interest for organic solar cells against first-principles \$gw\$ calculations](#), Computation **3**, 616 (2015).
- [38] J. P. Perdew, R. G. Parr, M. Levy, and J. L. Balduz, Jr., [Density-functional theory for fractional particle number: Derivative discontinuities of the energy](#), Phys. Rev. Lett. **49**, 1691 (1982).
- [39] K. R. Lykke, K. K. Murray, and W. C. Lineberger, [Threshold photodetachment of \$H^-\$](#) , Phys. Rev. A **43**, 6104 (1991).
- [40] R. T. Sharp and G. K. Horton, [A variational approach to the unipotential many-electron problem](#), Phys. Rev. **90**, 317 (1953).
- [41] J. D. Talman and W. F. Shadwick, [Optimized effective atomic central potential](#), Phys. Rev. A **14**, 36 (1976).
- [42] M. E. Casida, [Generalization of the optimized effective potential model to include electron correlation: A variational derivation of the Sham–Schluter equation for the exact exchange-correlation potential](#), Phys. Rev. A **51**, 2005 (1995).
- [43] J. B. Krieger, Y. Li, , and G. J. Iafrate, [Derivation and application of an accurate Kohn-Sham potential with integer discontinuity](#), Phys. Lett. A **146**, 256 (1990).
- [44] J. B. Krieger, Y. Li, , and G. J. Iafrate, [Construction and application of an accurate local spin-polarized Kohn-Sham potential with integer discontinuity: Exchange-only theory](#), Phys. Rev. A **45**, 101 (1992).
- [45] J. C. Slater, [A simplification of the Hartree-Fock method](#), Phys. Rev. **81**, 3455 (1951).

- [46] S. Hamel, M. E. Casida, and D. R. Salahub, Exchange-only optimized effective potential for molecules from resolution-of-the-identity techniques: Comparison with the local density approximation, with and without asymptotic correction, *J. Chem. Phys.* **116**, 8276 (2002).
- [47] S. Hamel, P. Duffy, M. E. Casida, and D. R. Salahub, Kohn-Sham orbitals and orbital energies: Fictitious constructs but good approximations all the same, *J. Electr. Spectr. and Related Phenomena* **123**, 345 (2002).
- [48] F. D. Sala and A. Görling, Efficient localized HartreeFock methods as effective exact-exchange KohnSham methods for molecules, *J. Chem. Phys.* **115**, 5718 (2001).
- [49] O. Gritsenko and E. J. Baerends, Exchange kernel of density functional response theory from the common energy denominator approximation (CEDA) for the Kohn-Sham Green's function, *Research on Chemical Intermediates* **30**, 87 (2004).
- [50] V. N. Staroverov, G. E. Scuseria, and E. R. Davidson, Effective local potentials for orbital-dependent density functionals, *J. Chem. Phys.* **125**, 081104 (2006).
- [51] J. P. Perdew and K. Schmidt, Jacobs ladder of density functional approximations for the exchange-correlation energy, in *Density Functional Theory and its Applications to Materials*, edited by V. E. V. Doren, K. V. Alseoy, and P. Geerlings, page 1, American Institute of Physics, Melville, New York, 2001.
- [52] J. P. Perdew, A. Ruzsinsky, L. A. Constantin, J. Sun, and G. Csonka, Some fundamental issues in ground-state density functional theory: a guide for the perplexed, *J. Chem. Theor. Comput.* **5**, 902 (2009).
- [53] L. Goerigk and N. Mehta, A trip to the density functional theory zoo: Warnings and recommendations for the user, *Aust. J. Chem.* **72**, 563 (2019).
- [54] P. A. M. Dirac, Note on exchange phenomena in the Thomas atom, *Proc. Camb. Phil. Soc.* **26**, 376 (1930).
- [55] S. H. Vosko, L. Wilk, and M. Nusair, Accurate spin-dependent electron liquid correlation energies for local spin density calculations: a critical analysis, *Can. J. Phys.* **58**, 1200 (1980).
- [56] J. P. Perdew and Y. Wang, Accurate and simple analytic representation of the electron-gas correlation energy, *Phys. Rev. B* **45**, 13244 (1992).
- [57] J. P. Perdew and Y. Wang, Accurate and simple density functional for the electronic exchange energy: Generalized gradient approximation, *Phys. Rev. B* **33**, 8800 (1986).
- [58] J. P. Perdew and Y. Wang, Erratum: Accurate and simple density functional for the electronic exchange energy: Generalized gradient approximation, *Phys. Rev. B* **34**, 7406(E) (1986).
- [59] J. P. Perdew, Density-functional approximation for the correlation energy of the inhomogeneous electron gas, *Phys. Rev. B* **33**, 8822(R) (1986).
- [60] J. P. Perdew, Erratum: Density-functional approximation for the correlation energy of the inhomogeneous electron gas, *Phys. Rev. B* **34**, 7406 (1986).
- [61] A. D. Becke, Density-functional exchange-energy approximation with correct asymptotic behavior, *Phys. Rev. A* **38**, 3098 (1988).

- [62] R. Colle and D. Salvetti, [Approximate calculation of the correlation energy for the closed shells](#), *Theor. Chim. Acta* **37**, 329 (1975).
- [63] R. Colle and D. Salvetti, [A general method for approximating the electronic correlation energy in molecules and solids](#), *J. Chem. Phys.* **79**, 1404 (1983).
- [64] C. Lee, W. Yang, and R. G. Parr, [Development of the Colle-Salvetti correlation-energy formula into a functional of the electron density](#), *Phys. Rev. B* **37**, 785 (1988).
- [65] N. C. Handy and A. J. Cohen, [Left-right correlation energy](#), *Mol. Phys.* **99**, 403 (2001).
- [66] J. P. Perdew, J. A. Chevary, S. H. Vosko, K. A. Jackson, M. R. Pederson, D. J. Singh, and C. Fiolhais, [Atoms, molecules, solids, and surfaces: Applications of the generalized gradient approximation for exchange and correlation](#), *Phys. Rev. B* **46**, 6671 (1992).
- [67] J. P. Perdew, K. Burke, and M. Ernzerhof, [Generalized gradient approximation made simple](#), *Phys. Rev. Lett.* **77**, 3865 (1996).
- [68] J. P. Perdew, K. Burke, and M. Ernzerhof, [Generalized gradient approximation made simple \[Phys. Rev. Lett. 77, 3865 \(1996\)\]](#), *Phys. Rev. Lett.* **78**, 1396(E) (1997).
- [69] J. P. Perdew, A. Ruzsinszky, G. I. Csonka, O. A. Vydrov, G. E. Scuseria, L. A. Constantin, X. Zhou, and K. Burke, [Restoring the density-gradient expansion for exchange in solids and surfaces](#), *Phys. Rev. Lett.* **100**, 136406 (2008).
- [70] J. P. Perdew, A. Ruzsinszky, G. I. Csonka, O. A. Vydrov, G. E. Scuseria, L. A. Constantin, X. Zhou, and K. Burke, [Erratum: Restoring the density-gradient expansion for exchange in solids and surfaces \[phys. rev. lett. 100, 136406 \(2008\)\]](#), *Phys. Rev. Lett.* **102**, 039902 (2009).
- [71] T. W. Keal and D. J. Tozer, [The exchange-correlation potential in KohnSham nuclear magnetic resonance shielding calculations](#), *J. Chem. Phys.* **119**, 3015 (2003).
- [72] T. W. Keal and D. J. Tozer, [A semiempirical generalized gradient approximation exchange-correlation functional](#), *J. Chem. Phys.* **121**, 5654 (2004).
- [73] R. Peverati, Y. Zhao, and D. G. Truhlar, [Generalized gradient approximation that recovers the second-order density-gradient expansion with optimized across-the-board performance](#), *J. Phys. Chem. Lett.* **2**, 1991 (2011).
- [74] R. Peverati and D. G. Truhlar, [Exchange-correlation functional with good accuracy for both structural and energetic properties while depending only on the density and its gradient](#), *J. Chem. Theor. Comput.* **8**, 2310 (2012).
- [75] H. S. Yu, W. Zhang, P. Verma, Z. He, and D. G. Truhlar, [Nonseparable exchange-correlation functional for molecules, including homogeneous catalysis involving transition metals](#), *Phys. Chem. Chem. Phys.* **17**, 12146 (2015).
- [76] J. Carmona-Espíndola, J. L. Gázquez, A. Vela, and S. B. Trickey, [Generalized gradient approximation exchange energy functional with correct asymptotic behavior of the corresponding potential](#), *J. Chem. Phys.* **142**, 054105 (2015).
- [77] J. P. Perdew and L. A. Constantin, [Laplacian-level density functionals for the kinetic energy density and exchange-correlation energy](#), *Phys. Rev. B* **75**, 155109 (2007).

- [78] T. van Voorhis and G. E. Scuseria, [A novel form for the exchange-correlation energy functional](#), J. Chem. Phys. **109**, 400 (1998).
- [79] T. van Voorhis and G. E. Scuseria, [Erratum: "A novel form for the exchange-correlation energy functional" \[j. chem. phys. 109, 400 \(1998\)\]](#), J. Chem. Phys. **129**, 219901 (2008).
- [80] J. P. Perdew, S. Kurth, A. Zupan, and P. Blaha, [Accurate density functional with correct formal properties: A step beyond the generalized gradient approximation](#), Phys. Rev. Lett. **82**, 2544 (1999).
- [81] J. P. Perdew, S. Kurth, A. Zupan, and P. Blaha, [Erratum: Accurate density functional with correct formal properties: A step beyond the generalized gradient approximation \[phys. rev. lett. 82, 2544 \(1999\)\]](#), Phys. Rev. Lett. **82**, 5197 (1999).
- [82] J. Tao, J. P. Perdew, V. N. Staroverov, and G. E. Scuseria, [Climbing the density functional ladder: Nonempirical meta-generalized gradient approximation designed for molecules and solids](#), Phys. Rev. Lett. **91**, 146401 (2003).
- [83] J. Tao, J. P. Perdew, V. N. Staroverov, and G. E. Scuseria, [Meta-generalized gradient approximation: Explanation of a realistic nonempirical density functional](#), J. Chem. Phys. **120**, 6898 (2004).
- [84] Y. Zhao and D. G. Truhlar, [A new local density functional for main-group thermochemistry, transition metal bonding, thermochemical kinetics, and noncovalent interactions](#), J. Chem. Phys. **125**, 194101 (2006).
- [85] R. Peverati and D. G. Truhlar, [M11-L: A local density functional that provides improved accuracy for electronic structure calculations in chemistry and physics](#), J. Phys. Chem. Lett. **3**, 117 (2012).
- [86] R. Peverati and D. G. Truhlar, [An improved and broadly accurate local approximation to the exchange-correlation density functional: The MN12-L functional for electronic structure calculations in chemistry and physics](#), Phys. Chem. Chem. Phys. **14**, 13171 (2012).
- [87] P. M. W. Gill, [Obituary: Density-functional theory \(1927-1993\)](#), Aust. J. Chem. **54**, 661 (2001).
- [88] A. D. Becke, [A new mixing of Hartree-Fock and local densityfunctional theories](#), J. Chem. Phys. **98**, 1372 (1993).
- [89] J. Harris and R. O. Jones, [The surface energy of a bounded electron gas](#), J. Phys. F **4**, 1170 (1974).
- [90] A. Seidl, A. Görling, P. Vogl, and J. A. Majewski, [Generalized kohn-sham schemees and band-gap problem](#), Phys. Rev. B **53**, 3764 (1996).
- [91] D. Mejía-Rodriguez and A. M. Köster, [Robust and efficient variational fitting of Fock exchange](#), J. Chem. Phys. **141**, 124114 (2014).
- [92] A. D. Becke, [Density-functional thermochemistry. III. The role of exact exchange](#), J. Chem. Phys. **98**, 5648 (1993).
- [93] P. J. Stephens, F. J. Devlin, C. Chabalowski, and M. Frisch, [Ab initio calculation of vibrational absorption and circular dichroism spectra using density functional force fields](#), J. Chem. Phys. **98**, 11623 (1994).

- [94] J. P. Perdew, M. Ernzerhof, and K. Burke, [Rationale for mixing exact exchange with density functional approximations](#), *J. Chem. Phys.* **105**, 9982 (1996).
- [95] C. Adamo and V. Barone, [Toward reliable density functional methods without adjustable parameters: The PBE0 model](#), *J. Chem. Phys.* **110**, 6158 (1999).
- [96] Y. Zhao and D. G. Truhlar, [The M06 suite of density functionals for main group thermochemistry, thermochemical kinetics, noncovalent interactions, excited states, and transition elements: two new functionals and systematic testing of four M06-class functionals and 12 other functionals](#), *Theor. Chem. Acc.* **120**, 215 (2007).
- [97] A. L. Fetter and J. D. Walecka, *Quantum Theory of Many-Particle Systems*, McGraw-Hill Book Company, New York, 1971.
- [98] F. Furche and T. Van Voorhis, [Fluctuation-dissipation theorem density-functional theory](#), *J. Chem. Phys.* **122**, 164106 (2005).
- [99] S. Grimme and M. Steinmetz, [A computationally efficient double hybrid density functional based on the random phase approximation](#), *Phys. Chem. Chem. Phys.* **18**, 20926 (2016).
- [100] G. Haeffler, D. Hanstorp, I. Kiyan, A. E. Klinkmüller, U. Ljungblad, and D. J. Pegg, [Electron affinity of Li: A state-selective measurement](#), *Phys. Rev. A* **53**, 4127 (1996).
- [101] R. L. Kelly, [Atomic and ionic spectrum lines below 2000 ångstöms: Hydrogen through krypton. Part I \(H-Cr\)](#), *J. Phys. Chem. Ref. Data* **16**, Suppl. 1, 1 (1987).
- [102] H. A. S. Eriksson, [Ionization energy of \$\text{Li}^+\$ and He](#), *Nature* **140**, 151 (1937).
- [103] M. Hellgren and T. Gould, [Strong correlation and charge localization in Kohn-Sham theories with fractional orbital occupations](#), *J. Chem. Theory. Comput.* **15**, 4907 (2009).
- [104] H. Olivares-Pilón and A. V. Turbiner, [H₂⁺, HeH and H₂: Approximating potential curves, calculating rovibrational states](#), *Ann. Physics* **393**, 335 (2018).
- [105] H. Olivares-Pilón and A. V. Turbiner, [Corrigendum to “H₂⁺, HeH and H₂: Approximating potential curves, calculating rovibrational states” \[ann. physics 393 \(2018\) 335-357\]](#), *Ann. Physics* **51**, 408 (2019).
- [106] W. Kolos and C. C. J. Roothaan, [Accurate electronic wave functions for the H₂ molecule](#), *Rev. Mod. Phys.* **32**, 219 (1960).
- [107] A. G. Robiette, [The variation theorem applied to H₂⁺: A simple quantum chemistry computer project](#), *J. Chem. Ed.* **52**, 95 (1975).
- [108] T. E. Sharp, [Potential-energy curves for molecular hydrogen and its ions](#), *Atomic Data* **2**, 119 (1971).
- [109] H. Chermette, C. Daul, and F. Mariotti, [Correct dissociation behavior of radical ions such as H₂⁺ in density functional calculations](#), *J. Chem. Phys.* **114**, 1447 (2001).
- [110] W. J. Moore, *Physical Chemistry*, Prentice-Hall, Englewood Cliffs, New Jersey, fourth edition edition, 1972.

- [111] T. Ziegler, A. Rauk, and E. J. Baerends, [On the calculation of multiplet energies by the Hartree-Fock-Slater method](#), *Theor. Chim. Acta* **4**, 877 (1977).
- [112] C. Daul, [Density functional theory applied to the excited states of coordination compounds](#), *Int. J. Quantum Chem.* **52**, 867 (1994).
- [113] C. A. Coulson, *Valence*, Clarendon Press, Oxford, England, UK, 1952.
- [114] G. N. Lewis, [The atom and the molecule](#), *J. Am. Chem. Soc.* **38**, 762 (1916).
- [115] P. Löwdin, [Quantum theory of many-particle systems. II. Study of the ordinary Hartree-Fock approximation](#), *Phys. Rev.* **97**, 1490 (1955).
- [116] A. Ipatov, F. Cordova, L. Joubert Doriol, and M. E. Casida, [Excited-state spin-contamination in time-dependent density-functional theory for molecules with open-shell ground states](#), *J. Mol. Struct. (Theochem)* **914**, 60 (2009).
- [117] K. Yamaguchi, F. Jensen, A. Dorigo, and K. Houk, [A spin correction procedure for unrestricted Hartree-Fock and Möller-Plesset wavefunctions for singlet diradicals and polyyradicals](#), *Chem. Phys. Lett.* **149**, 537 (1988).
- [118] A. D. Bacon and M. C. Zerner, [An intermediate neglect of differential overlap theory for transition metal complexes: Fe, co and cu chlorides](#), *Theor. Chim. Acta* **53**, 21 (1979).
- [119] Y. Yamaguchi, Y. Osamura, J. D. Goddard, and H. F. Schaefer III, *A New Dimension to Quantum Chemistry: Analytic Derivative Methods in Ab Initio Molecular Electronic Structure Theory*, Oxford University Press, Oxford, 1994.
- [120] P. Pulay, [Analytical derivatives, forces, force constants, molecular geometries, and related response properties in electronic structure theory](#), *WIREs Comput. Mol. Sci.* **4**, 169 (2014).
- [121] P. Güttinger, [Das Verhalten von Atomen im magnetischen Drehfeld](#), *Z. Physik* **73**, 169 (1932).
- [122] W. Pauli, [Principles of wave mechanics](#), in *Handbuch der Physik*, volume 24, page 162, Springer, Berlin, 1933.
- [123] H. Hellmann, [Einführung in die Quantenchemie](#), Franz Deuticke, Leipzig, 1937, p. 285.
- [124] R. P. Feynman, [Forces in molecules](#), *Phys. Rev.* **56**, 340 (1939).
- [125] M. Paris, [Global method for electron correlation](#), *Phys. Rev. Lett.* **119**, 063002 (2017).
- [126] P. M. Morse, [Diatomc molecules according to the wave mechanics. II. Vibrational levels](#), *Phys. Rev.* **34**, 57 (1929).
- [127] Z. Farooq, D. A. Chestakov, B. Yan, G. C. Groenenboom, W. J. van der Zande, and D. H. Parker, [Photodissociation of singlet oxygen in the UV region](#), *Phys. Chem. Chem. Phys.* **16**, 3305 (2014).
- [128] A. Rohatgi, [WEBPLOTDIGITIZER: Webbased plot digitizer](#), <https://apps.automeris.io/wpd/>, Last accessed 3 June 2021.
- [129] P. H. Krupenie, [The spectrum of molecular oxygen](#), *J. Phys. Chem. Ref. Data* **1**, 423 (1972).

- [130] R. P. Saxon and B. Liu, *Ab initio* configuration interaction study of the valence states of O₂, J. Chem. Phys. **67** (1977).
- [131] M. C. G. N. van Vroonhoven and G. C. Groenenboom, *Reassignment of the O₂ spectrum just below dissociation threshold based on ab initio calculations*, J. Chem. Phys. **117**, 5240 (2002).
- [132] W. T. Borden, R. Hoffmann, T. Stuyver, and B. Chen, *Dioxygen: What makes this triplet diradical kinetically persistent?*, J. Am. Chem. Soc. **139**, 9010 (2017).
- [133] C. C. J. Roothaan, *Self-consistent field theory for open shells of electronic systems*, Rev. Mod. Phys. **32**, 179 (1960).
- [134] T. V. Russo, R. L. Martin, and P. J. Hay, *Density functional calculations on first-row transition metals*, J. Chem. Phys. **101**, 7729 (1994).
- [135] I. Frank, J. Hutter, D. Marx, and M. Parrinello, *Molecular dynamics in low-spin excited states*, J. Chem. Phys. **108**, 4060 (1997).
- [136] M. Filatov and S. Shaik, *Spin-restricted density functional approach to the open-shell problem*, Chem. Phys. Lett. **288**, 689 (1998).
- [137] R. McWeeny and G. Diercksen, *Self-consistent perturbation theory. II. Extension to open shells*, J. Chem. Phys. **49**, 4852 (1968).
- [138] E. R. Davidson, *Spin-restricted open-shell self-consistent-field theory*, Chem. Phys. Lett. **21**, 565 (1973).
- [139] J. S. Binkley, J. A. Pople, and P. A. Dobosh, *The calculation of spin-restricted single-determinant wavefunctions*, Mol. Phys. **28**, 1423 (1974).
- [140] M. F. Guest and V. R. Saunders, *On methods for converging open-shell hartree-fock wavefunctions*, Mol. Phys. **28**, 819 (1974).
- [141] B. N. Plakhutin, E. V. Gorelik, and N. N. Breslavskaya, *Koopmans' theorem in the ROHF method: Canonical form for the Hartree-Fock hamiltonian*, J. Chem. Phys. **125**, 204110 (2006).
- [142] K. E. Hyde, *Methods for obtaining Russell-Saunders term symbols from electronic configurations*, J. Chem. Ed. **52**, 87 (1975).
- [143] National institute of standards and technologies atomic spectra database, https://physics.nist.gov/PhysRefData/ASD/levels_form.html, Last accessed 22 June 2021.
- [144] M. E. Casida and M. Huix-Rotllant, *Progress in time-dependent density-functional theory*, Annu. Rev. Phys. Chem. **63**, 287 (2012).
- [145] L. Noodleman, *Valence bond description of antiferromagnetic coupling in transition metal dimers*, J. Chem. Phys. **74**, 5737 (1981).
- [146] J. Friedrichs and I. Frank, *Mechanism of electrocyclic ring-opening of diphenyloxirane: 40 years after Woodward and Hoffmann*, Chemistry — A European Journal **15**, 10825 (2009).

- [147] J. Guan, F. Wang, T. Ziegler, and H. Cox, **Time-dependent density functional study of the electronic potential energy curves and excitation spectrum of the oxygen molecule**, *J. Chem. Phys.* **125**, 044314 (2006).
- [148] E. Cancés, **Self-consistent field algorithms for Kohn-Sham models with fractional occupation numbers**, *J. Chem. Phys.* **114**, 10616 (2001).
- [149] K. Scharz, **Optimization of the statistical exchange parameter α for the free atoms H through Nb**, *Phys. Rev. B* **5**, 2466 (1972).
- [150] A. Fouqueau, S. Mer, M. E. Casida, L. M. L. Daku, A. Hauser, T. Mineva, and F. Neese, **Comparison of density functionals for energy and structural differences between the high [$^5T_{2g}$: $(t_{2g})^4(e_g)^2$] and low [$^1A_{1g}$: $(t_{2g})^6(e_g)^0$] spin states of the hexaquoferrous cation, $[\text{Fe}(\text{H}_2\text{O})_6]^{2+}$** , *J. Chem. Phys.* **120**, 9473 (2004).
- [151] A. Fouqueau, M. E. Casida, L. M. L. Daku, A. Hauser, and F. Neese, **Comparison of density functionals for energy and structural differences between the high [$^5T_{2g}$: $(t_{2g})^4(e_g)^2$] and low [$^1A_{1g}$: $(t_{2g})^6(e_g)^0$] spin states of iron(II) coordination compounds: II. More functionals and the hexaminoferrous cation, $[\text{Fe}(\text{NH}_3)_6]^{2+}$** , *J. Chem. Phys.* **122**, 044110 (2005).
- [152] G. Ganzenmüller, N. Berkaïne, A. Fouqueau, M. E. Casida, and M. Reiher, **Comparison of density functionals for differences between the high ($^5T_{2g}$) and low ($^1A_{1g}$) spin states of iron(II) coordination compounds: IV. Results for the ferrous complexes $[\text{Fe}(\text{L})(\text{'NHS}_4\text{'})]$** , *J. Chem. Phys.* **122**, 234321 (2005).
- [153] L. M. L. Daku, A. Vargas, A. Hauser, A. Fouqueau, and M. E. Casida, **Assessment of density functionals for the high-spin/low-spin energy difference in the low-spin iron(II) tris(2,2'-bipyridine) complex**, *ChemPhysChem* **6**, 1393 (2005).
- [154] S. Zein, S. A. Borshch, P. Fleurat-Lessard, M. E. Casida, and H. Chermette, **Assessment of the exchange-correlation functionals for the physical description of spin transition phenomena by DFT methods: All the same?**, *J. Chem. Phys.* **126**, 014105 (2007).
- [155] L. M. L. Daku and M. E. Casida, **Modeling the physical properties of environmentally-friendly optical magnetic switches: DFT and TD-DFT**, in *Green Chemistry and Computational Chemistry: Shared Lessons in Sustainability*, edited by L. Mammino, Elsevier, 2021, *preprint* <https://arxiv.org/abs/1201.2398>.
- [156] E. Cancès and G. Dusson, **Discretization error cancellation in electronic structure theory: Toward a quantitative study**, *ESAIM: M2AN* **51**, 1617 (2017).
- [157] D. Bressanini, M. Mella, and G. Morosi, **Nonadiabatic wavefunctions as linear expansions of correlated exponentials. A quantum Monte Carlo application to H_2^+ and Ps_2** , *Chem. Phys. Lett.* **272**, 370 (1997).
- [158] A. Galano and J. R. Alvarez-Idaboy, **Kinetics of radical-molecule reactions in aqueous solution: A benchmark study of the performance of density functional methods**, *J. Comput. Chem.* **35**, 2019 (2014).
- [159] P. Hohenberg and W. Kohn, **Inhomogeneous electron gas**, *Phys. Rev.* **136**, B864 (1964).

- [160] Wikipedia, [Singlet oxygen](https://en.wikipedia.org/wiki/Singlet_oxygen), https://en.wikipedia.org/wiki/Singlet_oxygen, Last accessed 24 June 2021.
- [161] [Virtualbox](https://www.virtualbox.org/), <https://www.virtualbox.org/>, Last accessed 19 January 2022.